Theoretical Studies of Some Inelastic Collision Processes

by

Neil Peter Donaldson French, B.Sc.

Submitted to the University of Edinburgh as
a thesis as required for the degree of
Doctor of Philosophy in the Faculty of Science.

Ph.D.

University of Edinburgh

1975

DECLARATION

I hereby declare that this thesis has been composed by me and that the work described in it is my own and was carried out at the University of Edinburgh except where due acknowledgement is made.

SIGNED:

DATE: 27/9/76

ACKNOWLEDGEMENTS

I wish to express my sincere thanks to Dr K.P. Lawley for many helpful suggestions throughout the past three years and in the preparation of this thesis.

I should also like to record my gratitude to the University of Edinburgh for the use of library and computing facilities and to the Science Research Council for financial support.

My sincere thanks are due to Mrs Hosie for the excellent work done in typing this thesis. Every page is a tribute to her patience and perseverance.

Finally, I dedicate this thesis to my parents without whose help and encouragement this thesis would never have been written.

ABSTRACT

The work reported in part I of this thesis concerns ionisation and spin exchange in systems $M + X \rightleftarrows M^+ + X^-$. The familiar time-dependent perturbation equations are derived from the time-independent Schrödinger wave equation. Coriolis coupling is explicitly taken account of, the relevant coupled equations are set up for several M + X systems and are solved numerically. The results are presented in §I.10 and §I.11 where the solutions are compared with the Landau-Zener approximation and with the numerical solution of a simple two-state problem.

In Part II elastic and inelastic differential cross sections for two crossing monotonic repulsive potentials are calculated. Two model potentials are used and the scattering amplitudes are evaluated as a partial wave summation. The S-matrix elements are calculated using the Landau-Zener-Stueckelberg approximation and phase shifts are evaluated analytically by using a straight line approximation to the trajectory. The results, which are interpreted in an analysis due to Ford and Wheeler, are presented in §II.6.

In part III the quadrupole-quadrupole mechanism for fine structure transitions in heavy atoms induced by collision with H_2 HD and D_2 is considered.* The quadrupole-quadrupole term of the multipolar expansion of the electrostatic interaction potential is evaluated in two co-ordinate systems. An analytic expression for the transition probabilities is obtained in terms of atomic and molecular matrix

* Transition probabilities were evaluated using first order time-dependent perturbation theory.

elements, atomic and molecular quantum numbers and an integral over the collision trajectory. The matrix elements were evaluated using the best available wave functions. Transition probabilities as functions of impact parameter and velocity were obtained by numerically integrating the trajectory integrals. The probability functions were numerically integrated first over impact parameter and finally over the Boltzmann velocity distribution to obtain rate constants as functions of temperature. The rate constants so calculated were compared with experimental values and the results are presented in §III.5.

CONTENTS

PART I

Ionisation and Spin-flip in Some Systems

$$M + X \rightleftarrows M^{+} + X^{-}$$

C O N T E N T S

I.1 Introduction

It is known that, at infinite separation, the energy of the system $M^+(^1S_o) + X^-(^1S_o)$ where M = Li, Na, K and X = F, Cl, Br or I, lies between 0.21 eV (KF) and 2.25 eV (LiI) above that of the system $M(^2S_{\frac{1}{2}}) + X(^2P_{3/2})$, the ground state of the M - X system at infinite separation. However, in their lowest electronic states, which have binding energies of between 3.16 eV (NaI) and 6.6 eV (LiF) relative to $M(^2S_{\frac{1}{2}}) + X(^2P_{3/2})$, the diatomic alkali halide molecules seem to behave essentially like pairs of oppositely-charged ions. If the M + X system is described in terms of diabatic potential energy curves, it is clear that the ionic surface must cross the (manifold of) covalent one(s). Furthermore, the ionic and (one of) the covalent curve(s) have the same symmetry ($^1\Sigma^+$ or $\Omega = o^+$) so that there is a non-vanishing matrix element of the Hamiltonian between these two diabatic states.

One question that is often asked about such a system is "what is the probability of crossing from the (manifold of) covalent surface (s) to the ionic surface, or vice versa, as a result of the collision between M and X?". The method frequently adopted to answer this question is to set up the time-dependent perturbation (TDP) equations in a limited expansion basis of diabatic states - frequently including only two states in the expansion - and then solve the set of coupled, first order differential equations either numerically or by approximation - for example using the Landau-Zener (ZEN32) or

Landau-Zener-Stueckelberg (STU32) approximations. Such a treatment entirely neglects two factors:

a. The single ionic curve crosses manifolds of surfaces corresponding to pairs of M and X atoms in a variety of j, m_j states. I(1.1)

b. States whose Z-component of the total angular momentum (defined about the internuclear axis) differ by $\pm$ one unit are coupled by the rotational motion of the two atoms (except in a "head-on" collision). This is the so-called Coriolis Coupling.

The existence of manifolds of neutral surfaces becomes apparent on consideration of the correlation diagram.

For the case of KI, the coupling between the total orbital angular momentum, L, and the total spin angular momentum, S, in the separated atoms appears to be strong (for I at least) and J and M_J are good quantum numbers. In this situation, a space quantisation of J rather than L takes place in the electric field produced when the atoms approach each other. This corresponds to Hund's case (c) coupling (HER50, MUL30). The component of the total electronic angular momentum along the internuclear axis of the molecule, Ω, is then obtained by adding the M_J values of the two atoms:

$$|\Omega| = |M_{J_1} + M_{J_2}|$$

At larger internuclear separations, then, the 'molecular' states arising from the atomic states $M(^2S_{\frac{1}{2}}) + X(^2P_{3/2})$ and $M(^2S_{\frac{1}{2}}) + X(^2P_{\frac{1}{2}})$

figure 1

Diabatic Correlation Diagram for MX

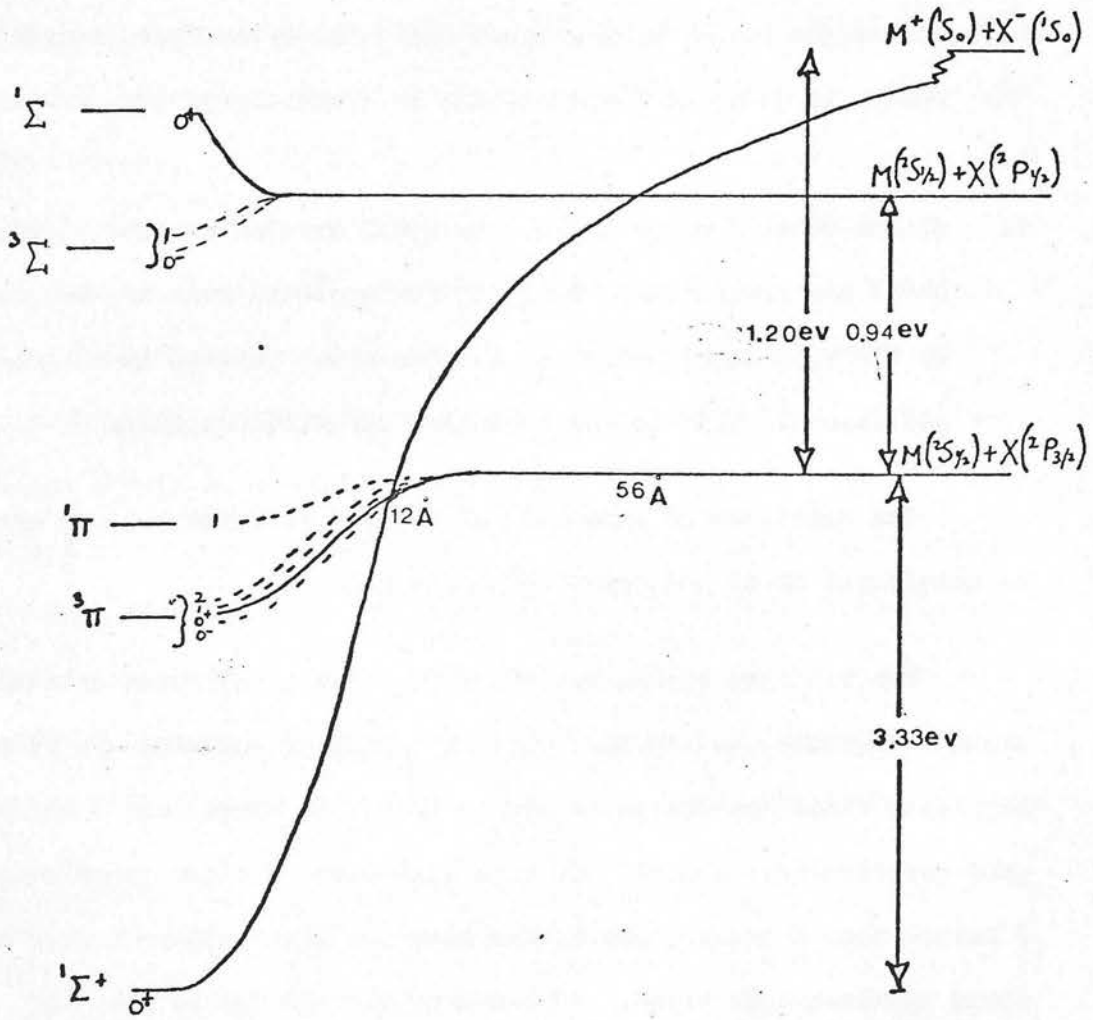

Curves of Symmetry $\Omega = 0^+$ are Shown as Full Lines

may be described as

$$^2S_{\frac{1}{2}} + {}^2P_{3/2} \rightarrow \Omega = 2,1,1,0^+,0^- \qquad \text{(8 states)}$$

$$^2S_{\frac{1}{2}} + {}^2P_{\frac{1}{2}} \rightarrow \Omega = 1,0^+,0^- \qquad \text{(4 states)}$$

At smaller separations it may be that coupling more nearly approaches Hund's case (a) when $\underline{L}$ and $\underline{S}$ become good quantum numbers. In this description the molecular states arising from the separated atoms may be described as

$$^2S + {}^2P \rightarrow {}^1\Sigma(\Omega = 0^+),\ {}^3\Sigma(\Omega = 1,0^-),\ {}^1\pi(\Omega = 1)$$

and ${}^3\pi(\Omega = 2,1,0^+,0^-)$ - 12 states in all.

In addition there is the possibility of a transition to something like Hund's case (c) in which the <u>total</u> angular momentum of each electron ($\underline{\ell} + \underline{s}$) combine to produce the total electronic angular momentum.

In order to determine the states present at still smaller separations (e.g. 3Å), the ordering and occupancy of molecular energy levels must be known. An attempt to predict this for a molecule as large as KI would be rather speculative. However it is known that the molecular ground state is the ionic ${}^1\Sigma^+(\Omega=0^+)$ state.

A correlation diagram may be tentatively constructed using Ω-Ω correlations and assuming that the low lying molecular states derive entirely from the states arising from ${}^2S + {}^2P$ together with the ionic ${}^1\Sigma^+$ state. One such possible diabatic correlation diagram is shown in Figure 1.

In the calculations, atomic J's were taken to be good quantum numbers, ie Hund's case (c) was used throughout the collision.

In the calculations described below, processes of the type

$$M + X \rightleftarrows M^+ + X^-$$

not specific to the alkali halide systems were considered:

$$\left.\begin{array}{ll} 1. & M(^2S_{\frac{1}{2}}) + X(^1S_o) \rightleftarrows M^+(^1S_o) + X^-(^2S_{\frac{1}{2}}) \\ 2. & M(^2S_{\frac{1}{2}}) + X(^1S_o) \rightleftarrows M^+(^1S_o) + X^-(^2P_{3/2}) \end{array}\right\} \text{one electron calculations}$$

$$\left.\begin{array}{ll} 3. & M(^2S_{\frac{1}{2}}) + X(^2S_{\frac{1}{2}}) \rightleftarrows M^+(^1S_o) + X^-(^1S_o) \\ 4. & M(^2S_{\frac{1}{2}}) + X(^2P_{3/2}) \rightleftarrows M^+(^1S_o) + X^-(^1S_o) \end{array}\right\} \text{two electron calculations}$$

I(1.2)

In model (1) two neutral potentials cross two ionic potentials, and in model (2) two neutral potentials cross four ionic potentials. Due to coriolis coupling, transitions can take place between the members of each manifold in each case. The component of electron spin, m_s, is not defined in the ion $X^-(^2P_{3/2})$, and it is expected that transitions from non-selected neutral states to the ionic substates with $m_j = \pm \frac{1}{2}$ and $m_j = \pm 3/2$ may not be of equal importance. (The ground state of an ion with electron configuration $(np)^1$ will be $^2P_{\frac{1}{2}}$ not $^2P_{3/2}$, and this point will be taken up in § (I.5)). In addition, the possibilities for spin-flip in M are quite different in (1) than in (2). In both M atom and X^- ion in (1) m_s is a good quantum number and, in fact, it is expected that spin flip is impossible in such a system. In (2), however, m_s is not defined in X^- due to spin-orbit coupling, and for this system non-zero spin-flip probabilities are expected.

In models (3) and (4) the single ionic potential crosses a manifold of four and eight neutral potentials respectively. Transitions are again possible between the members of a manifold. Now ion production processes depend (differently for the two models) upon the initial neutral state in which the system is prepared. As far as spin-flip in M is concerned, two electron processes are now possible. In terms of model (3), two such processes are

i. $M(\uparrow) + X(\downarrow) \rightarrow M^+ + X^-(\uparrow\downarrow) \rightarrow M(\downarrow) + X(\uparrow)$

ii. $M(\uparrow) + X(\downarrow) \rightarrow M(\downarrow) + X(\uparrow)$

where $\uparrow$ and $\downarrow$ represent the two possible orientations of electron spin. Processes of the type (i) and (ii) are also possible in model (4) except that m_s is not defined in the X atom or X^- ion.

Hence, from these various models, it should be possible to determine the effect upon collision-induced ionisation of making allowance for I(1.1) (a) and (b). In addition, the probability of spin-flip in M can be compared for the four systems in the hope of obtaining information about the mechanism for this process, and to determine whether or not it is a useful tool for investigating curve crossing.

In all the calculations, the Hamiltonian matrix elements were modelled on the KI system and collision energies were such that all exit channels were open.

As indicated above, only the crossing of the ionic potential with the ground neutral manifold of MX potentials was considered. The validity of neglecting other manifolds must be considered.

The second crossing of the ionic curve (working outwards from the minimum) is with the manifold of states arising from the atomic states $M(^2S_{\frac{1}{2}}) + X(^2P_{\frac{1}{2}})$. This additional crossing was incorporated in a simple semi-classical analysis in which only coupling due to the Hamiltonian was considered. In this analysis the probability, p, of emerging on the ionic surface after entering on the neutral ground surface was found to be

$$p = P_{LZS} \times p^1$$

where P_{LZS} is the probability of the same transition where the second crossing is ignored (see § I.8) and p^1 is the probability of remaining on the ionic surface after the outward traverse of the second crossing at separation R_{c_2}. In the case of KI, the outer crossing is at such a large internuclear separation ($R_{c_2} \approx 56$ Å) that $p^1 = 1$ (or very nearly) for all impact parameters less than R_{c_1} (the inner crossing distance) at the energies used. For this system, then, it is expected that ionisation probabilities and cross sections can be adequately computed ignoring the second crossing since the $^2P_{\frac{1}{2}}$ state does not appear to be an accessible exit channel via the outer crossing. This expectation was confirmed by computation.

Approximate values of R_{c_1} and R_{c_2} for other alkali-metal/Halogen systems are presented in the table following. It can be seen that the other systems for which a significant ionisation cross section is expected (R_{c_1} not too large) and for which the outer crossing can be neglected are K Br, Rb Br and Rb I.

The appropriate time-dependent perturbation equations will be derived in I.2 taking account of I(1.1) (a) and (b). Restrictions on their usefulness and validity will also be indicated.

I.2 MATHEMATICAL FORMULATION of the PROBLEM

The Coupled Equations

The method employed is to expand the complete wave function of the system in W.K.B.-type functions for the nuclear motion and in atomic wave functions for the electronic motion. The various assumptions made and approximations used will be specified as they are encountered.

The Hamiltonian of the system is given by

$$H = -(\hbar^2/2\mu)\nabla_N^2 + H_e \quad \text{(the co-ordinates of the C.M. are cyclical)} \qquad \text{I(2.1)}$$

where $$H_e = \Sigma_i\{-(\hbar^2/2\mu_e)\nabla_i^2 + V(\underline{r}^m, \underline{R})\} \quad ,$$

First and Second Ionic/Neutral Crossing Distances

(Å) for the Alkali-metal/Halogen Systems

MX	R_{c_1}/Å	R_{c_2}/Å
Li F	11.4	11.9
Li Cl	8.6	9.2
Li Br	7.6	10.0
Li I	6.4	11.0
Na F	14.3	15.0
Na Cl	10.2	11.0
Na Br	8.7	12.1
Na I	7.2	13.7
KF	68.6	90.1
K Cl	23.2	28.2
K Br	16.9	36.6
K I	12.0	56.0
RbF	313.0	None
RbCl	31.6	41.5
Rb Br	21.0	62.8
Rb I	13.9	154.5
Cs F	None	None
Cs Cl	83.2	225.7
Cs Br	35.7	None
Cs I	19.1	None

$\underline{\nabla}_N$ is the gradient with respect to nuclear co-ordinates and $\underline{\nabla}_i$ is the gradient with respect to the co-ordinates of the i^{th} electron. Electronic and nuclear co-ordinates are denoted $\underline{r}^m$ and $\underline{R}$ respectively. The Schrodinger time independent equation is

$$H\Psi = E\Psi \qquad \text{I(2.2)}$$

and the complete wave function Ψ is expanded in electronic and nuclear eigenfunctions:

$$\Psi = \Sigma_{n,\ell} a_{n\ell}(R)\phi_n(\underline{r}^m,\underline{R})\,\chi_{n\ell}(R)P_\ell(\cos\theta) \qquad \text{I(2.3)}$$

$$\text{and} \quad \chi_{n\ell} = (1/\rho_{n\ell})^{\frac{1}{2}} \exp\,(i/\hbar)\int \rho_{n\ell}\,dR \qquad \text{I(2.4)}$$

where $p_{n\ell} = \mu v_{n\ell} = (2E\mu)^{\frac{1}{2}}\left[1-H_{nn}/E-\ell(\ell+1)\hbar^2/2\mu ER^2\right]^{\frac{1}{2}}$

in which $H_{nn} = \langle\phi_n|H_e|\phi_n\rangle$

The electronic wave functions are written $\phi_n(\underline{r}^m,\underline{R})$ because

$$\phi_n = \phi_n(\underline{r}^m_A) \quad \text{or} \quad \phi_n(\underline{r}^m_B)$$

depending on which atom ϕ_n is centred upon.

Substituting I(2.3) into I(2.2) making use of I(2.1) and I(2.4), multiplying throughout by ϕ^*_m and integrating over electronic co-ordinates yields the result

$$\Sigma_{n,\ell}(C_{n\ell} + R_{n\ell}) = 0$$

where $C_{n\ell} = \left[-i\hbar v_{n\ell} S_{mn} \frac{da_{n\ell}}{dR} \chi_{n\ell} - i\hbar v_{n\ell} a_{n\ell} \{\frac{\partial}{\partial R}\}_{mn} \chi_{n\ell}\right.$

I(2.5)

$\left. + a_{n\ell}(H_{mn} - H_{nn} S_{mn}) \chi_{n\ell}\right] P_\ell(\cos\theta) - \frac{\hbar^2}{\mu R^2} a_{n\ell} \chi_{n\ell} \{\frac{\partial}{\partial\theta}\}_{mn} \frac{dP_\ell}{d\theta}$

and $R_{n\ell} = \frac{-\hbar^2}{2\mu} (a_{n\ell} \chi_{n\ell} \{\nabla_N^2\}_{mn} + S_{mn} \chi_{n\ell} \nabla_N^2 a_{n\ell} + 2\chi_{n\ell} \frac{da_{n\ell}}{dR} \{\frac{\partial}{\partial R}\}_{mn}) P_\ell(\cos\theta)$

$S_{mn} = \langle \phi_m | \phi_n \rangle$, $\{\hat{F}\}_{mn}$ is the mn^{th} matrix element of the operator $\hat{F}$, and it has been assumed that

$\partial \chi_{n\ell}/\partial R \approx i p_{n\ell} \chi_{n\ell}/\hbar$, $\frac{-\hbar^2}{2\mu} \{\frac{1}{R^2} \frac{d}{dR} R^2 \frac{d}{dR} - \frac{\ell(\ell+1)}{R^2} + \frac{2\mu(E-H_{nn})}{\hbar^2}\} \chi_{n\ell} \approx 0$

Making use of the relations

$$(1-x^2) dP_\ell/dx = (\ell+1) x P_\ell - (\ell+1) P_{\ell+1}$$

and $P_\ell(\cos\theta) \sim \frac{\alpha}{2i} \left[\exp(i\eta_\ell) - \exp(-i\eta_\ell)\right]$, $\alpha = \left[\frac{4}{(2\ell+1)\pi \sin\theta}\right]^{\frac{1}{2}}$, $\eta_\ell =$

$(\ell+\frac{1}{2})\theta + \pi/4$

it is readily demonstrated that

$$dP_\ell(\cos\theta)/d\theta \approx \frac{\alpha(\ell+1)}{2} \left[\exp(i\eta_\ell) + \exp(-i\eta_\ell)\right], \ell >> 1$$

And providing $a_{n\ell}$ is a moderately slowly varying function of R,

$$C_{n\ell} >> R_{n\ell}$$

Hence I(2.5) becomes

$$\Sigma_\ell \alpha f_\ell^+ \exp(i\eta_\ell) + \Sigma_\ell \alpha f_\ell^- \exp(-i\eta_\ell) \approx o$$

so that $$f_\ell^\pm = o \qquad \text{I(2.6)}$$

where $$f_\ell^\pm = \Sigma_n \{-i\hbar v_{n\ell} S_{mn} \frac{d a_{n\ell}}{dR} \chi_{n\ell} - i\hbar v_{n\ell} a_{n\ell} \{\frac{\partial}{\partial R}\}_{mn}$$

$$+ a_{n\ell}(H_{mn} - H_{nn} S_{mn}) \chi_{n\ell} \pm i\hbar \left[\frac{(\ell+1)\hbar}{\mu R^2}\right] \{\frac{\partial}{\partial \theta}\}_{mn} \chi_{n\ell}\}$$

Noting that $\left[\ell(\ell+1)\right]^{\frac{1}{2}} \hbar \approx (\ell+1)\hbar = \mu v_{n\ell} b = \mu R^2 \dot{\theta}$ (classical equation of motion) and that

$$\chi_{n\ell} \approx \exp\left[\frac{i}{\hbar}\int (2E\mu - \frac{\ell(\ell+1)\hbar^2}{R^2}) dR\right] \exp\left[\frac{-i}{\hbar}\int \frac{H_{nn} dR}{(2E/\mu)^{\frac{1}{2}}}\right]$$

for E large, making the approximation that

$$(2E/\mu)^{\frac{1}{2}} \approx v_{n\ell}$$

utilising the identity $\partial/\partial t \equiv \underline{v}_{n\ell} \cdot \underline{\nabla}_N$ and making a change of coefficient.

$$C_{n\ell} = a_{n\ell} \exp\left[-(i/\hbar)\int H_{nn} dt\right],$$

I(2.6) becomes

$$\Sigma_n \dot{C}_{n\ell} S_{mn} + \{\partial/\partial t\}_{mn} + (i/\hbar) H_{mn} C_{n\ell} = o \qquad \text{I(2.7)}$$

which is valid for $\ell \gg 1$, $E/H_{nn} \gg 1$, $da_{n\ell}/dR \gg 1$

It is very desirable and not difficult to show that equations I(2.7) are such that probability is conserved.

In matrix notation, equations I(2.7) used

$$\dot{\underline{C}} = -i\,\underline{V}\,\underline{C}\ ,\quad \underline{V} = \frac{1}{\hbar}\,\underline{S}^{-1}\,\underline{H} - i\underline{S}^{-1}\{\frac{\partial}{\partial t}\} \qquad \text{I(2.8)}$$

The criterion for conservation of probability is

$$\frac{d}{dt}\langle\Psi|\Psi\rangle = o \qquad \text{I(2.9)}$$

Since $\langle\Psi|\Psi\rangle = \Sigma_{ij} C_i^* C_j S_{ij} = \underline{C}^+\,\underline{S}\,\underline{C}$ (second suffix on coefficients is redundant), I(2.9) may be written, with $f = \langle\Psi|\Psi\rangle$

$$\dot{f} = \dot{\underline{C}}^+\,\underline{S}\,\underline{C} + \underline{C}^+\dot{\underline{S}}\,\underline{C} + \underline{C}^+\underline{S}\,\dot{\underline{C}}$$

On substituting the Hermitian conjugate of I(2.8), $\dot{f}$ becomes

$$\dot{f} = \underline{C}^+(\dot{\underline{S}} + i\underline{V}^+\underline{S} - i\underline{S}\underline{V})\underline{C}$$

$$= \underline{C}^+\{\dot{\underline{S}} + (i/\hbar)(\underline{H}^+ - \underline{H}) - (\{\frac{\partial}{\partial t}\} + \{\frac{\partial}{\partial t}\}^+)\}\underline{C}$$

($\underline{S}$ and $\underline{S}^{-1}$ are real symmetric matrices).

Since $\underline{H}$ is a Hermitian matrix and

$\{\partial/\partial t\} + \{\partial/\partial t\}^+ = \dot{\underline{S}}$, it is clear that $\dot{f} = o$

as required for conservation of probability.

In similar fashion it can be shown that it is always possible to transform the equations in the diabatic ϕ basis to a set of equations in an adiabatic ψ basis in which microscopic reversibility is obeyed. To demonstrate this, consider a transformation

$$\psi_j = \Sigma_i \phi_i d_{ij} \ , \ \psi_\ell = \Sigma_k b_{k\ell} \psi_k$$

such that the adiabatic ψ basis is orthogonal.

In matrix notation

$$\underline{C} = \underline{d}.\underline{b} \ , \ \underline{H}^{\psi} = \underline{d}^{+} \underline{H} \underline{d} = \underline{H}^{\dagger_\psi} \qquad \text{I(2.10)}$$

and $$\underline{S}^{\psi} = \underline{d}^{+} \underline{S} \underline{d} = \underline{I}$$

Making the replacement $\underline{C} = \underline{d}\,\underline{b}$ in I(2.7) and premultiplying the resulting equation throughout by $\underline{d}^{+}$, yields the equation

$$\dot{\underline{b}} = -\underline{V}\,\underline{b} \ , \ \underline{V} = \underline{A} + (i/h)\underline{H}^{\psi} \ , \ \underline{A} = \underline{d}^{+}\underline{S}\underline{d} + \underline{d}^{+}\{\partial/\partial t\}\underline{d}$$

$$\underline{A} + \underline{A}^{+} = \partial/\partial t\{\underline{d}^{+}\,\underline{S}\,\underline{d}\} = o$$

$$\therefore \ \underline{V}^{+} = -\underline{V} \qquad \text{I(2.11)}$$

Thus $\underline{V}$ is anti-hermitian, and microscopic reversibility is obeyed in the ψ basis.

figure 2

Attractive and Repulsive Trajectories in the CM Frame

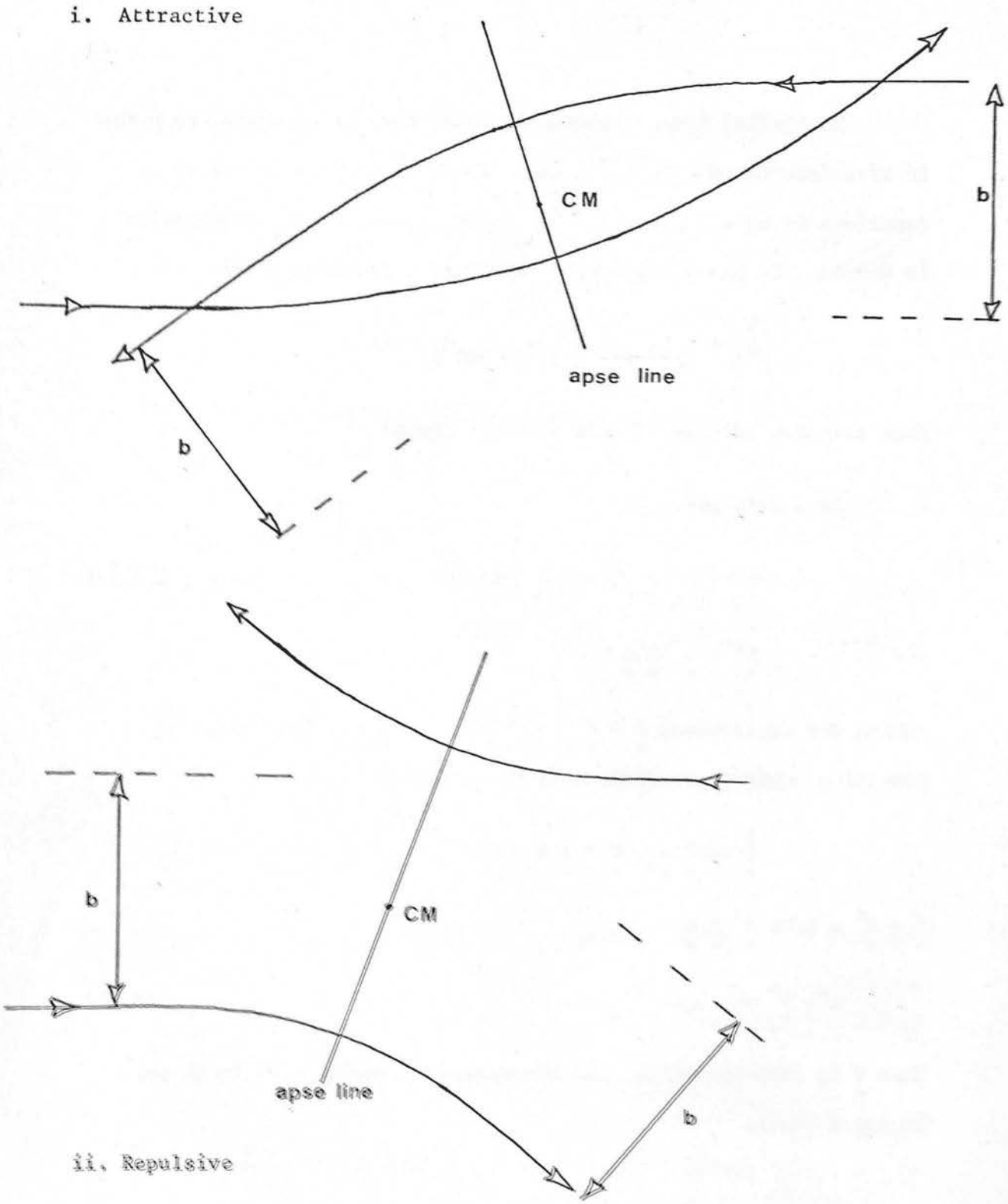

b is the impact parameter and the apse line is the interparticle vector at the instant of closest approach.

I.3 Evaluation of the Matrix $\{\partial/\partial t\}$

It is assumed that the nuclear motion is, to a good approximation, classical. Hence $\underline{R}(t)$ is known, where $\underline{R}$ is the internuclear vector, and it is useful to write

$$\frac{\partial}{\partial t} \equiv \underline{V}.\nabla_R \equiv \dot{R}\frac{\partial}{\partial R} + \dot{\Theta}\frac{\partial}{\partial \Theta} + \dot{\Phi}\frac{\partial}{\partial \Phi} \qquad \text{I(3.1)}$$

The interatomic potential is taken to be central, and it is known from classical mechanics (GOL50) that

$$\begin{aligned} \dot{\Phi} &= 0 \\ \dot{R} &= v\left[1-b^2/R^2 - u(R)/E\right]^{\frac{1}{2}} \\ \dot{\Theta} &= vb/R^2 \quad , \quad v = (2E/\mu)^{\frac{1}{2}} \end{aligned} \qquad \text{I(3.2)}$$

and b is the impact parameter for the trajectory (see Figure 2).

Energy transfer due to changes of quantum state during the collision was neglected since ΔE (1.2 eV for $M + X \rightarrow M^+ + X^-$) is $<<E$ ($E \gtrsim 50$ eV), so that one impact parameter and asymptotic velocity are defined for a trajectory.

In all the calculations that follow, the ϕ basis is an atomic one, that is, each ϕ is expressed in terms of atomic orbitals centred on M or X. Hence the evaluation of $\partial\phi_n/\partial t$ requires the evaluation of

$$\frac{\partial \psi_{jm}}{\partial t} = \dot{R}\frac{\partial \psi_{jm}}{\partial R}, + \dot{\Theta}\frac{\partial \psi_{jm}}{\partial \Theta}$$

figure 4

System of Euler Angles used.

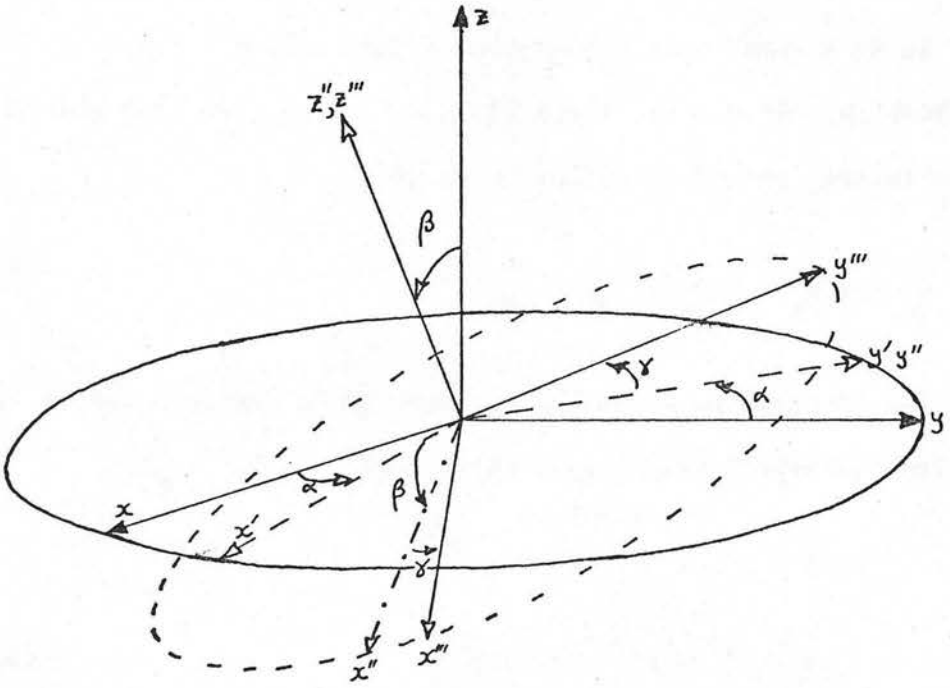

figure 3

Space-fixed and Rotating Co-ordinate Systems

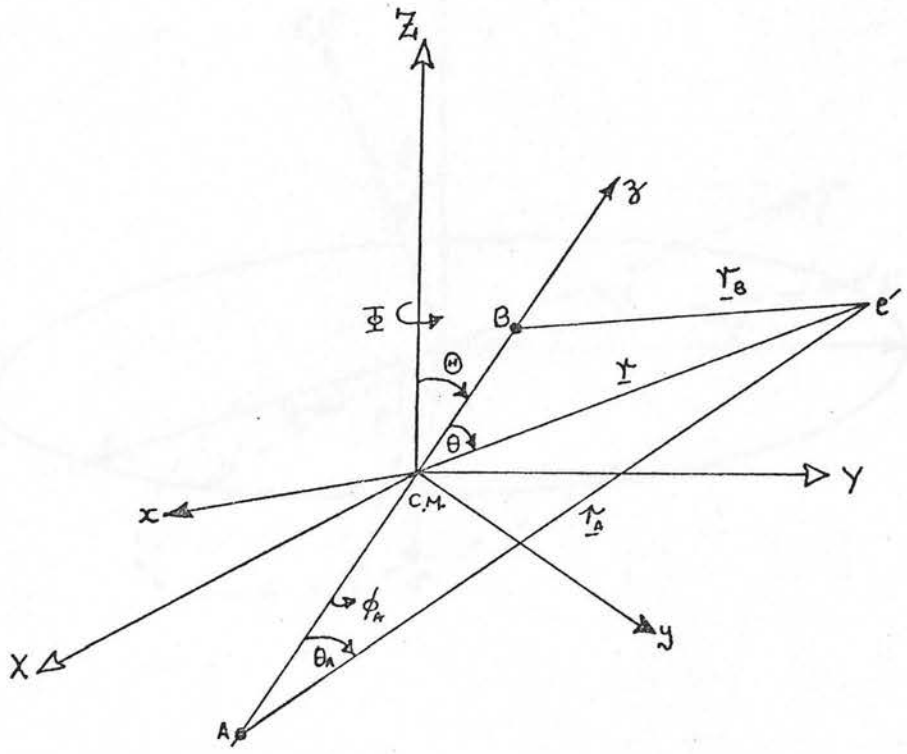

X, Y, Z, denote the axes of the space-fixed co-ordinate system.

x, y, z, are the axes of the rotating co-ordinate system.

where $\psi_{jm} = \psi_{jm}(\underline{r}_A) = \psi_{jm}(\underline{r},\underline{R})$ (see Figure 3).

Furthermore, throughout the collision, the axis of quantisation is taken to be the internuclear vector, that is, the basis is defined relative to a rotating co-ordinate system (see Figure 3). However, the operators $\partial/\partial R$ and $\partial/\partial\Theta$ in I(3.1) refer to a space-fixed system of co-ordinates. The two co-ordinate systems are related by the set of Euler angles shown in Figure 4 (EDM57). In any physical system of the atom - atom sort, only two angles

$$\Theta = \beta, \quad \Phi = \alpha \quad \text{are needed.}$$

The transformation between the ψ_{jm} in the rotating co-ordinate frame, ψ^R_{jm}, and the ψ_{jm} in the space-fixed frame, ψ^S_{jm}, is well known (ROS53):

$$\psi^R_{jm} = \Sigma_{m_1} \psi^S_{jm_1} D^j_{m_1 m}(\Phi,\Theta,O) \qquad \text{I(3.3)}$$

where $D^j_{m_1 m}(\alpha\beta\gamma)$ are the familiar rotation matrices

$$D^j_{m_1 m}(\alpha,\beta,\gamma) = e^{im_1\alpha} d^j_{m_1 m}(\beta)\, e^{im\gamma} \qquad \text{I(3.4)}$$

From I(3.3) and I(3.4) and the relationship

$$d/d\beta(d^j_{m_1 m}(\beta)) = \tfrac{1}{2}\{\left[(j-m+1)(j+m)\right]^{\frac{1}{2}} d^j_{m_1 m-1}$$

$$- \left[(j+m+1)(j-m)\right]^{\frac{1}{2}} d^j_{m_1 m+1}\}$$

it follows that

$$\partial\psi^{R}_{jm}/\partial\Theta = \tfrac{1}{2}\left[(j-m+1)(j+m)\right]^{\frac{1}{2}}\psi^{R}_{jm-1} - \tfrac{1}{2}\left[(j+m+1)(j-m)\right]^{\frac{1}{2}}\psi^{R}_{jm+1} \qquad \text{I(3.5)}$$

Finally, $\partial\psi_{jm}(\underline{r}_A)/\partial R$ and $\partial\psi_{jm}(\underline{r}_B)/\partial R$ must be evaluated.

$$x_A = x,\ y_A = y,\ z_A = z + m_B R/(m_A+m_B)$$

$$x_B = x,\ y_B = y,\ z_B = z - m_A R/(m_A+m_B)$$

where the co-ordinates x, x_A etc, are as shown in Figure 3.

It can be shown that

$$\partial f(\underline{r}_A)/\partial R = m_B/(m_A+m_B)\frac{\partial f}{\partial z}$$

and similarly that

$$\partial g(\underline{r}_B)/\partial R = -\, m_A/(m_A+m_B)\partial g/\partial z$$

Using these results, it is not difficult to demonstrate that

$$\int f^{*}(\underline{r}_A)\frac{\partial}{\partial R}g(\underline{r}_B)dr^3 = \frac{m_A}{(m_A+m_B)}\frac{\partial}{\partial R}\int f^{*}(\underline{r}_A)g(\underline{r}_B)dr^3$$

$$\int g^{*}(\underline{r}_B)\frac{\partial}{\partial R}f(\underline{r}_A)dr^3 = \frac{m_B}{(m_A+m_B)}\frac{\partial}{\partial R}\int g^{*}(\underline{r}_B)f(\underline{r}_A)dr^3 \qquad \text{I(3.6)}$$

The calculations for the process I(1.2) (i), (ii), (iii) and (iv) will now be considered in turn.

I.4 $\underline{M(^2S_{\frac{1}{2}}) + X(^1S_0) \rightleftarrows M^+(^1S_0) + X^-(^2S_{\frac{1}{2}}) \quad \text{(One-electron model)}}$

In all the calculations described, ψ_{jm} are the eigenfunctions of the total angular momentum operator, and $\chi_{M_L M_S}$ are the eigen functions of the total orbital angular momentum and spin angular momentum operators. In addition, the one electron spin-orbitals

$$S^M\{_{\beta}^{\alpha} \quad , \quad S^X\{_{\beta}^{\alpha} \quad , \quad P_m^X\{_{\beta}^{\alpha}$$

respectively denote the ns atomic orbital centred on M, the n^1s atomic orbital centred on X and the n^1p_m atomic orbital on X. α and β are the usual spin functions.

Suppose, for the sake of argument, that the system is prepared initially in a neutral state, M + X. In a one-electron treatment, the electron is supposed to be located initially on the M atom:

$$\psi_{cov} \simeq \psi_M$$

If the system emerges in the ionic state, $M^+ + X^-$ it is represented by a description in which the electron is located on the X atom:

$$\psi_{ionic} \simeq \psi_{X^-}$$

Hence the basis used was

$$\left.\begin{aligned} \psi_1 &= \psi^X_{\frac{1}{2}\frac{1}{2}} = \chi^X_{o\frac{1}{2}} \quad (L=o, S=\tfrac{1}{2}) \\ \psi_2 &= \psi^X_{\frac{1}{2}-\frac{1}{2}} = \chi^X_{o-\frac{1}{2}} \end{aligned}\right\} \text{ ionic channels}$$

$$\left.\begin{aligned} \psi_3 &= \psi^M_{\frac{1}{2}\frac{1}{2}} = \chi^M_{o\frac{1}{2}} \\ \psi_4 &= \psi^M_{\frac{1}{2}-\frac{1}{2}} = \chi^M_{o-\frac{1}{2}} \end{aligned}\right\} \text{ neutral channels} \qquad \text{I(4.1)}$$

In this basis, the overlap matrix $\underset{\sim}{S}$, is

$$\underset{\sim}{S} = \begin{vmatrix} 1 & o & x & o \\ o & 1 & o & x \\ x & o & 1 & o \\ o & x & o & 1 \end{vmatrix} \qquad x = \langle S^X | S^M \rangle \qquad \text{I(4.2)}$$

For the purpose of comparing the various models, the function

$$\varsigma = \langle \psi_{ionic} | \psi_{cov} \rangle \qquad \text{I(4.3)}$$

was assigned the same form in all the models. In equation I(4.3) ψ_{ionic} and ψ_{cov} are the wave functions for ionic and covalent states in an atomic description.

For the basis I(4.1),

$$\varsigma = \langle \psi_1 | \psi_3 \rangle = \langle \psi_2 | \psi_4 \rangle = \langle S^M | S^X \rangle$$

so that

$$x = \varsigma \qquad \text{I(4.4)}$$

Evaluating the matrix $\underset{\sim}{S}^{-1}$, making use of I(3.5) and I(3.6), the form of the matrices $\underset{\sim}{S}^{-1}\{\partial/\partial\theta\}$ and $\underset{\sim}{S}^{-1}\{\partial/\partial R\}$ was readily established:

$$\underset{\sim}{S}^{-1}\{\partial/\partial\theta\} = \begin{vmatrix} 0 & -\frac{1}{2} & 0 & 0 \\ \frac{1}{2} & 0 & 0 & 0 \\ 0 & 0 & 0 & -\frac{1}{2} \\ 0 & 0 & \frac{1}{2} & 0 \end{vmatrix} \qquad \text{I(4.4)}$$

$$\underset{\sim}{S}^{-1}\{\partial/\partial R\} = x^{1}(1-x^{2})^{-1}\begin{vmatrix} -\alpha x & 0 & \beta & 0 \\ 0 & -\alpha x & 0 & \beta \\ \alpha & 0 & -\beta x & 0 \\ 0 & \alpha & 0 & -\beta x \end{vmatrix} \qquad \text{I(4.5)}$$

where $\alpha = m_M/(m_M+m_X)$, $\beta = 1-\alpha$ and $x^1 = dx/dR$.

In all the calculations described, magnetic and relativistic terms in the Hamiltonian were ignored. Making use of the invariance of the Hamiltonian with respect to simultaneous arbitrary rotation of all electronic co-ordinates about the M-X axis, it can be shown that the only non-vanishing matrix elements of the Hamiltonian, H, are:

$$H_{11} = H_{22} \; ; \; H_{33} = H_{44} \; ; \; H_{13} = H_{31} \quad H_{24} = H_{42} = H$$

Hence it is trivial to show that the matrix $\underset{\sim}{S}^{-1}\{H\}$ is given by

$$\underset{\sim}{S}^{-1}\{H\} = (1-x^{2})^{-1}\begin{vmatrix} (H_{11}-xH) & 0 & (H-xH_{33}) & 0 \\ 0 & (H_{11}-xH) & 0 & (H-xH_{33}) \\ (H-xH_{11}) & 0 & (H_{33}-xH) & 0 \\ 0 & (H-xH_{11}) & 0 & (H_{33}-xH) \end{vmatrix}$$

I(4.6)

Throughout these calculations, for the purpose of comparing one model with another, corresponding matrix elements of the Hamiltonian were assigned the same functional form in all models (see § I.9).

The quantum states of M and X were taken to be defined relative to a space-fixed axis of quantisation at $R = \infty$. In what follows, R_o is chosen so that coupling due to the Hamiltonian is negligible for R greater than R_o, so that, in this region, pure rotation only is taking place. Hence, if the quantum states of M and X defined relative to the space-fixed axis of quantisation, at $R = \infty$ are denoted by the quantum numbers $j^M m_j^M$ and $j^X m_j^X$, then for $R \geq R_o$, the quantum states of M and X relative to the same axis of quantisation are denoted by the same quantum numbers. For $R \geq R_o$, the quantum states of M and X, ψ^R_{jm}, defined relative to the rotating interparticle vector as quantisation axis are defined by the relation

$$\psi^R_{jm} = \Sigma_m D^j_{m_1 m}(\Phi,\Theta,o)\,\psi_{jm'} \qquad \text{I(4.7)}$$

and $\Phi \equiv o$.

Hence

$$|\psi^X_{\frac{1}{2}\frac{1}{2}}\ \psi^X_{\frac{1}{2}-\frac{1}{2}}\ \psi^M_{\frac{1}{2}\frac{1}{2}}\ \psi^M_{\frac{1}{2}-\frac{1}{2}}>^R = |\psi^X_{\frac{1}{2}\frac{1}{2}}\ \psi^X_{\frac{1}{2}-\frac{1}{2}}\ \psi^M_{\frac{1}{2}\frac{1}{2}}\ \psi^M_{\frac{1}{2}-\frac{1}{2}}>D(\Theta) \qquad \text{I(4.8)}$$

figure 5

Co-ordinate System for Initial and Final Free Rotation

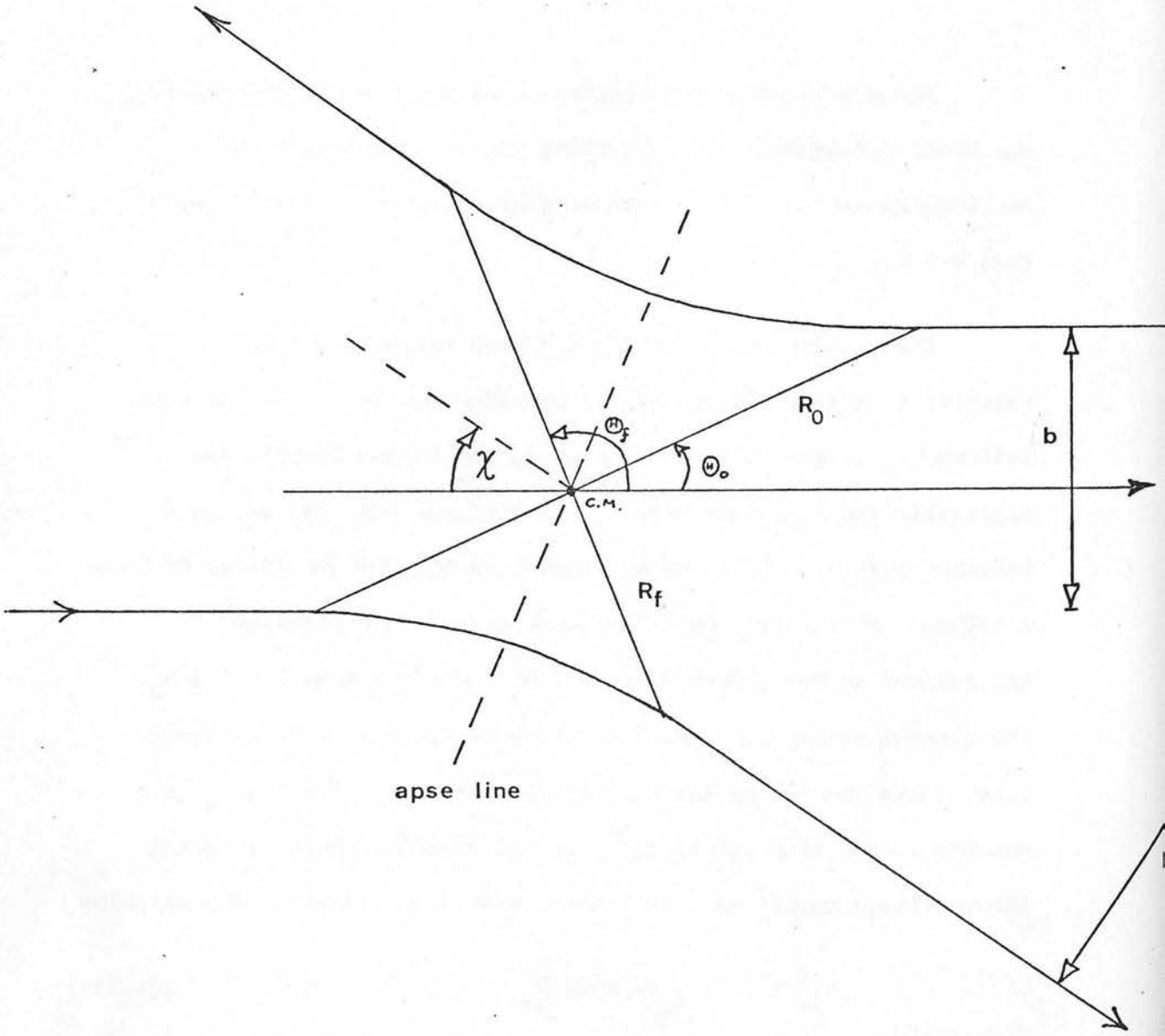

The CM angle of deflection, χ, is given by

$$\chi = \pi - \left[\Theta_f + \sin^{-1}(b/R_f)\right]$$

where

I(4.8)

$$D(\theta) = \begin{vmatrix} d^{\frac{1}{2}}_{\frac{1}{2}\frac{1}{2}} & d^{\frac{1}{2}}_{\frac{1}{2}-\frac{1}{2}} & 0 & 0 \\ d^{\frac{1}{2}}_{-\frac{1}{2}\frac{1}{2}} & d^{\frac{1}{2}}_{-\frac{1}{2}-\frac{1}{2}} & 0 & 0 \\ 0 & 0 & d^{\frac{1}{2}}_{\frac{1}{2}\frac{1}{2}} & d^{\frac{1}{2}}_{\frac{1}{2}-\frac{1}{2}} \\ 0 & 0 & d^{\frac{1}{2}}_{-\frac{1}{2}\frac{1}{2}} & d^{\frac{1}{2}}_{-\frac{1}{2}-\frac{1}{2}} \end{vmatrix} = \begin{vmatrix} C & -S & 0 & 0 \\ S & C & 0 & 0 \\ 0 & 0 & C & -S \\ 0 & 0 & S & C \end{vmatrix}$$

(see I(3.3) and I(3.4)) where $C = \cos \theta/2$, $S = \sin \theta/2$. Consider the inward part of the trajectory from $R = \infty \rightarrow R = R_o$ (see Figure 5).

At $R = R_o$, $\theta = \theta_o$, $t = t_o$,

and $\Psi(t_o) = |\psi\rangle^R \underset{\sim}{a}(t_o) = |\psi\rangle \underset{\sim}{D}(\theta_o)\, \underset{\sim}{a}(t_o)$

where $\underset{\sim}{a}$ is the vector of amplitudes of the states defined relative to a rotating axis of quantisation.

And $\Psi(t_o) = |\psi\rangle\, \underset{\sim}{b}(t_o)$

where $\underset{\sim}{b}(t_o)$ is the vector of the amplitudes of the states defined relative to space-fixed axes, and $\underset{\sim}{b}(t_o) \equiv \underset{\sim}{b}_o$, where $\underset{\sim}{b}_o$ is the initial vector at $R = \infty$.

Hence $\underset{\sim}{a}(t_o) = \underset{\sim}{D}^{-1}(\theta_o)\, \underset{\sim}{b}_o$ I(4.9)

Now consider the outward part of the trajectory from $R = R_o \rightarrow R = \infty$.

At $R = R_o$, $\Theta = \Theta_f$, $t = t_f$, and

$$\underset{\sim}{b}(t_f) = \underset{\sim}{b}_f = \underset{\sim}{D}(\Theta_f)\ \underset{\sim}{a}(t_f) \qquad \text{I(4.10)}$$

where $\underset{\sim}{b}_f$ is the final vector of amplitudes at $R = \infty$

I.5 $M(^2S_{\frac{1}{2}}) + X(^1S_o) \rightleftarrows M^+ + X^-(^2P_{3/2})$ (One-Electron Model)

The basis used was

$$\left.\begin{aligned}
\psi_1 &= \psi^X_{3/2\,3/2} = \chi^X_{1\frac{1}{2}} \quad (L=1,\ S=\tfrac{1}{2}) \\
\psi_2 &= \psi^X_{3/2\,\frac{1}{2}} = (1/\sqrt{3})(\chi^X_{1-\frac{1}{2}} + \sqrt{2}\chi^X_{o\frac{1}{2}}) \\
\psi_3 &= \psi^X_{3/2-\frac{1}{2}} = (1/\sqrt{3})(\chi^X_{-1\frac{1}{2}} + \sqrt{2}\chi^X_{o-\frac{1}{2}}) \\
\psi_4 &= \psi^X_{3/2-3/2} = \chi^X_{-1-\frac{1}{2}}
\end{aligned}\right\} \text{ ionic channels} \qquad \text{I(5.1)}$$

$$\left.\begin{aligned}
\psi_5 &= \psi^M_{\frac{1}{2}\frac{1}{2}} = \chi^M_{o\frac{1}{2}} \quad (L=o,\ S=\tfrac{1}{2}) \\
\psi_6 &= \psi^M_{\frac{1}{2}-\frac{1}{2}} = \chi^M_{o-\frac{1}{2}}
\end{aligned}\right\} \text{ Neutral channels}$$

The matrices $\underset{\sim}{S}$, $\underset{\sim}{S}^{-1}\{\partial/\partial\Theta\}$, $\underset{\sim}{S}^{-1}\{\partial/\partial R\}$ and $\underset{\sim}{S}^{-1}\{H\}$ are presented in Appendix I.

figure 6

Correlation diagram for $M(^2S_{\frac{1}{2}}) + X(^1S_o) \rightleftarrows M^+(^1S_o) + X^-(^2P_{3/2})$

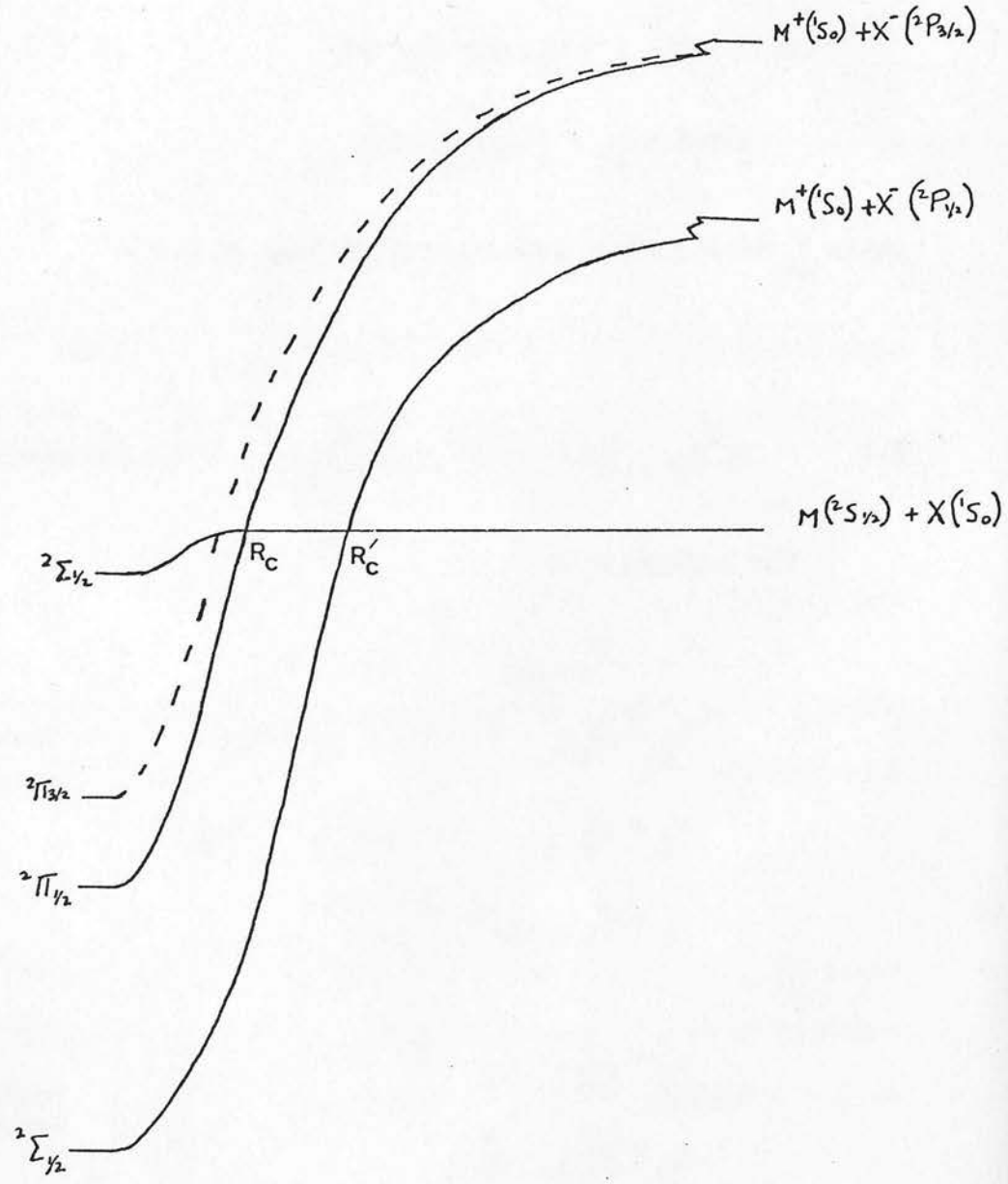

The valence-shell electron configuration of the two atoms were taken to be $M(ns)^1$, $X(n^1s)^2$, and making the assumptions described in §I.1, the correlation diagram is as shown in Figure 6. Provided the fine-structure splitting in the X^- ion is quite large, R_c and R_c^1 may be sufficiently widely separated that the two crossings may be treated separately in a semi-classical analysis. It is assumed here that this is the case.

The initial vector of amplitudes of states defined relative to a rotating axis at $R = R_o$, $\underset{\sim}{a}(t_o)$, and the final vector of amplitudes of states defined relative to space-fixed axes at $R = \infty$, $\underset{\sim}{b}_f$, are given by equations I(4.9) and I(4.10) and $D(\theta)$ is presented in Appendix 1.

I.6 $\underline{M(^2S_{\frac{1}{2}}) + X(^2S_{\frac{1}{2}}) \rightleftharpoons M^+(^1S_o) + X^-(^1S_o)}$ (Two electron model)

For this calculation a 'molecular' basis, ϕ, was used since the various coupling matrices are more clearly diagonalised in this basis.

$$\phi_1 = (1/\sqrt{2})\{s^M(1)s^X(2) - s^M(2)s^X(1)\}\alpha(1)\alpha(2)$$
$$\phi_2 = (1/\sqrt{2})\{s^M(1)s^X(2) - s^M(2)s^X(1)\}\tfrac{1}{\sqrt{2}}\{\alpha(1)\beta(2) + \alpha(2)\beta(1)\}$$ neutral $^3\Sigma$ channel
$$\phi_3 = (1/\sqrt{2})\{s^M(1)s^X(2) - s^M(2)s^X(1)\}\beta(1)\beta(2)$$

$$\phi_4 = (1/\sqrt{2})\{s^M(1)s^X(2) + s^M(2)s^X(1)\}(1/\sqrt{2})\{\alpha(1)\beta(2) - \alpha(2)\beta(1)\}$$ neutral $^1\Sigma$ channel

$$\phi_5 = (1/\sqrt{2})s^X(1)s^X(2)\{\alpha(1)\beta(2) - \alpha(2)\beta(1)\}$$ ionic channel

where S^M is an atomic s orbital centred on atom M, and α and β are the spin functions $s = \frac{1}{2}$, $m_s = +\frac{1}{2}$, $s = \frac{1}{2}$, $m_s = -\frac{1}{2}$ respectively. This molecular basis is related to an atomic basis (a description more appropriate to a scattering experiment) as follows:

$$\begin{aligned}
\phi_1 &= |\tfrac{1}{2},\tfrac{1}{2}| = \psi_1 \\
\phi_2 &= (1/\sqrt{2})(|\tfrac{1}{2},-\tfrac{1}{2}| + |-\tfrac{1}{2},\tfrac{1}{2}|) = (1/\sqrt{2})(\psi_2 + \psi_3) \\
\phi_3 &= |-\tfrac{1}{2},-\tfrac{1}{2}| = \psi_4 \\
\phi_4 &= (1/\sqrt{2})(|\tfrac{1}{2},-\tfrac{1}{2}| - |-\tfrac{1}{2},\tfrac{1}{2}|) = (1/\sqrt{2})(\psi_2 - \psi_3) \\
\phi_5 &= |\tfrac{1}{2},-\tfrac{1}{2}|^X = \psi_5
\end{aligned} \qquad \text{I(6.2)}$$

where $|m_1,m_2| = (\frac{1}{\sqrt{2}})(\psi^M_{j_1m_1}(1)\psi^X_{j_2m_2}(2) - \psi^M_{j_1m_1}(2)\psi^X_{j_2m_2}(1))\, j_1=j_2=\frac{1}{2}$

and $|m_1,m_2|^X = (1/\sqrt{2})(\psi^X_{j_1m_1}(1)\psi^X_{j_2m_2}(2) - \psi^X_{j_1m_1}(2)\psi^X_{j_2m_2}(1))$

The matrices $\underset{\sim}{S}$, $\underset{\sim}{S}^{-1}\{\partial/\partial R\}$, $\underset{\sim}{S}^{-1}\{\partial/\partial\Theta\}$ and $\underset{\sim}{S}^{-1}\{H\}$ are presented in Appendix II.

Since a molecular basis has been used, equations I(4.9) and I(4.10) cannot be used unmodified to describe pure rotation of the system.

In vector notation, the basis $|\Psi\rangle^R$, may be written

$$|\Psi\rangle^R = (1/\sqrt{2})|\Psi\rangle^R_a + (1/\sqrt{2})|\Psi\rangle^R_b \qquad \text{I(6.3)}$$

In the case of the present basis,

$$|\Psi\rangle_a^R = |(1/\sqrt{2})\psi_1\ \psi_3\ (1/\sqrt{2})\psi_4\ \psi_2\ (1/\sqrt{2})\psi_5\rangle$$

and

$$|\Psi\rangle_b^R = |(1/\sqrt{2})\psi_1\ \psi_2\ (1/\sqrt{2})\psi_4\ -\psi_3\ (1/\sqrt{2})\psi_5\rangle$$

It follows from I(6.3) that

$$|\Psi\rangle^R \underset{\sim}{a} = (1/\sqrt{2})|\Psi\rangle_a \underset{\sim}{b}^a + (1/\sqrt{2})|\Psi\rangle_b \underset{\sim}{b}^b$$

where

$$\underset{\sim}{b}^a = \underset{\sim}{D}^a(\Theta)\ \underset{\sim}{a} \qquad \text{I(6.4)}$$

and

$$\underset{\sim}{b}^b = \underset{\sim}{D}^b(\Theta)\ \underset{\sim}{a} = (\underset{\sim}{D}^b\ \underset{\sim}{D}^{a\,-1})\ \underset{\sim}{b}^a$$

define the amplitudes of the j, m_j states of M and X relative to a space-fixed axis of quantisation.

Now, ψ_5 can be written

$$\psi_5 = f^X(1,2)\ \xi^R(1,2)$$

where $f^X(1,2)$ is not affected by rotation of the axis of quantisation and

$$\xi^R(1,2) = \alpha(1)\ \beta(2) - \alpha(2)\ \beta(1)$$

It is not difficult to show that $\xi^R(1,2)$ is invariant under axis rotation. Making use of this result, and substituting from the various $d^j_{m_1 m}$, the matrices $\underset{\sim}{D}^a(\Theta)$ and $\underset{\sim}{D}^b(\Theta)$ were evaluated and are presented in Appendix II.

In what follows, p(n) is the probability of finding the system in state ψ_n, where ψ_n is now defined relative to a space-fixed axis of quantisation.

$$p(1) = (1/4)|b_1^a + b_1^b|^2$$

$$p(2) = (1/2)|b_4^a + b_2^b|^2$$

$$p(3) = (1/2)|b_2^a - b_4^b|^2 \qquad \text{I(6.5)}$$

$$p(4) = (1/4)|b_3^a + b_3^b|^2$$

$$p(5) = (1/4)|b_5^a + b_5^b|^2$$

Noting that $\underset{\sim}{b}^b = \underset{\sim}{D}\,\underset{\sim}{b}^a$, $\underset{\sim}{D} = \underset{\sim}{D}^b\,\underset{\sim}{D}^{a\,-1}$ (I(6.4)), defining $p_n^o = p(n)$ at $R = \infty$ initially, and assuming that b_i^a are real initially, it follows that

$$\underset{\sim}{R}(\theta_o)\,\underset{\sim}{b}^a = \underset{\sim}{Q}^o \qquad \text{I(6.6)}$$

For the present basis,

$$\underset{\sim}{R}(\theta_o) = \begin{vmatrix} (1+D_{11}) & D_{12} & D_{13} & D_{14} & D_{15} \\ D_{21} & D_{22} & D_{23} & (1+D_{24}) & D_{25} \\ -D_{41} & (1-D_{42}) & -D_{43} & -D_{44} & -D_{45} \\ D_{31} & D_{32} & (1+D_{33}) & D_{34} & D_{35} \\ D_{51} & D_{52} & D_{53} & D_{54} & (1+D_{55}) \end{vmatrix} \qquad \text{I(6.7)}$$

$$\text{and} \quad \underset{\sim}{Q}^{o} = \begin{vmatrix} 2(p_1^o)^{\frac{1}{2}} \\ 2(p_2^o)^{\frac{1}{2}} \\ 2(p_3^o)^{\frac{1}{2}} \\ 2(p_4^o)^{\frac{1}{2}} \\ 2(p_5^o)^{\frac{1}{2}} \end{vmatrix} \qquad \text{I(6.8)}$$

Equation I(6.6) is more usefully written as

$$\underset{\sim}{b}^{a} = \underset{\sim}{R}^{-1}_{(\theta_o)} \underset{\sim}{Q}^{o} \qquad \text{I(6.9)}$$

Hence the initial vector of amplitudes of states defined relative to a rotating axis at $R = R_o$, $\underset{\sim}{a}(t_o)$, is given by

$$\underset{\sim}{a}(t_o) = \underset{\sim}{D}^{a\,-1}(\theta_o)\, \underset{\sim}{b}^{a} \qquad \text{I(6.10)}$$

where $\underset{\sim}{b}^{a}$ is determined by I(6.9), and the final vector of amplitudes of states defined relative to space-fixed axes at $R = \infty$, $\underset{\sim}{b}_f$, is given by

$$\underset{\sim}{b}^{a}_f = \underset{\sim}{D}^{a}(\theta_f)\, \underset{\sim}{a}(t_f)$$

$$\underset{\sim}{b}^{b}_f = \underset{\sim}{D}^{b}(\theta_f)\, \underset{\sim}{a}(t_f) \qquad \text{I(6.11)}$$

The final transition probabilities can be calculated by substituting the results of I(6.11) in I(6.5).

I.7 $\underline{M(^2S_{\frac{1}{2}}) + X(^2P_{3/2}) \rightleftarrows M^+(^1S_o) + X^-(^1S_o)}$ (Two-electron Model)

The choice of basis (a molecular basis) which block diagonalises the overlap matrix is

$$\phi_1 = (1/\sqrt{2})(\psi_7 - \psi_8) \quad |\Omega| = o \qquad \psi_1 = |3/2, \tfrac{1}{2}|$$

$$\phi_2 = (1/\sqrt{2})(\psi_1 - \psi_6) \quad |\Omega| = 2 \qquad \psi_2 = |3/2, -\tfrac{1}{2}|$$

$$\phi_3 = (1/\sqrt{2})(\psi_2 + \psi_5) \quad |\Omega| = 1 \qquad \psi_3 = |\tfrac{1}{2}, \tfrac{1}{2}|$$

$$\phi_4 = (1/\sqrt{2})(\psi_3 + \psi_4) \quad |\Omega| = 1 \qquad \psi_4 = |-\tfrac{1}{2}, -\tfrac{1}{2}|$$

$$\phi_5 = \psi_9 = \psi^{X^-}_{oo} \text{ (ionic channel)} \Omega = o \qquad \psi_5 = |-3/2, \tfrac{1}{2}| \qquad \text{I(7.1)}$$

$$\phi_6 = (1/\sqrt{2})(\psi_3 - \psi_4) \quad |\Omega| = 1 \qquad \psi_6 = |-3/2, -\tfrac{1}{2}|$$

$$\phi_7 = (1/\sqrt{2})(\psi_7 + \psi_8) \quad |\Omega| = o \qquad \psi_7 = |\tfrac{1}{2}, -\tfrac{1}{2}|$$

$$\phi_8 = (1/\sqrt{2})(\psi_1 + \psi_6) \quad |\Omega| = 2 \qquad \psi_8 = |-\tfrac{1}{2}, \tfrac{1}{2}|$$

$$\phi_9 = (1/\sqrt{2})(\psi_2 - \psi_5) \quad |\Omega| = 1$$

where $|m_1 m_2| = (1/\sqrt{2})\ (\psi^X_{j_1 m_1}(1)\ \psi^M_{j_2 m_2} - \psi^X_{j_1 m_1}(2)\ \psi^M_{j_2 m_2}(1))$

$$j_1 = 3/2,\ j_2 = \tfrac{1}{2}$$

and $\psi^{X^-}_{oo} = (1/\sqrt{3})(|x^X_{1\frac{1}{2}}, x^X_{-1}{}_{-\frac{1}{2}}| - |x^X_{1-\frac{1}{2}} x^X_{-1\frac{1}{2}}| - |x^X_{o\frac{1}{2}}, x^X_{o-\frac{1}{2}}|)$ is the wave function of a state of X^- with $L=S=M_L=M_S=o$

TABLE 1

The Molecular Basis in Terms of Atomic Orbitals

$$\phi_1 = (1/\sqrt{12})\{\left[p_1^x(1)s^M(2)-p_1^x(2)s^M(1)\right]\beta(1)\beta(2)-\left[p_{-1}^x(1)s^M(2)-p_{-1}^x(2)s^M(1)\right]\alpha(1)\alpha(2)+\sqrt{2}\left[p_o^x(1)s^M(2)+p_o^x(2)s^M(1)\right]$$
$$\left[\alpha(1)\beta(2)-\alpha(2)\beta(1)\right]\}$$

$$\phi_2 = (1/2)\{\left[p_1^x(1)s^M(2)-p_1^x(2)s^M(1)\right]\alpha(1)\alpha(2)-\left[p_{-1}^x(1)s^M(2)-p_{-1}^x(2)s^M(1)\right]\beta(1)\beta(2)\}$$

$$\phi_3 = (1/2)\{\left[p_1^x(1)s^M(2)-p_{-1}^x(2)s^M(1)\right]\alpha(1)\beta(2)+\left[p_{-1}^x(1)s^M(2)-p_1^x(2)s^M(1)\right]\alpha(2)\beta(1)\}$$

$$\phi_4 = (1/\sqrt{12})\{\sqrt{2}\left[p_o^x(1)s^M(2)-p_o^x(2)s^M(1)\right]\left[\alpha(1)\alpha(2)+\beta(1)\beta(2)\right]+\left[p_1^x(1)s^M(2)-p_{-1}^x(2)s^M(1)\right]\alpha(2)\beta(1)-\left[p_1^x(2)s^M(1)$$
$$-p_{-1}^x(1)s^M(2)\right]\alpha(1)\beta(2)\}$$

$$\phi_5 = (1/\sqrt{6})\left[p_1^x(1)p_{-1}^x(2)+p_1^x(2)p_{-1}^x(1)-p_o^x(1)p_o^x(2)\right]\left[\alpha(1)\beta(2)-\alpha(2)\beta(1)\right]$$

$$\phi_6 = (1/\sqrt{12})\{\sqrt{2}\left[p_o^x(1)s^M(2)-p_o^x(2)s^M(1)\right]\left[\alpha(1)\alpha(2)-\beta(1)\beta(2)\right]+\left[p_1^x(1)s^M(2)+p_{-1}^x(2)s^M(1)\right]\alpha(2)\beta(1)-\left[p_1^x(2)s^M(1)$$
$$+p_{-1}^x(1)s^M(2)\right]\alpha(1)\beta(2)\}$$

$$\phi_7 = (1/\sqrt{12})\{\left[p_1^x(1)s^M(2)-p_1^x(2)s^M(1)\right]\beta(1)\beta(2)+\left[p_{-1}^x(1)s^M(2)-p_{-1}^x(2)s^M(1)\right]\alpha(1)\alpha(2)+\sqrt{2}\left[p_o^x(1)s^M(2)-p_o^x(2)s^M(1)\right]$$
$$\left[\alpha(1)\beta(2)+\alpha(2)\beta(1)\right]\}$$

$$\phi_8 = (1/2)\{\left[p_1^x(1)s^M(2)-p_1^x(2)s^M(1)\right]\alpha(1)\alpha(2)+\left[p_{-1}^x(1)s^M(2)-p_{-1}^x(2)s^M(1)\right]\beta(1)\beta(2)\}$$

$$\phi_9 = (1/2)\{\left[p_1^x(1)s^M(2)+p_{-1}^x(2)s^M(1)\right]\alpha(1)\beta(2)-\left[p_{-1}^x(1)s^M(2)+p_1^x(2)s^M(1)\right]\alpha(2)\beta(1)\}$$

To see which functions (if any) represent singlet and which represent triplet molecular states, it is convenient to decompose the functions ϕ_n into atomic spin-orbitals by expanding the various determinants, making use of I(5.1) to express the ψ_{jm} eigen functions in terms of the $\chi_{M_L M_S}$ eigen functions. The ϕ_n are listed in terms of atomic orbitals in Table 1 from which it can be seen that only ϕ_2 ϕ_7 and ϕ_8 (triplet states) and ϕ_5 (singlet) are eigen functions of the total spin operator.

The matrices $\underset{\sim}{S}$, $\underset{\sim}{S}^{-1}\{\partial/\partial\Theta\}$, $\underset{\sim}{S}^{-1}\{\partial/\partial R\}$ and $\underset{\sim}{S}^{-1}\{H\}$ are presented in Appendix III.

The valence-shell electron configurations of the two atoms were taken to be $M(ns)^1$, $X(ns)^2$ $(n^1p)^5$ (as in the halogens) to ensure that $M(^2S_{\frac{1}{2}}) + X(^2P_{\frac{1}{2}})$ lies higher in energy than $M(^2S_{\frac{1}{2}}) + X(^2P_{3/2})$.

In this description the diabatic correlation diagram is as shown in Figure 1, and it is again assumed that the two crossings may be treated separately.

Proœeding as in § I.6, the initial vector of amplitudes of states defined relative to a rotating axis of quantisation at $R = R_o$, $\underset{\sim}{a}(t_o)$ is given by

$$\underset{\sim}{a}(t_o) = \underset{\sim}{D}^{a^{-1}}(\Theta_o)\ \underset{\sim}{b}^{a} \qquad \text{(I(6.10))}$$

where $\underset{\sim}{b}^{a} = \underset{\sim}{R}(\Theta_o)\ \underset{\sim}{Q}^{o}$ and $\underset{\sim}{R}(\Theta_o)$, $\underset{\sim}{D}(\Theta_o)$ and $\underset{\sim}{Q}^{o}$ are presented in Appendix III.

The final vector of amplitudes of states defined relative to space-fixed axes at $R = \infty$, b_f is given by I(6.11), and the final transition probabilities in the atomic basis can be calculated by substituting the results of I(6.11) in

$$p(1) = \tfrac{1}{2}|b_2^a + b_8^b|^2$$

$$p(2) = \tfrac{1}{2}|b_9^a + b_3^b|^2$$

$$p(3) = \tfrac{1}{2}|b_6^a + b_4^b|^2$$

$$p(4) = \tfrac{1}{2}|b_4^a - b_6^b|^2$$

$$p(5) = \tfrac{1}{2}|b_3^a - b_9^b|^2$$

$$p(6) = \tfrac{1}{2}|b_8^a - b_2^b|^2$$

$$p(7) = \tfrac{1}{2}|b_1^a + b_7^b|^2$$

$$p(8) = \tfrac{1}{2}|b_7^a - b_1^b|^2$$

$$p(9) = \tfrac{1}{4}|b_5^a + b_5^b|^2$$

I.8 Two-state Approximation, Coupling via Hamiltonian only

As was noted in § I.1, the ionic-neutral curve-crossing situation is usually described in terms of a Landau-Zener or Landau-Zener Stueckelberg model. Since it is of interest to compare the present calculations with such models, a brief description of one such model is relevant here.

It is assumed that an expansion of the wave function in two diabatic states ϕ_1 (neutral) and ϕ_2 (ionic) provides an adequate description of the system. Inherent in the assumption is the idea that the basic problem is preserved if the manifold of (closely spaced) neutral states is replaced by a single neutral state. In addition, either ϕ_1 and ϕ_2 are so chosen that, to a good approximation, the basis is orthogonal ($\underset{\sim}{S} = \underset{\sim}{I}$) and time independent ($\{\partial/\partial t \equiv \underset{\sim}{o}$) or it is assumed that the effect of including the non orthogonality and time dependence of the basis is negligible. Under these conditions, the system of coupled equations I(2.7) reduces to

$$\begin{pmatrix} \dot{a}_1 \\ \dot{a}_2 \end{pmatrix} = \frac{-i}{\hbar} \begin{pmatrix} H_{11} & H_{12} \\ H_{12} & H_{22} \end{pmatrix} \begin{pmatrix} a_1 \\ a_2 \end{pmatrix} \qquad \text{I(8.1)}$$

The equations I(8.1) can be solved numerically or by approximation. The numerical solution will be discussed in § I.10.

Defining

$$a_n = C_n \exp\left[-(i/\hbar)\int H_{nn}\,dt\right] \qquad \text{I(8.2)}$$

figure 7

Crossing of two diabatic potential curves.

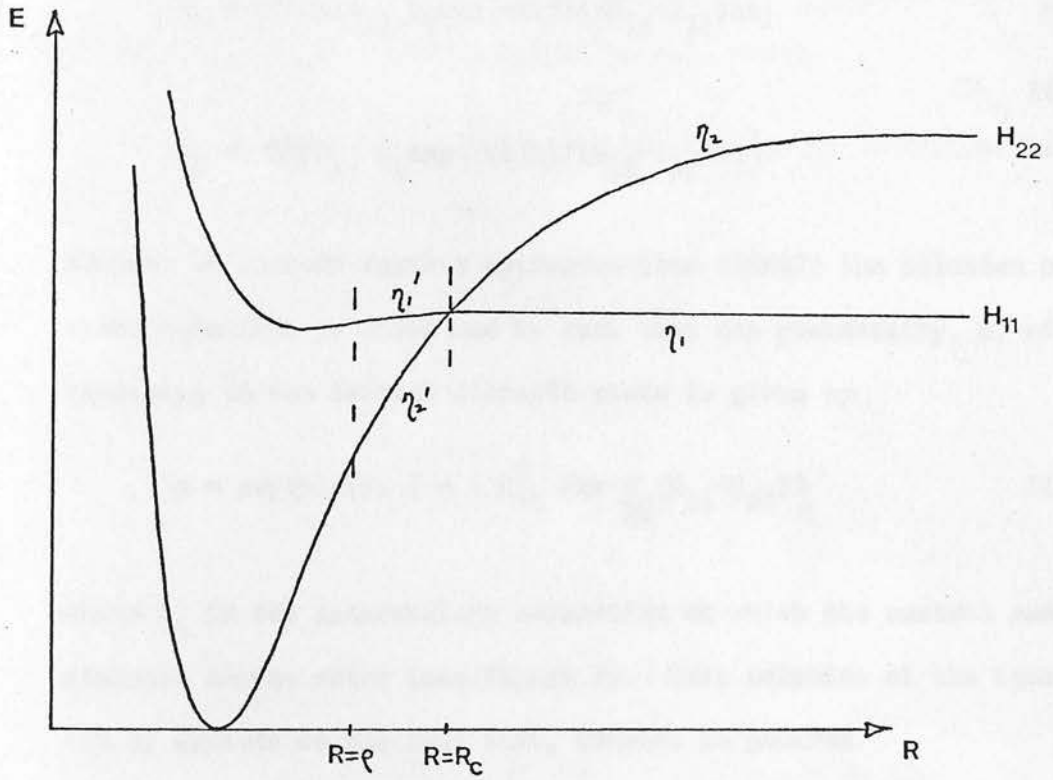

H_{11} (covalent) and H_{22} (ionic) are two diabatic potential curves. η_1 is the phase shift associated with motion along H_{11} from $R = \infty \rightarrow R_c$, η_2 is the phase shift associated with motion along H_{22} from $R = \infty \rightarrow R_c$, η_1' and η'_2 are defined analogously in the region $R = R_c \rightarrow \rho$.

equations I(8.1) may be written

$$\dot{c}_1 = -(i/\hbar)H_{12}\, c_2 \exp\left[-(i/\hbar)\int(H_{22}-H_{11})dt\right]$$

$$\dot{c}_2 = -(i/\hbar)H_{12}\, c_1 \exp\left[-(i/\hbar)\int(H_{11}-H_{22})dt\right] \qquad \text{I(8.3)}$$

Subject to certain further approximations (ZEN32) the solution of these equations is known and is such that the probability, p, of remaining in the initial diabatic state is given by

$$p = \exp(-2\pi\bar{\gamma}),\ \bar{\gamma} = \left\{ H_{12}^2 / \hbar v \frac{d}{dR}(H_{11}-H_{22}) \right\}_{R_c} \qquad \text{I(8.4)}$$

where R_c is the internuclear separation at which the neutral and ionic diabatic curves cross (see Figure 7). This solution of the equations I(8.3) depends on the fact that, whereas in general

$$\exp\left[-(i/\hbar)\int(H_{22}-H_{11})dt\right]$$

is a rapidly oscillating function of t (or R), so that changes in $|c_1|$ and $|c_2|$ are very slight, the time around which $R \approx R_c$ is a region of stationary phase in which there are significant changes in $|c_1|$ and $|c_2|$ (depending on the magnitude of H_{12}).

Consider the system semiclassically and suppose the crossing is approached in channel 2. After the crossing, there is amplitude both in channel 1 and channel 2. When the crossing is approached for the second time, there is both amplitude and phase in channels 1 and 2 and the phase difference must be taken into account in calculating the amplitudes in the two channels after the second crossing.

This analysis only applies, of course, when the distance of closest approach, ρ, is less than R_c. When ρ is greater than R_c, no transitions are possible according to this model.

It is assumed then, that the solution of the equations I(8.3) can be divided into four regions:

a. Inward half of the trajectory $\dot{R} < o$

Define an amplitude vector

$$\underset{\sim}{A}(t) = \begin{Bmatrix} a_1(t) \\ a_2(t) \end{Bmatrix}$$

i. $t = t_c = t(R_c)$

$$\underset{\sim}{A}(t_c) = \underset{\sim}{\Phi}_1 \underset{\sim}{A}(-\infty)$$

$$\underset{\sim}{\Phi}_1 = \begin{Bmatrix} \exp(-i\eta_1) & o \\ o & \exp(-i\eta_2) \end{Bmatrix} \qquad \eta_n = \int_{-\infty}^{t_c} H_{nn}\, dt$$

ii. $t = t_\rho = t(R = \rho)$

$$A(t_\rho) = \underset{\sim}{\Phi}_2 \underset{\sim}{B} \underset{\sim}{\Phi}_1 \underset{\sim}{A}(-\infty)$$

$$\underset{\sim}{B} = \begin{Bmatrix} a\, p^{\frac{1}{2}} & b(1-p)^{\frac{1}{2}} \\ c(1-p)^{\frac{1}{2}} & d\, p^{\frac{1}{2}} \end{Bmatrix}, \qquad \underset{\sim}{\Phi}_2 = \begin{Bmatrix} \exp(-i\eta_1^1) & o \\ o & \exp(-i\eta_2^1) \end{Bmatrix}$$

$$\eta_n^1 = \int_{t_c}^{t_\rho} H_{nn}\, dt$$

b. Outward half of the trajectory, $\dot{R} > 0$

iii. $t = t_c^1 = t(R_o)$

$$\underset{\sim}{A}(t_c^1) = (\underset{\sim}{\Phi}_2 \; \underset{\sim}{\Phi}_2 \; \underset{\sim}{B} \; \underset{\sim}{\Phi}_1) \; \underset{\sim}{A}(-\infty)$$

iv. $t = \infty$

$$\underset{\sim}{A}(\infty) = \underset{\sim}{S} \; \underset{\sim}{A}(-\infty)$$

$$\underset{\sim}{S} = (\underset{\sim}{\Phi}_1 \; \underset{\sim}{B}^* \; \underset{\sim}{\Phi}_2 \; \underset{\sim}{\Phi}_2 \; \underset{\sim}{B} \; \underset{\sim}{\Phi}_1)$$

$$\underset{\sim}{B}^* = \begin{Bmatrix} a^* p^{\frac{1}{2}} & b^*(1-p)^{\frac{1}{2}} \\ c^*(1-p)^{\frac{1}{2}} & d^* p^{\frac{1}{2}} \end{Bmatrix} \quad \text{(* does not denote complex conjugate)}$$

It is not difficult to show that the $\underset{\sim}{S}$ matrix is given by

$$\underset{\sim}{S} = \begin{vmatrix} aa^* p e^{-2i(\eta_1+\eta_1^1)} + b^* c(1-p) e^{-2i(\eta_1+\eta_2^1)} & p(1-p)^{\frac{1}{2}} a^* b e^{-i(\eta_1+\eta_2+2\eta_1^1)} \\ & \quad + b^* d e^{-i(\eta_1+\eta_2+2\eta_2^1)} \\ p(1-p)^{\frac{1}{2}} a c^* e^{-i(\eta_1+\eta_2+2\eta_1^1)} + c d^* e^{-i(\eta_1+\eta_2+2\eta_2^1)} & dd^* p e^{-2i(\eta_2+\eta_2^1)} \\ & \quad + bc^*(1-p) e^{-2i(\eta_2+\eta_1^1)} \end{vmatrix}$$

The matrix $\underset{\sim}{S}$ must be such that the system is microscopically reversible and probability is conserved.

If the phase factors a, b, c and d are defined as

$a = e^{i\alpha}$, $a^* = e^{i\alpha^*}$ etc., the conditions for microscopic reversibility and conservation of probability are found to be

$$\left.\begin{array}{l} \alpha - \beta - \gamma + \delta = \pi \\ \\ \alpha^* - \beta^* - \gamma^* + \delta^* = \pi \end{array}\right\} \qquad \text{I(8.5)}$$

One choice of α, α^* which satisfies equations I(8.5), and leads to the result derived from a more rigorous analysis due to Stueckelberg (STU32, RAA73) is

$$\alpha = \alpha^* = \delta = \delta^* = o$$

$$\beta = \xi, \quad \gamma = -\pi - \xi \qquad \text{I(8.6)}$$

$$\beta^* = -\pi - \xi$$

$$\gamma^* = \xi$$

and $\underset{\sim}{S}$ is given by

$$\begin{aligned} S_{11} &= pe^{-2i(\eta_1+\eta_1^1)} + (1-p)\, e^{-2i(\eta_1+\eta_2^1+\xi)} \\ S_{12} &= \left[p(1-p)\right]^{\frac{1}{2}}\left\{e^{-i(\eta_1+\eta_2+2\eta_1^1-\xi)} - e^{-i(\eta_1+\eta_2+2\eta_2^1+\xi)}\right\} \\ S_{21} &= \left[p(1-p)\right]^{\frac{1}{2}}\left\{e^{-i(\eta_1+\eta_2+2\eta_1^1-\xi)} - e^{-i(\eta_1+\eta_2+2\eta_2^1+\xi)}\right\} \\ S_{22} &= pe^{-2i(\eta_2+\eta_2^1)} + (1-p)e^{-2i(\eta_1+\eta_2^1-\xi)} \end{aligned} \qquad \text{I(8.7)}$$

In any calculations using the relations I(8.7) it was assumed that

$$\xi = o$$

as was originally assumed by Stueckelberg (STU 32) although the form

$$\xi = \gamma \ln \gamma - \gamma - \arg \Gamma(i\gamma) - \pi/4 \qquad b \ll R_c$$

was derived subsequently (KOT69, CHI69).

Results for ion-production probabilities obtained using I(8.7) will be compared in § I.10 with the numerical solution of I(8.1) and with the results of the calculations described in § I.4, § I.5, § I.6 and § I.7.

I.9 Computational Details

The complete system of equations to be solved is

$$\dot{\underline{a}} = -(i/\hbar)\, \underline{U}\, \underline{a} - \underline{W}\, \underline{a}\,, \quad \underline{U} = \underline{S}^{-1}\{H\}, \quad \underline{W} = \dot{\theta}\underline{S}^{-1}\{\partial/\partial\theta\} + \dot{R}\underline{S}^{-1}\{\partial/\partial R\}$$

$$\dot{R} = \mp v(1 - V(R)/E - b^2/R^2)^{\frac{1}{2}}, \quad \dot{\theta} = vb/R^2\,, \quad v = (2E/\mu)^{\frac{1}{2}} \qquad \text{I(9.1)}$$

It is convenient to define a system of dimensionless variables. In what follows, lengths are reduced by a_o ($a_o = 0.5292\text{Å}$), energies are reduced by 2 x Ry (Ry = 13.6054 eV), masses are reduced by the electron rest mass, m_e ($m_e = 9.10908 \times 10^{-31}$ kg), and time is reduced by the quantity

$$\tau = \hbar/2\text{Ry} = 2.419 \times 10^{-17} \text{ sec.}$$

It is also desirable, from the point of view of computation, to cast the coupled equations I(.1) into a form which is entirely real. This is achieved by making the replacement

figure 8

Co-ordinate system for evaluation of overlap matrix element

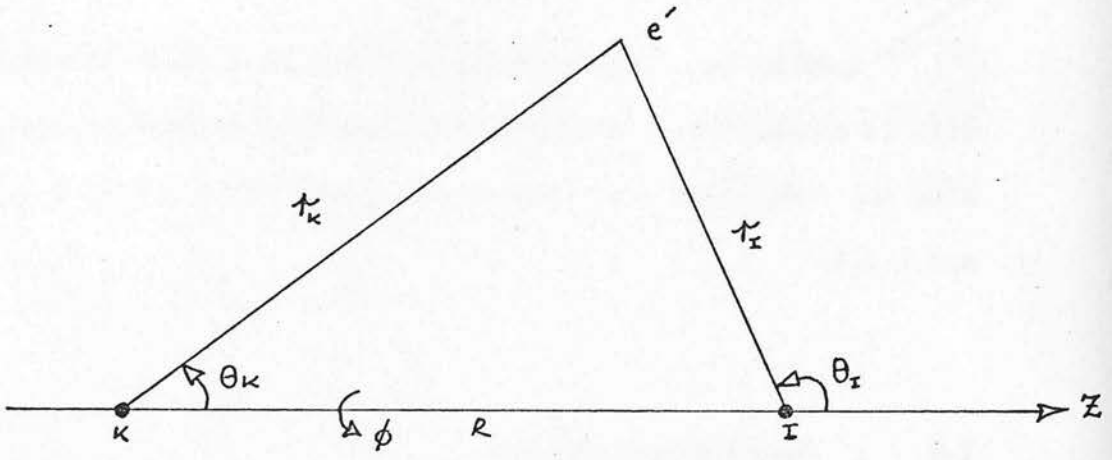

$$\phi_K = \phi_I = \phi$$

$$\underline{a} = \underline{\alpha} + i\underline{B} \qquad \text{I(9.2)}$$

The system of equation which results is

$$\begin{aligned} d\alpha/dt^* &= \underline{U}^*\underline{\beta} - \underline{W}^*\underline{\alpha} \\ d\beta/dt^* &= -\underline{U}^*\underline{\alpha} - \underline{W}^*\underline{\beta} \qquad \text{I(9.3)} \\ dR^*/dt^* &= \pm v^*(1-V^*(R^*)/E^* - b^{*2}/R^{*2}), \\ d\theta/dt^* &= v^* b^*/R^{*2} \end{aligned}$$

and $v^* = (2E^*/\mu^*)^{\frac{1}{2}}$

where * denotes reduced variables. Henceforth the * notation will be dropped and it is understood that reduced variables are used.

Functional fit to overlap matrix element

In all the models used, the basis functions are composed of K4s and I5p wave functions, and the only non-zero contribution to an off-diagonal element of the overlap matrix is

$$S = \langle \psi^I_{5p_z} | \psi^K_{4s} \rangle$$

S was first computed as

$$S = \int R^K_{40}(r_K)\, Y_{oo}(\theta_K,\phi_K)\, R^I_{51}(r_I)\, Y_{10}(\theta_I,\phi_I)\, dv$$

where the co-ordinate system is displayed in Figure 8,

$$Y_{oo}(\theta_K,\phi_K) = 1/2\sqrt{\pi},\ Y_{10}(\theta_I,\phi_I) = (\sqrt{3}/2\sqrt{\pi})\cos\theta_I$$

Overlap Matrix Element as a function of Internuclear Separation R/a.u.

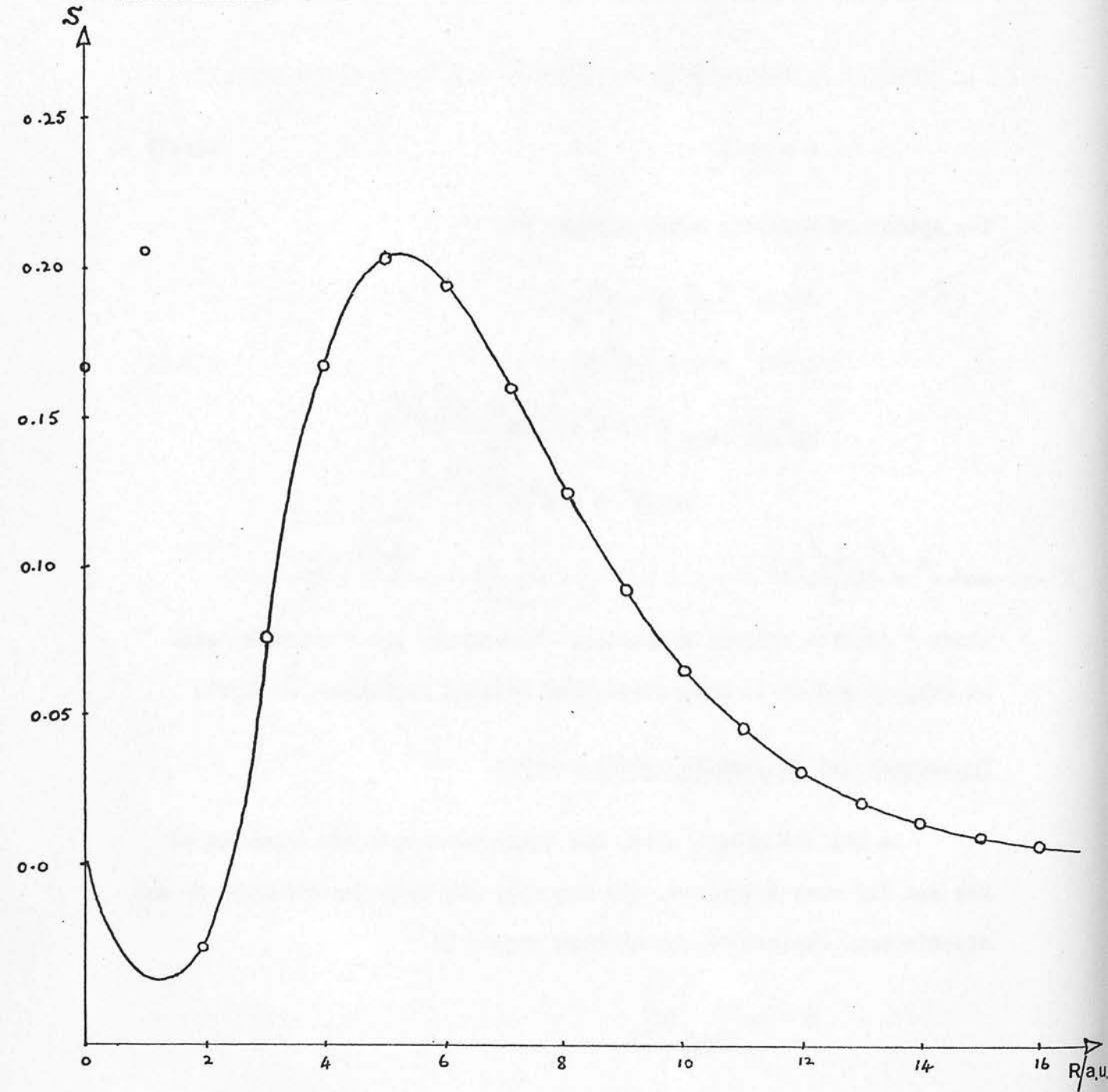

The full curve represents the function S (equation I(9.4)) as a function of R/a.u., the points o are for S_f as a function of R (equation I(9.5)).

TABLE 2

Parameters for Functional Fit

to Overlap Matrix Elements.

A = -0.9085960902781

B = 4.596521439883

C = 3.500801655621

α = -0.7027046944309

β = 0.2861425388080

γ = -0.3961018181228

and for R^K_{40} and R^I_{51}, Hartree-Fock-Slater wave functions (HER63) were used. The integration was performed over the spherical polar coordinates of the K atom as centre:

$$S = -(\sqrt{3}/2)\int R^K_{40}(r_K)\, R^I_{51}(r_I)\, \cos\theta_I\, r_K^2 dr_K dx \qquad I(9.4)$$

where $r_I = (r_K^2 + R^2 - 2r_K Rx)^{\frac{1}{2}}$, $x = \cos\theta_K$ and $\cos\theta_I = (r_K x - R)/r_I$

I(9.4) was evaluated numerically as a function of R by scanning a close mesh of r_K and x. The resulting function $S_f(R)$ was then fitted by the functional form

$$S_f(R) = 2\exp(\alpha R)\{A\cos\beta R - B\sin\beta R\} + C\exp(\gamma R) \qquad I(9.5)$$

A, B, C, α, β and γ are listed in Table 2 and S(R) and $S_f(R)$ are displayed in Figure 9.

Functional fit to the matrix elements of the Hamiltonian

As far as possible, for the purpose of comparison between the various models, corresponding matrix elements were assigned the same functional form.

a. $M(^2S_{\frac{1}{2}}) + X(^1S_0) \rightleftarrows M^+(^1S_0) + X^-(^2S_{\frac{1}{2}})$ one electron model

$$H_{11} = H_{22} = \langle\psi(X^{-2}S_{\frac{1}{2}})|H|\psi(X^{-2}S_{\frac{1}{2}})\rangle = \bar{E}_{ionic}$$

$$H_{33} = H_{44} = \langle\psi(M^2S_{\frac{1}{2}})|H|\psi(M^2S_{\frac{1}{2}})\rangle = \bar{E}_{cov}$$

$$H_{13} = H_{31} = H_{24} = H_{42} = \langle\psi(\ ^{-2}S_{\frac{1}{2}})|H|\psi(M^2S_{\frac{1}{2}})\rangle = \bar{H}$$

$\bar{E}_{ionic}$ was required to reproduce the experimental values for the depth and position of the minimum in the energy of the ground electronic state of KI, and the parameters in $\bar{E}_{cov}$ were chosen so that the position of the ionic/covalent curve crossing is reproduced.

A simplifiedRittner Potential (RIT51) was used to fit the data for $\bar{E}_{ionic}$

$$\bar{E}_{ionic} = V_o \exp(-R/\rho) - 1/R + E(\infty) \qquad I(9.6)$$

where, for speed of computation, charge-quadrupole, dispersion and other higher order interaction effects were ignored.

$\bar{E}_{cov}$ was assigned the convenient functional form

$$\bar{E}_{cov} = 4\varepsilon\{(\sigma/R)^{12} - (\sigma/R)^{6}\} \qquad I(9.7)$$

for which the location of the minimum, $R = R_e^{cov}$ is given by

$$R_e^{cov} = \sigma/(0.5)^{1/6} \qquad I(9.8)$$

To ensure that the minimum in the neutral and ionic curves were located at approximately the same internuclear separation, σ was taken equal to R_e^{ionic}, the position of the minimum in $\bar{E}_{ionic}$. ε was chosen so that $\bar{E}_{cov}(R_c) = \bar{E}_{ionic}(R_c)$, where R_c is the crossing distance. The value of R_c used was 22.67 a.u. (12.0Å) which compares favourably with the value used by Grice and Hershbach (GRI74), 11.3Å.

TABLE 3

Parameters for Functional Fit

to Hamiltonian Matrix Elements

a. $\overline{E}_{ionic} = V_o \exp(-R/\rho) - 1/R + E(\infty)$

ρ = 0.738039 a.u.

V_o = 77.0774 A.U.

R_e^{ionic} = 6.10 a.u. , D_e = 0.10 A.U. (true D_e = 0.1229 A.U. cannot be fitted)

$E(\infty)$ = 0.0441 A.U.

b. $\overline{E}_{cov} = 4\varepsilon\{(\sigma/R)^{12} - (\sigma/R)^{6}\}$

ε = 7.35367×10^{-3} A.U.

σ = 6.10 a.u.

R_c = 22.67 a.u.

c. $\overline{H} = \exp(-\lambda R)$

λ = 0.419859 $a.u.^{-1}$

$\overline{H}(R_c)$ = 2×10^{-3} eV

The element $\bar{H}$ was represented by

$$\bar{H} = \exp(-\lambda R) \qquad \text{I(9.9)}$$

where λ was chosen so that $\bar{H}(R_c) = 2.0 \times 10^{-3}$eV (A value of 2.7×10^{-3}eV was obtained from a semi-empirical relation (OLS71) and $H_{12}(11.3\text{Å})$ has been calculated (GRI74) to be 1.45×10^{-3}eV). V_o, ρ, $E(\infty)$, R_e^{ionic}, D_e^{ionic}, $(= \bar{E}_{ionic}(R_e^{Ionic}))$. ϵ, σ, R_c and λ are listed in Table 3.

b. $\underline{M(^2S_{\frac{1}{2}}) + X(^1S_o) \rightleftarrows M^+(^1S_o) + X^-(^2P_{3/2})}$

$$H_{11} = H_{44} = \langle\psi(X^{-2}P_{3/2\pm3/2})|H|\psi(X^{-2}P_{3/2\pm3/2})\rangle$$

$$H_{22} = H_{33} = \langle\psi(X^{-2}P_{3/2\pm\frac{1}{2}})|H|\psi(X^{-2}P_{3/2\pm\frac{1}{2}})\rangle = \bar{E}_{ionic}$$

$$H_{55} = H_{66} = \langle\psi(M^2S_{\frac{1}{2}})|H|\psi(M^2S_{\frac{1}{2}})\rangle = \bar{E}_{cov}$$

$$H_{25} = H_{36} = H_{52} = H_{63} = \langle\psi(X^{-2}P_{3/2\pm\frac{1}{2}})|H|\psi(M^2S_{\frac{1}{2}\pm\frac{1}{2}})\rangle = \bar{H}$$

I(9.10)

The difference between the energy of an atom, A(j,m), in an electric field $\underline{E} = \hat{e}_z E$, and the same atom in a zero field is given by

$$\Delta E^A(j,m) = -\tfrac{1}{2}\alpha^A_{zz}(j,m)E^2 \qquad \text{I(9.11)}$$

and the field at a distance R from an ion charge Q is given by

$$|\underline{E}| = Q/R^2 \qquad \text{I(9.12)}$$

Substituting I(9.11) into I(9.10) and introducing dimensionless variables yields the result

$$E^{X^-}(3/2,\tfrac{1}{2}) - E^{X^-}(3/2,3/2) = -(1/2R^4)\left[\alpha_{zz}^{X^-}(3/2,\tfrac{1}{2}) - \alpha_{zz}^{X^-}(3/2,3/2)\right]$$

For a system with axial symmetry

$$\alpha_{zz} = \bar{\alpha} + 2\Delta\alpha/3,\ \bar{\alpha} = (\alpha_{xx}+\alpha_{yy}+\alpha_{zz})/3,\ \Delta\alpha = \alpha_{zz}-\alpha_{xx}$$

Assuming that

$$\bar{\alpha}^{X^-}(3/2,3/2) = \bar{\alpha}^{X^-}(3/2,\tfrac{1}{2}) = \bar{\alpha}(x^-),$$

$$\Delta\alpha^{X^-}(3/2,3/2) = -\Delta\alpha^{X^-}(3/2,\tfrac{1}{2}) = 0.1\bar{\alpha}(X^-), \qquad \text{I(9.13)}$$

that this is the sole source of splitting between H_{11} and H_{22}, and substituting the value of the polarisability of the normal $I^-(^1S_o)$ ion, ($\bar{\alpha} = 7.60 \times 10^{-24}$ c m ^{3}) in appropriate units, for $\bar{\alpha}(X^-)$, H_{11} was evaluated as

$$H_{11} = \bar{E}_{ionic} - 3.419/R^4 \text{ A.U.} \qquad \text{I(9.14)}$$

c. $M(^2S_{\frac{1}{2}}) + X(^2S_{\frac{1}{2}}) \rightleftarrows M^+(^1S_0) + X^-(^1S_0)$ two electron model

$$H_{11} = H_{22} = H_{33} = \tfrac{1}{2}\{\langle|\tfrac{1}{2},-\tfrac{1}{2}||H||\tfrac{1}{2},-\tfrac{1}{2}\rangle + \langle|-\tfrac{1}{2},\tfrac{1}{2}||H||-\tfrac{1}{2},\tfrac{1}{2}\rangle + 2\langle|\tfrac{1}{2},-\tfrac{1}{2}||H||-\tfrac{1}{2},\tfrac{1}{2}|\rangle\}$$

$$H_{44} = \tfrac{1}{2}\{\langle|\tfrac{1}{2},-\tfrac{1}{2}||H||\tfrac{1}{2},-\tfrac{1}{2}|\rangle + \langle|-\tfrac{1}{2},\tfrac{1}{2}||H||-\tfrac{1}{2},\tfrac{1}{2}|\rangle - 2\langle|\tfrac{1}{2},-\tfrac{1}{2}||H||-\tfrac{1}{2},\tfrac{1}{2}|\rangle\} = \bar{E}_{cov}$$

$$H_{55} = \langle|\tfrac{1}{2},-\tfrac{1}{2}|^X|H||\tfrac{1}{2},-\tfrac{1}{2}|^X\rangle = \bar{E}_{ionic}$$

$$H_{45} = H_{54} = \sqrt{2}\langle|\tfrac{1}{2},-\tfrac{1}{2}||H||\tfrac{1}{2},-\tfrac{1}{2}|^X\rangle = \sqrt{2}\bar{H}$$

in the notation of § I.6.

ϕ_1, ϕ_2 and ϕ_3 are the three components of a $^3\Sigma$ state, whereas ϕ_4 is a $^1\Sigma$ state (see § I.6). H_{11} was therefore assigned the form

$$H_{11} = (3/4)\bar{E}_{cov} \qquad \text{I(9.15)}$$

d. $M(^2S_{\frac{1}{2}}) + X(^2P_{3/2}) \rightleftarrows M^+(^1S_o) + X^-(^1S_o)$ two electron model

$$H_{11} = (\tfrac{1}{2})\left[\langle|\tfrac{1}{2},-\tfrac{1}{2}||H||\tfrac{1}{2},-\tfrac{1}{2}|\rangle+\langle|-\tfrac{1}{2},\tfrac{1}{2}||H||-\tfrac{1}{2},\tfrac{1}{2}|\rangle-2\langle|\tfrac{1}{2}-\tfrac{1}{2}||H||-\tfrac{1}{2},\tfrac{1}{2}|\rangle\right] = \bar{E}_{cov}$$

$$H_{22} = H_{33} = H_{88} = H_{99} = (\tfrac{1}{2})\left[\langle|3/2,\tfrac{1}{2}||H||3/2,\tfrac{1}{2}|\rangle+\langle|-3/2,-\tfrac{1}{2}||H||-3/2,-\tfrac{1}{2}|\rangle\right]$$

$$H_{44} = H_{66} = H_{77} = (\tfrac{1}{2})\left[\langle|\tfrac{1}{2},\tfrac{1}{2}||H||\tfrac{1}{2},\tfrac{1}{2}|\rangle+\langle|-\tfrac{1}{2},\tfrac{1}{2}||H||-\tfrac{1}{2},\tfrac{1}{2}|\rangle\right]$$

$$H_{55} = \langle\psi_{oo}^{X^-}|H|\psi_{oo}^{X^-}\rangle$$

$$H_{15} = H_{51} = \sqrt{2}\langle|\tfrac{1}{2},-\tfrac{1}{2}||H|\psi_{oo}^{X^-}\rangle = -(2/3)\langle p_o^X(1)S^M(2)|H|p_o^X(1)S^M(2)\rangle$$

in the notation of § I.7 $= -\sqrt{2}\bar{H}$

Using the expanded form of ϕ_1, ϕ_2 and ϕ_4 given in Table 1 (§ I.6), it is readily seen that

$$H_{11} = (1/3)\{\langle p_1^X(1)S^M(2)|H|p_1^X(1)S^M(2)\rangle + 2\langle p_o^X(1)S^M(2)|H|p_o^X(1)S^M(2)\rangle + 2\langle p_o^X(1)S^M(2)|H|S^M(1)p_o^X(2)\rangle\}$$

$$H_{22} = \langle p_1^X(1)S^M(2)|H|p_1^X(1)S^M(2)\rangle$$

$$H_{44} = (1/3)\{\langle p_1^X(1)S^M(2)|H|p_1^X(1)S^M(2)\rangle + 2\langle p_o^X(1)S^M(2)|H|p_o^X(1)S^M(2)\rangle - 2\langle p_o^X(1)S^M(2)|H|S^M(1)p_o^X(2)\rangle\}$$

where p_1^X etc are as defined in § I.7.

TABLE 4

(Contd/-...)

The Forms used for the

Hamiltonian Matrix Elements

d. $M(^2S_{\frac{1}{2}}) + X(^2P_{3/2}) \rightleftarrows M^+(^1S_o) + X^-(^1S_o)$

$$H_{11} = \bar{E}_{cov}$$

$$H_{22} = H_{33} = H_{88} = H_{99} = (3/4)\bar{E}_{cov}$$

$$H_{44} = H_{66} = H_{77} = (\tfrac{1}{4})\bar{E}_{cov}$$

$$H_{55} = \bar{E}_{ionic}$$

$$H_{15} = H_{51} = -\sqrt{2}\bar{B}$$

TABLE 4

The Forms used for the

Hamiltonian Matrix Elements

a. $M(^2S_{\frac{1}{2}}) + X(^1S_o) \rightleftarrows M^+(^1S_o) + X^-(^2S_{\frac{1}{2}})$

$$H_{11} = H_{22} = \overline{E}_{ionic}$$

$$H_{33} = H_{44} = \overline{E}_{cov}$$

$$H_{13} = H_{31} = H_{24} = H_{42} = \overline{H}$$

b. $M(^2S_{\frac{1}{2}}) + X(^1S_o) \rightleftarrows M^+(^1S_o) + X^-(^2P_{3/2})$

$$H_{11} = H_{44} = \overline{E}_{ionic} - 3.419/R^4$$

$$H_{22} = H_{33} = \overline{E}_{ionic}$$

$$H_{55} = H_{66} = \overline{E}_{cov}$$

$$H_{25} = H_{36} = H_{52} = H_{63} = \overline{H}$$

c. $M(^2S_{\frac{1}{2}}) + X(^2S_{\frac{1}{2}}) \rightleftarrows M^+(^1S_o) + X^-(^1S_o)$

$$H_{11} = H_{22} = H_{33} = (3/4)\overline{E}_{cov}$$

$$H_{44} = \overline{E}_{cov}$$

$$H_{55} = \overline{E}_{ionic}$$

$$H_{45} = H_{54} = \sqrt{2}\overline{H}$$

Figure 10

$\overline{H}$, $\overline{E}_{cov}$ and $\overline{E}_{ionic}$ as functions of R

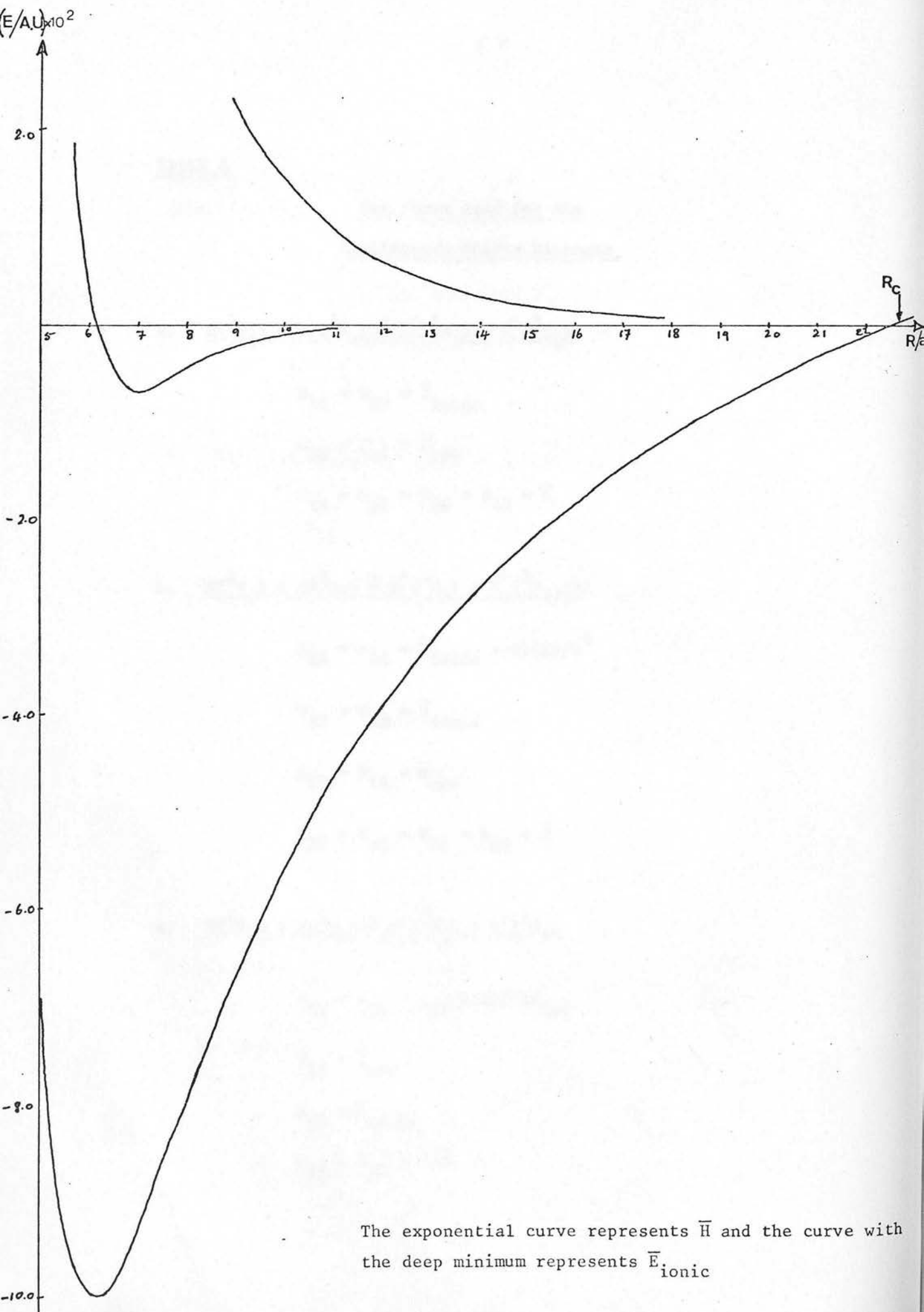

The exponential curve represents $\overline{H}$ and the curve with the deep minimum represents $\overline{E}_{ionic}$

It was assumed that

$$(1/3)\{\langle p_1^X(1)S^M(2)|H|p_1^X(1)S^M(2)\rangle + 2\langle p_o^X(1)S^M(2)|H|p_o^X(1)S^M(2)\rangle\}$$
$$= \langle p_1^X(1)S^M(2)|H|p_1^X(1)S^M(2)\rangle = \bar{E}$$

and that $\bar{E} = (3/4)\bar{E}_{cov}$

with the result that

$$H_{22} = (3/4)\bar{E}_{cov}$$
$$H_{44} = (1/2)\bar{E}_{cov} \qquad \text{I(9.16)}$$

The various matrix elements as functions of R are displayed in Figure 10, and the functional forms of all the matrix elements are summarised in Table 4.

Solving the Coupled Equations

The coupled equations I(9.1) were solved (for each of the models described) by means of Hammings modified predictor-corrector method (RAL60). It is a fourth order method using four preceding points for computation of a new vector of the dependent variables. The fourth order Runge-Kutta method suggested by Ralston was used for adjustment of the initial increment in the independent variable (time) and for computation of starting values. The increment was adjusted during the whole computation by halving or doubling. The program

allowed up to ten bisections of the initial increment, but the increment never exceeded its initial value. Accordingly the initial increment had to be selected quite carefully.

Care also had to be exercised in the evaluation of $\dot{R}$ and $\ddot{R}$ in the neighbourhood of the turning points of the motion, $R = \rho$, where ρ is defined by the zero of $\dot{R}$ and is the root of the equation

$$1-V(R)/E - b^2/R^2 = o$$

Given the form of $V(R)$, this equation can be solved iteratively for ρ. $V(R)$ was assigned the form

$$V(R) = W(\sigma/R)^{12}$$

in which the same value was used for σ as was used in $\bar{E}_{cov}$ (equation I(9.7))

$$= 6.10 \text{ a.u.}$$

The repulsive contribution to the ionic (diabatic) potential at $R = R_e$ is $\simeq 0.5$ eV It therefore seemed reasonable to choose

$$W = 0.5 \text{ eV}$$

To select a value for R_o, the value of R at which the computation was started, the simplest model of all was considered, namely that in which the expansion basis consists of two diabatic states ϕ_1 and ϕ_2, and coupling is due to the Hamiltonian only. The

system of equations to be solved for such a model is given by I(8.1), subject to the boundary conditions $a_2(o) = 1$. Initially R_o was taken to be 25.0 a.u. (R_c = 22.67 a.u.). Consider the effect upon a_1 and a_2 of starting the computation not at $R = R_o$, but at $R = R_o^1$ ($R_o^1 > R_o$). In the region

$$R_o \leq R \leq R_o^1$$

the system of equations I(8.1) can be approximated by

$$\text{a.} \quad \dot{a}_1 = -iH_{12} \qquad (a_2 \simeq 1)$$

$$\text{b.} \quad \dot{a}_2 = -iH_{22}$$

Consider the solution of equation a.

$$\Delta a_1 = -i\int_{t_o^1}^{t_o} H_{12}\,dt = -i\int_{R_o^1}^{R_o} \frac{H_{12}}{v}\,dR$$

Substituting $v = (2E/\mu)^{\frac{1}{2}}(1-b^2/R^2)^{\frac{1}{2}}$ (the trajectory is approximately rectilinear in this region) and $H_{12} = \exp(-\lambda R)$, Δa_1 becomes

$$\Delta a_1 = -i(\mu/2E)^{\frac{1}{2}}\int_{R_o}^{R_o^1} \frac{\exp(-\lambda R)\,dR}{(1-b^2/R^2)^{\frac{1}{2}}} \qquad \text{I(9.17)}$$

the integral in I(9.17) was evaluated approximately by binomially expanding $(1-b^2/R^2)^{-\frac{1}{2}}$ and making use of the tabulated function

$$E_1(x) = \int_x^\infty (e^{-t}/t)\,dt$$

TABLE 5

Change in Transition Amplitude as a Function of the Distance at Which Computation is started

R_o^1 a.u.	$\lvert\Delta a_1\rvert$
30	5.4×10^{-3}
35	6.0×10^{-3}
40	6.1×10^{-3}

$b = 10.0$ a.u., $R_o = 25.0$ a.u., $E = 100.0$ eV

The results for different values of R_o^1 are displayed in Table 5. It is not desirable to allow R_o to be too large, since then the computation is very time consuming if a high accuracy is to be maintained. It was therefore decided, by way of a compromise, to take R_o = 30.0 a.u. for all the calculations. The result of this choice for the above model is that for E = 100.0 eV and b = 10.0 a.u., microscopic reversibility is satisfied to 2 parts in 10^5 and probability is conserved to better than 4 parts in 10^5.

As a final check on the program, the Hamiltonian coupling was "switched off" for each of the models by setting all the Hamiltonian matrix elements equal to zero. This corresponds to two atoms colliding in the absence of any interaction (for a straight line trajectory)! The expected outcome of such a collision is merely to leave the quantum states of the collision partners, defined relative to a space-fixed co-ordinate system, unchanged. For E = 100.0 eV , b = 10.0 a.u., all "transition amplitudes" (for all models) were found to be less than 10^{-6}.

I.10 RESULTS and DISCUSSION

Part I Ionisation

A. $M(^2S_{\frac{1}{2}}) + X(^1S_o) \rightleftarrows M^+(^1S_o) + X^-(^2S_{\frac{1}{2}})$

The basis used (see § I.4) was

$$\psi_1 = \psi^{X^-}(j=\tfrac{1}{2}\ m=\tfrac{1}{2})$$

$$\psi_2 = \psi^{X^-}(j=\tfrac{1}{2}\ m=-\tfrac{1}{2}) \qquad \text{I(10.1)}$$

$$\psi_3 = \psi^{M}(j=\tfrac{1}{2}, m=\tfrac{1}{2})$$

$$\psi_4 = \psi^{M}(j=\tfrac{1}{2}, m=-\tfrac{1}{2})$$

The average ionisation probability which would be measured in an experiment in which the M atoms were not state selected, is given by

$$\bar{P}_{ion}(X^1S_o \rightarrow X^{-2}S_{\frac{1}{2}}) = \tfrac{1}{2}(P_{31} + P_{41} + P_{32} + P_{42}) \qquad \text{I(10.2)}$$

The probabilities of emerging in the ionic channel with $j = \frac{1}{2}$, $m = \frac{1}{2}$, and with $j = \frac{1}{2}$ $m = -\frac{1}{2}$, are respectively given by

$$P^{\frac{1}{2}}_{ion}(X^1S_o \rightarrow X^{-2}S_{\frac{1}{2}}) = \tfrac{1}{2}(P_{31} + P_{41}) \qquad \text{I(10.3)}$$

$$P^{-\frac{1}{2}}_{ion}(X^1S_o \rightarrow X^{-2}S_{\frac{1}{2}}) = \tfrac{1}{2}(P_{32} + P_{42})$$

and the expectation that these two probabilities are equal was confirmed by computation.

B. $M(^2S_{\frac{1}{2}}) + X(^1S_o) \rightleftarrows M^+(^1S_o) + X^-(^2P_{3/2})$

$$\psi_1 = \psi^{X^-}(j=3/2,\ m=3/2)$$

$$\psi_2 = \psi^{X^-}(j=3/2,\ m=\tfrac{1}{2})$$

$$\psi_3 = \psi^{X^-}(j=3/2,\ m=-\tfrac{1}{2})$$

$$\psi_4 = \psi^{X^-}(j=3/2,\ m=-3/2) \qquad \text{I(10.4)}$$

$$\psi_5 = \psi^{M}(j=\tfrac{1}{2},\ m=\tfrac{1}{2})$$

$$\psi_6 = \psi^{M}(j=\tfrac{1}{2},\ m=-\tfrac{1}{2})$$

For this system the average ionisation probability $\bar{P}_{ion}(X^1S_o \rightarrow X^{-2}P_{3/2})$ is given by

$$\bar{P}_{ion}(X^1S_o \rightarrow X^{-2}P_{3/2}) = \{P^{3/2}_{ion}(X^1S_o \rightarrow X^{-2}P_{3/2}) + P^{\frac{1}{2}}_{ion}(X^{-1}S_o \rightarrow X^{-2}P_{3/2}) + P^{-\frac{1}{2}}_{ion}(X^1S_o \rightarrow X^{-2}P_{3/2}) + P^{-3/2}_{ion}(X^1S_o \rightarrow X^{-2}P_{3/2})\} \qquad \text{I(10.5)}$$

where $P^{m}_{ion}(X^1S_o \rightarrow X^{-2}P_{3/2})$ denotes the probability of emerging in the ionic channel with $j = 3/2$, $m_j = m$. Specifically,

$$P^{3/2}_{ion}(X^1S_o \rightarrow X^{-2}P_{3/2}) = \tfrac{1}{2}(p_{51} + p_{61}),\ P^{-3/2}_{ion}(X^1S_o \rightarrow X^{-2}P_{3/2}) = \tfrac{1}{2}(p_{54} + p_{64}) \qquad \text{I(10.6)}$$

(I.(10.6) contd/-...)

$$P^{\frac{1}{2}}_{ion}(X^1S_o \rightarrow X^{-2}P_{3/2}) = \tfrac{1}{2}(P_{52} + P_{62}) \ , \ P^{-\frac{1}{2}}_{ion}(X^1S_o \rightarrow X^{-2}P_{3/2}) = \tfrac{1}{2}(P_{53} + P_{63}) \qquad \text{I(10.6)}$$

and the expectation that $P^{m}_{ion}(X^1S_o \rightarrow X^{-2}P_{3/2}) = P^{-m}_{ion}(X^1S_o \rightarrow X^{-2}P_{3/2})$ I(10.7)

($m = \frac{1}{2}, 3/2$) was again confirmed.

At this point, it is instructive to consider the description of the systems

$$\text{a.} \quad M(^2S_{\frac{1}{2}}) + X(^1S_o) \rightleftarrows M^+(^1S_o) + X^-(^2S_{\frac{1}{2}}) \qquad \text{I(10.8)}$$

$$\text{b.} \quad M(^2S_{\frac{1}{2}}) + X(^1S_o) \rightleftarrows M^+(^1S_o) + X^-(^2P_{3/2})$$

in terms of the Landau-Zener approximation.

In the basis used to describe the system I(10.8) (a), the only non-zero matrix elements of the Hamiltonian are

$$H_{11} = H_{22}, \ H_{33} = H_{44}, \ H_{13} = H_{31} = H_{24} = H_{42}$$

If the Hamiltonian is the only source of coupling, then, the states 1 and 3 are coupled in identical fashion to the coupling between 2 and 4, but there is no coupling between 1 and 2 or 1 and 4 or between 3 and 2 or 3 and 4. Hence

$$P_{13} = P_{24} = P_{LZ} \qquad \text{I(10.9)}$$

P_{LZ}(-0-), $\overline{P}_{ion}(X^1S_o \rightarrow X^{-2}S_{\frac{1}{2}})$ (-.-.), $\overline{P}_{ion}(X^1S_o \rightarrow X^{-2}P_{3/2})$ (-) as functions of impact parameter b.

figure 11

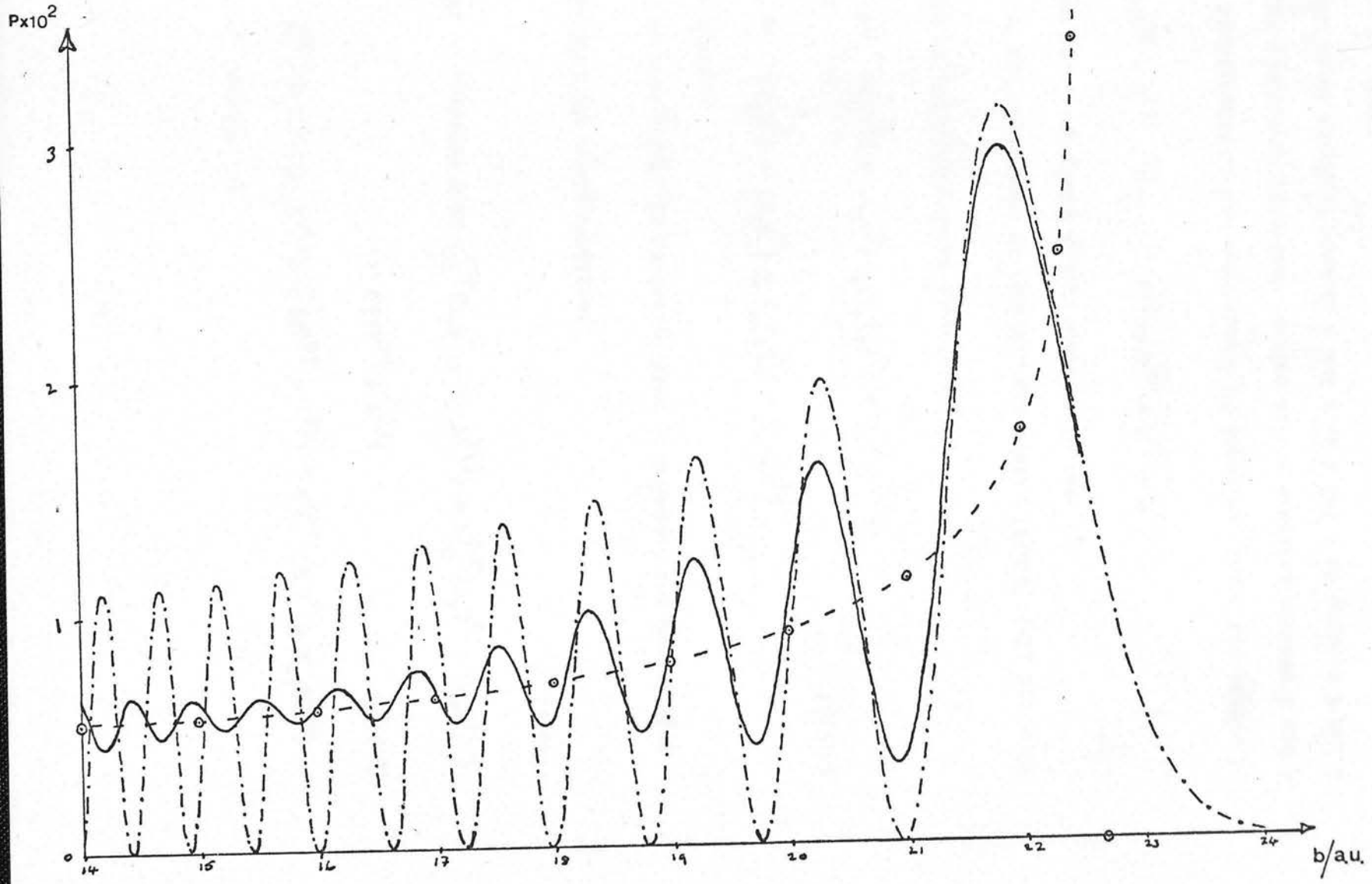

and $$\bar{P}_{ion}(x^1S_o \rightarrow X^{-2}S_{\frac{1}{2}}) = P_{LZ} \qquad I(10.10)$$

Similarly, for the system I(10.8) (b), states 2 and 5 are coupled in the same way as 3 and 6 are coupled but no coupling exists between the two sets:

$$P_{25} = P_{36} = P_{LZ} \qquad I(10.11)$$

and $$\bar{P}_{ion}(X^1S_o \rightarrow X^{-2}P_{3/2}) = P_{LZ} \qquad I(10.12)$$

(P_{LZ} in I(10.11) and I(10.9) are the same since corresponding Hamiltonian matrix elements in the two systems were assigned identical functional forms). $\bar{P}_{ion}$ for the two systems (obtained by numerical solution of the relevant coupled equations) and P_{LZ} are displayed as functions of impact parameter (E = 50 eV) in Figure 11 which shows several interesting features.

i. The high frequency structure in the two functions $\bar{P}_{ion}(X^1S_o \rightarrow X^{-2}S_{\frac{1}{2}})$ and $\bar{P}_{ion}(X^1S_o \rightarrow X^{-2}P_{3/2})$, although quite different in amplitude in the two cases, is in each case nearly perfectly centred on P_{LZ} except in the region $b = R_c$ where the Landau-Zener approximation is known to break down. In the simple semi-classical analysis of § I.8, this high frequency structure is due to the difference in the phases of the two terms contributing to the transition (ionic) amplitude. A very good estimate of $\bar{\sigma}_{ion}$, the total cross section for ionisation measured

in an experiment in which the M atoms are not state-selected (for either I(10.8) (a) or (b)) is given by

$$\bar{\sigma}_{ion} = \bar{\sigma}_{ion}(X^1S_o \rightarrow X^{-2}S_{\frac{1}{2}}) = \bar{\sigma}_{ion}(X^1S_o \rightarrow X^{-2}P_{3/2}) = \sigma_{LZ}$$

where I(10.13)

$$\sigma_{LZ} = 2\pi \int_o^\infty 2p(1-p)b\, db,$$

$$p = \exp(-2\pi\gamma), \quad \gamma = \{H_{12}^2/v \frac{d}{dR}|H_{11} - H_{22}|\}_{R_c} \quad \text{(atomic units)}.$$

If the velocity is assumed to be well approximated at R_c by

$$v = (2E/\mu)^{\frac{1}{2}} \left[1-b^2/R_c^2\right]^{\frac{1}{2}}$$

(straight line trajectory - an excellent approximation in the present case where R_c is large (22.67 a.u.) and E is high (50 eV)), then it can be shown that

$$\sigma_{LZ} = 2\pi\{(R_c^2-\alpha R_c)e^{-\alpha/R_c} - (R_c^2-\beta R_c)e^{-\beta/R_c} + \alpha^2 \int_{zc_1}^\infty (e^{-z}/z)dz$$

$$-\beta^2 \int_{zc_2}^\infty (e^{-z}/z)dz\} \qquad \text{I(10.14)}$$

in units of a_o^2, where

$$\alpha = R_c\zeta, \quad \beta = 2\alpha, \quad zc_1 = \alpha R_c, \quad zc_2 = 2zc_1$$

and $$\zeta = \left[2\pi/(2E/\mu)^{\frac{1}{2}}\right]\{H_{12}^2/\frac{d}{dR}|H_{11} - H_{22}|\}R_c$$

when the integrals are evaluated, σ_{LZ} is found to be

figure 12 $P^{3/2}_{ion}(X^1S_o \rightarrow X^{-2}P_{3/2})$ (---), approximation I(10.16) (O and Δ), $P^{\frac{1}{2}}_{ion}(X^1S_o \rightarrow X^{-2}P_{3/2})$ (-) as functions of impact parameter, b.

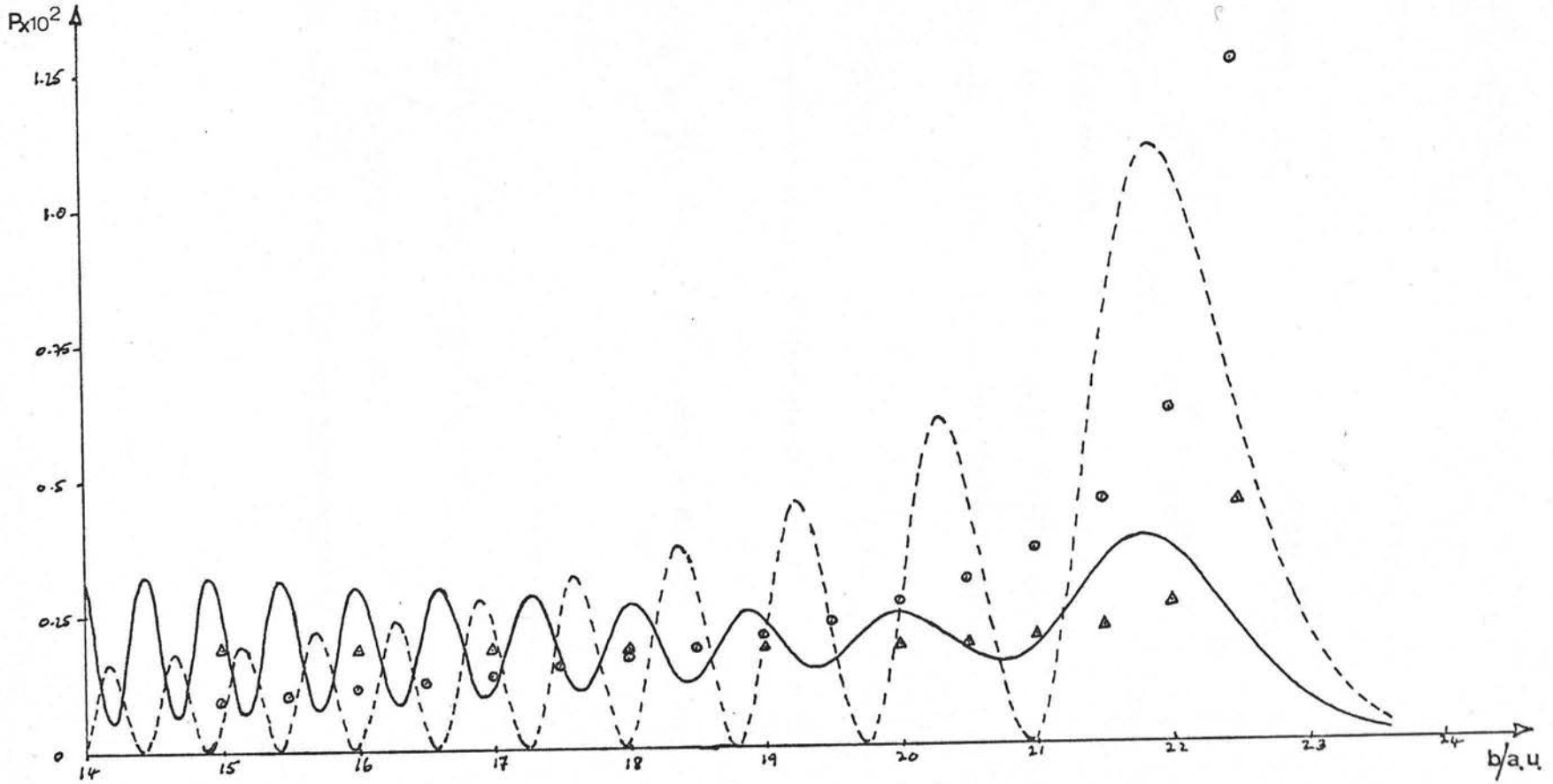

$$\sigma_{LZ} = 3.77\ \text{Å}^2$$

the expected dependence of σ_{LZ} on energy and $H_{12}(R_c)$ will be discussed below.

ii. The oscillations in $\bar{P}_{ion}(X^1S_o \rightarrow X^{-2}P_{3/2})$ do not range from zero to twice p_{LZ} as do those in $\bar{P}_{ion}(X^1S_o \rightarrow X^{-2}S_{\frac{1}{2}})$. In addition, the amplitude of the oscillations in $\bar{P}_{ion}(X^1S_o \rightarrow X^{-2}P_{3/2})$ appears to be smallest at b $\simeq$ 15.5 a.u. The reason for this can be seen by noting that

$$\bar{P}_{ion}(X^1S_o \rightarrow X^{-2}P_{3/2}) = 2\{P^{3/2}_{ion}(X^1S_o \rightarrow X^{-2}P_{3/2}) + P^{\frac{1}{2}}_{ion}(X^1S_o \rightarrow X^{-2}P_{3/2})\}.$$

$P^{3/2}_{ion}(X^1S_o \rightarrow X^{-2}P_{3/2})$ and $P^{\frac{1}{2}}_{ion}(X^1S_o \rightarrow X^{-2}P_{3/2})$ are displayed as functions of impact parameter, b (E = 50 eV) in Figure 12 from which it can be seen that $P^{3/2}_{ion}(X^1S_o \rightarrow X^{-2}P_{3/2})$ decreases as b decreases and increases to nearly three times $P^{\frac{1}{2}}_{ion}(X^1S_o \rightarrow X^{-2}P_{3/2})$ at the outermost maximum in the two functions (b = 22 a.u.). This, together with the fact that the oscillations in $P^{3/2}_{ion}(X^1S_o \rightarrow X^{-2}P_{3/2})$ appear to be $\sim 90^\circ$ out of phase with those in $P^{\frac{1}{2}}_{ion}(X^1S_o \rightarrow X^{-2}P_{3/2})$ in the range $14 \lesssim b \lesssim 18$ a.u., accounts for the modulation in the amplitude of the oscillations in $\bar{P}_{ion}(X^1S_o \rightarrow X^{-2}P_{3/2})$.

To account for these observations, consider the following model:

At R_c on the inward half trajectory

$$\theta = \theta_c = \sin^{-1}(b/R_c) \qquad \text{(See Figure 5)}$$

and at R_c on the outward half trajectory

$$\theta = \theta_c^1 = \pi - \chi - \theta_c$$

Suppose that i. there are no transitions between states defined relative to space-fixed axes for $R > R_c$, and that

ii. for $R < R_c$ transitions between states defined relative to rotating axes are possible only if the states are connected by the Hamiltonian (coriolis coupling neglected).

It follows from i. that $\underset{\sim}{a}(t_c)$, the vector of amplitudes of states defined relative to a rotating quantisation axis at R_c on the inward half of the trajectory, is given, neglecting phase factors, by

$$\underset{\sim}{a}(t_c) = \underset{\sim}{D}^{-1}(\theta_c)\ \underset{\sim}{b}_o \qquad \text{(c.p. eq'n. I(4.9))}$$

where $\underset{\sim}{D}(\theta)$ is given by equation I(5.6).

It follows from ii. that $\underline{a}(t_c^1)$, the vector of amplitudes of states defined relative to a rotating quantisation axis at R_c on the outward half of the trajectory, is given by

$$\underline{a}(t_c^1) = \underline{\underline{S}}\,\underline{\underline{D}}^{-1}(\Theta_c)\,\underline{b}_o$$

where $\underline{\underline{S}}$ is the 'transition matrix' whose only offdiagonal elements are $S_{25} = S_{52} = S_{36} = S_{63} = s$. Finally, $\underline{b}^f$, the vector of amplitudes of states defined relative to space fixed axes at $R = \infty$ on the outward half trajectory, is given (neglecting phase factors) by

$$\underline{b}^f = \left[\underline{\underline{D}}(\Theta_c^1)\,\underline{\underline{S}}\,\underline{\underline{D}}^{-1}(\Theta_c)\right]\underline{b}_o = \underline{\underline{T}}.\underline{b}_o \qquad \text{I(10.15)}$$

Now $P_{ion}^{3/2}(X^1S_o \to X^{-2}P_{3/2}) = \frac{1}{2}(P_{51}+P_{61}) = \frac{1}{2}\{|T_{15}|^2 + |T_{16}|^2\}$

and $P_{ion}^{\frac{1}{2}}(X^1S_o \to X^{-2}P_{3/2}) = \frac{1}{2}(P_{52}+P_{62}) = \frac{1}{2}\{|T_{25}|^2 + |T_{26}|^2\}$

The appropriate elements of the T matrix can be evaluated from I(10.15) with the result that

$$P_{ion}^{3/2}(X^1S_o \to X^{-2}P_{3/2}) \sim (3/8)\sin^2\Theta_c^1|s|^2 = (3/8)\sin^2(\chi+\Theta_c)|s|^2$$

and $\qquad \text{I(10.16)}$

$$P_{ion}^{\frac{1}{2}}(X^1S_o \to X^{-2}P_{3/2}) \sim (1/8)(1+3\cos^2\Theta_c^1)|s|^2 = (1/8)\left[4-3\sin^2(\chi+\Theta_c)\right]|s|^2$$

$$P_{ion}^{\frac{1}{2}}(X^1S_o \to X^{-2}P_{3/2}) + P_{ion}^{3/2}(X^1S_o \to X^{-2}P_{3/2}) = \tfrac{1}{2}|s|^2$$

These approximations for the two ionisation probabilities, together with the additional assumption that

$$|s|^2 = P_{LZ}$$

are displayed in Figure 12. This model reproduces the following features of the observed behaviour of the two functions:

a. $P_{ion}^{3/2}(X^1S_o \to X^{-2}P_{3/2}) \to 0$ as $b \to 0$ and

b. $P_{ion}^{3/2}(X^1S_o \to X^{-2}P_{3/2}) \to 3\, P_{ion}^{\frac{1}{2}}(X^1S_o \to X^{-2}P_{3/2})$ as $b \to R_c$

It does not account for the difference in the phase and amplitude of the high frequency oscillations in the two cases.

c. $M(^2S_{\frac{1}{2}}) + X(^2S_{\frac{1}{2}}) \rightleftarrows M^+(^1S_o) + X^-(^1S_o)$

The basis used was a molecular basis (§ I.6) derived from linear combinations of the atomic basis functions

$$\begin{aligned}
\psi_1 &= |\psi^M(j=\tfrac{1}{2}m=\tfrac{1}{2}),\ \psi^X(j=\tfrac{1}{2}.m=\tfrac{1}{2})| \\
\psi_2 &= |\psi^M(j=\tfrac{1}{2},m=\tfrac{1}{2}),\ \psi^X(j=\tfrac{1}{2},m=-\tfrac{1}{2})| \\
\psi_3 &= |\psi^M(j=\tfrac{1}{2},m=-\tfrac{1}{2})\ \psi^X(j=\tfrac{1}{2},m=\tfrac{1}{2})| \\
\psi_4 &= |\psi^M(j=\tfrac{1}{2},m=-\tfrac{1}{2}),\ \psi^X(j=\tfrac{1}{2}\ m=-\tfrac{1}{2})| \\
\psi_5 &= \psi_{ionic}
\end{aligned} \qquad \text{I(10.17)}$$

where | | denotes the usual determinant. For this system, the average ionisation probability, $\overline{P}_{ion}(X^2S_{\frac{1}{2}} \rightarrow X^{-1}S_o)$ is given by

$$\overline{P}_{ion}(X^2S_{\frac{1}{2}} \rightarrow X^{-1}S_o) = (\tfrac{1}{4})(p_{15}+p_{25}+p_{35}+p_{45}) \qquad \text{I(10.18)}$$

and the expectation that

$$p_{15} = p_{45} \simeq 0, \quad \text{and} \quad p_{25} = p_{35}$$

was confirmed by computation.

The above basis is not amenable to an analysis using the Landau-Zener approximation because H_{23} is non-zero as well as H_{25} and H_{35}. Hence it is necessary to define a molecular basis

$$\begin{aligned} \phi_I &= \psi_1 \\ \phi_{II} &= (1/\sqrt{2})(\psi_2 + \psi_3) \\ \phi_{III} &= \psi_4 \\ \phi_{IV} &= (1/\sqrt{2})(\psi_2 - \psi_3) \\ \phi_V &= \psi_5 \end{aligned} \qquad \text{I(10.19)}$$

in which $\langle\phi_{IV}|H|\phi_V\rangle$ is the only non-zero offdiagonal matrix element of the Hamiltonian.

$$p(IV \rightarrow V) = p(V \rightarrow IV) = P_{LZ}$$

where P_{LZ} is given by I(10.13) except that H_{12} is now $\sqrt{2}$ times the value used for I(10.8) (a) and (b) (See Table 4 and § I.9,(c)).

figure 13

$\overline{P}_{ion}(X^2S_{\frac{1}{2}} \rightarrow X^{-1}S_o)$ (-) and $\overline{P}^{LZ}_{ion}(X^2S_{\frac{1}{2}} \rightarrow X^{-1}S_o)$ (- o -) as functions of impact parameter, b.

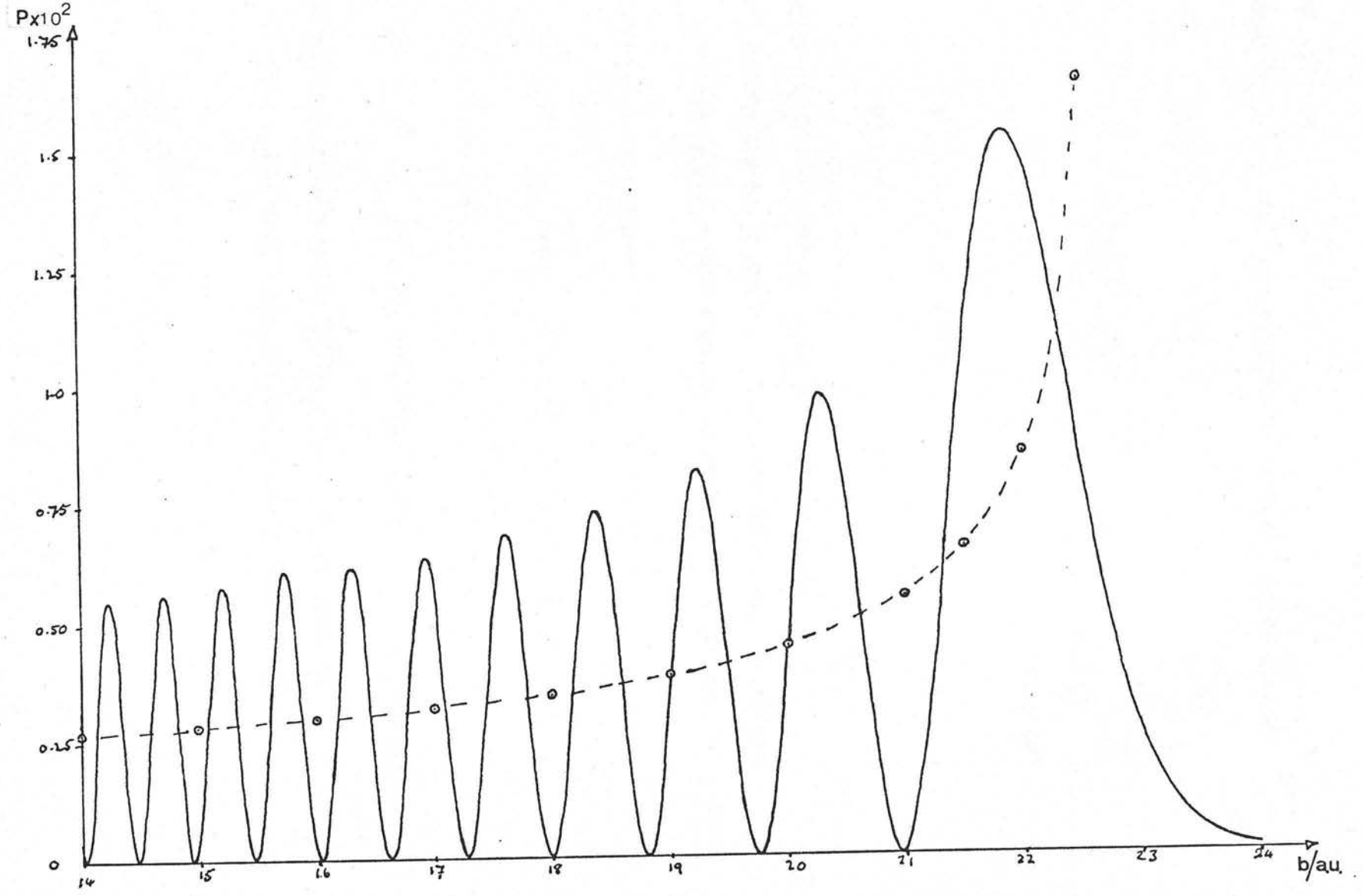

To convert p(IV → V) into a transition probability in the atomic basis note that the total wave function, Ψ, is given by

$$\Psi = a_I\phi_I + a_{II}\phi_{II} + a_{III}\phi_{III} + a_{IV}\phi_{IV} + a_V\phi_V$$

Suppose the system is prepared initially in state ψ_5 or ϕ_V ie $a_V(o) = 1$. After 'collision' only a_{IV} and a_V can be non-zero. Hence p_2, the probability of finding the system after the collision in the state described by ψ_2, is given by

$$p_2 = \tfrac{1}{2}|a_{IV}|^2 \qquad \text{(See I(10.19)).}$$

(Both bases are orthonormal at R = ∞.)

Similarly

$$p_3 = \tfrac{1}{2}|a_{IV}|^2$$

and
$$p(V \to IV) = |a_{IV}|^2 = p_{LZ} \qquad \text{I(10.20)}$$

$$\therefore \quad p_{25} = p_{52} = p_{53} = p_{35} = \tfrac{1}{4} p_{LZ}$$

and
$$\bar{P}^{LZ}_{ion}(X^2S_{\frac{1}{2}} \to X^{-1}S_o) = \tfrac{1}{4} p_{LZ} \qquad \text{I(10.21)}$$

$\bar{P}_{ion}(X^2S_{\frac{1}{2}} \to X^{-1}S_o)$ and $\bar{P}^{LZ}_{ion}(X^2S_{\frac{1}{2}} \to X^{-1}S_o)$ are displayed as functions of impact parameter, b, in Figure 13. The close similarity between $\bar{P}_{ion}(X^2S_{\frac{1}{2}} \to X^{-1}S_o)$ and $\bar{P}_{ion}(X^1S_o \to X^{-2}S_{\frac{1}{2}})$ (Figure 11) should be noted.

The oscillations are of the same frequency in each case, and corresponding maxima and minima are located at identical b values. When the Landau-Zener cross section $\bar{\sigma}^{LZ}_{ion}(X^2S_{\frac{1}{2}} \rightarrow X^{-1}S_o)$ (Equation I(10.14)) was evaluated for the present case, it was found that

$$\bar{\sigma}^{LZ}_{ion}(X^2S_{\frac{1}{2}} \rightarrow X^{-1}S_o) = 1.86\ \text{Å}^2$$

which is very close to half the value for the process

$$M(^2S_{\frac{1}{2}}) + X(^1S_o) \rightarrow M^+(^1S_o) + X^-(^2S_{\frac{1}{2}}) \qquad (3.77\text{Å}^2)$$

It would appear then, that so far as ion production from unselected collision partners is concerned, the process

$$M(^2S_{\frac{1}{2}}) + X(^1S_o) \rightarrow M^+(^1S_o) + X^{-1}(^2S_{\frac{1}{2}})$$

and $$M(^2S_{\frac{1}{2}}) + X(^2S_{\frac{1}{2}}) \rightarrow M^+(^1S_o) + X^-(^1S_o)$$

are virtually identical after account is taken of the different multiplicities of initial (neutral) states.

D. $$M(^2S_{\frac{1}{2}}) + X(^2P_{3/2}) \rightarrow M^+(^1S_o) + X^-(^1S_o)$$

The basis used was a molecular basis (§ I.7) derived from linear combinations of the atomic basis functions

$$\psi_1 = |\psi^X(j=3/2\ m=3/2),\ \psi^M(j=\tfrac{1}{2}\ m=\tfrac{1}{2})|$$

$$\psi_2 = |\psi^X(j=3/2,\ m=3/2),\ \psi^M(j=\tfrac{1}{2},\ m=-\tfrac{1}{2})|$$

$$\psi_3 = |\psi^X(j=3/2,\ m=\tfrac{1}{2}),\ \psi^M(j=\tfrac{1}{2},\ m=\tfrac{1}{2})|$$

$$\psi_4 = |\psi^X(j=3/2,\ m=-\tfrac{1}{2}),\ \psi^M(j=\tfrac{1}{2}\ m=-\tfrac{1}{2})|$$

$$\psi_5 = |\psi^X(j=3/2,\ m=-3/2),\ \psi^M(j=\tfrac{1}{2},\ m=\tfrac{1}{2})| \qquad \text{I(10.22)}$$

$$\psi_6 = |\psi^X(j=3/2,\ m=-3/2),\ \psi^M(j=\tfrac{1}{2},\ m=-\tfrac{1}{2})|$$

$$\psi_7 = |\psi^X(j=3/2,\ m=\tfrac{1}{2}),\ \psi^M(j=\tfrac{1}{2},\ m=-\tfrac{1}{2})|$$

$$\psi_8 = |\psi^X(j=3/2,\ m=-\tfrac{1}{2}),\ \psi^M(j=\tfrac{1}{2},\ m=\tfrac{1}{2})|$$

$$\psi_9 = \psi_{ionic}$$

where $|\ |$ denotes the usual determinant.

The average ionisation probability $\bar{P}_{ion}(X^2P_{3/2} \rightarrow X^{-1}S_o)$, is given by

$$\bar{P}_{ion}(X^2P_{3/2} \rightarrow X^{-1}S_o) = (\tfrac{1}{4})\{P^{ion}_{3/2}(X^2P_{3/2} \rightarrow X^{-1}S_o) + P^{ion}_{-3/2}(X^2P_{3/2} \rightarrow X^{-1}S_o) + P^{ion}_{\frac{1}{2}}(X^2P_{3/2} \rightarrow X^{-1}S_o) + P^{ion}_{-\frac{1}{2}}(X^2P_{3/2} \rightarrow X^{-1}S_o)\} \qquad \text{I(10.23)}$$

where $$P^{ion}_{3/2}(X^2P_{3/2} \rightarrow X^{-1}S_o) = (\tfrac{1}{2})(P_{19} + P_{29})$$

$$P^{ion}_{\frac{1}{2}}(X^2P_{3/2} \rightarrow X^{-1}S_o) = (\tfrac{1}{2})(P_{39} + P_{79})$$

$$P^{ion}_{-\frac{1}{2}}(X^2P_{3/2} \rightarrow X^{-1}S_o) = (\tfrac{1}{2})(P_{89} + P_{49})$$

$$P^{ion}_{-3/2}(X^2P_{3/2} \rightarrow X^{-1}S_o) = (\tfrac{1}{2})(P_{59} + P_{69})$$

are the probabilities of ionisation starting from the 4 substates of the X atom, as would be measured by an experiment in which the X atom was state-selected. Computation confirmed the expectation that

$$P^{ion}_{m}(X^2P_{3/2} \rightarrow X^{-1}S_o) = P^{ion}_{-m}(X^2P_{3/2} \rightarrow X^{-1}S_o)$$

$$m = 3/2,\ \tfrac{1}{2} \qquad \text{I(10.24)}$$

In order to make use of the Landau-Zener approximation, it is again necessary to define a molecular basis (see § I.7). Proceeding as before it is found that

$$P_{79} = P_{89} = \tfrac{1}{2} P_{LZ}$$

where, as before, P_{LZ} is given by I(10.13) except that H_{12} is now $-\sqrt{2}$ times the value used in I(10.8) (a) and (b). (See Table 4 and § I.9 (d)).

Hence

$$\bar{P}^{LZ}_{ion}(X^2P_{3/2} \rightarrow X^{-2}S_{\frac{1}{2}}) = \tfrac{1}{8} P_{LZ} \qquad \text{I(10.25)}$$

figure 14

$\overline{P}_{ion}(X^2P_{3/2} \rightarrow X^{-1}S_o)$ (-) and $\overline{P}_{ion}(X^2P_{3/2} \rightarrow X^{-1}S_o)$ (---) as functions of impact parameter, b.

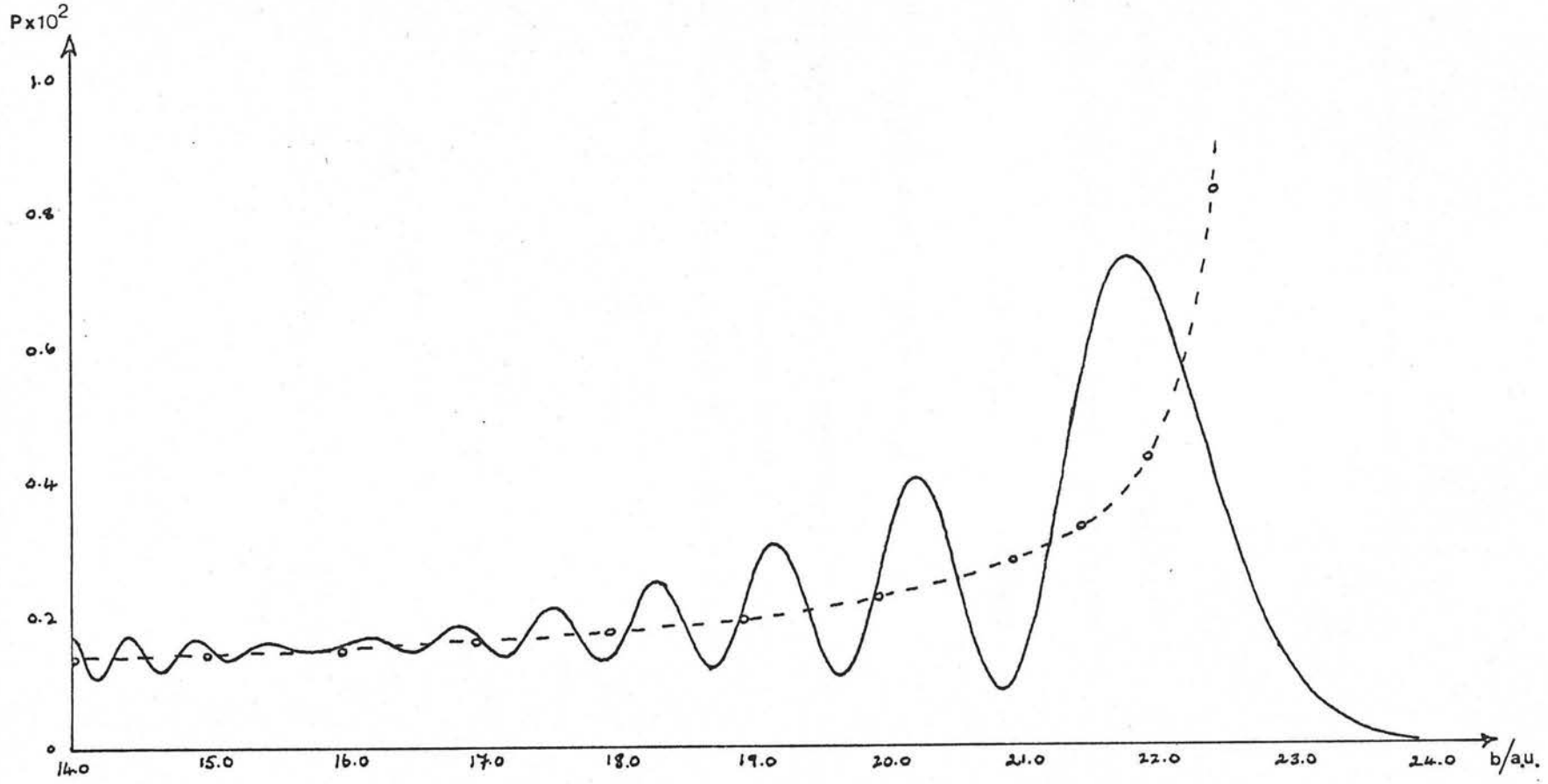

$\bar{P}_{ion}(X^2P_{3/2} \rightarrow X^{-1}S_o)$ and $\bar{P}^{LZ}_{ion}(X^2P_{3/2} \rightarrow X^{-1}S_o)$ are displayed as functions of impact parameter, b, in Figure 14. The close similarity of the functions $\bar{P}_{ion}(X^2P_{3/2} \rightarrow X^{-1}S_o)$ and $\bar{P}_{ion}(X^1S_o \rightarrow X^{-2}P_{3/2})$ should be noted. The oscillations are of the same frequency in each case, corresponding extrema are located at identical b values, and even the modulation in the amplitude of the oscillations is very similar. When the Landau-Zener cross section was evaluated for the present case, it was found that

$$\bar{\sigma}^{LZ}_{ion}(X^2P_{3/2} \rightarrow X^{-1}S_o) = 0.93\text{Å}^2$$

which is very close to one quarter of the value for the process

$$M(^2S_{\frac{1}{2}}) + X(^1S_o) \rightarrow M^+(^1S_o) + X^-(^2P_{3/2})$$

It would again appear then, that so far as ion production from unselected collision partners is concerned, the two processes are virtually identical after account is taken of the different multiplicities of initial (neutral) states.

The damping of the oscillations in $\bar{P}_{ion}(X^2P_{3/2} \rightarrow X^{-1}S_o)$ for b ~ 15.5 a.u. can be accounted for by noting that

$$\bar{P}_{ion}(X^2P_{3/2} \rightarrow X^{-1}S_o) = (\tfrac{1}{2})\{P^{ion}_{3/2}(X^2P_{3/2} \rightarrow X^{-1}S_o) + P^{ion}_{\frac{1}{2}}(X^2P_{3/2} \rightarrow X^{-1}S_o)\} \qquad \text{I(10.26)}$$

figure 15

$P^{ion}_{3/2}(X^2P_{3/2} \rightarrow X^{-1}S_o)$ (---) and $P^{ion}_{\frac{1}{2}}$ $(X^2P_{3/2} \rightarrow X^{-1}S_o)$ (-) as functions of impact parameter, b.

83

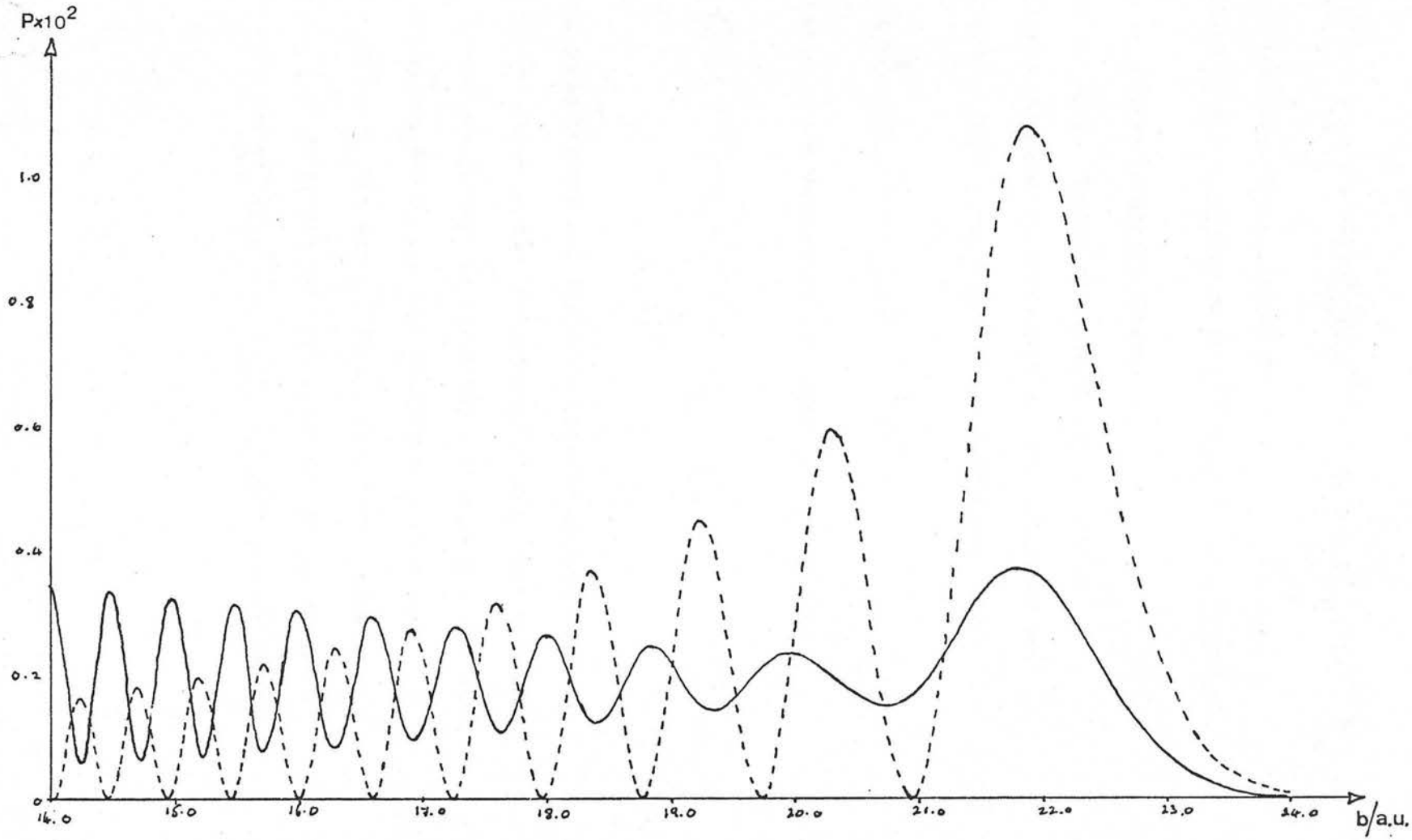

$P^{ion}_{3/2}(X^2P_{3/2} \rightarrow X^{-1}S_o)$ and $P^{ion}_{\frac{1}{2}}(X^2P_{3/2} \rightarrow X^{-1}S_o)$ are displayed as functions of impact parameter (E = 50 eV) in Figure 15 where it can be seen that $P^{ion}_{3/2}(X^2P_{3/2} \rightarrow X^{-1}S_o)$ decreases as b decreases and increases to nearly three times $P^{ion}_{\frac{1}{2}}(X^2P_{3/2} \rightarrow X^{-1}S_o)$ at the outermost maximum in the two functions (b ≈ 22 a.u.). This, together with the fact that the oscillations in the two functions appear to be ~ 90° out of phase in the region 14 ≲ b ≲ 18 a.u., accounts for the modulation in the amplitude of the oscillations in $\bar{P}_{ion}(X^2P_{3/2} \rightarrow X^{-1}S_o)$.

An analysis similar to that used to account for the behaviour of $P^{3/2}_{ion}(X^1S_o \rightarrow X^{-2}P_{3/2})$ may be used again here.

At R_c on the inward half trajectory,

$$\theta = \theta_c = \sin^{-1}(b/R_c)$$

and there are again two limiting cases of interest:

a. $b \approx o, \quad \theta_c \approx o$

b. $b \approx R_c, \quad \theta_c \approx \pi/2$

Suppose it is assumed that

i. there are no transitions between states defined relative to space fixed axes for $R > R_c$, and that

ii. for $R < R_c$ transitions are possible only between states (defined relative to rotating axes) which are connected by the Hamiltonian.

Similarly, by considering the magnitudes of $a_1(t_c)$ when the system is initially prepared in atomic states $1 \to 8$, it can be shown that

$$P^{ion}_{3/2}(X^2P_{3/2} \to X^{-1}S_o) = 3\, P^{ion}_{\frac{1}{2}}(X^2P_{3/2} \to X^{-1}S_o) \text{ at } b = R_c.$$

It is of interest to estimate the relative magnitudes of the cross-sections for ionisation from the states $M(j = \frac{1}{2}\ m = \pm\frac{1}{2})\ X(j=3/2,\ m = 3/2)$, $\sigma^{ion}_{3/2}(X^2P_{3/2} \to X^{-1}S_o)$ and $M(j=\frac{1}{2},\ m=\pm\frac{1}{2})\ X(j = 3/2,\ m = \frac{1}{2})$ $\sigma^{ion}_{\frac{1}{2}}(X^2P_{3/2} \to X^{-1}S_o)$, since these cross sections would be measured in a scattering experiment in which the X atom is substate selected but the M atom is unselected. From I(10.26) it is clear that

$$\bar{\sigma}_{ion}(X^2P_{3/2} \to X^{-1}S_o) = \tfrac{1}{2}\{\sigma^{ion}_{3/2}(X^2P_{3/2} \to X^{-1}S_o) + \sigma^{ion}_{\frac{1}{2}}(X^2P_{3/2} \to X^{-1}S_o)\}$$

and I(10.25) suggests that

$$\bar{\sigma}_{ion}(X^2P_{3/2} \to X^{-1}S_o) = (\tfrac{1}{8})\sigma_{LZ}$$

so that $$\sigma^{ion}_{3/2}(X^2P_{3/2} \to X^{-1}S_o) + \sigma^{ion}_{\frac{1}{2}}(X^2P_{3/2} \to X^{-1}S_o) = \tfrac{1}{4}\sigma_{LZ}$$

I(10.29)

Because of the strongly oscillatory behaviour of $P^{ion}_m(X^2P_{3/2} \to X^{-1}S_o)$ (as a function of b), the cross sections are rather difficult to evaluate. However they were evaluated approximately as follows.

It is convenient to define

$$S_m^{ion}(b_o \to b_f) = 2\pi \int_{b_o}^{b_f} b\, P_m^{ion}(X^2P_{3/2} \to X^{-1}S_o)db \qquad I(10.30)$$

so that $$\sigma_{3/2}^{ion}(X^2P_{3/2} \to X^{-1}S_o) = S_{3/2}^{ion}(o \to 17.2) + S_{3/2}^{ion}(17.2 \to 24.0)$$

and $$\sigma_{\frac{1}{2}}^{ion}(X^2P_{3/2} \to X^{-1}S_o) = S_{\frac{1}{2}}^{ion}(o \to 16.9) + S_{\frac{1}{2}}^{ion}(16.9 \to 24.0)$$

$S_{3/2}^{ion}(17.2 \to 24.0)$ and $S_{\frac{1}{2}}^{ion}(16.9 \to 24.0)$ were evaluated by integrating separately over each of the last five maxima in the functions $P_m^{ion}(X^2P_{3/2} \to X^{-1}S_o)$. A 32-point Gaussian Quadrature was used for the integrations, the values of the functions at the required points being obtained by 6-point interpolation. In addition, it was assumed that

$$S_{3/2}^{ion}(o \to 17.2) \approx S_{3/2}^{ion}(17.2 \to 24.0) - S_{3/2}^{ion}(18.0 \to 24.0)$$

$$= 0.04 \text{ Å}^2$$

which will almost certainly result in $\sigma_{3/2}^{ion}(X^2P_{3/2} \to X^{-1}S_o)$ being underestimated.

Finally, making use of I(10.29), it was found that

$$\sigma_{3/2}^{ion}(X^2P_{3/2} \to X^{-1}S_o)/\sigma_{\frac{1}{2}}^{ion}(X^2P_{3/2} \to X^{-1}S_o) \geq 0.87$$

In addition it is expected that the ratio $\sigma_{ion}^{3/2}(X^1S_o \to X^{-2}P_{3/2})/\sigma_{ion}^{\frac{1}{2}}(X^1S_o \to X^{-2}P_{3/2})$ will have approximately the same value, where $\sigma_{ion}^{m}(X^1S_o \to X^{-2}P_{3/2})$ are the cross sections appropriate to the

figure 16

σ_{LZ} as a function of energy, E, H_{12}(molecular) = $\frac{1}{2}\bar{H}$, $\bar{H}$, $3/2\bar{H}$

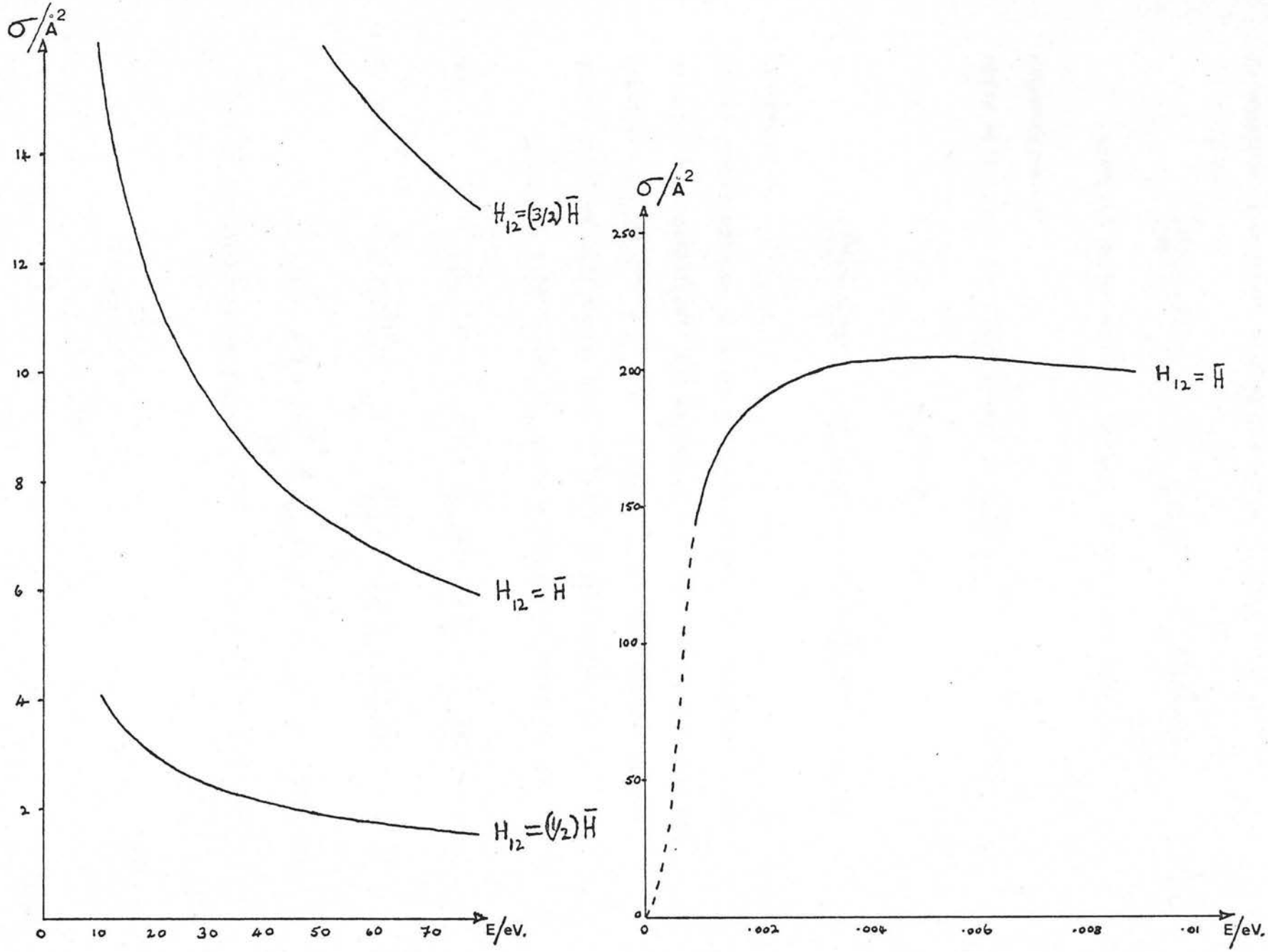

probabilities $P^{m}_{ion}(X\,^1S_o \rightarrow X^{-2}P_{3/2})$ (eq'n I(10.6)).

An indication of the dependence of the average cross section for ionisation on Energy and H_{12} for the various systems, can be obtained from the dependence of σ_{LZ} on these parameters. σ_{LZ} (H_{12} appropriate to a two-electron molecular basis) is displayed as a function of E (E = 10-80 eV) and $H_{12}(R_c)$ ($H_{12}(R_c) = \frac{1}{2}\bar{H}, \bar{H}, 3/2\bar{H}$, $\bar{H} = 2.0 \times 10^{-3}$ eV) in figure 16 where it can be seen that the chosen parameterisation of H_{11}, H_{12} and H_{22} is such that the high energy 'tail' of the $\sigma(E)$ function is being used.

E. Different Values of Energy and $H_{12}(R_c)$

The basic fact that has emerged from § I.10(A) _ (D) is that for the energy (50 eV) and value of $H_{12}(R_c)$ ($\bar{H} = 2 \times 10^{-3}$ eV) considered, the Landau-Zener approximation compares very favourably with a complete numerical solution including Coriolis coupling in the range of impact parameters considered.

The reasons for this are

i. the Landau-Zener adiabatic transition probabilities, p, are ≈1 (p(b = 14 a.u.) = 0.997) and

ii. the Massey parameter for Coriolis coupling, λ, is <<1

$\lambda = \frac{\Delta v \tau}{h} = \Delta v \tau$ in atomic units.

$\tau = 1/v$ and states 1 and 3 (see eq'n I(7.1)) are connected by Coriolis coupling, so that

$$\Delta v = |H_{11} - H_{33}| = \tfrac{1}{4}|\bar{E}_{cov}| \qquad \text{(See Table 4)}$$

Hence $$\lambda \sim |\bar{E}_{cov}|/4v \; ; \; v = (2E/\mu)^{\frac{1}{2}}(1-(b/R)^2-U/E)^{\frac{1}{2}}$$

For b = 18 a.u. and E = 50 eV λ varies from $\sim 5 \times 10^{-3}$ at R = 18.5 a.u. to $\sim 3 \times 10^{-4}$ at R = 24.5 a.u. Clearly for the impact parameters considered the Massey parameter for coriolis coupling is very small for all but a very short part of the trajectory near the turning point.

It is therefore interesting to examine the situation when the parameters are so chosen that $p \sim 0.5$ and the Massey parameter is somewhat larger. This can be achieved by increasing $H_{12}(R_c)$ and decreasing E. If however, $H_{12}(R_c)$ is increased too much or E is decreased too much, the distance at which computation is started may have to be made very large (see § I.9 equations I(9.16) and I(9.17)).

For this reason the compromise values

$$E = 2.0 \text{ eV} \quad \text{and} \quad H_{12}(R_c) = 5 \times \text{original value}$$

were chosen and computation was started at 40 a.u. For these parameters

$p_{LZ}(b = 14 \text{ a.u.}) = 0.5$

and for b = 18 a.u. λ varies from $\sim 2.5 \times 10^{-2}$ at R = 18.5 a.u. to $\sim 1.5 \times 10^{-3}$ at R = 24.5 a.u. Coriolis coupling, though still weak, is somewhat stronger than previously.

Of course E = 2.0 eV is rather close to the threshold for ionisation (1.2 eV) and since a single energy is assumed for the

figure 17

$\overline{P}^{LZ}_{ion}(X^2P_{3/2} \rightarrow X^- {}^1S_o)$ (—●—), numerical solution of 2-state problem (--o--) and $\overline{P}_{ion}(X^2P_{3/2} \rightarrow X^- {}^1S_o)$ (—△—) as functions of b, E = 2.0 e.V., H_{12} = 5 x original

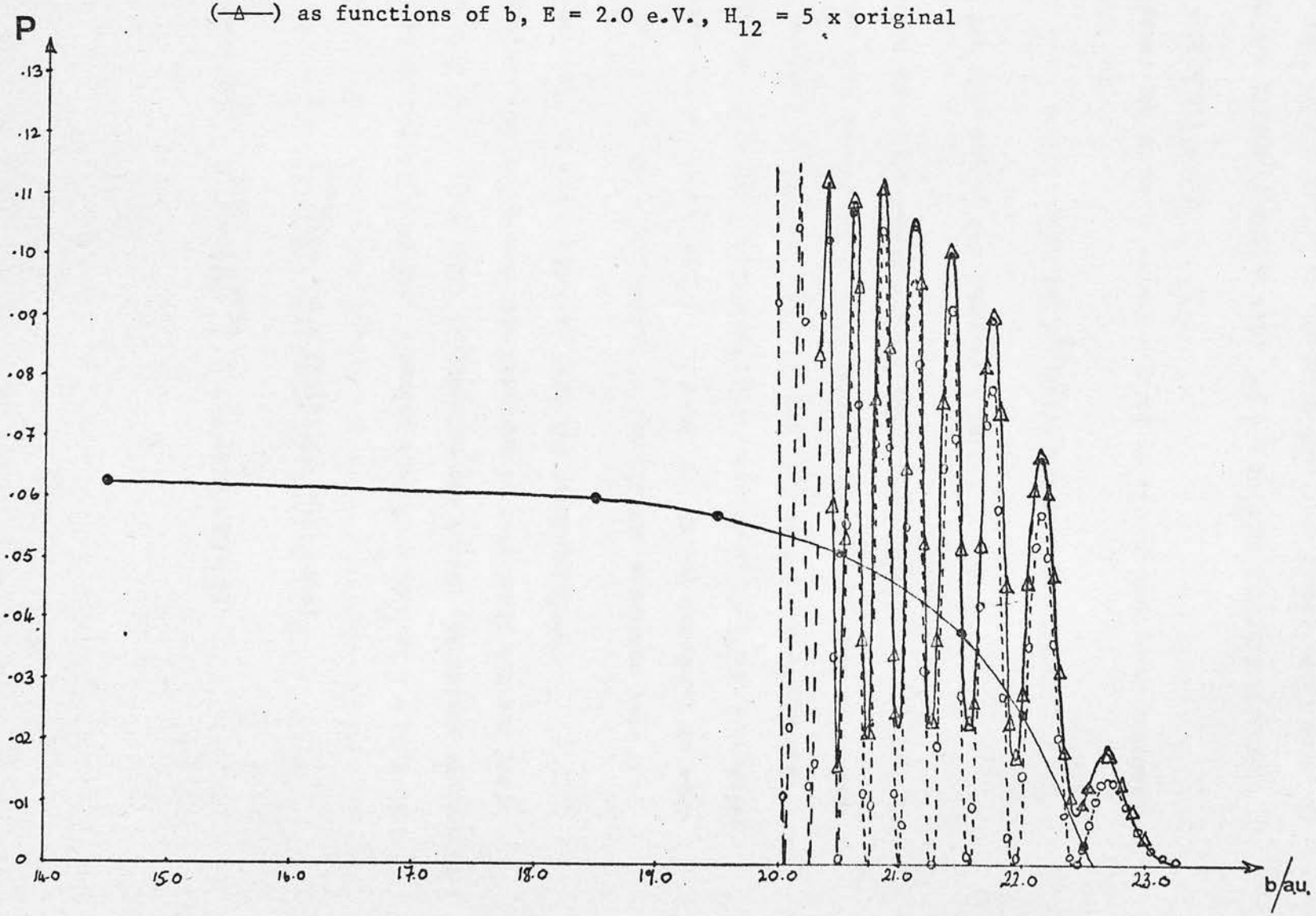

trajectory, the actual numerical values cannot be taken as being particularly meaningful.

$\bar{P}_{ion}(X^2P_{3/2} \rightarrow X^{-1}S_o)$, $\bar{P}^{LZ}_{ion}(X^2P_{3/2} \rightarrow X^{-1}S_o)$ and the numerical solution of the 2-state problem are displayed as functions of impact parameter for the new values of E and $H_{12}(R_c)$ in Figure 17.

It can be seen that although the 2-state oscillating solution is no longer perfectly centred on the Landau-Zener approximation even for $b \neq R_c$, the displacement is within a factor of two and becomes much smaller as b decreases. In view of the rather strong coupling which now exists between the two states, this result is noteworthy.

It can also be seen that the numerical 2-state solution is still rather a good approximation to the numerical solution of the 9-state system including coriolis coupling, the periodicity of the oscillations being identical in the two cases. The fact that there is only slight distortion of the 2-state solution is probably due to the fact that coriolis coupling is still rather weak as already noted.

SUMMARY

i. The Landau-Zener approximation, carefully applied, accurately estimates substate-averaged ionisation probabilities when $p_{LZ} \approx 1$ and is still accurate within a factor of two when $p_{LZ} \approx 0.5$ provided the Massey parameter, λ, for coriolis

coupling is $< 10^{-2}$ for most of the trajectory.

ii. High frequency structure in the ionisation probabilities is well accounted for in terms of Stueckelberg oscillations.

iii. A more detailed analysis of the ionisation process may be given in terms of a simple model which assumes that

A. there are no transitions between states defined relative to space-fixed axes for $R > R_c$ (free rotation)

B. for $R < R_c$ transitions between states defined relative to rotating axes are possible only if the states are connected by the Hamiltonian (coriolos coupling neglected).

This model reproduces the numerical results rather well when the $p_{LZ} \sim 1$ and λ is $\lesssim 5 \times 10^{-3}$ over nearly all of the trajectory.

iv. The processes

$$\left.\begin{array}{l} M(^2S_{\frac{1}{2}}) + X(^1S_o) \rightleftarrows M^+(^1S_o) + X^-(^2S_{\frac{1}{2}}) \\ M(^2S_{\frac{1}{2}}) + X(^2S_{\frac{1}{2}}) \rightleftarrows M^+(^1S_o) + X^-(^1S_o) \end{array}\right.$$

and

$$\left.\begin{array}{l} M(^2S_{\frac{1}{2}}) + X(^1S_o) \rightleftarrows M^+(^1S_o) + X^-(^2P_{3/2}) \\ M(^2S_{\frac{1}{2}}) + X(^2P_{3/2}) \rightleftarrows M^+(^1S_o) + X^-(^1S_o) \end{array}\right.$$

are virtually identical so far as ion production from unselected collision partners is concerned, after account has been taken of the different multiplicities, w, of neutral states:

$$w.\bar{\sigma}_{ion} \propto 3.8 \text{Å}^2 \qquad (E = 50 \text{ eV})$$

v. $\sigma^{ion}_{3/2}(X^2P_{3/2} \rightarrow X^{-1}S_o)/\sigma^{ion}_{\frac{1}{2}}(X^2P_{3/2} \rightarrow X^{-1}S_o) \geq 0.87$

($E = 50$ eV) (See I(10.23)).

vi. At least for KI, the crossing of the ionic potential with the manifold of potentials arising from

$$M(^2S_{\frac{1}{2}}) + X^*(^2P_{\frac{1}{2}})$$

does not significantly affect the ionisation probabilities predicted when these crossings are ignored, provided $\lambda \ll 1$.

I.11 Results and Discussion

Part II Spin-flip in the M atom

(A) $M(^2S_{\frac{1}{2}}) + X(^1S_o) \rightleftarrows M^+(^1S_o) + X^-(^2S_{\frac{1}{2}})$

$$P_{sf}(A) = P_{34} = P_{43} \qquad \left[\text{see } I(10.1)\right] \qquad I(11.1)$$

(B) $M(^2S_{\frac{1}{2}}) + X(^1S_o) \rightleftarrows M^+(^1S_o) + X^-(^2P_{3/2})$

$$P_{sf}(B) = P_{56} = P_{65} \qquad \left[\text{see } I(10.4)\right] \qquad I(11.2)$$

In the simplest possible model in which coupling is due only to the Hamiltonian and only first order transitions are considered,

$$P_{sf}(A) = P_{sf}(B) = 0$$

But if the same model is used here as was used in §I.10 [equation I(10.15)], it is predicted that

$$P_{sf}(A) = P_{sf}(B) \sim \sin^2(\chi + 2\Theta_c)(1 - P_{LZ}) \qquad I(11.3)$$

At b = 14.0 a.u. the value of this function is approximately 0.94. Spin-flip is made possible by the presence of Coriolis coupling.

However, on solving the appropriate coupled equations numerically for the range of impact parameters

$$14.0 \leqslant b \leqslant 24.0 \text{ a.u.}$$

it was found that

$$P_{sf}(A) < 1.0 \times 10^{-13} \text{ and } P_{sf}(B) < 4.5 \times 10^{-5}$$

figure 18

$P_{sf}(B)$ as a function of impact parameter, b.

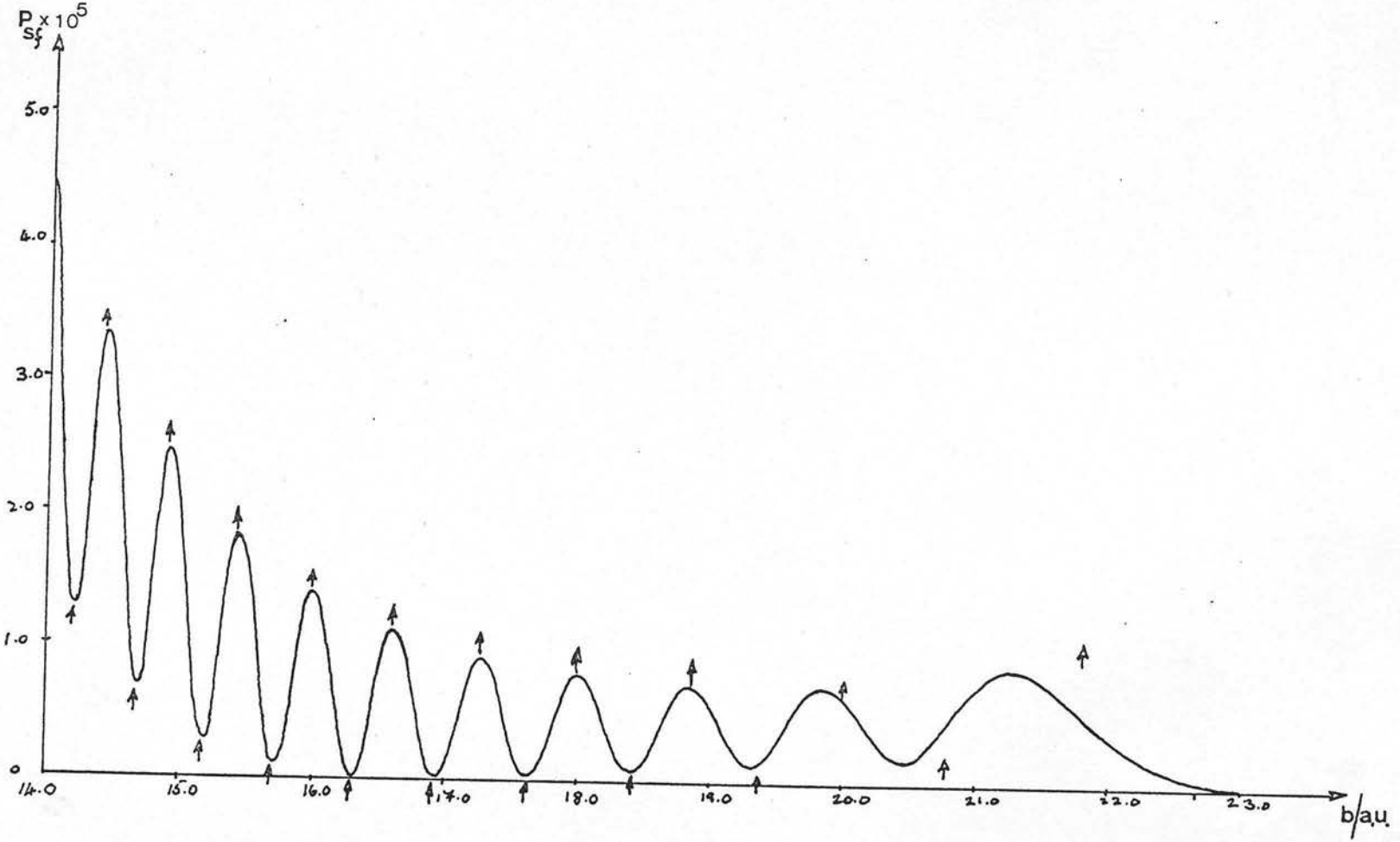

(In this calculation the overlap matrix elements used were those appropriate to the KI system.) It may be that the model represented by equation I(11.3) is not appropriate to spin-flip transitions because Coriolis coupling is important in these processes in the region $R < R_c$, even though λ is small.

$P_{sf}(B)$ is displayed as a function of impact parameter in figure 18. The positions of the extrema in $P_{ion}^{\frac{1}{2}}(X^1S_o \to X^- {}^2P_{3/2})$ are also shown in figure 18 and it is clear that the oscillations in $P_{sf}(B)$ and in $P_{ion}^{\frac{1}{2}}(X^1S_o \to X^- {}^2P_{3/2})$ are of the same frequency and corresponding extrema are located at identical b values (at least for $14 \lesssim b \lesssim 19$ a.u.). In semiclassical terms, this and the fact that $P_{sf}(B)$ quickly $\to 0$ for $R > R_c$, suggests that the spin is flipped at $R \sim R_c$ so that amplitude in the state with spin opposite to the original has two components - one due to motion along the neutral curve from R_c to the distance of closest approach and the other due to motion along the ionic curve.

However, since $P_{sf}(B) < 10^{-2}\, \overline{P}_{ion}(X^1S_o \to X^- {}^2P_{3/2})$ the experimentalist would most readily obtain information about the curve crossing by measuring the ion production cross section.

(C) $M(^2S_{\frac{1}{2}}) + X(^2S_{\frac{1}{2}}) \rightleftarrows M^+(^1S_o) + X^-(^1S_o)$

$$P_{sf}(c) = \tfrac{1}{2}(P_{13} + P_{14} + P_{23} + P_{24}) \quad \left[\text{see I(10.17)}\right] \qquad \text{I(11.4)}$$

For $14 \lesssim b \lesssim 24$ a.u. it was found that

$$P_{13} = P_{24} \lesssim 1.25 \times 10^{-18}$$

$$P_{14} < 1.1 \times 10^{-23}$$

and $P_{23} < 0.132$ (at b = 14 a.u.)

Thus the spin-exchange process in this system appears to be completely dominated by the two-electron process

$$M(j = \tfrac{1}{2}, m = \tfrac{1}{2}) + X(j = \tfrac{1}{2}, m = -\tfrac{1}{2}) \rightarrow M(j = \tfrac{1}{2}, m = -\tfrac{1}{2}) + X(j = \tfrac{1}{2}, m = \tfrac{1}{2})$$

The only non-vanishing matrix elements of the Hamiltonian in the atomic basis are

$$\left\langle \left| \psi^M(j = \tfrac{1}{2}, m = \tfrac{1}{2}),\ \psi^X(j = \tfrac{1}{2}, m = -\tfrac{1}{2}) \right| \right| H \left| \left| \psi^M(j = \tfrac{1}{2}, m = -\tfrac{1}{2})\ \psi^X(j = \tfrac{1}{2}, m = \tfrac{1}{2}) \right| \right\rangle$$

and $$\left\langle \left| \psi^M(j = \tfrac{1}{2}, m = \pm\tfrac{1}{2}),\ \psi^X(j = \tfrac{1}{2}, m = \mp\tfrac{1}{2}) \right| \right| H \left| \psi_{\text{ionic}} \right\rangle$$

Hence spin-flip may occur by two mechanisms, one involving an ionic intermediate and the other involving simultaneous inversion of the spin in M and X i.e. in the atomic description spin-flip may proceed via the transitions $2 \rightarrow 5 \rightarrow 3$ and $2 \rightarrow 3$. Neither of these two mechanisms is available in systems (A) or (B). It is for this reason that $P_{sf}(C) >> P_{sf}(A), P_{sf}(B)$.

In trying to assess the importance of the ionic intermediate mechanism consider the following argument. A simple semiclassical analysis suggests that

$$p(2 \rightarrow 5 \rightarrow 3) = p_{25} \times p^1$$

where p^1 is the probability of the transition $5 \rightarrow 3$ at a single traverse of the curve crossing (in an atomic description), and

figure 20

$P_{sf}(c)$ as a function of impact parameter, b.

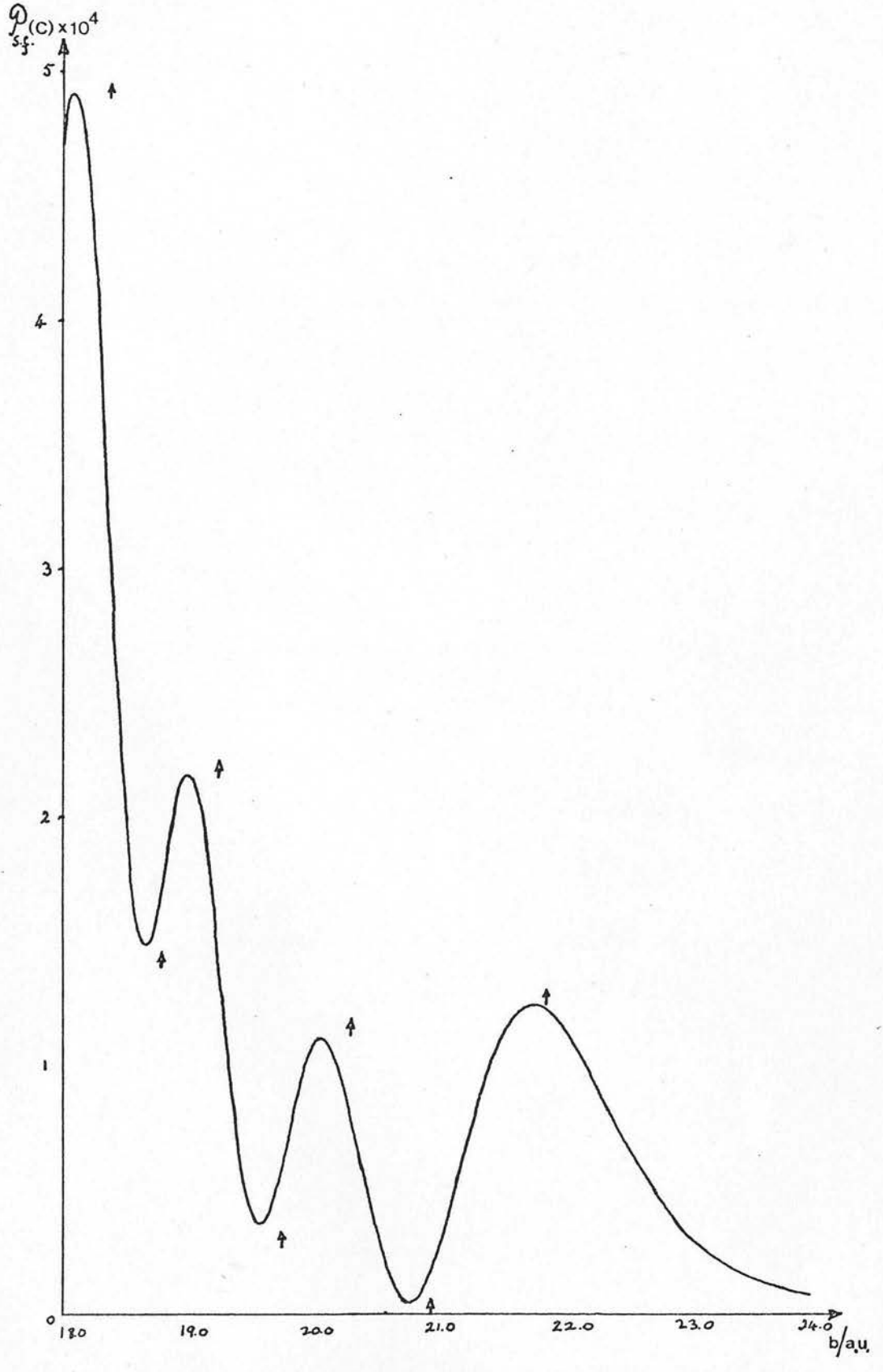

figure 19

$P_{sf}(C)$ as a function of impact parameter, b.

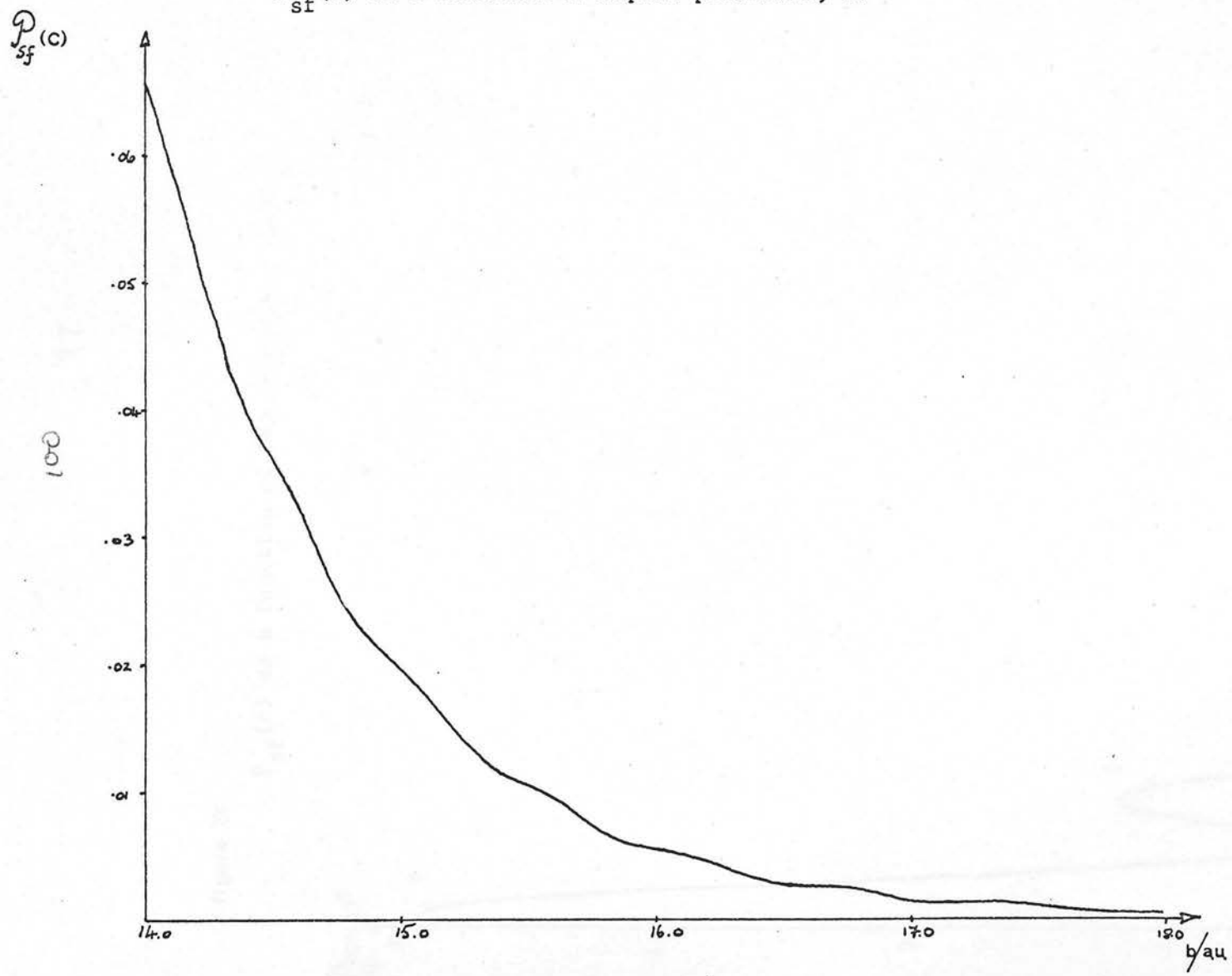

$$p_{25} = \tfrac{1}{2}\rho_{LZ} \qquad \left[I(10.20)\right]$$

At $b = 14$ a.u., $p(2 \to 5 \to 3) = 5.4 \times 10^{-3} p^1 < 5.4 \times 10^{-3}$ $(p^1 < 1)$

At $b = 16$ a.u., $p(2 \to 5 \to 3) = 6.0 \times 10^{-3} p^1 < 6.0 \times 10^{-3}$

and $p_{23}(b = 16) = 1.09 \times 10^{-2}$

Since ρ_{LZ} increases with increasing b and p_{23} (computed) decreases with increasing b, it appears that for $b < 14$ a.u. the simultaneous double spin exchange mechanism dominates, but that the ionic intermediate mechanism may become relatively more important as $b \to R_c$. These remarks only apply, of course to the parameters used in the various computations - values of Hamiltonian matrix elements, Energy (50 eV) and overlap matrix elements (appropriate to KI).

$P_{sf}(c)$ is displayed as a function of impact parameter in figures 19 and 20. The positions of the extrema in $\overline{P}_{ion}(X^2S_{\frac{1}{2}} + \overline{X}^1S_o)$ are also shown in figure 20 and it can be seen that the oscillations in $P_{sf}(c)$ are of approximately the same frequency as those in the ionisation probability, but the positions of the extrema are shifted slightly. The relatively small amplitude of these oscillations for $b \sim 14$ a.u. is in accord with the observations of the previous paragraph.

$P_{sf}(c) / \overline{P}_{ion}(X^2S_{\frac{1}{2}} \to \overline{X}^1S_o)$ varies from ~1.6 ($b = 16$ a.u.) to ~26 ($b = 14$ a.u.) so that, for this system, the differential cross section for spin-flip probably varies from ~1.6 times ($\chi = 0.36^o$) to ~26 times ($\chi = 0.35^o$) the differential cross section for ionisation.

figure 22 $P_{sf}(D)$ as a function of impact parameter, b.

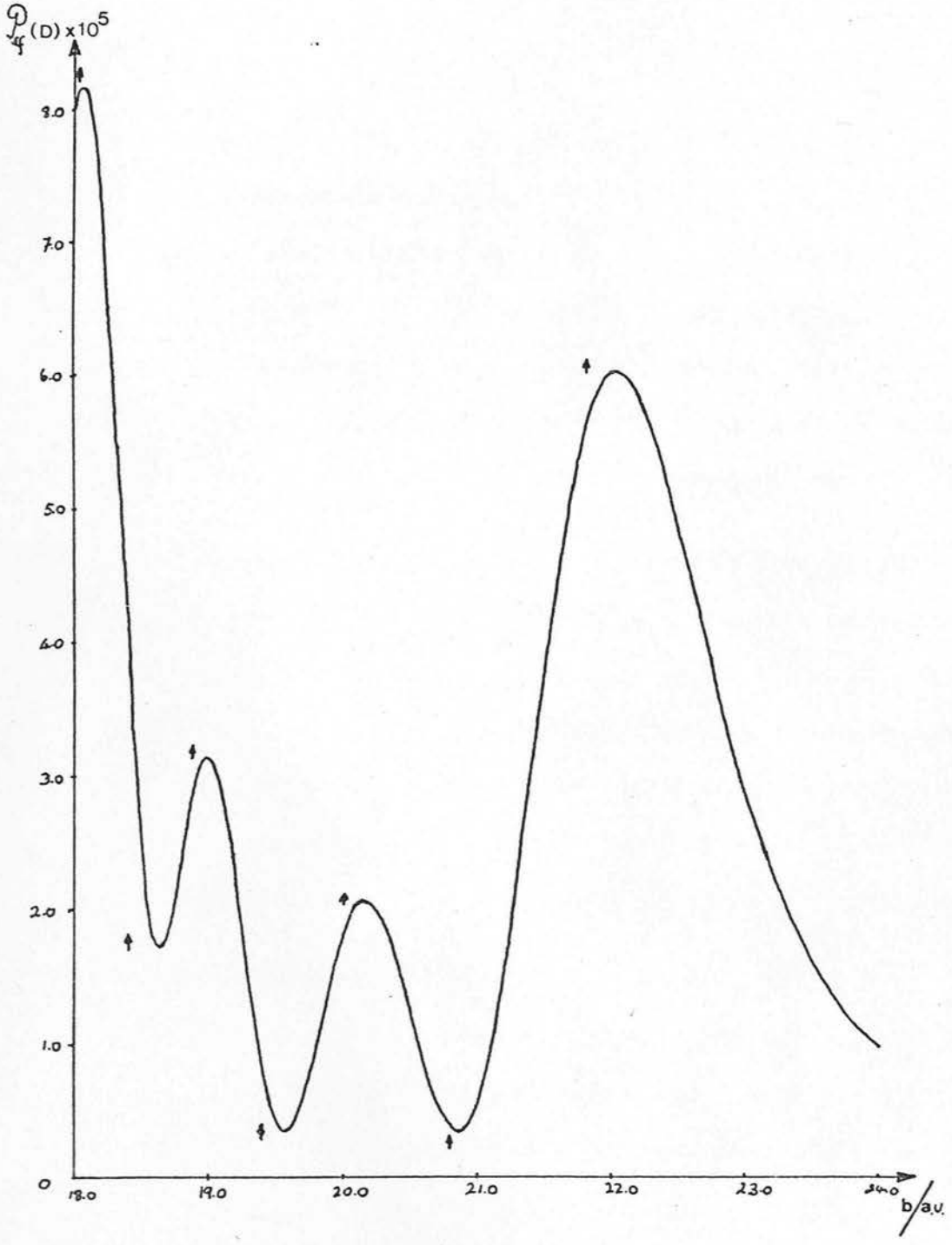

figure 21 $P_{sf}(D)$ as a function of impact parameter, b.

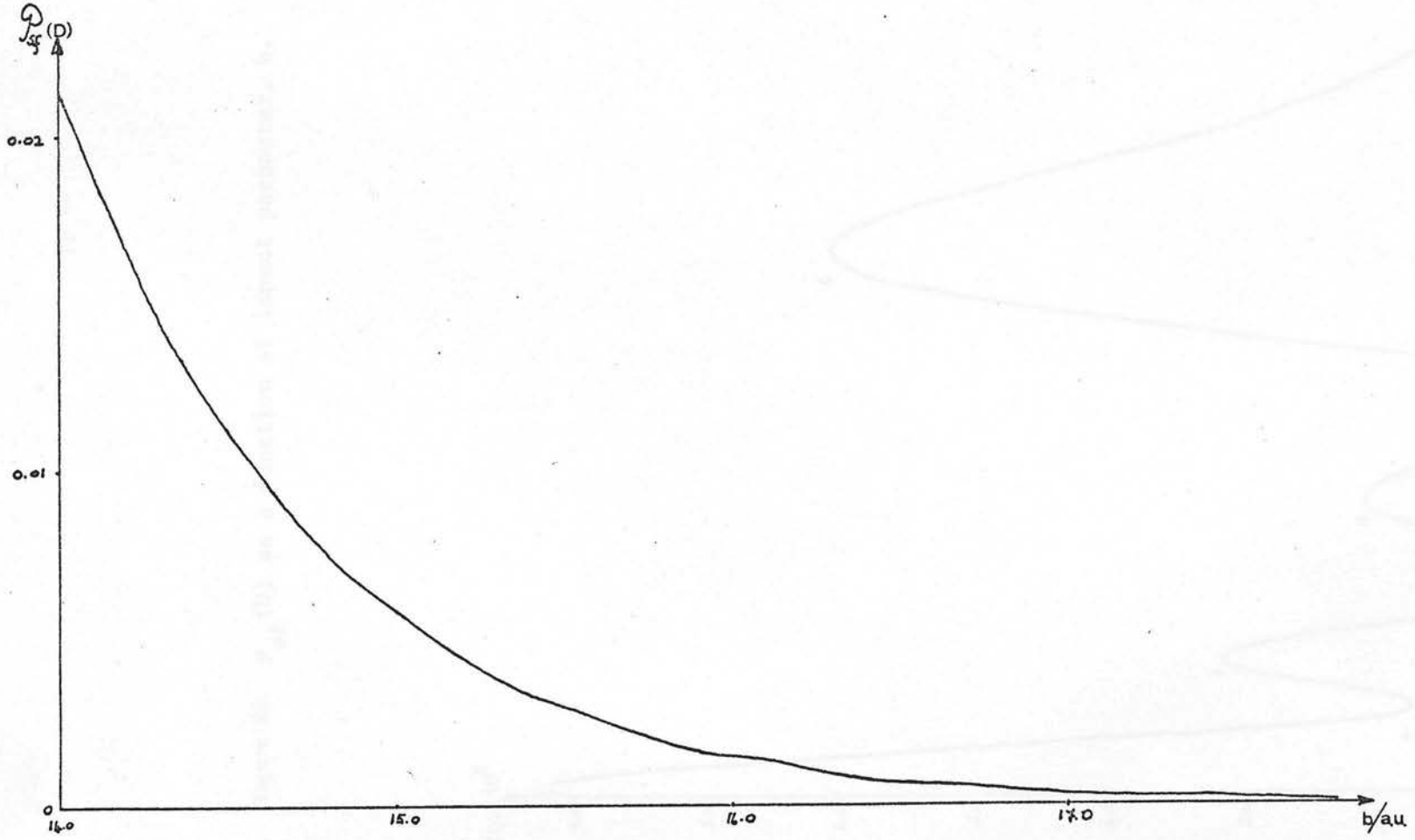

(D) $$M(^2S_{\frac{1}{2}}) + X(^2P_{3/2}) \rightleftarrows M^+(^1S_o) + \bar{X}(^1S_o)$$

$$P_{sf}(D) = \tfrac{1}{4}(P_{12} + P_{14} + P_{16} + P_{17} + P_{32} + P_{34} + P_{36} + P_{37} + P_{52} + P_{54} + P_{56} + P_{57} + P_{82} + P_{84} + P_{86} + P_{87}) \qquad I(11.5)$$

[see I(10.22)] .

It was found that for 14 a.u. $\leq b \leq$ 24 a.u. , P_{32}, P_{34}, P_{52} and P_{54} form the dominant contributions to $P_{sf}(D)$; that is, the dominant spin-flip transitions are

$M(j=\frac{1}{2}, m=\frac{1}{2}) + X(j=3/2, m=\frac{1}{2}) \rightarrow M(j=\frac{1}{2}, m=-\frac{1}{2}) + X(j=3/2, m=3/2)$

$M(j=\frac{1}{2}, m=\frac{1}{2}) + X(j=3/2, m=\frac{1}{2}) \rightarrow M(j=\frac{1}{2}, m=-\frac{1}{2}) + X(j=3/2, m=-\frac{1}{2})$

$M(j=\frac{1}{2}, m=\frac{1}{2}) + X(j=3/2, m=-3/2) \rightarrow M(j=\frac{1}{2}, m=-\frac{1}{2}) + X(j=3/2, m=3/2)$

$M(j=\frac{1}{2}, m=\frac{1}{2}) + X(j=3/2, m=-3/2) \rightarrow M(j=\frac{1}{2}, m=-\frac{1}{2}) + X(j=3/2, m=-\frac{1}{2})$

(All $\Omega = 1 \rightarrow 1$ transitions.)

None of the initial or final states are directly connected to each other or to the ionic state by the Hamiltonian. However, all initial and final states are connected by Coriolis coupling to states with $\Omega = 0$ which are coupled to the ionic state.

This system differs from (C) above in that the transition $M(j=\frac{1}{2}, m=\frac{1}{2}) + X(j=3/2, m=-\frac{1}{2}) \rightarrow M(j=\frac{1}{2}, m=-\frac{1}{2}) + X(j=3/2, m=\frac{1}{2})$, which could proceed (by Hamiltonian coupling alone) either directly or via an ionic intermediate, does not dominate the spin-flip process.

$P_{sf}(D)$ is displayed in figures 21 and 22 as a function of impact

parameter. Also shown in figure 22 are the positions of the extrema in $P^{ion}_{\frac{1}{2}}(X\ ^2P_{3/2} \rightarrow X^-\ ^1S_o)$. The oscillations in $P_{sf}(D)$ are of approximately the same frequency as those in the ionisation probability but the positions of the extrema are shifted slightly.

$P_{sf}(D) / \overline{P}_{ion}(X\ ^2P_{3/2} \rightarrow X^-\ ^1S_o)$ varies from ~0.14 (b = 17.2 a.u.) to ~15 (b = 14.0 a.u.) so that, for this system, the differential cross section for spin-flip probably varies from ~0.14 times ($\chi = 0.25^o$) to ~15 times ($\chi = 0.35^o$) the differential cross section for ionisation.

SUMMARY

The following are the observations when $p \simeq 1$ ($P_{LZ} = 2p(1-p)$, $\lambda << 1$, and KI overlap matrix elements are used.

(i) The total cross section for spin-flip, $\overline{\sigma}_{sf}$, in the system

$$M(^2S_{\frac{1}{2}}) + X(^1S_o) \rightleftarrows M^+(^1S_o) + X^-(^2S_{\frac{1}{2}})$$

is essentially zero.

(ii) For the system

$$M(^2S_{\frac{1}{2}}) + X(^1S_o) \rightleftarrows M^+(^1S_o) + X^-(^2P_{3/2})$$

$\overline{\sigma}_{sf} << \overline{\sigma}_{ion}$.

iii) The free rotation/Hamiltonian only model does <u>not</u> account for spin-flip cross sections. Presumably Coriolis coupling is important for $R < R_c$.

(iv) In the system (C)

$$M(^2S_{\frac{1}{2}}) + X(^2S_{\frac{1}{2}}) \rightleftarrows M^+(^1S_o) + X^-(^1S_o)$$

the differential cross section for spin flip, $\bar{I}_{sf}$, varies from ~1.6 times ($\chi = 0.36^o$) to ~26 times ($\chi = 0.35^o$) the differential cross section for ionisation, $\bar{I}_{ion}$.

(v) In system (C), spin flip appears to proceed mainly by either an ionic intermediate or simultaneous two-electron spin exchange depending on whether or not $b \sim R_c$.

(vi) For the system (D)

$$M(^2S_{\frac{1}{2}}) + X(^2P_{3/2}) \rightleftarrows M^+(^1S_o) + X^-(^1S_o)$$

$\bar{I}_{sf}$ varies from ~0.14 times ($\chi = 0.25^o$) to ~15 times ($\chi = 0.35^o$) $\bar{I}_{ion}$.

vii) Coriolis coupling plays a vital part in spin-flip in system (D).

PART II

Elastic and Inelastic Differential Cross Sections

for two crossing, monotonic repulsive potentials

II.1 Introduction

A commonly encountered situation in high energy scattering experiments is that of scattering from two monotonic repulsive potentials which have an accessible crossing. In such a situation there is the possibility of elastic and inelastic scattering with structure in both differential cross sections.

Differential cross section measurements for the systems K/CH_3I, K/SF_6, K/Ar and K/N_2 have recently been reported (KER74) for energies in the centre of mass (c.m.) frame of about 200 eV. Only very weak structure was seen for K/Ar and for none of the other systems was any structure seen in the angular range $0^\circ<\theta<4^\circ$. In these experiments, elastic and inelastic events were not distinguished. The purpose of the calculations to be described is to determine whether the lack of structure in the combined differential cross section is due to the fact that resolvable oscillations in the elastic and inelastic differential cross sections are necessarily out of phase. The effectiveness of this cancellation depends upon the magnitudes, periods and phases of the resolvable oscillations in the two differential cross sections.

Two model potentials were constructed for K(4s) + Q and $K^*(4p)$ + Q, where Q is some atomic or molecular species whose mass was assumed to be approximately that of potassium. The scattering amplitudes (for an energy of 200 eV in the c.m. frame) were evaluated in terms of the usual partial wave analysis, and the

elastic and inelastic phase shifts were calculated from an approximate semi-classical solution of the coupled equations describing transitions between the two states involved in the curve crossing. Each ℓ value in the partial wave summation is related (in a semi-classical analysis) to a particular value of impact parameter, b, by

$$p_o b = (\ell + \tfrac{1}{2})$$

where p_o is the asymptotic relative momentum of the colliding partners. In this relation, and in all other calculations, atomic units (as defined in §I) were used.

figure 1

Curve Crossing and Phase Shifts

(a)

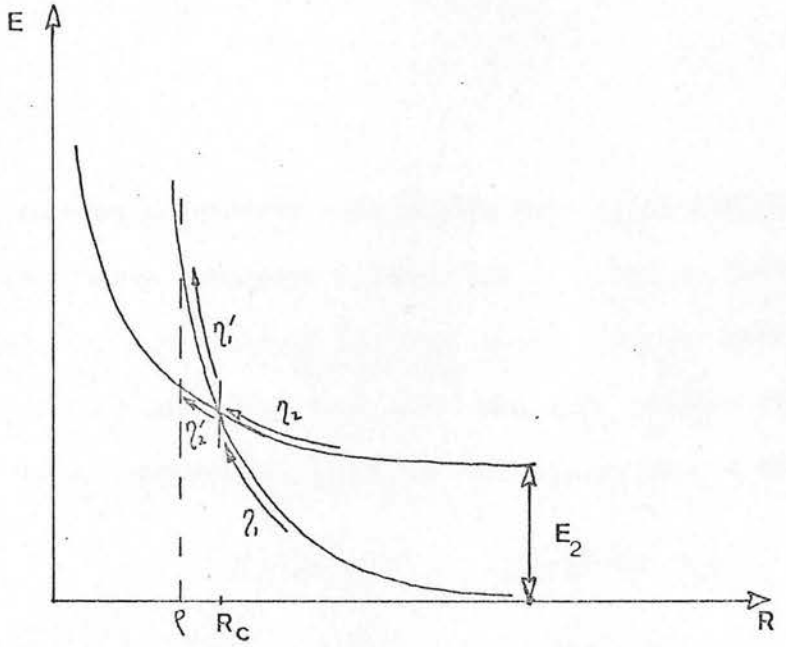

$\rho < R_c$

(b)

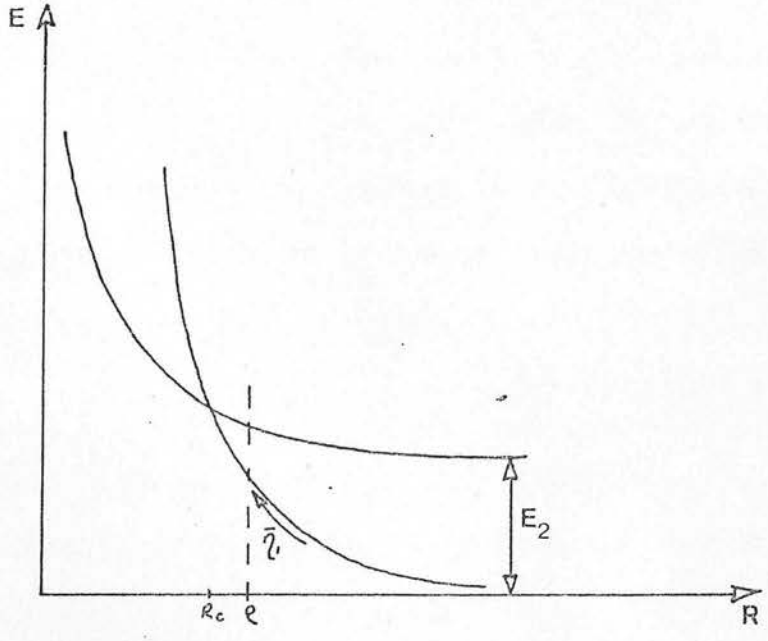

$\rho > R_c$

R_c is the crossing point of H_{11} and H_{22}, and η_1 etc are the phase shifts ρ is the distance of closest approach.

II.2 Differential Cross Sections - S matrix elements

The elastic and inelastic scattering differential cross sections are defined, by means of the usual partial wave analysis, as

$$\sigma_{e\ell}(\theta) = |f_{e\ell}(\theta)|^2 , \quad \sigma_{inel}(\theta) = |f_{inel}(\theta)|^2$$

where $$f_{e\ell}(\theta) = (1/2ik_{e\ell})\Sigma_{\ell=0}^{\infty}(2\ell+1)(S_{\ell\ell}^{e\ell}-1)P_{\ell}(\cos\theta)$$

$$f_{inel}(\theta) = (1/2ik_{\ell})\Sigma_{\ell=0}^{\infty}(2\ell+1)S_{\ell\ell}^{inel}P_{\ell}(\cos\theta) \quad \text{II(2.1)}$$

and $S_{\ell\ell}^{e\ell}$ and $S_{\ell\ell}^{inel}$ are the diagonal elements of the S-matrices for elastic and inelastic scattering respectively.

Calculation of S-matrix elements

Both elastic and inelastic events are discussed in terms of curve crossings (Figure 1). Suppose the system is initially prepared in diabatic state 1. In semi-classical terms, elastic scattering is the result of two possible processes.

a. The system remains in state 1 throughout the encounter

b. There is a transition from state 1 to state 2 at $R = R_c$ (the crossing distance) on the inward part of the trajectory, and there is a transition from state 2 to state 1 on the outward part of the trajectory, provided the distance of closest approach, ρ, lies inside the crossing distance R_c.

Inelastic scattering is the result of one of two different processes (provided $\rho < R_c$).

a. There is a transition from state 1 to state 2 at R_c on the inward part of the trajectory, after which the system remains in state 2.

b. The system remains in state 1 until the outward traverse of R_c when there is a transition from state 1 to state 2.

When the complete wave function of the system, Ψ, is expanded in terms of the wave functions ψ_1 and ψ_2 describing the diabatic states 1 and 2,

$$\Psi = a_1 \psi_1 + a_2 \psi_2$$

and this expansion is substituted into the time-dependent Schrodinger Equation

$$H\Psi = i\hbar\partial\Psi/\partial t$$

The solution of the resulting pair of coupled equations (in atomic units).

$$\begin{Bmatrix} \dot{a}_1 \\ \dot{a}_2 \end{Bmatrix} = -i \begin{Bmatrix} H_{11} & H_{12} \\ H_{12} & H_{22} \end{Bmatrix} \begin{Bmatrix} a_1 \\ a_2 \end{Bmatrix} \qquad \text{II(2.2)}$$

subject to the boundary condition $a_1(o) = 1$

$a_2(o) = 0$

(the basis has been assumed orthonormal and time-independent), determines the elastic ($a_1(\infty)$) and inelastic ($a_2(\infty)$) transition

amplitudes as functions of ℓ (when a trajectory analysis is used). $a_1(\infty)$ and $a_2(\infty)$ may be identified with the matrix elements $S^{el}_{\ell\ell}$ and $S^{inel}_{\ell\ell}$ respectively.

The equations II(2.2) were solved in the same approximate semi-classical scheme as that described in Section I.8.

An amplitude matrix

$$A_{\sim}(t) = \begin{Bmatrix} a_1(t) \\ a_2(t) \end{Bmatrix} ,$$

A transition matrix

$$\underset{\sim}{B} = \begin{Bmatrix} a\,p^{\frac{1}{2}} & b(1-p)^{\frac{1}{2}} \\ c(1-p)^{\frac{1}{2}} & d\,p^{\frac{1}{2}} \end{Bmatrix}$$

and phase matrices

$$\underset{\sim}{\Phi}_1 = \begin{Bmatrix} \exp(-i\eta_1) & o \\ o & \exp(-i\eta_2) \end{Bmatrix} \qquad \text{II(2.3)}$$

$$\text{and} \quad \underset{\sim}{\Phi}_2 = \begin{Bmatrix} \exp(-i\eta_1^1) & o \\ o & \exp(-i\eta_2^1) \end{Bmatrix}$$

were defined as before, a, b, c and d were chosen in the way described in §I.8,

and $$\eta_n = \int_{-\infty}^{\epsilon_c} H_{nn}\, dt$$

The approximate solution to equations II(2.2) was obtained for two cases

a. $\underline{\rho \leq R_c}$

$$\underline{A}(\infty) = (\underline{\Phi}_1 \cdot \underline{B}^* \cdot \underline{\Phi}_2 \, \underline{\Phi}_2 \, \underline{B} \, \underline{\Phi}_1)\underline{A}(o)$$

Hence it can easily be shown that

$$S_{\ell\ell}^{el} = a_1(\infty) = pe^{2i\zeta_1} + (1-p)e^{2i\zeta_2}, \quad \zeta_1 = -(\eta_1 + \eta_1^1),$$

$$\zeta_2 = -(\eta_1 + \eta_2^1)$$

$$S_{\ell\ell}^{inel} = a_2(\infty) = [p(1-p)]^{\frac{1}{2}}(e^{2i\zeta_3} - e^{2i\zeta_4}), \quad \zeta_3 = -(\eta_1 + \eta_2 + 2\eta_1^1)/2$$

$$\zeta_4 = -(\eta_1 + \eta_2 + 2\eta_2^1)/2 \qquad \text{II(2.4)}$$

where the transition phase ξ has been taken to be zero (as in I.8) and $p = p_{LZ}$ where p_{LZ}, the Landau-Zener probability (ZEN32), is given by

$$p_{LZ} = \exp(-2\pi\gamma), \quad \gamma = (1/\hbar)\{H_{12}^2 / v_\ell \left| \frac{d}{d_R}(H_{11} - H_{22}) \right|\}_{R_c}$$

as $\rho \to R_c$, $a_1(\infty) \to e^{2i\eta_1}$, $a_2(\infty) \to o$

b. $\rho > R_c$

In the simple Landau-Zener model,

$$a_1(\infty) = \exp(2i\bar{\zeta}_1), \; \bar{\zeta}_1 = -\bar{\eta}_1, \text{ and } a_2(\infty) = o \qquad \text{II(2.5)}$$

$$\bar{\eta}_1 = \int_{-\infty}^{t_e} H_{nn}\, dt$$

From II(2.1), II(2.4) and II(2.5) it can be shown that

$$\sigma_{el}(\theta) = (1/4k_{el}^2)\left[\sum_{l'l'=0}^{l_c}\left\{(2l+1)(2l^1+1)P_{ll}P_{l^1}\{pp^1\cos2(\zeta_1-\zeta_1^1)\right.\right.$$

$$+(1-p)(1-p^1)\cos2(\zeta_2-\zeta_2^1)+p(1-p^1)\cos2(\zeta_1-\zeta_2)+$$

$$\left.(1-p)p^1\cos2(\zeta_2-\zeta_1^1)\right\}+2\sum_{l=0}^{l_c}\sum_{l'=l_{c+1}}^{\infty}(2l+1)(2l'+1)P_l P_{l'}$$

$$\left\{p\cos2(\xi_1-\xi_1')+(1-p)\cos2(\xi_2-\xi_1')\right\}$$

$$\left.+\sum_{ll^1=l_{c+1}}^{\infty}(2l+1)(2l^1+1)P_l P_{l^1}\{\cos2(\zeta_1-\zeta_1^1)\}\right]$$

and

$$\sigma_{inel}(\theta) = (1/4k_{el}^2)\sum_{l,l^1=0}^{l_c}(2l+1)(2l^1+1)P_l P_{l^1}\left[p^1(1-p^1)\right]^{\frac{1}{2}}\left[p(1-p)\right]^{\frac{1}{2}}$$

$$\{\cos2(\zeta_3-\zeta_3^1)+\cos2(\zeta_4-\zeta_4^1)-\cos2(\zeta_3-\zeta_4^1)-\cos2(\zeta_4-\zeta_3^1)\}$$

II(2.6)

where primes denote functions evaluated at l^1.

Itis not possible to predict from the form of the relations II(2.6) whether or not the oscillations in $\sigma_{el}(\theta)$ and $\sigma_{inel}(\theta)$ are in or out of phase.

figure 4

Potential Curves H_{11} and H_{22} 115

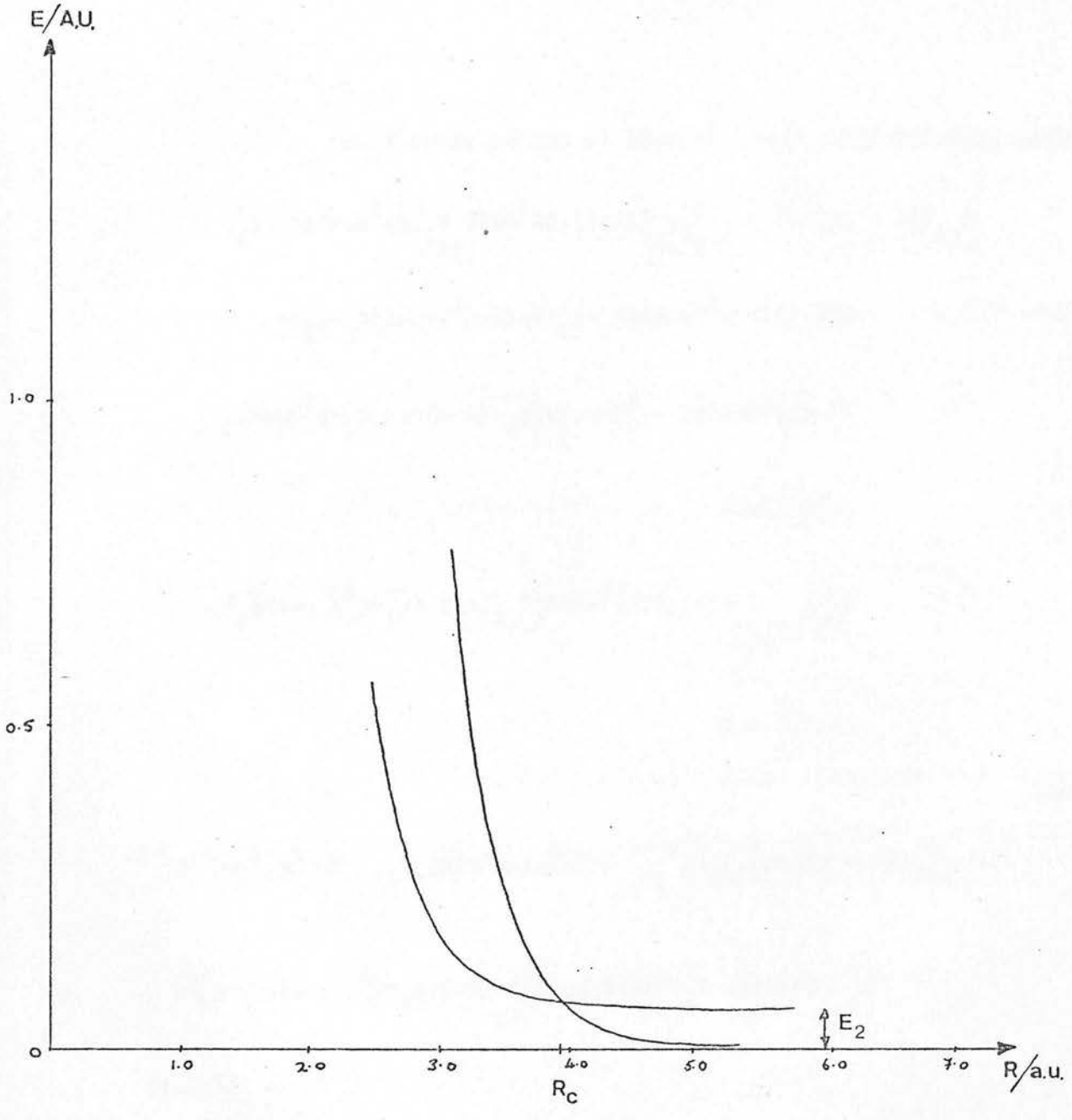

H_{11}/A.U. and H_{22}/A.U. v.s. R/a.u., E_2=0.0592 A.U., R_c=3.968 a.u.

figure 3

$P=|a_2(\infty)|^2$ v.s. ℓ (Landau-Zener Model), E = 200 eV, $H_{12}(R_c)$ = 0.25 eV

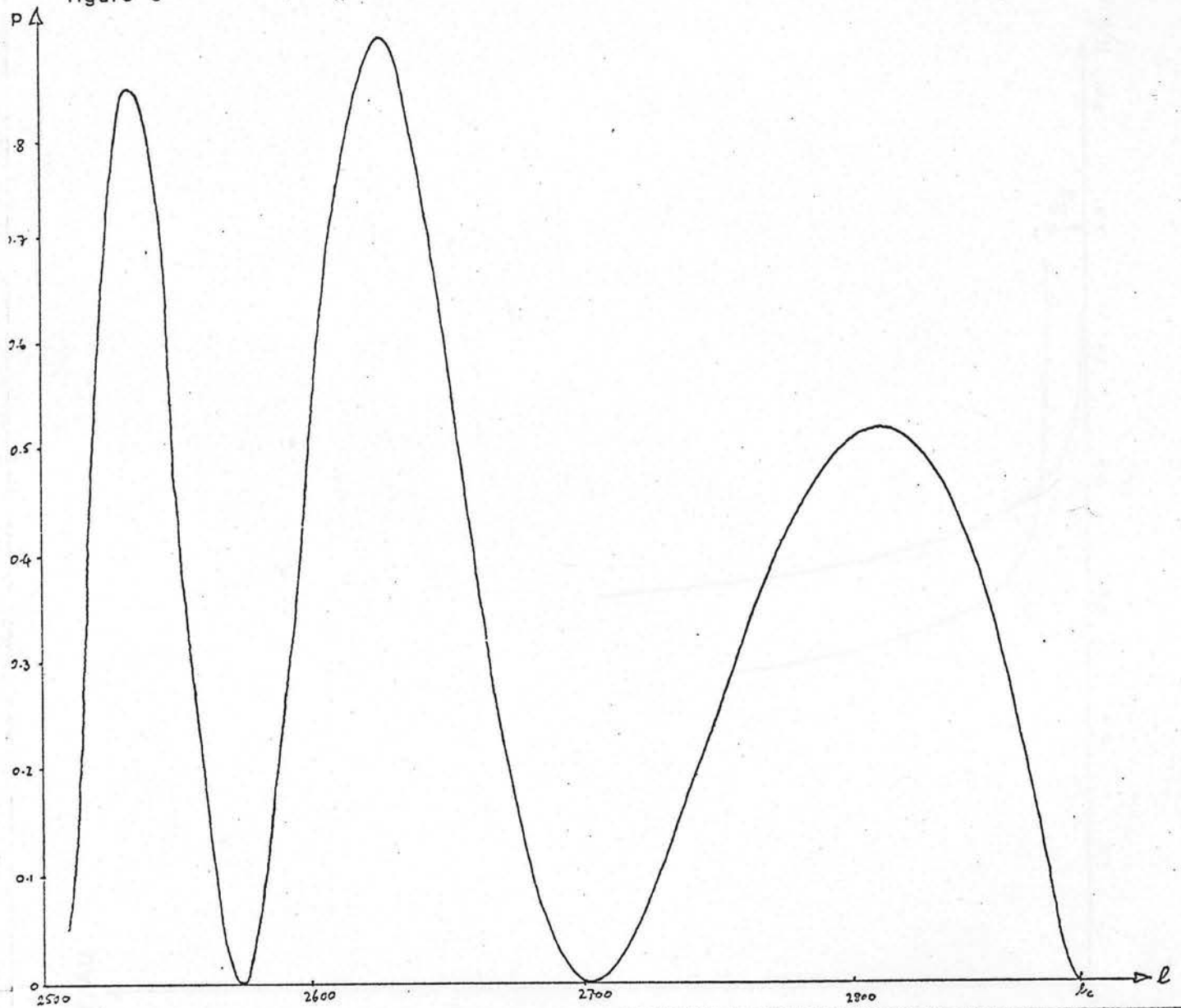

figure 2

Landau - Zener Probability Function

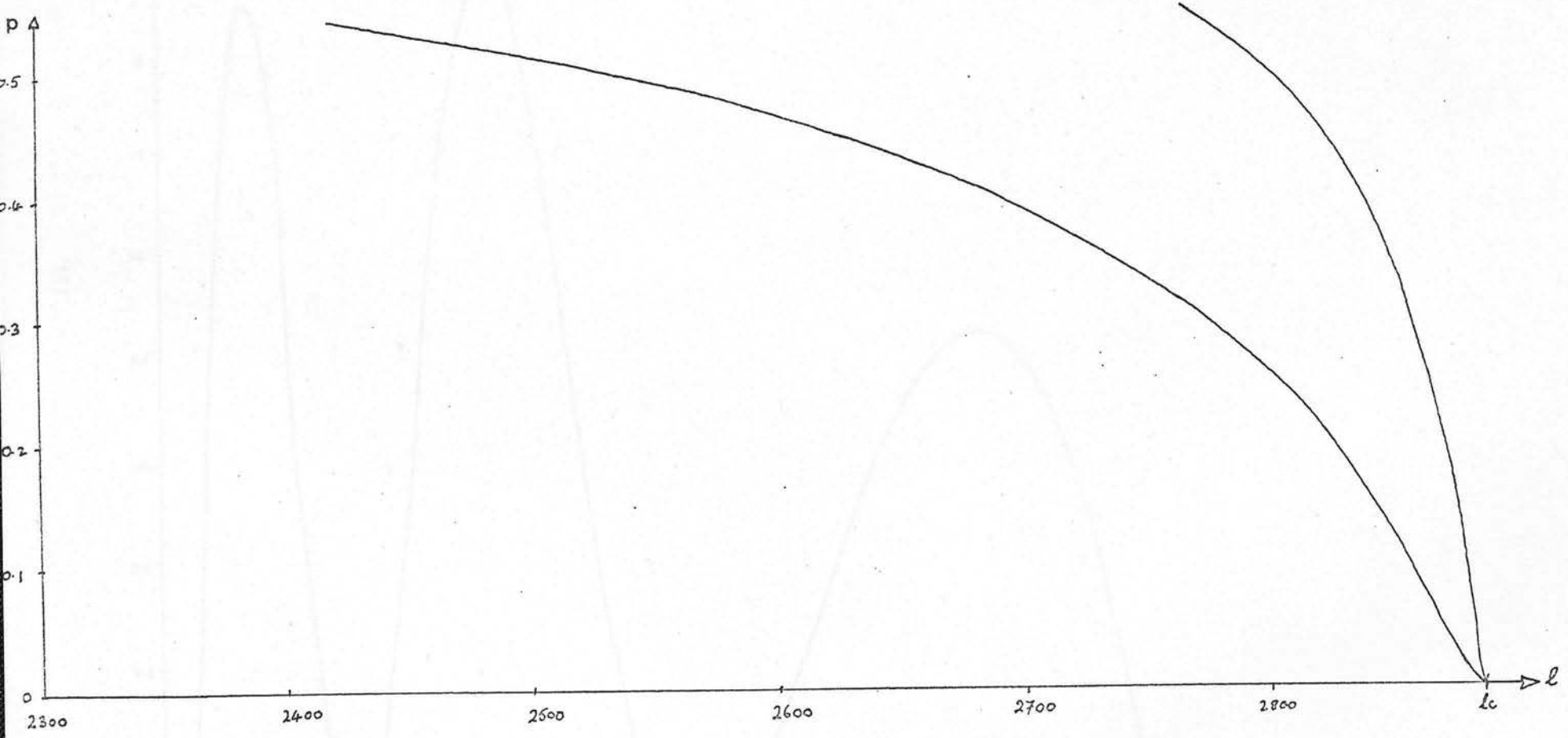

Landau - Zener probability, P, v.s. ℓ for $H_{12}(R_c)$=0.25 eV (upper curve) and 0.35 eV (lower curve),

E = 200 eV

P_{LZ} is displayed as a function of ℓ in Figure 2 for $H_{12}(R_c) = 0.25$ and 0.35 eV ., and $|a_2(\infty)|^2$ calculated from III(2.4) is displayed in Figure 3 for $H_{12}(R_c) = 0.25$ eV.

The cut-off of $a_2(\infty)$ for $\rho > R_c$ effectively truncates the partial wave summation for $f_{inel}(\theta)$ and may introduce oscillations in the inelastic differential cross section. The rapidly varying character of the functions p and (1-p) may also introduce oscillations in the elastic differential cross section. The period, τ, of such oscillations would be $\sim \pi/\ell_c$ radians, where ℓ_c is the value of ℓ corresponding to b for $\rho = R_c$ ($b=R_c$ in a straight line trajectory). Since for the system considered, $\ell_c \sim 2900$, $\tau \sim 0.06^{\circ}$. Oscillations of such high frequency are unlikely to be resolved experimentally.

In the evaluation of phases, a straight line trajectory was assumed. The use of rectilinear trajectories gives the same result for the phase shifts as the use of the small angle formula for the deflection function.

The functional forms used for H_{11} and H_{22} were

$$H_{11} = A_1/R^{10} \qquad A_1 = 6.93\times10^4 \text{ A.U.}$$

$$H_{22} = A_2/R^8 + E_2 \qquad A_2 = 7.65\times10^2 \text{ A.U.},$$

$$E_2 = 5.92\times10^{-2} \text{ A.U.}$$

and H_{11} and H_{22} are displayed as functions of R in Figure 4.

E_2 is the excitation energy for the process

$$K(4s) \rightarrow K^*(4p) \qquad (\Delta E = 1.61 \text{ eV})$$

and A_1 and A_2 were fixed arbitrarily except that the crossing distance R_c was chosen to be accessible within the energy and impact parameter range covered by the experiment.

At high incident energies, the attractive branches of the potentials for $K + Q$ and $K^* + Q$ are unimportant.

II.3 Phase Shifts for Elastic and Inelastic Scattering

Elastic Scattering

$$\zeta_1 = -\int_{-\infty}^{t_\rho} H_{11}\,dt = -\int_{\infty}^{\rho} \frac{H_{11}}{\dot{R}}\,dR$$

and $\dot{R} = -(p_o/\mu)\,(1-b^2/R^2 - H_{11}/E)^{\frac{1}{2}}$, $p_o = (2E\mu)^{\frac{1}{2}}$,

b is the impact parameter (see Section I).

It is assumed that at the energies considered (200 eV), the use of straight line trajectory

$$\dot{R} = -(p_o/\mu)\,(1-b^2/R^2)^{\frac{1}{2}}$$

is a useful approximation.

figure 9

120

Deflection Functions for Inelastic Scattering.

χ_3/radians (upper curve) and χ_4/radians (lower curve) as functions of ℓ.

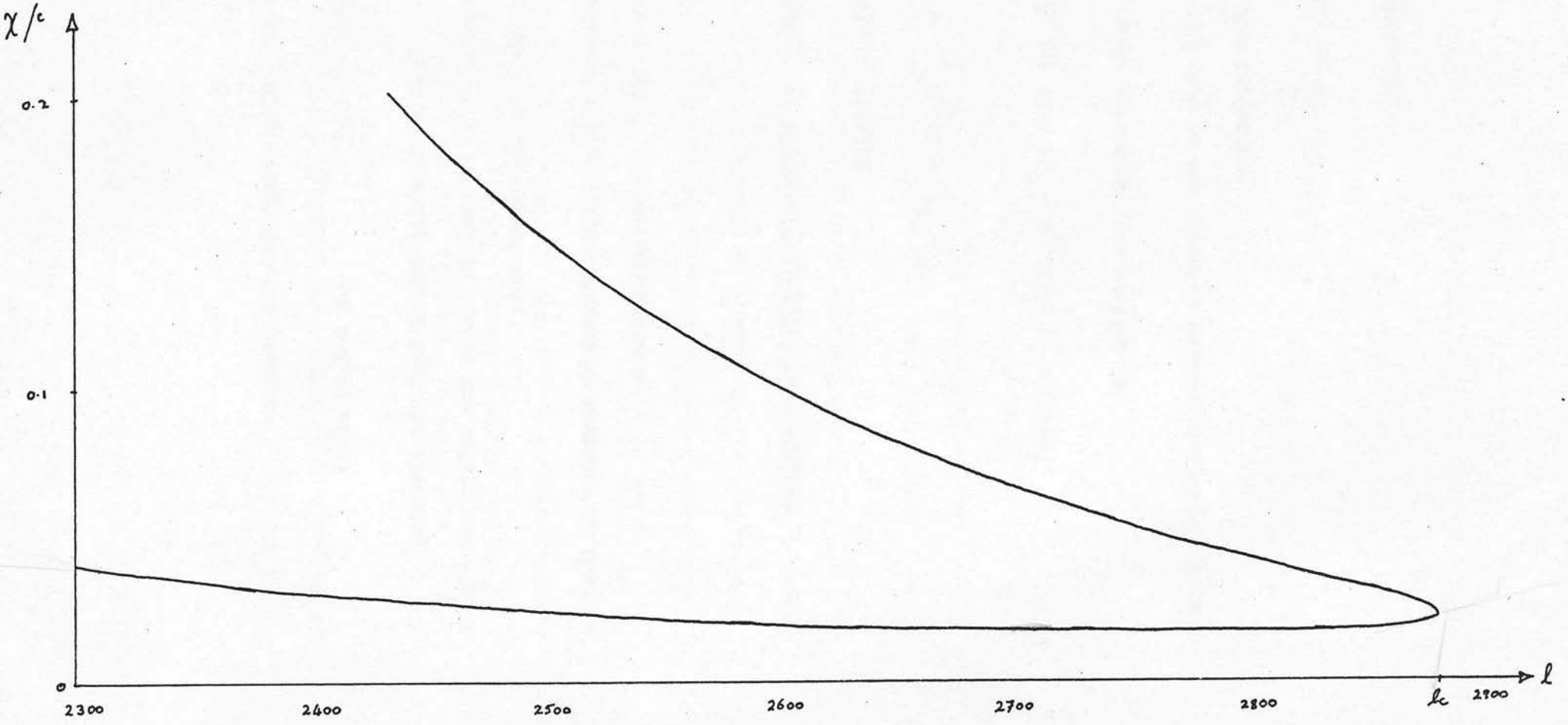

figure 8

Deflection Functions for Elastic Scattering.

χ_1/radians (upper curve) and χ_2/radians (lower curve) as functions of ℓ.

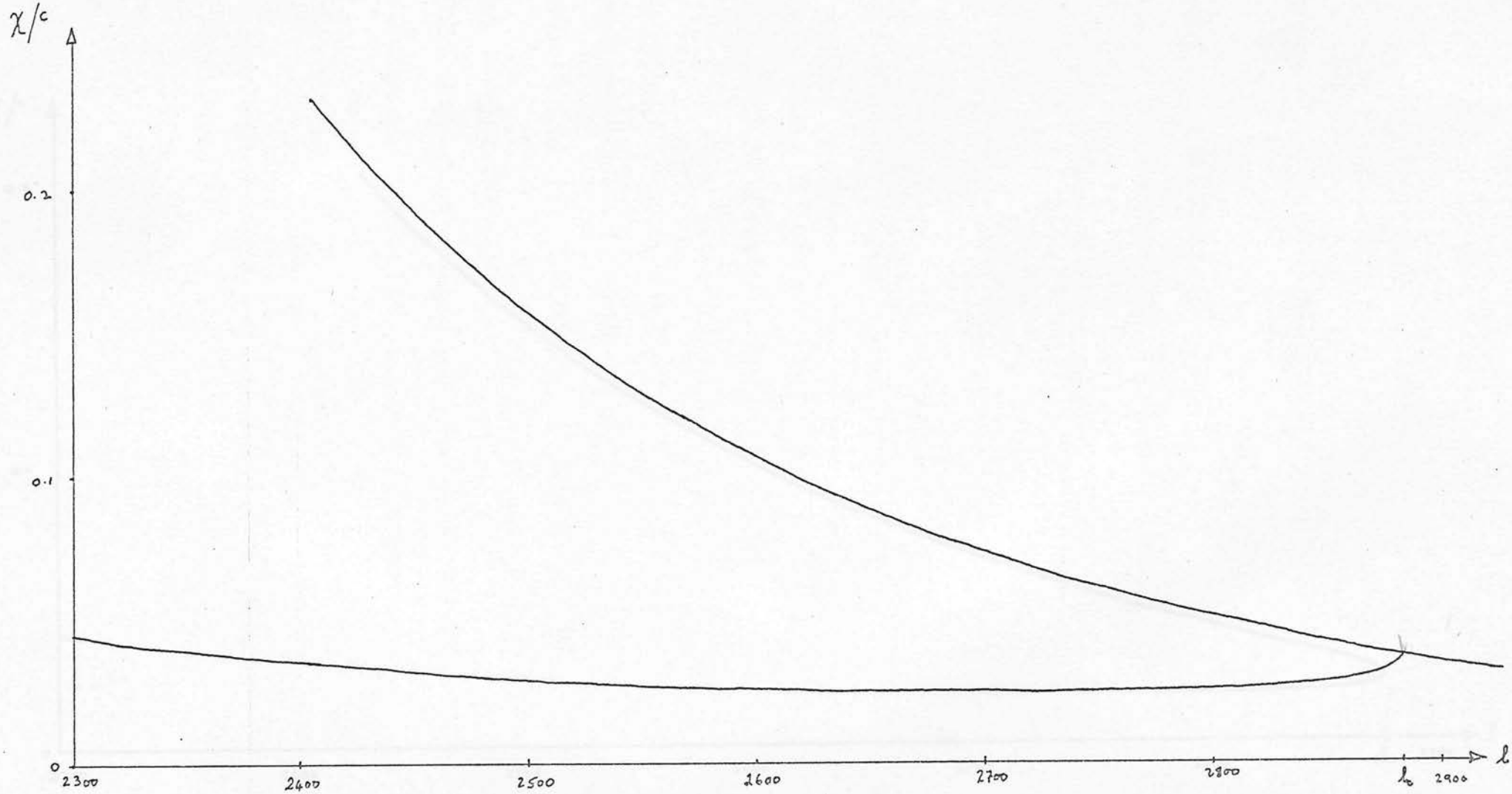

figure 7 Elastic and Inelastic Differential Cross Sections (caption as in Figure 5)

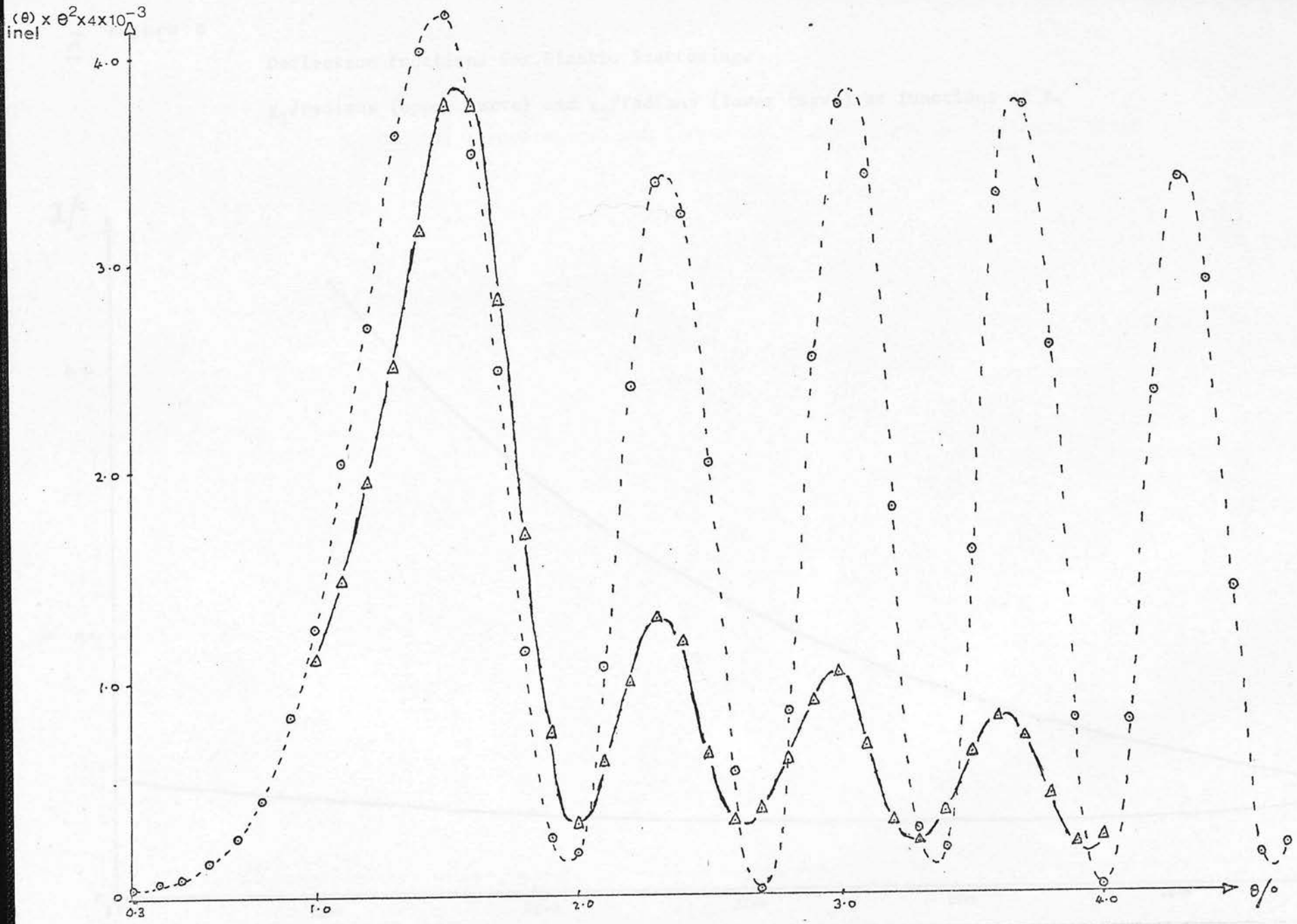

figure 6 Elastic and Inelastic Differential Cross Sections (caption as in Figures 5, $H_{12}(R_c)$=0.35 eV)

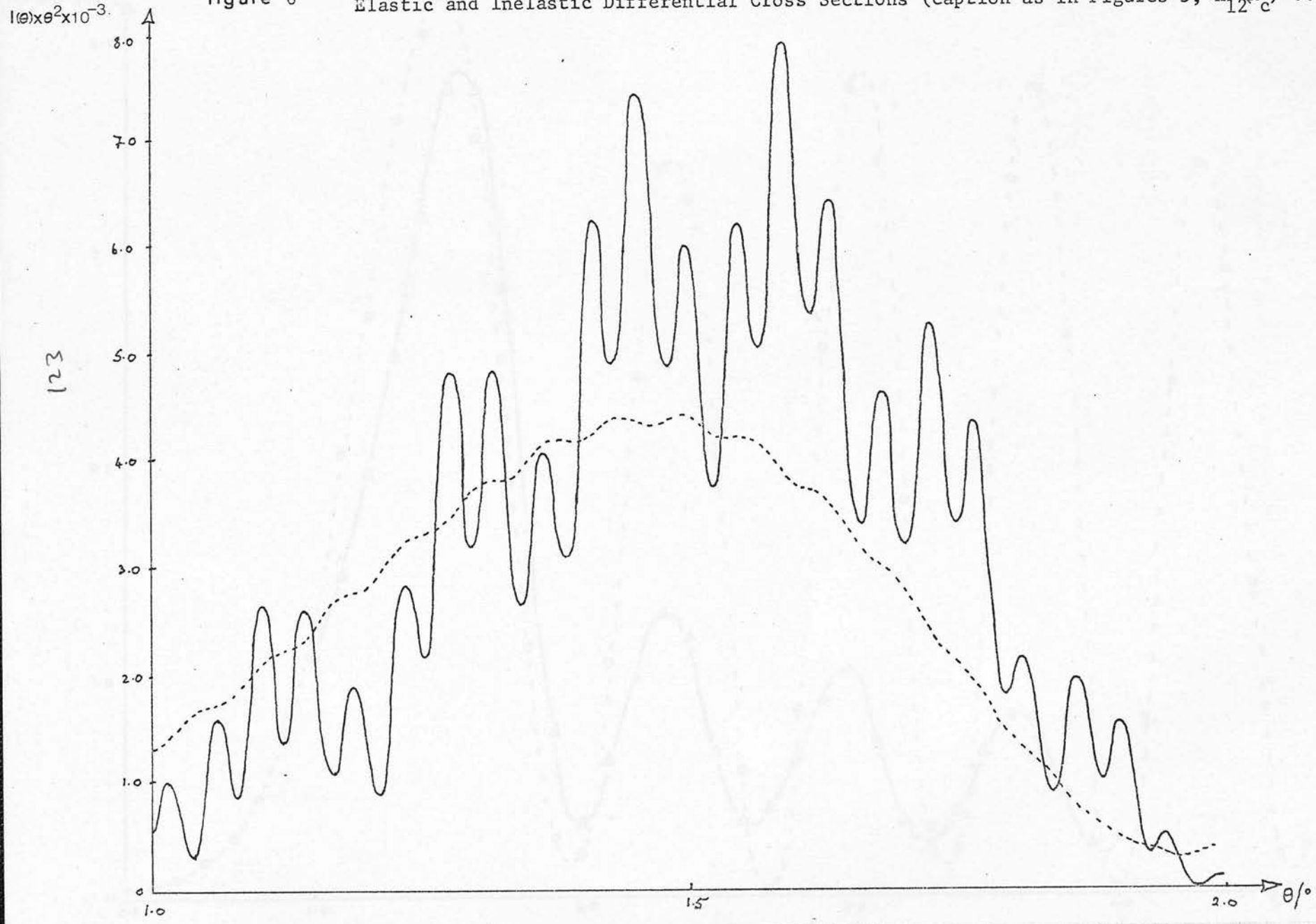

123

figure 5

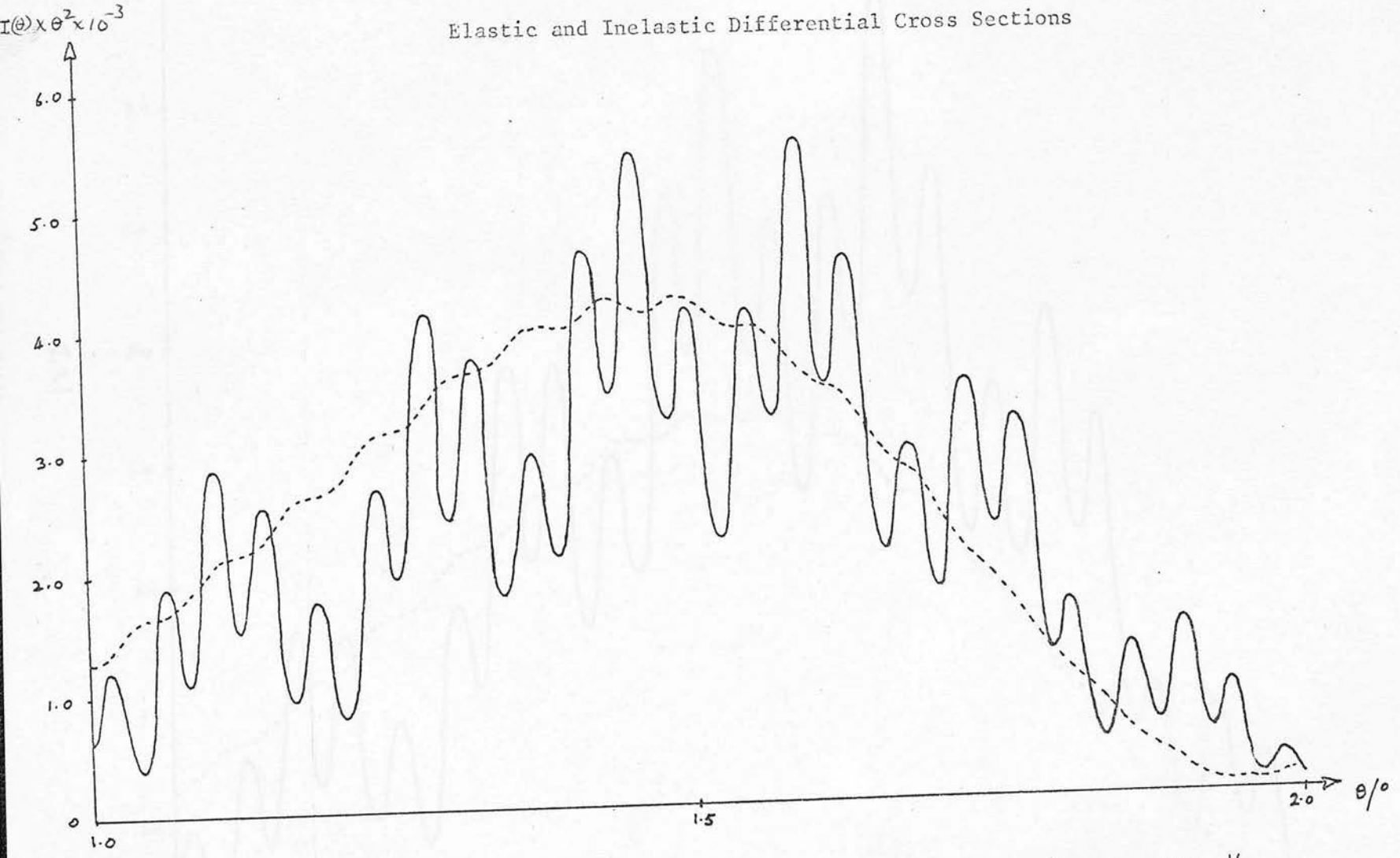

$I_{el}(\theta)x\theta^2x10^{-3}$(—) and $I_{inel}(\theta)x\theta^2x4x10^{-3}$(---) v.s. θ/degrees, $H_{12}(R_c)$=0.25 eV , E = 200 eV .

Subject to this approximation and neglecting any momentum change following transitions between the two states, phase shifts for elastic and inelastic scattering were evaluated analytically (see Appendix V)

II.4 Evaluation of Partial Wave Summation

As already noted (II(2.1)), the elastic and inelastic scattering amplitudes are given by

$$f_{el}(\theta) = (1/2ik_{el}) \sum_{l=0}^{\infty} (2l+1)(S_{ll}^{el} - 1) \; P_l(\cos\theta)$$

$$f_{inel}(\theta) = (1/2ik_{el}) \sum_{l=0}^{\infty} (2l+1) \; S_{ll}^{inel} \; P_l(\cos\theta)$$

The evaluation of the summations is discussed in Appendix V.

$I_{el}(\theta) = |f_{el}(\theta)|^2$ and $I_{inel}(\theta) = |f_{inel}(\theta)|^2$ are displayed as functions of θ ($\theta = 1\text{-}2^\circ$) in figure 5 for $H_{12}(R_c) = 0.25$ eV, and in figure 6 for $H_{12}(R_c) = 0.35$ eV, and $I_{el}(\theta)$ and $I_{inel}(\theta)$ are presented as functions of θ ($\theta = 0.3^\circ \rightarrow 4.7^\circ$) in figure 7.

II.5 Semi-classical Analysis of Elastic and Inelastic Differential Gross Sections

The analysis used was essentially that of Ford & Wheeler (FOR59) and is presented in detail in Appendix V. It is convenient to define "deflection functions," in terms of which the form of $f_{el}(\theta)$ may be analysed. There are two elastic deflection functions χ_1 and χ_2 and these are displayed as functio of l in figure 8 where it can be seen that χ_1 has a single branch and χ_2 has two branches.

The deflection functions χ_3 and χ_4 appropriate to inelastic scattering are displayed as functions of l in figure 9.

II.6 Discussion and Conclusions

As can be seen from Figures 5 and 6, both elastic and inelastic differential cross sections show high frequency structure (much more pronounced in the former case than in the latter) with a period of about 0.05°. This can probably be accounted for in terms of the behaviour of elastic and inelastic S-matrix elements ($S^{el}_{\ell\ell}$ and $S^{inel}_{\ell\ell}$ respectively) for ℓ near ℓ_c as already discussed in § II.3. The difference in the amplitudes of these oscillations in the two differential cross sections is presumably due to the different behaviour of $S^{el}_{\ell\ell}$ and $S^{inel}_{\ell\ell}$ for ℓ near ℓ_c. Only the elastic cross section shows a prominent rainbow (expected at 1.4°). The lack of prominence of the inelastic rainbow (expected at $\theta = 1^{\circ}$) is probably due to the fact that the minimum in the inelastic deflection function (χ_4, Figure 9) is too shallow to support a strong rainbow structure.

Furthermore, the inelastic rainbow is located not at $\theta = 1^{\circ}$, as expected from a Ford and Wheeler analysis, but at $\theta \simeq 1.5^{\circ}$. It would appear that in this situation, where the bowl of the inelastic deflection function is very shallow, Ford and Wheeler's analysis may not be applicable. The weakness of the interference structure in the inelastic D.CS. lends support to this notion. It is clear from Figure 7. that the semi-classical prediction of longer period (0.9°) Stueckelberg oscillations in elastic and inelastic differential cross sections is confirmed, as is the prediction that the inelastic cross section is negligible for $\theta<1^{\circ}$.

The relations (see Appendix V)

$$(2k^2_{el}\ \sin\theta)I_{inel}(\theta) = a_3^2+a_4^2-2a_3a_4\cos(\beta_3-\beta_4)\ ,\quad \theta>1.2^{\circ}$$

$$(2k^2_{el}\sin\theta)I_{el}(\theta) = a_1^2+a_2^2+2a_1a_2\cos(\beta_1-\beta_2)\ ,\quad \theta>2.15^{\circ}$$

do not imply that oscillations in $I_{el}(\theta)$ and $I_{inel}(\theta)$ are π out of phase for $\theta>2.15^{\circ}$ because the functions $(\beta_1-\beta_2)$ and $(\beta_3-\beta_4)$ are quite different.

Conclusions

For angles from one to four degrees (c.m frame) and a relative kinetic energy of 200 eV (c.m. frame) it is expected that oscillations with a period of $\sim 0.9^{\circ}$ will be observed in the sum of the elastic and inelastic differential cross sections for the system considered (see § II.1), at least when the Landau-Zener single crossing transition probability (p_{LZ}) is about 0.5.

Both differential cross sections show maxima in the low frequency modulation of their envelopes at angles of approximately 1.5°, 2.3°, 3.0° and 3.7° and the location of maxima and minima (even in thehighest frequency structure) appears to be independent of the magnitude of the off-diagonal matrix element of the Hamiltonian (H_{12}) at the point at which the two potential curves cross (R_c), at least in the range $H_{12}(R_c) = 0.25 \rightarrow 0.35$ eV for which $p_{LZ}(\ell = 2500) \approx 0.7$ and 0.5 respectively (curve crossing is not reached for $\ell > 2884$).

It can be seen from Figure 7 that the low frequency oscillations in the elastic and inelastic differential cross sections are not perfectly in phase. Over a wider angular range, therefore, the sum of the two cross sections will show oscillations with a period of several degrees (dependent on the form of the two potentials), as the low frequency oscillations in the two cross sections pass in and out of phase. It is expected that it will be difficult to interpret differential cross section measurements obtained from an experiment in which elastic and inelastic events are not distinguished, although a rather prominent rainbow should be observed in the summed differential cross sections.

PART III

FINE STRUCTURE TRANSITIONS IN HEAVY ATOMS INDUCED BY COLLISION WITH H_2, HD AND D_2

CONTENTS

III.1 Introduction

Transitions between the fine structure components of an electronic configuration of an atom, A,

$$A(j^{11},m^{11}) \rightarrow A(j^{1},m^{1})$$

and depolarisation transitions

$$A(j^{11}_{,}m^{11}) \rightarrow A(j^{11}_{,}m^{1})$$

which have been induced by collision with another atom have been extensively investigated both experimentally and theoretically, particularly for alkali - atom inert gas systems, and the work up to 1972 has been comprehensively reviewed in LIJ72. It is sufficient here to note that the cross sections for ^2P fine structure transitions in the alkalis vary between $104\mathring{A}^2$, for K and Xe at 300K, to 5.7×10^{-5} $\mathring{A}^2$ for Cs and He at 315K, and that calculations employing a model proposed by Nikitin (NIK65A, NIK65B) have reproduced the experimental results to within an order of magnitude throughout the series. The process was described as the occurrence of non-adiabatic transitions between the Σ and Π molecular states arising from the alkali ^2P states due to a breakdown of spin - orbit coupling in the excited atom at an interatomic distance for which

$$\Delta\varepsilon \approx \Delta V$$

where $\Delta\varepsilon$ is the fine structure splitting and ΔV is the splitting between the Σ and Π states. The theory took account of the change in nuclear velocity during the transition (significant for the heavier alkalis where $\Delta\varepsilon$ is larger), and of polarisation forces. When Coriolis Coupling was included (DAS70a, DAS70b) agreement between

TABLE 1

Atomic Transition	$\sigma H_2/cm^2$	$\sigma HD/cm^2$	$\sigma D_2/cm^2$	$\sigma H_2/\sigma D_2$
$I(5^2P_{\frac{1}{2}}) \rightarrow I(5^2P_{3/2})$	7.4×10^{-19}	2.1×10^{-18}	8.0×10^{-21}	92
$Te(5^3P_{1,0}) \rightarrow Te(5^3P_2)$	5.8×10^{-17}		6.9×10^{-20}	840
$Tl(6^2P_{3/2}) \rightarrow Tl(6^2P_{\frac{1}{2}})$	2.8×10^{-18}		3.9×10^{-19}	7

theory and experiment was further improved. It appears that exchange interaction is more important than polarisation interaction in these processes, but polarisation becomes more important for the heavier inert gases.

During the past few years, a large number of experimental measurements have been made of rate constants for atomic fine structure transitions induced by collision with small molecules, and this work has been reviewed in several recent reports (DON71, DON72, DON74). Attention has focussed particularly on the heavier atoms for which $\Delta\epsilon$ ~ 5000 - 8000 cm^{-1} whereas $\Delta\epsilon$ for the alkalis ranges from 0.34 cm^{-1} for Li to 554.0 cm^{-1} for Cs. Some recent papers have shown that unusually large isotope effects can be observed in such processes (DON73, STR73, DEA72, WIE73) and some crude cross sections ($\sigma = k/\bar{v}$) and ratios of cross sections are listed in Table 1.

Resonant energy transfer channels have been shown (MOO73, SNI71) to be important for vibration → vibration transfer and theories involving dipole - dipole (MOO73) and higher multipolar couplings (SHA73) have been quite successful in explaining these results. In view of this it has been suggested (BUT74,EWI74) that transfer of electronic → vibrational + rotational energy from atoms to small molecules may also occur by a multipolar coupling mechanism in which the energy to be transferred to translation is minimised.

Before considering this and other possible mechanisms, the experimental techniques employed in obtaining the data in Table 1 will be described briefly.

Flash spectroscopic or kinetic spectrophotometric techniques are usually employed to measure rate constants for fine structure transitions and for the quenching of excited atoms, and these techniques are described in POR73 and elsewhere. In these experiments, the population of a single component can be observed as a function of time by monitoring a transition from that state to a higher excited state, provided the wavelength for the transition can be isolated from those of other lines in the spectrum. In obtaining the rate constant for a fine structure transition induced by collision with some atomic or molecular species, Q, the measured rate constant must be corrected for loss of the initial j state by diffusion and first order processes other than collision with Q.

In the case where Q is a diatomic molecule, BC, the fine structure splitting may be transferred to electronic and or vibrational and rotational excitation of the BC molecule and to translation:

III (1.1)

$$A(j^{11},m^{11})+BC(\Omega^{11}v^{11}J^{11}M^{11}) \rightarrow A(j^{1}m^{1})+BC(\Omega^{1}v^{1}J^{1}M^{1})+\Delta E(\Omega^{11}\,\Omega^{1}:j^{11}j^{1}:v^{11}v^{1}:J^{11}J^{1})$$

where ΔE is the energy transferred to or from relative motion of the A - BC pair, Ω denotes the electronic state of the BC and v and J are the usual vibrational and rotational quantum numbers. The cross section $\sigma_{j^{11}j^{1}}(v)$ for the fine structure transition

$$A(j^{11}) \rightarrow A(j^{1})$$

resulting from processes like III(1.1) is given by

$$(2j^{11}+1)\sigma_{j^{11}}^{j^{1}}(v)=\sum_{\Omega^{11}\Omega^{1}}\frac{f(\Omega^{11})}{\omega^{11}}\sum_{V^{11}V^{1}J^{11}J^{1}}\frac{f(V^{11},J^{11})}{(2J^{11}+1)}\sum_{M^{11}M^{1}m^{11}m^{1}}\sigma_{\Omega^{11}:V^{11}J^{11}M^{11}:j^{11}m^{11}}^{\Omega^{1}:V^{1}J^{1}M^{1}:j^{1}m^{1}}(v)$$

III(1.2)

where v is the relative velocity of A and BC before collision, $f(\Omega^{11})$ and $f(V^{11}J^{11})$ are the populations of the electronic and vibration - rotation levels of BC respectively at the time measurement starts, ω^{11} is the degeneracy of the state Ω^{11} and $\sigma_{\Omega^{11}:V^{11}J^{11}M^{11}:j^{11}m^{11}}^{\Omega^{1}:V^{1}J^{1}M^{1}:j'm'}(v)$ is the cross section for the process III(1.1). Consideration of the experimental conditions, and of the various energy differences involved, leads to a simplification of III(1.2).

First, the action of the flash does not significantly perturb the pre-flash (thermal) distribution of electronic states of BC in which only the ground state is effectively populated. The electronic groundstate of H_2, HD and D_2 is $^1\Sigma_g^+$ which is non-degenerate. Calculations were performed only for BC = H_2, HD or D_2, since for these molecules reliable electronic wave functions are available. For the present purpose then, there is no loss of generality in writing

$$\sigma_{j^{11}}^{j^{1}}(v)=\frac{1}{(2j^{11}+1)}\sum_{V^{11}V^{1}J^{11}J^{1}}\frac{f(V^{11}J^{11})}{(2J^{11}+1)}\sum_{M^{11}M^{1}m^{11}m^{1}}\sigma_{V^{11}J^{11}M^{11}:j^{11}m^{11}}^{V^{1}J^{1}M^{1}:j^{1}m^{1}}(v)$$

III(1.3)

Second, the pre-flash thermal distribution of VJ states of BC is only slightly perturbed and has completely relaxed to equilibrium at a temperature which is only slightly different from the initial

ambient temperature before measurement starts. Hence, to a good approximation

$$f(v^{11}J^{11}) = f_T(v^{11}J^{11}) = P_{J^{11}}\exp\left[E(v^{11}J^{11})/kT\right]/N \qquad \text{III(1.4)}$$

where N is a normalising constant, $P_{J^{11}}=(2J^{11}+1)g_n$, and g_n is a nuclear spin factor. For identical nuclei of integer spin I,

$$g_n = (I+1)(2I+1) \quad \text{for Jeven}$$

$$= I(2I+1) \quad \text{for Jodd,}$$

for identical nuclei with ½ integer spin, I,

$$g_n = I(2I+1) \quad \text{for Jeven}$$

$$= (I+1)(2I+1) \quad \text{for Jodd,}$$

and for non-identical nuclei $g_n = 1$.

The same assumption is made about thermal equilibration of velocities as was made for the distribution of VJ states. If the A + BC mixture is in thermal equilibrium, the distribution of relative velocities is given by

$$f_T(v)dv = \left(\frac{4}{\sqrt{\pi}}\right)\frac{v^2}{v_m^3}\exp(-v^2/v_m^2)dv \qquad \text{III(1.5)}$$

where v_m, the most probable velocity, is given by

$$v_m = (2kT/\mu)^{\frac{1}{2}}$$

Hence the rate constant for processes III(1.1), $k^{j}_{j^{11}}(T)$ is given by

$$k^{j^1}_{j^{11}}(T) = \frac{1}{(2j^{11}+1)} \sum_{V^{11}J^{11}V^1J^1} \frac{f_T(V^{11},J^{11})}{(2J^{11}+1)} k^{V^1J^1j^1}_{V^{11}J^{11}j^{11}}(T)$$

where

$$k^{V^1J^1j^1}_{V^{11}J^{11}j^{11}}(T) = \int_{v_o}^{\infty} v\, \sigma^{V^1J^1j^1}_{V^{11}J^{11}j^{11}}(v)\, f_T(v)dv,$$

$$\sigma^{V^1J^1j^1}_{V^{11}J^{11}j^{11}}(v) = \sum_{M^{11}M^1} \sum_{m^{11}m^1} \sigma^{V^1J^1M^1j^1m^1}_{V^{11}J^{11}M^{11}j^{11}m^{11}}(v),$$

$$v_o = o \quad \text{when } \Delta E(j^{11}j^1V^{11}V^1J^{11}J^1) \text{ is } <o \qquad \text{III(1.6)}$$

$$= 2\Delta E(j^{11}j^1V^{11}V^1J^{11}J^1)/\mu^{\frac{1}{2}} \quad \text{when } \Delta E \text{ is } >o$$

It is clear from the set of equations III(1.6) that $\sigma^{V^1J^1j^1}_{V^{11}J^{11}j^{11}}$ must be evaluated as a function of velocity in order to evaluate the rate constant $k^{j^1}_{j^{11}}(T)$.

Formally, a solution to the Schrodinger time dependent wave equation

$$H\psi = i\hbar\, \partial\psi/\partial t$$

must be found by expanding the wave function ψ in an appropriate basis:

$$\psi = \Sigma_q A_q \Phi_q$$

where q is a collective subscript for Ω V JMjm, and evaluating the

figure 1

Two Curve Crossing Situations

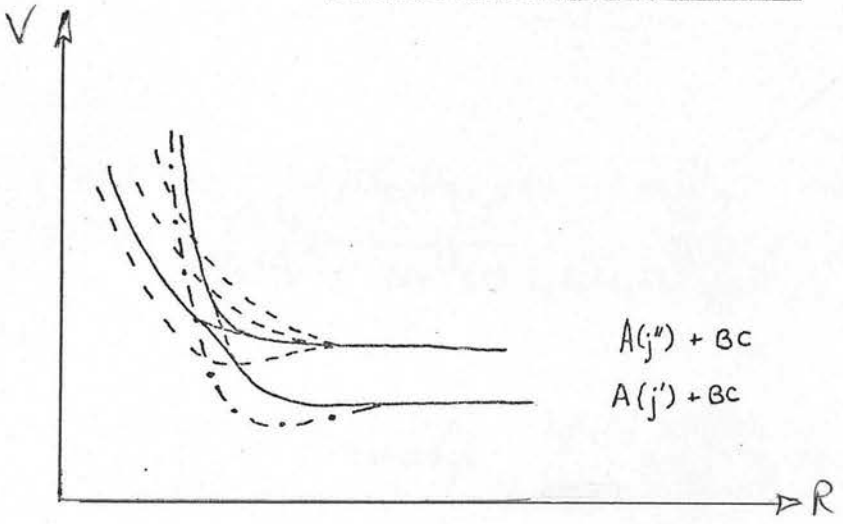

i. There is an avoided crossing between curves of the same symmetry – .
Other curves - - - and – . – cross.

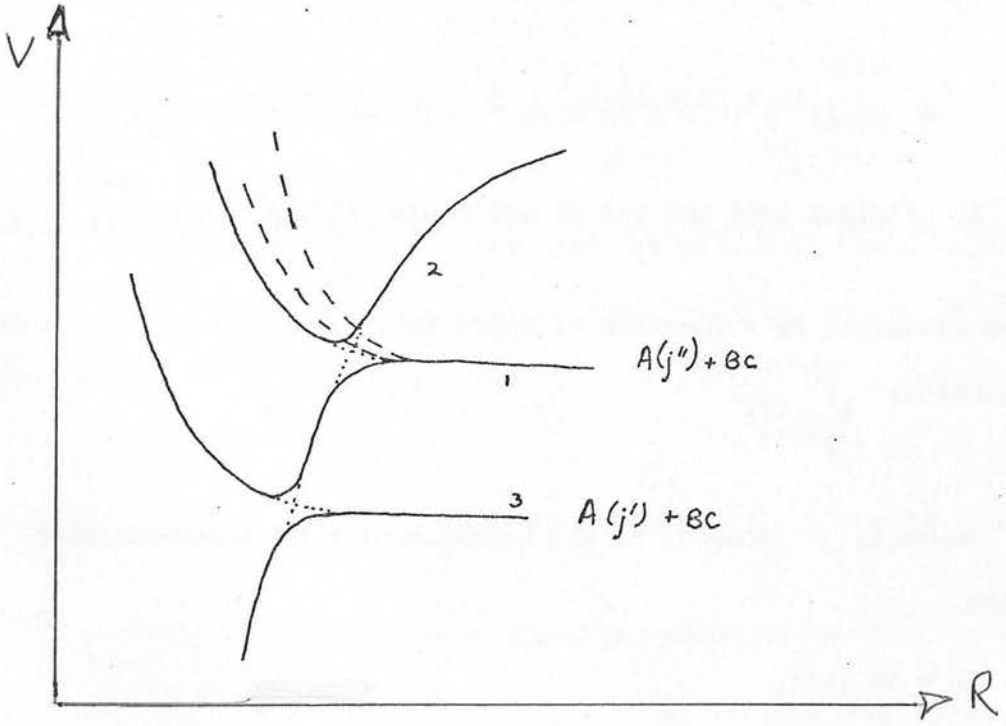

ii. The transition 1 → 3 occurs via the intermediate state 2 by two avoided curve crossings.

amplitudes Aq after the 'collision' is over, given some starting condition

$$|Aq|^2 = \delta_{iq}$$

However, the basis functions are eigen functions of the unperturbed Hamiltonian, Ho :

H = Ho +V, where V, the interaction, →o as R → ∞

thus, if Aq = Cq.exp(-iEqt/ħ) and Ho ϕq = Eq ϕq, then, in matrix notation

$$i\hbar\{\dot{C}(t)\} = \{G\}\{C(t)\},\ \hat{G} = V - i\hbar\partial/\partial t \qquad \text{III(1.7)}$$

and the basis has been assumed orthonormal.

The probability of transition to a final state f is identified with $|a_f(\infty)|^2 = |C_f(\infty)|^2$, and from these probabilities the cross sections $\sigma^{(v)}_{v^1J^1M^1j^1m^1 \; v^{11}J^{11}M^{11}j^{11}m^{11}}$ can be evaluated.

In principle, the system of coupled equations III(1.7) can be solved as it stands. Not only is this a rather formidable undertaking since V may be difficult to evaluate, but it is not physically instructive since there is no way of knowing which part of the interaction is responsible for these transitions. It is important, therefore, to consider some possible mechanisms for coupling.

a. Curve Crossing (see Figure 1)

There are two possible cases:

i. The potential surface of a member of the manifold of molecular

states arising from $A(j^{11})+BC$ may cross a potential surface of the same symmetry arising from $A(j^{1})+BC$, so that there is the possibility of a direct $j^{11} \rightarrow j^{1}$ transition. This is the classic case of curve crossing considered by Landau and Zener (ZEN32), Stueckelberg (STU32) and others.

ii. Two potential surfaces of the same symmetry arising from $A(j^{11})+BC$ (1) and $A(j^{1})+BC$ (3) may be crossed by a third surface (2) of the same symmetry so that transitions $1 \rightarrow 2 \rightarrow 3$ result in an overall $j^{11} \rightarrow j^{1}$ transition.

In a curve crossing situation equations III(1.7) must be solved as they stand, possibly by means of one of the well known approximation schemes.

b. Coupling via exchange forces - the repulsive part of the interaction

This mechanism has been extensively discussed for the alkali - inert gas systems (LIJ72) and no more need be said about it here.

c. Long range coupling via a term or terms in the electrostatic multipole expansion for the interaction, V.

Since the purpose of this work is to examine the suggestion (BUT74, EWI74) that (c) is the dominant mechanism for the transfer of electronic to vibrational + rotational energy from atoms to small molecules, the form of the solution of III(1.7) appropriate to such an assumption will be considered.

Each basis function in the expansion is a product of molecular and atomic electronic wave functions, ζ_Ω and ψ_{jm} respectively and molecular vibrational and rotational wave functions χ_{VJ} and Y_J^M respectively:

$$\phi_i = \psi_{jm}(\underline{r}^n)\zeta_\Omega(\underline{r}_1,\underline{r}_2)\chi^{VJ}(\xi)Y_J^M(\theta,\phi)$$

Clearly the electronic wave function has not been completely antisymmetrised , but it should provide a good approximation to the correct wave function at least for larger interparticle separations. The basis is obviously orthonormal.

V is written as a multipole expansion, and it is assumed that equations III(1.7) can be solved to first or second order in this perturbation, V. The perturbation equations are derived in standard fashion (SCH49):

$$^{(o)}C_f(t) = C_f(o)$$

$$i\hbar\,^{(s+1)}\dot{C}_f(t) = \Sigma_q\,^{(s)}C_q(t)V_{fq}\exp(-i\,\omega_{fq}t)$$

where the superscript (s) denotes the order of the perturbation,

$$V_{fq} = \langle\Omega_f : j_f m_f : V_f J_f M_f | V | \Omega_q : j_q m_q : V_q J_q M_q\rangle$$

and $\omega_{fq} = [E(f) - E(q)]/\hbar$ III(1.8)

Applying the boundary conditions

$$C_q(o) = \delta_{qi}$$

the first and second order solutions are

$$^{(1)}C_f(t) = (i\hbar)^{-1}\int_{-\infty}^{t} V_{fi}\, \exp(i\,\omega_{fi}t^{1})dt^{1} \qquad \text{III(1.9)}$$

and

$$^{(2)}C_f(t) = (i\hbar)^{-2}\sum_q \int_{-\infty}^{t} V_{fq}\, \exp(i\omega_{fq}t^{1})$$

$$\{\int_{-\infty}^{t^{1}} V_{qi}\, \exp(i\omega_{qi}t^{11})dt^{11}\}dt^{1} \qquad \text{III(1.10)}$$

where f is the final state (usually denoted ^{1}) and i is the initial state (^{11}).

First of all consider only the leading term - the dipole-dipole term for two uncharged species - in the perturbation. In the first order approximation, this term only accounts for dipole-allowed transitions in the atom and molecule. But the experimentalist focuses his attention upon metastable states of the atom, that is upon those states for which there is <u>not</u> a dipole allowed transition to the lower state.

However, these transitions are allowed in the second order of approximation in which the overall transition takes place by means of two consecutive dipole-allowed transitions first to an intermediate or virtual state and then from that intermediate state to the final state. Alternatively, the transition of interest may proceed under the influence of a higher term in the expansion, for example the quadrupole-quadrupole term. It is therefore necessary to estimate the relative importance of these first and second order processes.

If the perturbation can be taken to be zero for $t<o$ and $t>t$, and the matrix elements of the perturbation to be slowly-varying functions of t, then

$$C_f^{(1)}(t) \approx -(\hbar)^{-1} V_{fi} f(t)$$

and

$$C_f^{(2)}(t) \approx (\hbar)^{-2} \sum_q \frac{V_{fq} V_{qi}}{\omega_{qi}} \{f(t) - (e^{i\omega_{fq} t} - 1)\}$$

$$= (\hbar)^{-2} \left(\sum_q \frac{V_{fq} V_{qi}}{\omega_{qi}} \right) f(t) \quad , \quad f(t) = \frac{(e^{i\omega_{fi} t} - 1)}{\omega_{fi}}$$

if there are no energy conserving transitions in first order. If ω_{qi} ≈constant = $\hbar \bar{E}$, then

$$C_f^{(2)}(t) \sim \frac{(\hbar)^{-1}}{\bar{E}} (\Sigma_q V_{fq} V_{qi}) f(t) = \frac{(\hbar)^{-1}}{\bar{E}} \langle f | V^2 | i \rangle f(t)$$

Hence the second order process is expected to be important compared to first order if $\langle f|V^2|i\rangle/\bar{E}$ is comparable to V_{fi}.

In the present calculations it was assumed that the first order, quadrupole quadrupole mechanism dominates (H_2, HD and D_2 have zero or very small dipole moment), so that the effective perturbation V was taken to be this term in the multipole expansion. A semi-classical analysis was used in which

$$\sigma^{V^1 J^1 j^1}_{V^{11} J^{11} j^{11}}(v) = 2\pi \int_0^\infty b \, \mathcal{P}^{V^1 J^1 j^1}_{V^{11} J^{11} j^{11}}(b) \, db \qquad \text{III(1.11)}$$

where b is the impact parameter for a given trajectory (see §I Figure 2) and

$$\mathcal{P}^{V^1 J^1 j^1}_{V^{11} J^{11} j^{11}}(b) = \sum_{M^{11} M^1} \sum_{m^{11} m^1} P^{V^1 J^1 M^1 j^1 m^1}_{V^{11} J^{11} M^{11} j^{11} m^{11}}(b) \qquad \text{III(1.12)}$$

in which $P^{V^1 J^1 M^1 j^1 m^1}_{V^{11} J^{11} M^{11} j^{11} m^{11}}(b)$ is the probability of the transition

$$A(j^{11} m^{11}) + BC(V^{11} J^{11} M^{11}) \rightarrow A(j^1 m^1) + BC(V^1 J^1 M^1)$$

for impact parameter b and is computed to first order of perturbation as

$$P^{V^1 J^1 M^1 j^1 m^1}_{V^{11} J^{11} M^{11} j^{11} m^{11}}(b) = |{}^{(1)}C_f(\infty)|^2 \qquad \text{III(1.13)}$$

where ${}^{(1)}C_f(\infty)$ is defined in equation III(1.9)

The use of first order perturbation theory was found to be justified (see Section III.5) when cross sections were computed. The choice of co-ordinate system will be discussed in Section III.5 but two co-ordinate systems will be used throughout

a. "Rotating" co-ordinate system in which the interparticle vector is chosen as the Z axis.

b. "Space fixed" co-ordinate system where the apse line (for a given trajectory) is chosen as the Z axis.

For ease of computation, a system of dimensionless variables was introduced in which the units were as follows:

Energy: 2 x Rydberg = 27.106 eV

Length: The first Bohr radius (a_o) = 0.5292Å

Mass: Electron rest mass = 9.10908×10^{-31} kg

Time: $\hbar/2Ry = 2.419 \times 10^{-17}$ secs.

In this system of variables, equations III(1.9) read

$$^{(1)}C_f(\infty) = \frac{1}{i}\int_{-\infty}^{\infty} V^*_{fi} \exp(i\Delta E^*_{fi} t^*)\,dt^* \qquad \text{III(1.14)}$$

where * denotes dimensionless variables.

In order to evaluate the transition probabilities in this scheme, the form of the perturbation V must be known.

figure 2

Two Co-ordinate Systems for the Interaction Potential

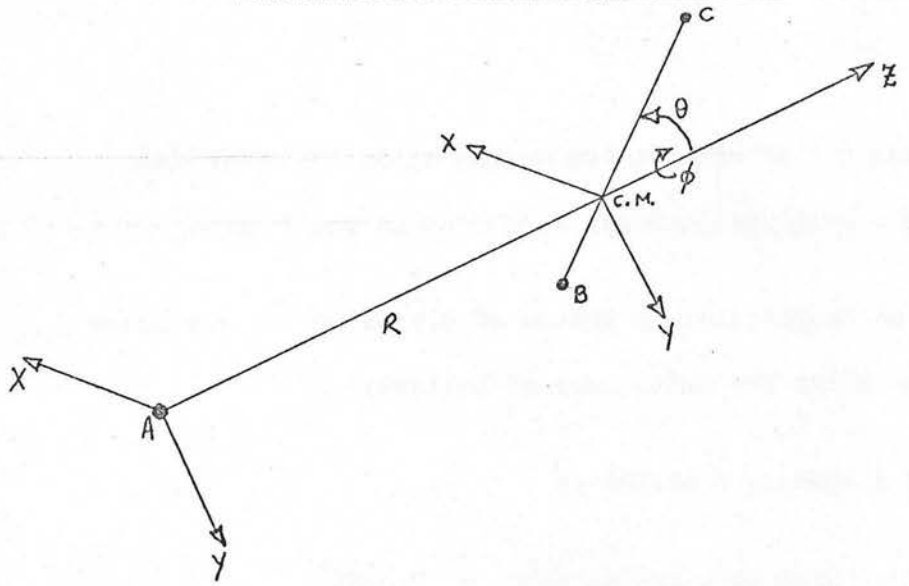

(a) 'Rotating Co-ordinate System

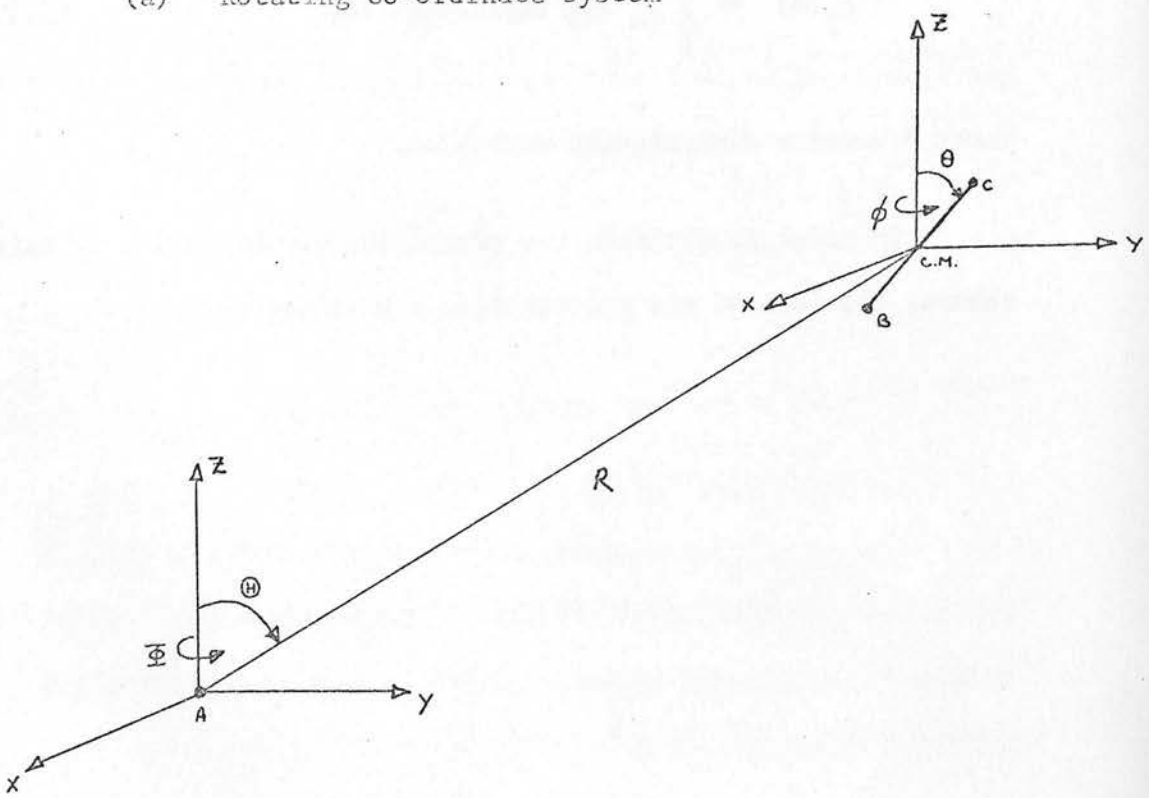

(b) 'Space-fixed Co-ordinate System

III.2 The Electrostatic Interaction Potential, V

The electrostatic potential energy of the charge distribution is given by

$$\phi = \Sigma_{i,j}\, e_i e_j / r_{ij}$$

and this quantity may be identified with the electrostatic part of the interaction, V. ϕ may be written in terms of two centres, one in each distribution. One of two co-ordinate systems can be adopted and they are displayed in Figure 2. When the two distributions do not overlap, the appropriate expressions for ϕ are derived in CAR50:

a. A co-ordinate system in which the two origins lie on a mutually common Z-axis

$$\phi(r)=\sum_{\ell_a=0}^{\infty}\sum_{\ell_b=0}^{\infty}\frac{(-1)^{\ell_b}}{R^{\ell_a+\ell_b+1}}\left\{A^{m}_{\ell_a\ell_b}\sum_i e_i r_i^{\ell_a} Y^{m}_{\ell_a}(\theta_i,\phi_i)\sum_j e_j r_j^{\ell_b} Y^{m}_{\ell_b}(\theta_j,\phi_j)\right\}_{m=-\ell_<}^{\ell_<} \qquad \text{III(2.1)}$$

where

$$A^{m}_{\ell_a\ell_b}=\left[4\pi(\ell_a+\ell_b)!\right]/\left[(2\ell_a+1)(2\ell_b+1)(\ell_a+m)!(\ell_a-m)!(\ell_b+m)!(\ell_b-m)!\right]^{\frac{1}{2}}$$

b. The origin of the second set of axes has co-ordinates R, Θ,Φ with respect to the origin of the first set:

$$\phi(r)=\sum_{\ell_a=0}^{\infty}\sum_{\ell_b=0}^{\infty}\frac{(-1)^{\ell_b}}{R^{\ell_a+\ell_b+1}}\sum_{m_a=-\ell_a}^{\ell_a}\sum_{m_b=-\ell_b}^{\ell_b} R^{m_a m_b}_{\ell_a\ell_b}\, Y^{-(m_a+m_b)}_{\ell_a+\ell_b}(\Theta,\Phi)$$

$$\sum_i e_i r_i^{\ell_a} Y^{m_a}_{\ell_a}(\theta_i,\phi_i)\sum_j e_j r_j^{\ell_b} Y^{m_b}_{\ell_b}(\theta_j,\phi_i) \qquad \text{III(2.2)}$$

where

$$B^{m_a m_b}_{\ell_a \ell_b} = \frac{(-1)^{m_a+m_b}(4\pi)^{3/2}}{[(2\ell_a+1)(2\ell_b+1)(2\ell_a+2\ell_b+1)]^{\frac{1}{2}}} \left\{ \frac{(\ell_a+\ell_b+m_a+m_b)!(\ell_a+\ell_b-m_a-m_b)!}{(\ell_a+m_a)!(\ell_a-m_a)!(\ell_a+m_b)!(\ell_b-m_b)!} \right\}^{\frac{1}{2}}$$

In each case the summation over i and j runs over electrons and nuclei. Co-ordinate system a. is appropriate to calculations in which the basis functions are defined relative to a rotating co-ordinate system, and co-ordinate system b. is appropriate where the basis functions are defined relative to axes fixed in space.

Throughout this work, the convention adopted for the phases of the spherical harmonics was that used in CON53, namely

$$Y_\ell^{-m}(\theta,\phi) = (-1)^m Y_\ell^{*m}(\theta,\phi)$$

As can be seen from equation III(1.8) the matrix elements V_{fi} are of the form

$$V_{fi} = \langle j_f m_f : V_f J_f M_f | \bar{V} | j_i m_i : V_i J_i M_i \rangle$$

where $\bar{V} = \langle \Omega | V | \Omega \rangle$, $\Omega_f = \Omega_i = \Omega$ see III(1.3)

and when BC = H_2, HD or D_2, Ω denotes the state $^1\Sigma_g^+$

Consider then, the quantity

$$Q^m_{\ell_b} = \sum_j e_j r_j^{\ell_b} Y^m_{\ell_b}(\theta_j,\phi_j) \qquad \text{III(2.3)}$$

('b' denotes molecular co-ordinates), where the angles θ_j and ϕ_j are defined to either co-ordinate system (a) or (b). The molecular electronic Σ state is defined in a co-ordinate system where the inter-

nuclear (BC) vector is the Z axis (in either co-ordinate system). The transformation of $Y^M_{\ell_b}$ to the new system is well known:

$$Y^M_{\ell_b} = \sum_{M'} Y^{M'}_{\ell_b} D^{*\ell_b}_{MM'}(\alpha,\beta,\gamma) \text{ (inverse transformation)}$$

where $D^{\ell}_{M'M}$ are the familiar rotation matrices (ROS57) and α β γ Euler angles of the BC internuclear vector relative to the axes X, Y, Z (see §I Figure 4). In the terms of the polar angles θ, ϕ

$$\alpha = \phi, \beta = \theta, \gamma = 0$$

Hence III(2.3) transforms to

$$Q^m_{\ell_b} = e\{r_1^{\ell_b} Z_1 Y^m_{\ell_b}(\theta_1\phi_1) + r_2^{\ell_b} Z_2 Y^m_{\ell_b}(\theta_2,\phi_2)\} - e\sum_{m'}\sum_j r_j^{\ell_b} Y^{m'}_{\ell_b}(\theta_j\phi_j)$$

$$D^{*\ell_b}_{mm'}(\phi,\theta,0)$$

where 1 and 2 denote the co-ordinates of the two nuclei, j denotes electronic co-ordinates and functions of nuclear co-ordinates have not been transformed. In addition,

$$\theta_1\phi_1 = \theta,\phi$$

$$\theta_2\ \phi_2 = \pi-\theta, \phi+\pi \quad \text{and} \quad Y^m_\ell(\pi-\theta,\phi+\pi) = (-1)^\ell Y^m_\ell(\theta,\phi)$$

Hence

$$Q^m_{\ell_b} = e\left\{\left[Z_1 r_1^{\ell_b} + (-1)^{\ell_b} Z_2 r_2^{\ell_b}\right] Y^m_{\ell_b}(\theta,\phi) - e\sum_{m'}\sum_j r_j^{\ell_b} Y^{m'}_{\ell_b}(\theta_j\phi_j) D^{*\ell_b}_{mm'}(\phi,\theta,0)\right\}$$

III(2.4)

In the case of H_2, HD and D_2, $\bar{V}$ and $\phi_{(r)}$ are identical except that terms like $Q^m_{l_b}$ in $\phi(r)$ are replaced by

$$\langle {}^1\Sigma_g^+ | Q^m_{l_b} | {}^1\Sigma_g^+ \rangle \quad \text{in } \bar{V}. \qquad \text{Noting that}$$

$$\langle {}^1\Sigma | Y^m_\ell | {}^1\Sigma \rangle = \langle {}^1\Sigma | Y^o_\ell | {}^1\Sigma \rangle \delta_{mo}$$

and that $$D^\ell_{mo}(\phi,\theta,o) = (4\pi/2\ell+1)^{\frac{1}{2}} Y^{*m}_\ell(\theta,\phi)$$

it is easy to show that

$$\langle {}^1\Sigma | Q^m_{\ell_b} | {}^1\Sigma \rangle = \bar{Q}_{\ell_b} Y^m_{\ell_b}(\theta,\phi)$$

where $$\bar{Q}_{\ell_b} = e\left[r_1^{\ell_b} + (-1)^{\ell_b} r_2^{\ell_b}\right] - 2e\left[\frac{4\pi}{(2\ell_b+1)}\right]^{\frac{1}{2}} \langle {}^1\Sigma | r^{\ell_b} Y^o_{\ell_b} | {}^1\Sigma \rangle \qquad \text{III(2.5)}$$

where θ, ϕ are the angles of orientation of the internuclear vector in the co-ordinate system X Y Z in (a) or (b).

Hence $\bar{V}$ in the two co-ordinate systems is given by

a. $$\bar{V} = \sum_{\ell_a=0}^{\infty} \sum_{\ell_b=0}^{\infty} \frac{(-1)^{\ell_b}}{R^{\ell_a+\ell_b+1}} \sum_{m=-\ell_<}^{\ell_<} A^m_{\ell_a \ell_b} \bar{Q}_{\ell_b} Y^{-m}_{\ell_b}(\theta,\phi)$$

$$\sum_i e_i r_i^{\ell_a} Y^m_{\ell_a}(\theta_i \phi_i) \qquad \text{III(2.6)}$$

(b) $$\overline{V}=\sum_{\ell_a=0}^{\infty}\sum_{\ell_b=0}^{\infty}\frac{(-1)^{\ell_b}}{R^{\ell_a+\ell_b+1}}\sum_{m_a=-\ell_a}^{\ell_a}\sum_{m_b=-\ell_b}^{\ell_b}B_{\ell_a\ell_b}^{m_a m_b}\,Y_{\ell_a+\ell_b}^{-(m_a+m_b)}(\Theta,\Phi)\;\overline{Q}_{\ell_b}\;Y_{\ell_b}^{m_b}(\theta,\phi)$$

$$\Sigma_i e_i r_i^{\ell_a} Y_{\ell_a}^{m_a}(\theta_i,\phi_i)$$

The atomic transitions to be considered are $I(5^2P_{\frac{1}{2}})\rightarrow I(5^2P_{3/2})$, $Tl(6^2P_{3/2})\rightarrow Tl(6^2P_{\frac{1}{2}})$, $Hg(6^3P_2)\rightarrow Hg(6^3P_o)$, $Te(6^3P_o)\rightarrow Te(6^3P_2)$ and $Te(6^3P_1)\rightarrow Te(6^3P_2)$. Only those terms in the multipole expansion which connect these states are therefore of interest in first order. Making use of the relation

$$\int Y_{\ell_3}^{*m_3}\,Y_{\ell_2}^{m_2}\,Y_{\ell_1}^{m_1}\sin\theta\,d\theta\,d\phi=\left[\frac{(2\ell_1+1)(2\ell_2+1)}{4\pi(2\ell_3+1)}\right]^{\frac{1}{2}}$$

$$\langle\ell_1\ell_2 m_1 m_2|\ell_1\ell_2\ell_3 m_3\rangle\langle\ell_1\ell_2\;oo|\ell_1\ell_2\ell_3 o\rangle \qquad \text{III(2.7)}$$

where <1> are Clebsch-Gordan coefficients in the notation adopted in CON53, and considering the symmetry properties of the Clebsch-Gordan coefficients, it can be shown that the above states are connected by terms involving the spherical harmonics Y_2^m. For uncharged molecules, terms with $\ell_a=2,\ell_b=1$ and $\ell_a=2,\ell_b=2$ are the lowest order multipole terms to satisfy this condition. However $\overline{Q}_1$, the dipole moment function, of BC is either very small (HD) or zero (H_2,D_2). The lowest order term of interest is therefore that with $\ell_a=\ell_b=2$, denoted $\overline{V5}$ which, in terms of co-ordinate systems (a) and (b) is given by

$$\overline{V5}=-(12\pi e/5R^5)\overline{Q}_2\,\hat{G}$$

where

$$\hat{G} = \Sigma_i r_i^2 \{A\, Y_2^2(i) + B\, Y_2^1(i) + C\, Y_2^o(i) + D\, Y_2^{-1}(i) + E\, Y_2^{-2}(i)\} \qquad \text{III(2.8)}$$

and the summation is over the electrons of atom A.

Co-ordinate System (a)

$$A = (1/3)Y_2^{-2}(\text{mol}),\ B = (4/3)Y_2^{-1}(\text{mol}),\ C = 2Y_2^o(\text{mol}),\ D = (4/3)Y_2^1(\text{mol}),$$

$$E = (1/3)Y_2^2(\text{mol}) \qquad \text{III(2.9)}$$

Co-ordinate System (b)

$$A = (35f_5/24)e^{-4i\Phi}Y_2^2(\text{mol}) - (35f_4/12)e^{-3i\Phi}Y_2^1(\text{mol}) + (\sqrt{3}f_3/12\sqrt{2})e^{-2i\Phi}$$
$$Y_2^o(\text{mol}) - (f_2/12)e^{-i\Phi}Y_2^{-1}(\text{mol}) + (f_1/24)Y_2^{-2}(\text{mol})$$

$$B = -(35f_4/12)e^{-3i\Phi}Y_2^2(\text{mol}) + (f_3/6)e^{-2i\Phi}Y_2^1(\text{mol}) - (\sqrt{3}f_2/6\sqrt{2})e^{-i\Phi}Y_2^o(\text{mol})$$
$$+ (f_1/6)Y_2^{-1}(\text{mol}) + (f_2/12)e^{i\Phi}Y_2^{-2}(\text{mol})$$

$$C = (\sqrt{3}f_3/12\sqrt{2})e^{-2i\Phi}Y_2^2(\text{mol}) - (\sqrt{3}f_2/6\sqrt{2})e^{-i\Phi}Y_2^1(\text{mol}) + (f_1/4)Y_2^o(\text{mol})$$
$$+ (\sqrt{3}f_2/6\sqrt{2})e^{i\Phi}Y_2^{-1}(\text{mol}) + (\sqrt{3}f_3/12\sqrt{2})e^{2i\Phi}Y_2^{-2}(\text{mol})$$

figure 3

Co-ordinate System for H_2 Quadrupole Moment Calculation

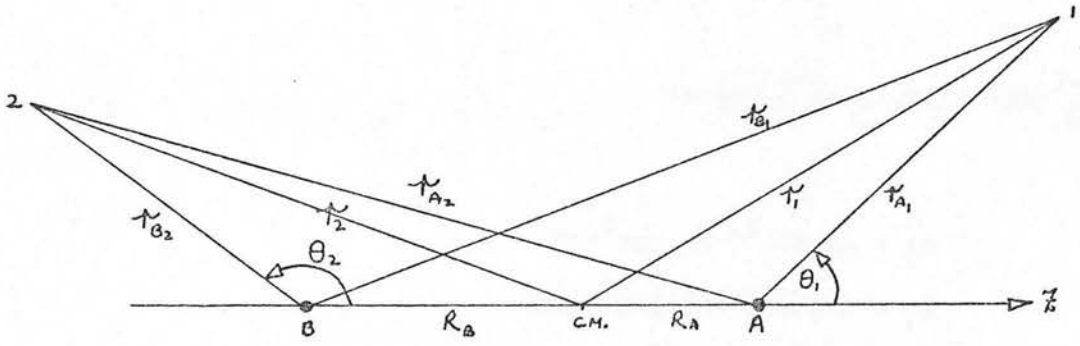

Approximation:

The Centre of mass (C.M.) of the AB molecule lies on the C.M. of the two nuclei.

III.3 Evaluation of Atomic and Molecular Matrix Elements

It can be seen from equations III(1.9) and III(1.13) that the transition probabilities ${}_{P}V^{1}J^{1}M^{1}j^{1}m^{1}$ / $V^{11}J^{11}M^{11}j^{11}m^{11}$ are proportional to

$$\langle V^{1}J^{1}|\bar{Q}_2|V^{11}J^{11}\rangle^2 \langle j^{1}m^{1}|\hat{G}|j^{11}m^{11}\rangle^2$$

Clearly then, these matrix elements must be evaluated accurately if the mte constant in equation III(1.6) is to be estimated reliably.

Hydrogen Molecule Quadrupole Moment Matrix Elements

In a more familiar notation, $\bar{Q}_2 = \bar{\Theta}zz$ (BUC59) where $\bar{\Theta}zz = \langle {}^{1}\Sigma_g^{+}|\Theta zz|{}^{1}\Sigma_g^{+}\rangle$ and Θzz is the zz component of the nine-element Quadrupole moment tensor.

As a first step, an approximate ab initio calculation of $\bar{\Theta}zz$ was attempted for H_2. The co-ordinate system used is shown in Figure 3.

The Quadrupole moment operator (zz component) is given by

$$\hat{\Theta}zz = e(R_A^2+R_B^2) - (e/2)(\hat{g}_1+\hat{g}_2),\ \hat{g}_n = 3z_n^2 - r_n^2 \qquad \text{III(3.1)}$$

c.p. III(2.5).

If the Heitler-London function

$$\Psi_{el} = \left[2(1+S^2)\right]^{-\frac{1}{2}}\{\phi_A(1)\phi_B(2)+\phi_A(2)\phi_B(1)\}\frac{1}{\sqrt{2}}$$

$$\{\alpha(1)\beta(2)-\alpha(2)\beta(1)\}$$

is used, where $\phi = H_{1_s} = (a_o^{3/2}\sqrt{\pi})^{-1}\exp(-r/a_o)$

and $S = \langle\phi_A(1)|\phi_B(1)\rangle$ III(3.2)

then

$$\bar{\theta}_{zz} = e(R_A^2+R_B^2) - \frac{e}{2(1+S^2)}\{\langle\phi_A(1)\phi_B(2)|\hat{g}_1+\hat{g}_2|\phi_A(1)\phi_B(2)\rangle$$

$$+\langle\phi_A(1)\phi_B(2)|\hat{g}_1+\hat{g}_2|\phi_A(2)\phi_B(1)\rangle\}$$

Noting that

$$\langle\phi_A(1)\phi_B(2)|\hat{g}_1+\hat{g}_2|\phi_A(1)\phi_B(2)\rangle = 2(R_A^2+R_B^2) \quad ,$$

$$\langle\phi_A(1)\phi_B(2)|\hat{g}_1+\hat{g}_2|\phi_A(2)\phi_B(1)\rangle = S\langle\phi_A(1)|\hat{g}_1|\phi_B(1)\rangle$$

$$+S\langle\phi_B(2)|\hat{g}_2|\phi_A(2)\rangle \quad ,$$

$$\langle\phi_A(1)|\hat{g}_1|\phi_B(1)\rangle = 2R_A^2S+Q, \quad \langle\phi_B(2)|\hat{g}_2|\phi_A(2)\rangle = 2R_B^2S+Q,$$

the result is obtained

$$\bar{\theta}_{zz} = \frac{-eSQ}{(1+S^2)} \quad , \quad Q = 2a_o^2\int_{-1}^{1}\{\int_o^{\infty} r^{*4}(3x^2-1)-2xr^{*3}R\, e^{-r^*+(r^{*2}-2xr^*R+R^2)^{\frac{1}{2}}}$$

$$dr^*\}dx$$

$$S = 2\int_{-1}^{1}\{\int_o^{\infty}\exp(-r^*+(r^{*2}-2xr^*R+R^2)^{\frac{1}{2}})r^{*2}\,dr^*\}dx \qquad \text{III(3.3)}$$

$r^* = r/a_o$, $x = -\cos\theta$, $R = (R_A + R_B)/a_o$

Thus when a two-centre representation is used to describe the $^1\Sigma^+$ electronic wave function, the same quadrupole moment is predicted for H_2, HD and D_2.

The x integrals were evaluated by summation ($\Delta x = 10^{-3}$) and the r* integrals were evaluated using a 24-point Gaussian-Laguerre Quadrature (KRY62).

Vibrational Wave functions

The vibrational wave functions, R, of diatomic molecules satisfy the equation

$$\frac{d^2S}{dr^2} + \left\{\frac{2\mu}{\hbar^2}\left[E-V(r)\right] - \frac{J(J+1)}{r^2}\right\} S = 0 \qquad \text{III(3.4)}$$

where $S = R/r$ and J is the rotational quantum number. When a parabolic potential is used for V(r),

$$V(r) = (k/2)\,(r-r_e^{\,2}) \qquad \text{III(3.5)}$$

and J=0 (the effect of neglecting the rotation of the molecule is considered below), the solutions of III(3.4) are the well known harmonic oscillator eigen functions (PAU35):

$$S_v(r) = N_v e^{-\xi^2/2} H_v(\xi)\ ,\ \xi = \alpha^{\frac{1}{2}}(r-r_e) \qquad \text{III(3.6)}$$

$$N_v = \{(\alpha/\pi)^{\frac{1}{2}} / 2^v.v!\}^{\frac{1}{2}}\ ,\ \alpha = 2\pi\mu\nu_{osc}/\hbar$$

and $H_v(\xi)$ are the familiar Hermite Polynomials. ν_{osc}., and hence k is

figure 4

Quadrupole moment function/ea_o^2 as a function of R/au.

Upper Curve - Kolos and Wolniewicz

Lower Curve - Heitler London

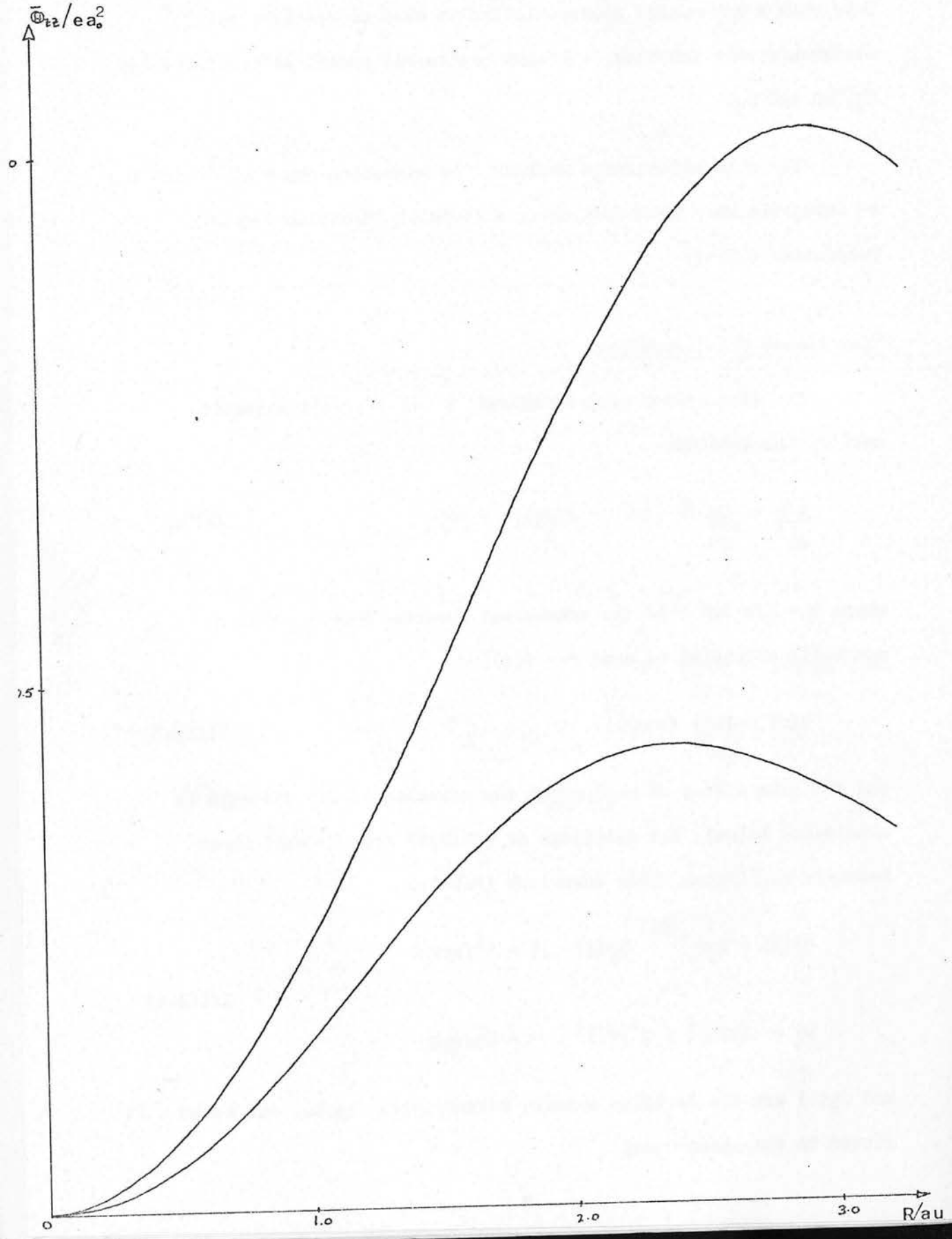

fitted to the spectroscopic data. For H_2, $\alpha = 18.3973\ a_o^{-2}$ and $r_e = 1.4016 a_o$.

If harmonic oscillator eigen functions are used for the vibrational wave functions of H_2, it follows that

$$\langle v^1 J^1 | \bar{\Theta}_{zz} | v^{11} J^{11} \rangle = \langle v^1 | \bar{\Theta}_{zz} | v^{11} \rangle = \Theta_{v^1 v^{11}}$$

The matrix elements Θ_{oo}, Θ_{o1} and Θ_{o2} are most conveniently written as

$$\Theta_{oo} = (1/\sqrt{\pi}) \int_{-\infty}^{\infty} e^{-z^{*2}} \bar{\Theta}_{zz}(x^*) dz^*$$

$$\Theta_{o1} = (1/\sqrt{2\pi}) \int_{-\infty}^{\infty} e^{-z^{*2}} z^* \bar{\Theta}_{zz}(x^*) dz^* \qquad \text{III(3.7)}$$

$$\Theta_{o2} = (1/2\sqrt{2\pi}) \int_{-\infty}^{\infty} e^{-z^{*2}} (4z^{*2}-2) \bar{\Theta}_{zz}(x^*) dz^*$$

where $\beta = a_o^2 \alpha$, $x^* = (r - r_e)/a_o$ and $z^* = \sqrt{\beta} x^*$.

The integrals in III(3.7) are particularly suitable for evaluation by Gaussian-Hermite Quadrature (KRY62) which gave the results

$$\Theta_{oo} = 0.2814 \quad e a_o^2$$

$$\Theta_{o2} = -2.64 \times 10^{-3} \quad e a_o^2$$

In fact, however, the Heitler London function, III(3.2), gives rather a poor approximation to the best calculated Quadrupole moment function (KOL(65)) as can be seen from Figure 4, and improved

vibrational wave functions are obtained by using the Morse Potential for V(r) in equation III(3.4):

$$V(r) = D\left[1-e^{-a(r-r_e)}\right]^2 \qquad \text{III(3.8)}$$

the solutions of equation III(3.4) are then given (PAU35) by

$$S_{VJ}(r) = (a/N_{VJ})^{\frac{1}{2}}\{e^{-z/2} z^{b/2} F_{VJ}(z)\}$$

where $z = 2d\ e^{-a(r-r_e)}$, $N_{VJ} = \int_o^\infty e^{-z}\ z^{b-1}\ F_{VJ}(z)dz$

$$F_{VJ}(z) = \Sigma_{n=o}^{V}\ a_n z^n \ , \quad a_o=1, \quad a_{n+1} = -(V-n)a_n/\left[(n+1)(n+k-2V)\right]$$

$$d = 2\mu(D_e+C_2)^{\frac{1}{2}}/a \ , \qquad \text{III(3.9)}$$

$$k = \left[(2\mu)^{\frac{1}{2}}(2D_e-C_1)\right] / \left[a(D_e+C_2)^{\frac{1}{2}}\right] \ , \quad b = k-1-2V$$

$$C_1 = A(4/ar_e-6/a^2r_e^2), \ C_2 = A(-1/ar_e+3/a^2r_e^2)$$

and $A = J(J+1)/2\mu r_e^2$ all in reduced units.

D_e and a are obtained by fitting the eigen energies of $S_{VJ}(r)$ to the spectroscopic data:

$$a = \frac{(2\mu\omega_e x_e)^{\frac{1}{2}}}{\hbar} \cdot \left(\frac{hc}{27.2106em_e}\right)^{\frac{1}{2}} \qquad \text{III(3.10)}$$

$$D_e = \left(\frac{\omega_e^2}{4\omega_e x_e}\right) \cdot \left(\frac{hc}{27.2106e}\right)$$

Wave functions for the Harmonic potential (- - -) and Morse potential (-) for the states, V=o, J=o and V=2, J=o of the $X^1\Sigma_g^+$ electronic ground state of H_2.

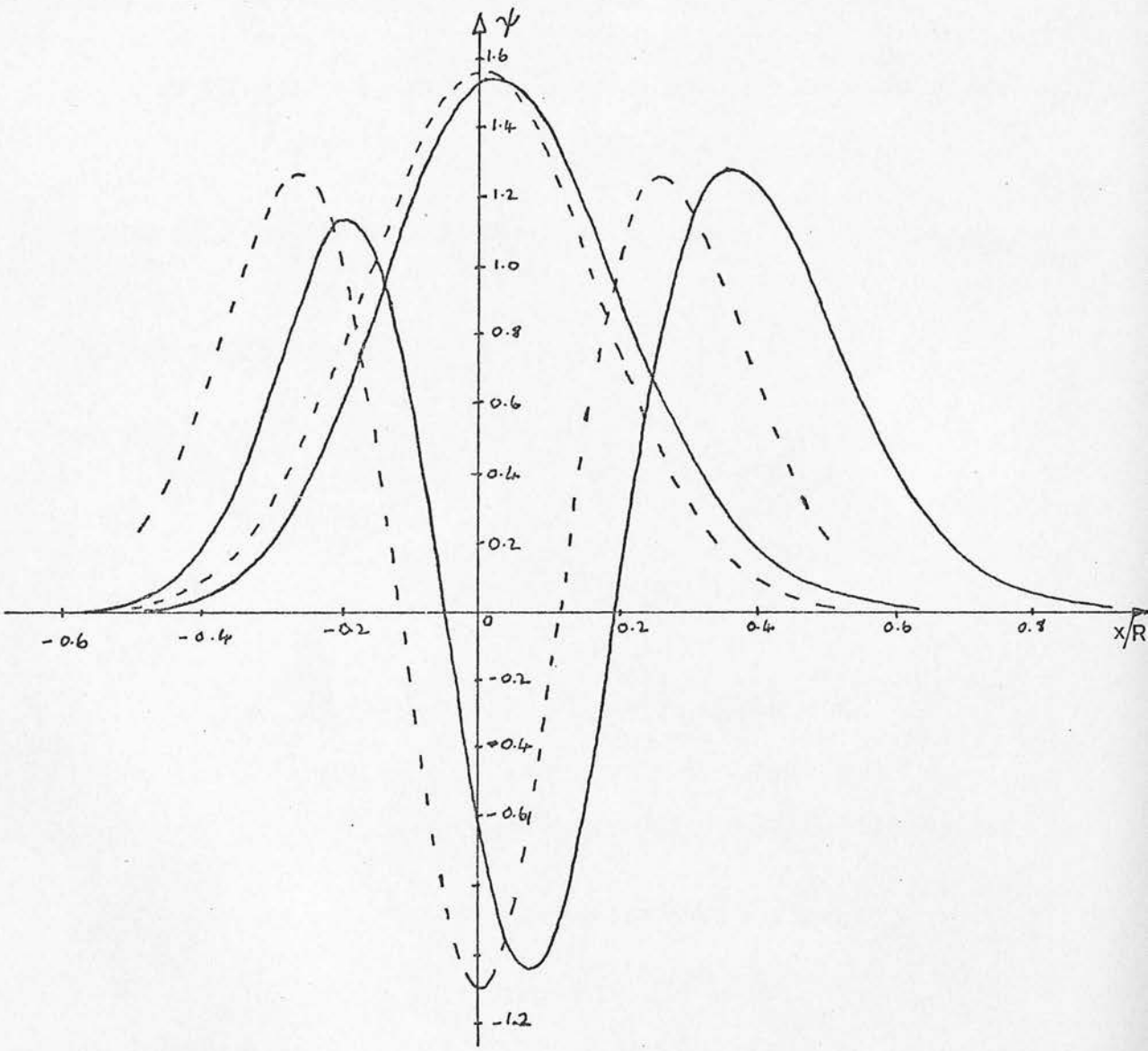

TABLE 2

Molecular Constants and Morse Parameters for H_2, HD and D_2.

Molecule	$\mu \times 10^{27}$/kg	ω_e/cm^{-1}	$\omega_e x_e$/cm^{-1}	B_e/cm^{-1}	r_e/Å	D_e/A.U.	a/a_o^{-2}
H_2	0.8367114	4401.217	121.343	60.8591	0.74140	0.181838	1.00788
HD	1.115329	3811.924	90.7113	45.6378	0.74155	0.182465	1.00611
D_2	1.672136	3118.36	64.097	30.442	0.74154	0.172810	1.03555

where ω_e and $\omega_e x_e$ are in cm^{-1}, μ is in kg, C is in cms sec^{-1}, e is the electronic charge in coulombs and m_e is the electron rest mass in kg. r_e was obtained from the rotational constant B_e:

$$B_e = h/8\pi^2 c\mu r_e^2 \quad (B_e \text{ in } cm^{-1}, r_e \text{ in m}). \qquad \text{III(3.11)}$$

The best spectroscopic data available for H_2 (FIN65), HD (ST057) and D_2 (ST057, BRE73) was used to determine a, D_e and r_e and some of this data, together with the values calculated for a, D_e and r_e are listed in Table 2 and the parabolic and Morse potential wave functions for the V=0 J=0 and V=2,J=0 states of H_2 are displayed in Figure 5.

The matrix elements $\langle oo|\Theta_{zz}|20\rangle$ and $\langle oo|\Theta_{zz}|oo\rangle$ were computed using three sets of wave functions

a. parabolic potential vibrational functions, Heitler-London Quadrupole moment function.

b. parabolic potential vibrational functions, numerical Quadrupole moment function (KOL65).

c. Morse potential vibrational functions, numerical Quadrupole moment function.

In the case of morse potential vibrational functions, the matrix elements $\langle VJ|\Theta_{zz}|V^1J^1\rangle$ are most conveniently written as:

$$\langle VJ|\Theta_{zz}|V^1J^1\rangle = \frac{(d^{b/2}d^{1^{b^1/2}}/d^{b})\int_o^\infty e^{-x}\,\Theta_{zz}(r)x^{b-1}\,F_{VJ}(\frac{dx}{d})F_{V^1J^1}(\frac{d^1x}{d})dx}{(N_{VJ}N_{V^1J^1})^{\frac{1}{2}}}.$$

TABLE 3

Matrix elements of $^{\Theta}zz$ for H_2 (calculated)

Calculation	$\langle oo\|^{\Theta}zz\|oo\rangle/ea_o^2$	$\langle oo\|^{\Theta}zz\|2o\rangle/ea_o^2$
(a)	0.2814	-2.64×10^{-3}
(b)	0.4594	1.56×10^{-3}
(c)	0.4811	-1.01×10^{-2}

TABLE 4

Available off diagonal matrix elements of $^{\Theta}zz$ for H_2

$\langle 1o\|^{\Theta}zz\|oo\rangle/D\text{Å}$	$\langle 2o\|^{\Theta}zz\|oo\rangle/D\text{Å}$	$\langle 3o\|^{\Theta}zz\|oo\rangle/D\text{Å}$	Ref.
-100×10^{-3}	-15.9×10^{-3}	-2.8×10^{-3}	Exp't.
-59.3×10^{-3}	-22.3×10^{-3}	-6.0×10^{-3}	JAM33
-125×10^{-3}	-12.2×10^{-3}	-3.8×10^{-3}	RAN62
-116×10^{-3}			JAM64
-123×10^{-3}	-20.7×10^{-3}	-3.5×10^{-3}	RAN63

Figure 6

Co-ordinate system for HD Quadrupole moment function

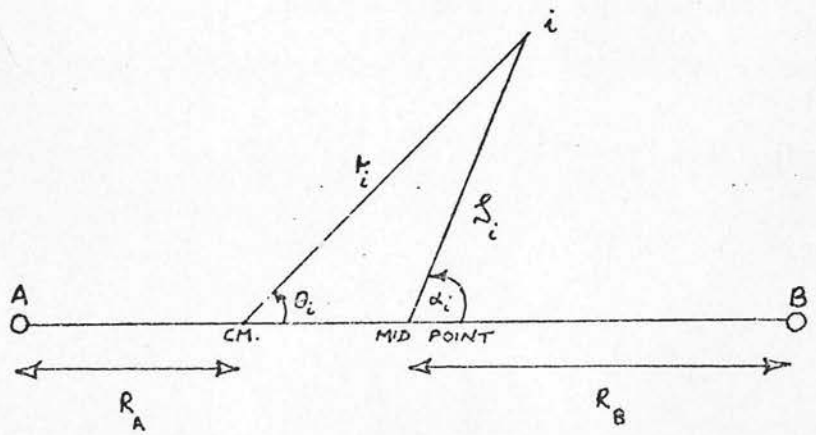

where $$N_{VJ} = \int_0^\infty e^{-z} z^{b-1} F^2_{VJ}(z)dz \qquad (z \text{ as in III(3.9)})$$

$$x = 2de^{-a(r-r_e)}, \quad \bar{d} = (d+d^1)/2, \quad \bar{b} = (b+b^1)/2 \qquad \text{III(3.12)}$$

in which the integrals are of a form suitable for evaluation by Gaussian-Laguerre Quadrature (KRY62), the values of $^{\Theta}zz$ at the quadrature points being obtained by interpolation of a table of $^{\Theta}zz$. The results obtained using the three sets of basis functions (a), (b) and (c) are presented in Table 3. In all 6 cases the numerical quadratures used were shown to have converged.

The best calculated value (WOL66) for $\langle oo|^{\Theta}zz|oo\rangle$ is

$$\langle oo|^{\Theta}zz|oo\rangle = 0.4842 \text{ A.U.}$$

The value obtained from calculation (c) was 99.4% of this value. In addition, expectation values of the operators R^2 and $(3z^2-r^2)$ were computed for the states V=0 J=0, V=1, J=0 and V=2, J=0 and in all cases the values obtained from scheme (c) were found to be between 97% and 99% of the best values. Accordingly scheme (c) was chosen for further calculation of matrix elements $\langle V\ J|^{\Theta}zz|V^1J^1\rangle$.

Available data on the off-diagonal elements of $^{\Theta}zz$, taken from 65 is summarised in Table 4. The values of $\langle o|^{\Theta}zz|oo\rangle$ and $\langle 2o|^{\Theta}zz|oo\rangle$ should be compared with the values obtained from the present calculation:

$$\langle 10|\,{}^{\Theta}zz|oo\rangle = 118.6\times10^{-3}\,DA^{2}$$

$$\langle 20|\,{}^{\Theta}zz|oo\rangle = -13.6\times10^{-3}\,DA$$

Quadrupole moment matrix elements for D_2 were calculated using the same scheme with parameters from Table 2.

Finally, it is necessary to consider the quadrupole moment function for HD. The co-ordinate systems are shown in Figure 6.

From the calculations of Kolos and Wolniewicz (KOL65), the expectation value of the operator

$$\Theta^{1}zz = eR^{2}/2 - e\Sigma_i \zeta_i^{2}(3\cos^{2}\alpha_i - 1) \qquad \text{III(3.13)}$$

for the $^{1}\Sigma_g^{+}$ electronic ground state of H_2 (and HD and D_2) is known. However, the operator of interest in the present calculation is

$$\Theta zz = e(R_A^{2} + R_B^{2}) - e\Sigma_i r_i^{2}(3\cos^{2}\theta_i - 1)$$

In the case of H_2 and D_2, where the c.m. of the two nuclei lies on the mid-point of the internuclear vector, the two operators are identical. Since the electronic wave function is (to a good approximation) the same for H_2, HD and D_2, it follows that

$$\langle\psi|\,{}^{\Theta 1}zz|\psi\rangle = \langle\phi H_2|\,{}^{\Theta 1}zz|\phi H_2\rangle = \langle\phi D_2|\,{}^{\Theta 1}zz|\phi D_2\rangle$$

where ψ is the wave function used by Kolos and Wolniewicz

In the case of HD is can readily be shown that

$$\Theta_{zz} = \Theta^1_{zz} + e\beta^2R^2 - 2e\beta R\Sigma_i\xi_i\cos\alpha_i, \quad \beta = (M_D - M_H)/(M_D + M_H)$$

$$\therefore \langle\phi_{HD}|\Theta_{zz}|\phi_{HD}\rangle = e\beta^2R^2 + \langle\psi|\Theta^1{}_{zz}|\psi\rangle \qquad \text{III(3.14)}$$

since $\langle\phi_{HD}|\Sigma_i\zeta_i\cos\alpha_i|\phi_{HD}\rangle = 0$

Various quadrupole moment matrix elements for H_2, HD and D_2 are displayed in Table 5 along with several atomic matrix elements.

Atomic Matrix Elements

As can be seen from equation III(2.8), the term $\bar{V}5$ in the multipole expansion of the A-BC potential may be written

$$\bar{V}5 = \alpha\Sigma_i r_i^2(A\,Y_2^2(i) + B\,Y_2^1(i) + CY_2^o(i) + DY_2^{-1}(i) + EY_2^{-2}(i)) \qquad \text{III(3.15)}$$

where the summation runs over the electrons of the atom,

$$\alpha = -12\pi e\,\bar{\Theta}_{zz}(BC)/5R^5$$

and A, B etc are given by equations III(2.9) or III(2.10).

The main elements of $\bar{V}5$ relevant to the transitions $I(5^2P_{\frac{1}{2}}) \rightarrow I(5^2P_{3/2})$, $Tl(6^2P_{3/2}) \rightarrow Tl(6^2P_{\frac{1}{2}})$, $Hg(6^3P_2) \rightarrow Hg(6^3P_o)$, $Te(5^3P_o) \rightarrow Te(5^3P_2)$ and $Te(5^3P_1) \rightarrow Te(5^3P_2)$ are considered in turn below.

The notation used is

$$|JM\rangle = \Sigma_{M_LM_S}\langle LSM_LM_S|LSJM\rangle|LSM_LM_S\rangle$$

where $|JM\rangle$ denotes eigen functions of the total angular momentum operator, $|LSM_L M_S\rangle$ denotes eigen functions of the orbital and spin angular momenta and $\langle LSM_L M_S|LSJM\rangle$ are Clebsch-Gordan coefficients in the notation of CON53.

a. Iodine $I(5^2P_{\frac{1}{2}}) \rightarrow I(5^2P_{3/2})$

The wave functions for the $^2P_{3/2}$ and $^2P_{\frac{1}{2}}$ states of an atom are given by

$$
\begin{aligned}
|3/2\ 3/2\rangle &= |1\tfrac{1}{2}\ 1\tfrac{1}{2}\rangle \\
|3/2\ \tfrac{1}{2}\rangle &= (1/\sqrt{3})\{|1\tfrac{1}{2}\ 1\text{-}\tfrac{1}{2}\rangle + \sqrt{2}|1\tfrac{1}{2}\,0\,\tfrac{1}{2}\rangle\} \\
|3/2\text{-}\tfrac{1}{2}\rangle &= (1/\sqrt{3})\{|1\tfrac{1}{2}\text{-}1\tfrac{1}{2}\rangle + \sqrt{2}|1\tfrac{1}{2}\,0\,\text{-}\tfrac{1}{2}\rangle\} \\
|3/2\text{-}3/2\rangle &= |1\tfrac{1}{2}\text{-}1\text{-}\tfrac{1}{2}\rangle \\
|\tfrac{1}{2}\ \tfrac{1}{2}\rangle &= (1/\sqrt{3})\{\sqrt{2}|1\tfrac{1}{2}1\text{-}\tfrac{1}{2}\rangle - |1\tfrac{1}{2}\,0\,\tfrac{1}{2}\rangle\} \\
|\tfrac{1}{2}\text{-}\tfrac{1}{2}\rangle &= (1/\sqrt{3})\{|1\tfrac{1}{2}\,0\,\text{-}\tfrac{1}{2}\rangle - \sqrt{2}|1\tfrac{1}{2}\text{-}1\tfrac{1}{2}\rangle\}
\end{aligned}
\qquad \text{III(3.16)}
$$

For the p^5 configuration, the functions $|LSM_L M_S\rangle$ are 5 x 5 determinants:

$$|1\tfrac{1}{2}\ 1\tfrac{1}{2}\rangle = (1/\sqrt{5!})\left|p_1^{\alpha}(1)p_1^{\beta}(2)p_0^{\alpha}(3)p_0^{\beta}(4)p_{-1}^{\alpha}(5)\right|$$

$$|1\tfrac{1}{2}1\text{-}\tfrac{1}{2}\rangle = (1/\sqrt{5!})\left|p_1^{\alpha}(1)p_1^{\beta}(2)p_0^{\alpha}(3)p_0^{\beta}(4)p_{-1}^{\beta}(5)\right|$$

$$|1\tfrac{1}{2}\,0\,\tfrac{1}{2}\rangle = (1/\sqrt{5!})\left|p_1^{\alpha}(1)p_1^{\beta}(2)p_0^{\alpha}(3)p_{-1}^{\alpha}(4)p_{-1}^{\beta}(5)\right|$$

$$|1\tfrac{1}{2}\,0\,\text{-}\tfrac{1}{2}\rangle = (1/\sqrt{5!})\left|p_1^{\alpha}(1)p_1^{\beta}(2)p_0^{\beta}(3)p_{-1}^{\alpha}(4)p_{-1}^{\beta}(5)\right|$$

$$|1\tfrac{1}{2}\,1\tfrac{1}{2}> = (1/\sqrt{5!})|p_1\alpha(1)p_0\alpha(2)p_0\beta(3)p_{-1}\alpha(4)p_{-1}\beta(5)|$$

$$|1\tfrac{1}{2}\,-1\,-\tfrac{1}{2}> = (1/\sqrt{5!})|p_1\beta(1)p_0\alpha(2)p_0\beta(3)p_{-1}\alpha(4)p_{-1}\beta(5)|$$

where $|a(1)b(2)c(3)d(4)e(5)|$ is an abbreviation for

$$\begin{vmatrix} a(1) & \dots & a(5) \\ b(1) & \dots & b(5) \\ c(1) & \dots & c(5) \\ d(1) & \dots & d(5) \\ e(1) & \dots & e(5) \end{vmatrix}$$

$$p_m = R^{5p}(r)Y_1^m(\theta\phi) \quad , \quad I(5^2P_{3/2})$$

$$= R^{5p}(r)Y_1^m(\theta\phi) \quad , \quad I(5^2P_{\frac{1}{2}})$$

III(3.17)

and α and β are the $m_s = +\frac{1}{2}$ and $-\frac{1}{2}$ spin functions respectively. Consider the matrix component of the operator $\bar{V}5$ between two determinants:

$$<p|\bar{V}5|q> = (1/N!)\int|U_1^*(1) \dots U_N^*(N)|\bar{V}5|U_1^1(1)\dots U_N^1|_{d\tau_1}\dots d\tau_N$$

where $\int\dots d\tau_1\dots d\tau_N$ includes summation over the spin variables.

Expanding the determinant on the left, noting that all N! resulting integrals have the same value since $\bar{V}5$ is symmetrical with respect to interchange of the electrons, yields the result

$$<p|\bar{V}5|q> = \int\{U_1^*(1)\dots U_N^*(N)\}\bar{V}5|U_1^1(1)\dots U_N^1(N)|d\tau_1\dots d\tau_N \quad .$$

Furthermore, $\bar{V}5$ may be written

$$\bar{V}5 = \Sigma_m \Sigma_i f_m(i)$$

where $f_m(i)$ is a one-electron operator for the i^{th} electron and does not operate on the spin function. Hence the only non-vanishing terms contributing to $\langle p|\bar{V}5|q\rangle$ are given by

$$\langle p|\bar{V}5|q\rangle = \Sigma_m \int U_1^*(1)\ldots U_i^*(i)\ldots U_N^*(N) f_m(i) U_1^1(1)\ldots U_i^1(i)\ldots$$

$$U_N^1(N)\, d\tau_1 \ldots d\tau_N$$

in which U_n^1 and U_n refer to the same orbital for all n except possibly n=i, so that

$$\langle p|\bar{V}5|q\rangle = \Sigma_m \int U_i^*(i) f_m(i) U_i^1(i)\, d\tau_i$$

where it has been assumed that

$$\int U_n^* U_n^1 d\tau = 1$$

Since U_n^1 and U_n describe one orbital for the atom in two different states, this is an approximation because all the orbitals are distorted in the excited state. However, it probably does not introduce an error greater than 10%.

Hence, for example,

$$\langle 1\tfrac{1}{2}1\tfrac{1}{2}|\bar{V}5|1\tfrac{1}{2}1\tfrac{1}{2}\rangle = \Sigma_m 2\langle p_1|f_m|p_1\rangle + 2\langle p_0|f_m|p_0\rangle + \langle p_{-1}|f_m|p_{-1}\rangle$$

$$= \langle R^{5p}(5^2P_{\frac{1}{2}})|r^2|R^{5p}(5^2P_{3/2})\rangle \Sigma_m a_m \{2\langle Y_1^1|Y_2^m|Y_1^1\rangle$$

$$+2\langle Y_1^o|Y_2^m|Y_1^o\rangle + \langle Y_1^{-1}|Y_2^m|Y_1^{-1}\rangle\}$$

Since $f_m(i) = \alpha a_m Y_2^m(i)$.

A well-known property of spherical harmonics is

$$\Sigma_m \int Y_\ell^{*m} Y_1^m Y_\ell^m \, d\Omega = o$$

Making use of this result it follows that

$$\langle 1\tfrac{1}{2}1\tfrac{1}{2}|\bar{V}5|1\tfrac{1}{2}1\tfrac{1}{2}\rangle = -\alpha\langle R^{5p}(5^2P_{\frac{1}{2}})|r^2|R^{5p}(5^2P_{3/2})\Sigma_m a_m\langle Y_1^{-1}|Y_2^m|Y_1^{-1}\rangle$$

$$= -\alpha\langle R^{5p}(5^2P_{\frac{1}{2}})|r^2|R^{5p}(5^2P_{3/2})\rangle a_o\langle Y_1^{-1}|Y_2^o|Y_1^{-1}\rangle$$

according to III(2.7).

"Off-diagonal" matrix elements of the operator $\bar{V}5$ are even simpler to calculate. For example:

$$\langle 1\tfrac{1}{2}1\tfrac{1}{2}|\bar{V}5|1\tfrac{1}{2}o\tfrac{1}{2}\rangle = -\Sigma_m\langle \rho_1^{\alpha}(1)\rho_1^{\beta}(2)\rho_o^{\alpha}(3)\rho_o^{\beta}(4)\rho_{-1}^{\alpha}(5)|f_m|$$

$$\rho_1^{\alpha}(1)\rho_1^{\beta}(2)\rho_o^{\alpha}(3)\rho_{-1}^{\beta}(4)\rho_{-1}^{\alpha}(5)\rangle$$

$$= \Sigma_m\langle \rho_o|f_m|\rho_{-1}\rangle$$

$$= -\alpha\langle R^{5p}(5^2P_{3/2})|r^2|R^{5p}(5^2P_{3/2})\rangle a_1\langle Y_1^o|Y_2^1|Y_1^{-1}\rangle$$

The matrix elements

$$\langle Y_1^{m_3} | Y_2^{m_2} | Y_1^{m_1} \rangle$$

were evaluated by making use of III(2.7) and tabulated values of Clebsch-Gordan Coefficients (CON53).

In this way matrix elements of the form $\langle LSM_L M_S | \bar{V}5 | L^1 S^1 M_L^1 M_S^1 \rangle$ involved in the evaluation of the matrix elements $\langle JM | \bar{V}5 | J^1 M^1 \rangle$ can be calculated. The eight matrix elements of interest are as below.

$$\langle 3/2\ 3/2 | \bar{V}5 | \tfrac{1}{2}\ \tfrac{1}{2} \rangle = \gamma BG$$

$$\langle 3/2\ 3/2 | \bar{V}5 | \tfrac{1}{2} -\tfrac{1}{2} \rangle = -2\gamma AG$$

$$\langle 3/2\ \tfrac{1}{2} | \bar{V}5 | \tfrac{1}{2}\ \tfrac{1}{2} \rangle = \sqrt{2}\gamma CG$$

$$\langle 3/2\ \tfrac{1}{2} | \bar{V}5 | \tfrac{1}{2} -\tfrac{1}{2} \rangle = \sqrt{3}\gamma BG$$

$$\langle 3/2 -\tfrac{1}{2} | \bar{V}5 | \tfrac{1}{2}\ \tfrac{1}{2} \rangle = -\sqrt{3}\gamma DG$$

$$\langle 3/2 -\tfrac{1}{2} | \bar{V}5 | \tfrac{1}{2} -\tfrac{1}{2} \rangle = -\sqrt{2}\gamma CG$$

$$\langle 3/2 -3/2 | \bar{V}5 | \tfrac{1}{2}\ \tfrac{1}{2} \rangle = 2\gamma EG$$

$$\langle 3/2 -3/2 | \bar{V}5 | \tfrac{1}{2} -\tfrac{1}{2} \rangle = \gamma DG \qquad , \qquad \gamma = (6\sqrt{\pi})/(8\sqrt{5})$$

where A-E are given in equation III(2.9) or III(2.10) and G is given by

$$G = \frac{-e\theta zz(BC)}{R^5} \langle R^{5p}(5^2P_{3/2}) | r^2 | R^{5p}(5^2P_{\frac{1}{2}}) \rangle \qquad \text{III(3.18)}$$

b. Thallium $Tl(6^2P_{3/2}) \rightarrow Tl(6^2P_{\frac{1}{2}})$

The spectroscopic states of the ground electronic configuration of the Tl atom $-(6p)^1$ - are $^2P_{\frac{1}{2}}$ and $^2P_{3/2}$ for which the wave functions III(3.16) are again appropriate. Now, however, the functions $|LSM_L M_S\rangle$ are one electron functions:

$$|1\tfrac{1}{2}1\tfrac{1}{2}\rangle = p_1\alpha, |1\tfrac{1}{2}1\text{-}\tfrac{1}{2}\rangle = p_1\beta, |1\tfrac{1}{2}0\,\tfrac{1}{2}\rangle = p_0\alpha, |\tfrac{1}{2}0\text{-}\tfrac{1}{2}\rangle = p_0\beta,$$

$$|1\tfrac{1}{2}\text{-}1\tfrac{1}{2}\rangle = p_{-1}\alpha \; |1\tfrac{1}{2}\text{-}1\text{-}\tfrac{1}{2}\rangle = p_{-1}\beta$$

where $p_m = R^{6p}(r)\, Y_1^m(\theta,\phi)$

In the evaluation of the appropriate matrix elements, III(2.7) may be invoked immediately, and the matrix elements are listed below:

$$\langle\tfrac{1}{2}\;\tfrac{1}{2}|\bar{V}5|3/2\;\;3/2\rangle = \gamma DG$$

$$\langle\tfrac{1}{2}\text{-}\tfrac{1}{2}|\bar{V}5|3/2\;\;3/2\rangle = 2\gamma EG$$

$$\langle\tfrac{1}{2}\;\tfrac{1}{2}|\bar{V}5|3/2\;\;\tfrac{1}{2}\rangle = -\sqrt{2}\gamma CG$$

$$\langle\tfrac{1}{2}\text{-}\tfrac{1}{2}|\bar{V}5|3/2\;\;\tfrac{1}{2}\rangle = -\sqrt{3}\gamma DG$$

$$\langle\tfrac{1}{2}\;\tfrac{1}{2}|\bar{V}5|3/2\text{-}\tfrac{1}{2}\rangle = \sqrt{3}\gamma BG$$

$$\langle\tfrac{1}{2}\text{-}\tfrac{1}{2}|\bar{V}5|3/2\text{-}\tfrac{1}{2}\rangle = \sqrt{2}\gamma CG$$

$$\langle\tfrac{1}{2}\;\tfrac{1}{2}|\bar{V}5|3/2\text{-}3/2\rangle = -2\gamma\, AG$$

$$\langle\tfrac{1}{2}\text{-}\tfrac{1}{2}|\bar{V}5|3/2\text{-}3/2\rangle = -\gamma BG \qquad \text{III(3.19)}$$

The functions $|LS\ M_L M_S\rangle$ appropriate to the configuration $(6s)^1(6p)^1$ are:

$$|1\ 1\ 1\ 1\rangle = (1/\sqrt{2})\ |s\alpha(1)\ p_1\alpha(2)|$$

$$|1\ 1\ 1\ 0\rangle = (1/\sqrt{2})\{(1/\sqrt{2})|s\alpha(1)\ p_1\beta(2)| + (1/\sqrt{2})|s\beta(1)p_1\alpha(2)|\}$$

$$|1\ 1\ 1\ -1\rangle = (1/\sqrt{2})|s\beta(1)\ p_1\beta(2)|$$

$$|1\ 1\ 0\ 1\rangle = (1/\sqrt{2})|s\alpha(1)\ p_o\alpha(2)|$$

$$|1\ 1\ o\ o\rangle = (1/\sqrt{2})\{(1/\sqrt{2})|s\alpha(1)\ p_o\beta(2) + (1/\sqrt{2})|s\beta(1)\ p_o\alpha(2)|\}$$

$$|1\ 1\ o\ -1\rangle = (1/\sqrt{2})|s\beta(1)\ p_o\beta(2)|$$

$$|1\ 1\ -1\ 1\rangle = (1/\sqrt{2})|s\alpha(1)\ p_{-1}\alpha(2)|$$

$$|1\ 1\ -1\ o\rangle = (1/\sqrt{2})\{(1/\sqrt{2})|s\alpha(1)\ p_{-1}\beta(2)|+(1/\sqrt{2})|s\beta(1)p_{-1}\alpha(2)|\}$$

$$|1\ 1\ -1\ -1\rangle = (1/\sqrt{2})|s\beta(1)\ p_{-1}\beta(2)|$$

where $s = R^{6s}\ Y_o^o\ (^3P_o)$ or $R^{6s}\ Y_o^o\ (^3P_2)$

and $_m = R^{6p}\ Y_1^m\ (^3P_o)$ or $R^{6p}\ Y_1^m\ (^3P_2)$ III(3.21)

The matrix elements $\langle jm|\bar{V}5|j^1_m{}^1_1\rangle$ are evaluated in the same manner as the corresponding Iodine atom matrix elements:

$$\langle o\ o|\overline{V}5|2\ 2\rangle = -\gamma EG$$

$$\langle o\ o|\overline{V}5|2\ 1\rangle = \gamma DG$$

$$\langle o\ o|\overline{V}5|2\ 0\rangle = -\gamma CG$$

$$\langle o\ o|\overline{V}5|2\text{-}1\rangle = \gamma BG$$

$$\langle o\ o|\overline{V}5|2\text{-}2\rangle = -\gamma AG \quad , \quad \gamma = 12\sqrt{\pi}/5\sqrt{10} \qquad \text{III(3.22)}$$

where A-E are as before and

$$G = \frac{-e\Theta_{zz}(BC)\langle R^{6p}(6^3P_o)|r^2|R^{6p}(6^3P_2)}{R^5}$$

d. Tellurium $\quad Te(5^3P_o) \rightarrow Te(5^3P_2)$

The J,M eigen-functions are defined in equation III(3.20). Now, however, the $|LS\ M_L M_S\rangle$ eigen functions are appropriate to a p^4 configuration.

$$|1\ 1\ 1\ 1\rangle = (1/\sqrt{4!})|\rho_1{}^{\alpha(1)}\rho_1{}^{\beta(2)}\rho_o{}^{\alpha(3)}\rho_{-1}{}^{\alpha(4)}|$$

$$|1\ 1\ 1\ o\rangle = (1/\sqrt{2})\{(1/\sqrt{4!})|\rho_1{}^{\alpha(1)}\rho_1{}^{\beta(2)}\rho_o{}^{\alpha(3)}\rho_{-1}{}^{\beta(4)}|+$$

$$(1/\sqrt{4!})|\rho_1{}^{\alpha(1)}\rho_1{}^{\beta(2)}\rho_o{}^{\beta(3)}\rho_{-1}{}^{\alpha(4)}|\}$$

$$|1\ 1\ 1\text{-}1\rangle = (1/\sqrt{4!})|\rho_1{}^{\alpha(1)}\rho_1{}^{\beta(2)}\rho_o{}^{\beta(3)}\rho_{-1}{}^{\beta(4)}|$$

$$|1\ 1\ o\ 1\rangle = (1/\sqrt{4!})|\rho_1{}^{\alpha(1)}\ \rho_o{}^{\alpha(2)}\rho_o{}^{\beta(3)}\rho_{-1}{}^{\alpha(4)}|$$

$$|1\ 1\ o\ o\rangle = (1/\sqrt{2})\{(1/\sqrt{4!})|p_1\alpha(1)p_o\alpha(2)p_o\beta(3)p_{-1}\beta(4)| +$$

$$(1/\sqrt{4!})|p_1\beta(1)p_o\alpha(2)p_o\beta(3)p_{-1}\alpha(4)|\}$$

$$|1\ 1\ o\ -1\rangle = (1/\sqrt{4!})|p_1\beta(1)p_o\alpha(2)p_o\beta(3)p_{-1}\beta(4)|$$

$$|1\ 1\ -1\ 1\rangle = (1/\sqrt{4!})|p_1\alpha(1)p_o\alpha(2)p_{-1}\alpha(3)p_{-1}\beta(4)|$$

$$|1\ 1\ -1\ o\rangle = (1/2)\{(1/\sqrt{4!})|p_1\alpha(1)p_o\beta(2)p_{-1}\alpha(3)p_{-1}\beta(4)| +$$

$$(1/\sqrt{4!})|p_1\beta(1)p_o\alpha(2)p_{-1}\alpha(3)p_{-1}\beta(4)|\}$$

$$|1\ 1\ -1\ -1\rangle = (1/\sqrt{4!})|p_1\beta(1)p_o\beta(2)p_{-1}\alpha(3)p_{-1}\beta(4)| \qquad \text{III(3.23)}$$

It follows that in the same manner as before

$$\langle 2\ 2|\bar{V}5|o\ o\rangle = -\gamma AG$$

$$\langle 2\ 1|\bar{V}5|o\ o\rangle = \gamma BG$$

$$\langle 2\ o|\bar{V}5|o\ o\rangle = +\gamma CG$$

$$\langle 2\ -1|\bar{V}5|o\ o\rangle = \gamma DG$$

$$\langle 2\ -2|\bar{V}5|o\ o\rangle = +\gamma EG \quad , \quad \gamma = 12\sqrt{\pi}/5\sqrt{10}$$

$$G = \frac{-eQ_{zz}(BC)\langle R^{5p}(5^3P_2)|r^2|R^{1}5p(5\ ^3P_o)\rangle}{R^5} \qquad \text{III(3.24)}$$

In addition for Te the transitions $^3P_1 \rightarrow {}^3P_o$ and $^3P_2 \rightarrow {}^3P_1$ must be considered. The J = 1 eigen functions are

$$|1\ 1\rangle = (1/\sqrt{2})\{|1\ 1\ 1\ 0\rangle - |1\ 1\ 0\ 1\rangle\}$$

$$|1\ 0\rangle = (1/\sqrt{2})\{|1\ 1\ 1\ -1\rangle - |1\ 1\ -1\ 1\rangle\}$$

$$|1\ -1\rangle = (1/\sqrt{2})\{|1\ 1\ 0\ -1\rangle - |1\ 1\ -1\ 0\rangle\} \qquad \text{III(3.25)}$$

It can be shown in the usual manner that $\langle 00|\bar{V}5|11\rangle = \langle 00|\bar{V}5|10\rangle = \langle 00|\bar{V}5|1\ -1\rangle = 0$, ie the transition $^3P_1 \rightarrow {}^3P_0$ is not quadrupole allowed for Te. However, the transition $Te(5^3P_1) \rightarrow Te(5^3P_2)$, is allowed.

e. $Te(5^3P_1) \rightarrow Te(5^3P_2)$

$$\langle 2\ 2|\bar{V}5|1\ 1\rangle = 2\sqrt{3}\gamma BG$$

$$\langle 2\ 2|\bar{V}5|1\ 0\rangle = 2\sqrt{6}\gamma AG$$

$$\langle 2\ 2|\bar{V}5|1\ -1\rangle = 0$$

$$\langle 2\ 1|\bar{V}5|1\ 1\rangle = -3\sqrt{2}\gamma CG$$

$$\langle 2\ 1|\bar{V}5|1\ 0\rangle = -\sqrt{6}\gamma BG$$

$$\langle 2\ 1|\bar{V}5|1\ -1\rangle = 2\sqrt{3}\gamma AG$$

$$\langle 2\ 0|\bar{V}5|1\ 1\rangle = 3\sqrt{2}\gamma DG$$

$$\langle 2\ 0|\bar{V}5|1\ 0\rangle = 0$$

$$\langle 2\ 0|\bar{V}5|1\ -1\rangle = 3\sqrt{2}\gamma BG$$

$$\langle 2\text{-}1|\bar{V}5|1\ 1\rangle = 2\sqrt{3}\gamma EG$$

$$\langle 2\text{-}1|\bar{V}5|1\ 0\rangle = -\sqrt{6}\gamma DG$$

$$\langle 2\text{-}\ 1|\bar{V}5|1\text{-}1\rangle = -3\sqrt{2}\gamma CG$$

$$\langle 2\text{-}2|\bar{V}5|1\ 1\rangle = 0$$

$$\langle 2\text{-}2|\bar{V}5|1\ 0\rangle = -2\sqrt{6}\gamma EG$$

$$\langle 2\text{-}2|\bar{V}5|1\text{-}1\rangle = 2\sqrt{3}\gamma DG \qquad , \qquad \gamma = 3\sqrt{\pi}/5\sqrt{1}0 \qquad \text{III(3.26)}$$

$$G = \frac{-e\Theta_{zz}(BC)\langle R^{5p}(^3P_2)|r^2|R^{5p}(^3P_1)\rangle}{R^5}$$

Hence all the atomic matrix elements $V_{fi} = \langle\psi_f|\bar{V}5|\psi_i\rangle$ can be reduced to the form

$$V_{fi} \propto \langle R_f|r^2|R_i\rangle$$

where only $\langle R_f|r^2|R_i\rangle$ involves atomic co-ordinates. In the case of the Iodine atom,

$$R_f = R^{5p}(5^2P_{3/2}) \quad \text{and} \quad R_i = R^{5p}(5^2P_{\frac{1}{2}})$$

and strictly $R_f \neq R_i$ since the $5^2P_{3/2}$ and $5^2P_{\frac{1}{2}}$ states are separated in energy by ~7600 cm^{-1}. For the present, however, it is assumed that

$$R_f \equiv R_i = \psi^{HFS}_{5p}(I)$$

where $\psi^{HFS}_{5p}(I)$ is the Iodine 5p wave function tabulated in HER(63).

The integral was evaluated using a 32-point Gaussian Quadrature (KRY62), the values of the integrand at the quadrature points being obtained by interpolation of the tabulated Hartree-Fock-Slater wave function:

$$\langle \psi_{5p}^{HFS}(I) | r^2 | \psi_{5p}^{HFS}(I) \rangle = 6.638\ a_o^2$$

The corresponding matrix elements for Thallium and Tellurium were evaluated in the same way:

$$\langle \psi_{6p}^{HFS}(Tl) | r^2 | \psi_{6p}^{HFS}(Tl) \rangle = 17.64\ a_o^2 \qquad \text{and}$$

$$\langle \psi_{5p}^{HFS}(Te) | r^2 | \psi_{5p}^{HFS}(Te) \rangle = 7.760\ a_o^2$$

Wave functions for mercury were available only for the ground electronic configuration.

The wave functions used in these calculations are non-relativistic Hartree-Fock-Slater wave functions which are reasonably good approximations to Hartree-Fock wave functions except that exchange is not rigourously dealt with - the free electron exchange approximation is used. However, the matrix elements are rather sensitive to the form of the atomic wave functions at large distances from the nucleus and it is known that the effects of electron exchange are important in this region.

In order to estimate the usefulness of the Hartree-Fock-Slater wave functions in the present calculations, the Tl matrix element was computed using the so-called 'Coulomb Wave functions' (HAR27, BAT49).

The asymptotic form of the potential seen by any electron in an atom is

$$V = -C/r$$

where C is the core charge (+1 for a neutral atom). When this form for V is used in the Schrodinger Equation with an arbitrary energy, the approximate solutions are the Coulomb wave functions. The wave functions obtained by such a procedure are discussed by Hartree (HAR27) and it is sufficient here to note the result:

$$\int_o^\infty R_i\, r^s R_f dr = \frac{f_i f_f}{C^{s+1}} \sum_{t,t^1} b_t^i\, b_{t^1}^f \left(\frac{n_i n_f}{n_i+n_f}\right)^{N+1} \Gamma(N+1)$$

where $N = n_i + n_f + s - t - t^1$,

$$f_i = 2^{n_i} C_i^{\frac{1}{2}} / \left(n_i^{(n_i+1)} \left[\Gamma(n_i+\ell_i+1)\ \Gamma(n_i-\ell_i)\right]^{\frac{1}{2}}\right)$$

$$b_t^i = C_i^t\, a_t^i \quad , \quad a_t^i = a_{t-1}^i \left(\frac{n_i}{2C_i t}\right)\left[\ell_i(\ell_i+1)-(n_i-t)(n_i-t+1)\right]$$

$$a_o^i = 1, \quad n_i = C/\epsilon_i^{\frac{1}{2}} \qquad \text{III(3.27)}$$

and ℓ_i is the azimuthal quantum number of the electron in state i.

(NOTE: There are several misprints in the corresponding expression quoted in BAT(49)).

The series can be evaluated with sufficient accuracy by ignoring terms for which

$$N < 2 \quad \text{(BAT49)}$$

For systems with a single electron outside closed shells (simple systems), ε (in Rydberg units), may reasonably be taken to be the energy required to remove the electron from the particular level concerned since it has been shown (HAR38) that the corresponding parameter in the Fock wave equation is identical with this energy. The position regarding complex systems (more than one electron outside closed shells) is less certain, but perhaps to a first approximation the same significance may be attached to ε.

Bates considered the usefulness of the Coulomb Approximation (BAT49) in evaluating oscillator strengths (s=1) and concluded that

i. The Coulomb approximation may be employed with confidence for all transitions in the lighter, simple systems.

ii. For the heavier simple systems, it is probably necessary to restrict the use of the method to those transitions for which the interference (cancellation of positive and negative contributions to the integrand) is small, eg ns → ns etc (diagonal matrix elements), 4s → 4p, 5s → 4p, 5s → 5p, 6s → 5p etc.

iii. The 'boundary' between light and heavy is located at or beyond Potassium for s → p transitions, and even further down the Periodic Table for p - d and d - f.transitions.

iv. For complex systems the Coulomb approximation also appears to meet with considerable success.

a. It is accurate when both levels are Class I (see below) and interference is slight.

b. Its accuracy is fair when both levels are Class II and interference is slight.

c. It is fair - accurate for lighter systems when both levels are Class I and interference is gross.

d. It is probably unreliable when either or both levels are Class II and interference is gross.

Class I: levels for which the active electron is in a shell by itself and for which the exchange forces are relatively small.

Class II: levels for which the active electron is in a shell containing other electrons or for which the exchange forces are relatively large.

Since conclusion iv(b) is applicable to Tl $(6s^2 6p)$ and Hg(6s6p), it was expected that using Coulomb wave functions the matrix elements of $r^2(s=2)$ could be computed quite accurately. The results were:

$$\langle \psi^{Coul}(Tl6p^2P_{\frac{1}{2}}) | r^2 | \psi^{Coul}(Tl6p^2P_{\frac{1}{2}}) \rangle = 6.372\ a_o^2$$

$$\langle \psi^{Coul}(Tl6p^2P_{\frac{1}{2}}) | r^2 | \psi^{Coul}(Tl6p^2P_{3/2}) \rangle = 8.326\ a_o^2$$

figure 7

P(r) = r R(r) vs r/a.u. for Tl 6p

The upper curve is that of the H.F.S. wave function and the lower curve is that of the Coulomb wave function.

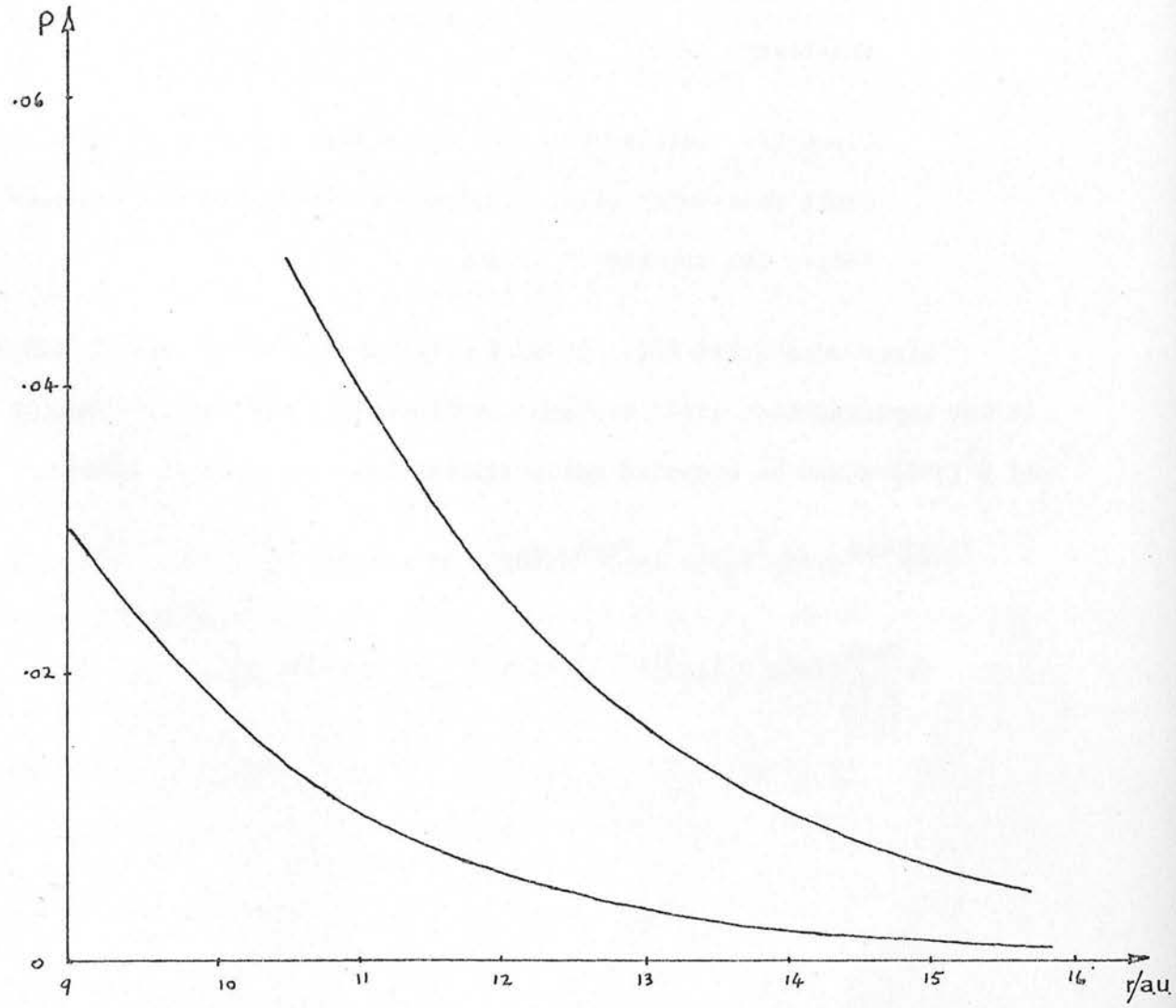

$$\langle\psi^{\text{Coul}}(\text{Tl}6p^2P_{3/2})|r^2|\psi^{\text{Coul}}(\text{Tl}6p^2P_{3/2})\rangle = 10.75\ a_o^2$$

$$\langle\psi^{\text{Coul}}(\text{Hg}6p^3P_o)|r^2|\psi^{\text{Coul}}(\text{Hg}6p^3P_o)\rangle = 7.843\ a_o^2$$

$$\langle\psi^{\text{Coul}}(\text{Hg}6p^3P_o)|r^2|\psi^{\text{Coul}}(\text{Hg}6p^3P_2)\rangle = 9.466\ a_o^2$$

$$\langle\psi^{\text{Coul}}(\text{Hg}6p^3P_2)|r^2|\psi^{\text{Coul}}(\text{Hg}6p^2P_2)\rangle = 11.72\ a_o^2 \qquad \text{III(3.28)}$$

Furthermore, the matrix elements of r^2 can be expressed in terms of oscillator strengths via the closure relation:

$$\langle i|r^2|f\rangle = \Sigma_j\langle i|r|j\rangle\langle j|r|f\rangle \qquad \text{III(3.29)}$$

When experimental oscillator strengths (GAL64) were used in III(3.29) it was found that

$$\langle r^2\rangle \text{Tl}(6p^2P_{\frac{1}{2}}) = 5.5\ a_o^2 \quad (\pm 10\%)$$

$$\langle r^2\rangle \text{Tl}(6p^2P_{3/2}) = 8.8\ a_o^2$$

In view of the fact that not all the oscillator strengths are known, these values are in good agreement with the Coulomb prediction. The asymptotic behaviour of $\psi_{6p}^{\text{HFS}}(\text{Tl})$ and $\psi^{\text{Coul}}(\text{Tl}6p^2P_{\frac{1}{2}})$ is displayed in Figure7, from which it is clear that the Hartree-Fock-Slater wave function is not sufficiently rapidly attenuated at large distances from the nucleus. It is this feature which leads to an over-estimate of $\langle r^2\rangle$ when this wave function is used.

As a check on the value of the r^2 matrix element for Iodine, the lifetime of the $^2P_{\frac{1}{2}}$ state for quadrupole radiation can be calculated.

The spontaneous emission transition probability for quadrupole radiation $Aq(j,j^1)$, is given (GAR57), by

$$Aq(j\ j^1) = \left[1/(2j+1)\right](32\pi^6\nu^5/5hc^5)\ Sq(j,j^1)$$

where $Sq(j,j^1) = \Sigma_{mm^1}|\langle jm|\ |j^1m^1\rangle|^2 = \Sigma_{mm^1}\Sigma_{\alpha\beta}|\langle_{jm}|\mathcal{N}_{\alpha\beta}|_{j^1m^1}\rangle|^2$,

the Dyadic $\mathcal{N}$ is given by $\mathcal{N} = \Sigma_s N_s$

and
$$N_s = -e\begin{Bmatrix} (x^2-1/3r^2) & xy & xz \\ xy & (y^2-1/3r^2) & yz \\ xz & yz & (z^2-1/3r^2) \end{Bmatrix} \qquad \text{III(3.30)}$$

The elements of N_s are written in terms of spherical harmonics:

eg $$x^2-1/3r^2 = (\sqrt{2\pi}/\sqrt{15})r^2\left[Y_2^2 + Y_2^{-2} - (\sqrt{2}/\sqrt{3})Y_2^o\right]$$

and the matrix elements can be evaluated in exactly the same fashion as for the matrix components of $\bar{V}5$. For Iodine the summation over electrons was only extended over the five 5p electrons. The result for $Sq(\frac{1}{2},3/2)$ was $Sq(\frac{1}{2},3/2) = \frac{40}{75}\ e^2|\langle R(I5^2P_{\frac{1}{2}})|r^2|R(I5^2P_{3/2})\rangle|^2$ III(3.31)

(N.B: The Units appropriate to III(3.30) are C.G.S. units in which $e = 4.803\times10^{-10}$ e.s.u., $a_o = 0.5292\times10^{-8}$cm, $h = 6.625\times10^{-27}$ erg. sec.).

Substituting in III(3.31) the value of the matrix element obtained by using Hartree-Fock-Slater wave functions, $A_q(\frac{1}{2},3/2)$ was found to be

$$Aq(\tfrac{1}{2},3/2) = 0.050 \text{ sec}^{-1}.$$

which compared very favourably with the value calculated by Garstang (GAR64)

$$Aq(\tfrac{1}{2},3/2) = 0.055 \text{ sec}^{-1}.$$

Garstang collected values of the radial integral for atoms in the $2p$ and $3p$ configurations, calculated values for the $4p^n$ configurations using s.c.f. with exchange wave functions, and extrapolated to the $5p^n$ configurations

It is perhaps worth noting that the spontaneous emission transition probability for magnetic dipole radiation is

$$Am(\tfrac{1}{2},3/2) = 7.8 \text{ sec}^{-1} \quad \text{(GAR64)}$$

and that the experimental Einstein A coefficient is

$$Aexp(\tfrac{1}{2},3/2) = 22 \text{ sec}^{-1} \quad \text{(HUS67)}$$

In view of the good agreement between the Hartree-Fock-Slater matrix element and the matrix element calculated by Garstang, and the fact that the Hartree-Fock-Slater matrix element is slightly smaller, the latter value was used for the Iodine matrix element in all further calculations. Since Tellurium is adjacent to Iodine in the periodic

TABLE 5

Atomic and Molecular Quadrupole Moment Matrix Elements

a. Molecular

BC	V	J	V^1	J^1	$\langle VJ\|\Theta_{zz}\|V^1J^1\rangle/ea_o^2$
H_2	0	1	1	3	7.2×10^{-2}
	0	2	1	4	6.6×10^{-2}
	0	1	2	3	-1.1×10^{-2}
	0	2	2	0	-9.5×10^{-3}
	0	2	2	4	-1.1×10^{-2}
	0	3	2	1	-9.0×10^{-3}
	0	3	2	5	-1.1×10^{-2}
	0	7	2	5	-6.6×10^{-3}
HD	0	5	1	7	8.6×10^{-2}
	0	6	1	8	8.0×10^{-2}
	0	7	1	9	7.3×10^{-2}
	0	1	2	3	-1.2×10^{-2}
	0	2	2	4	-1.2×10^{-2}
	0	3	2	5	-1.2×10^{-2}
	0	4	2	2	-7.9×10^{-3}
	0	4	2	6	-1.2×10^{-2}
	0	5	2	3	-7.1×10^{-3}
D_2	0	2	2	4	-7.6×10^{-3}
	0	3	2	5	-7.7×10^{-3}
	0	4	2	6	-7.7×10^{-3}
	0	5	2	7	-7.7×10^{-3}
	0	6	3	4	-8.0×10^{-5}
	0	7	3	5	-2.0×10^{-4}
	0	8	3	6	-3.1×10^{-4}

b. Atomic

$$\langle\psi_{5p}^{HFS}(Te)|r^2|\psi_{5p}^{HFS}(Te)\rangle = 7.760\ a_o^2$$

$$\langle\psi_{5p}^{HFS}(I)|r^2|\psi_{5p}^{HFS}(I)\rangle = 6.638\ a_o^2$$

$$\langle\psi^{Coul}(Hg6s6p\,^3P_o)|r^2|\psi^{Coul}(Hg6s6p\,^3P_2)\rangle = 9.466\ a_o^2$$

$$\langle\psi^{Coul}(Tl6p\,^2P_{\frac{1}{2}})|r^2|\psi^{Coul}(Tl6p\,^2P_{3/2})\rangle = 8.326\ a_o^2$$

table, it was felt that the Tellurium matrix element should be calculated in the same way. All atomic and molecular matrix elements used in evaluating cross-sections and rate constants are listed in Table 5.

It is now possible to consider the form of equation III(1.12) in greater detail with a view to evaluating cross-sections and, finally, rate constants.

III.4 Evaluation of Cross-Sections and Rate Constants

From equations III(1.8), III(1.9), III(1.12) and III(1.13) it is easily seen, in first order, that

$$\mathcal{P}^{v^1 J^1 j^1}_{v^{11} J^{11} j^{11}}(b) = \Sigma_{M^{11} M^1} \Sigma_{m^{11} m^1} \left| \int_{-\infty}^{\infty} V_{fi} \exp(i\Delta E_{fi} t)\, dt \right|^2 \qquad \text{III(4.1)}$$

where f denotes $\Omega^1 j^1 m^1 v^1 J^1 M^1$ and i denotes $\Omega^{11} j^{11} m^{11} v^{11} J^{11} M^{11}$.

Equating $\langle \Omega^1 | V | \Omega^{11} \rangle$, where $\Omega^1 = \Omega^{11}$ as already noted, to $\bar{V}5$ as given in equations III(2.8), III(2.9) and III(2.10) and noting the form of equations III(3.18), III(3.19), III(3.22), III(3.24) III(3.25) and III(3.26), equation III(4.1) may be written

$$\mathcal{P}^{v^1 J^1 j^1}_{v^{11} J^{11} j^{11}}(b) = \left[\beta(j^1, j^{11}) H(j^1 v^1 J^1, j^{11} v^{11} J^{11}) \right]^2 F(J^1, J^{11}) \,.$$

where $H(j^1v^1J^1, j^{11}v^{11}J^{11}) = -\langle v^1J^1|\Theta_{zz}(BC)|v^{11}J^{11}\rangle$

$$\langle R(j^1)|r^2|R(j^{11})\rangle ,$$

$\beta(j^1,j^{11})$ is a numerical constant, for example

$$\beta(\tfrac{1}{2},3/2) = \beta(3/2\ \tfrac{1}{2}) = (12\sqrt{\pi}/5\sqrt{5})$$

$$\beta(1,2) = \beta(2\ 1) = (18\sqrt{\pi}/5\sqrt{10})$$

$$\beta(o,2) = \beta(2,o) = (12\sqrt{\pi}/5\sqrt{10}) \qquad \text{III(4.2)}$$

and

$$F(J^1,J^{11}) = \Sigma_{M^{11}M^1}\Big\{\Big|\frac{\int_{-\infty}^{\infty}\langle J^1M^1|A|J^{11}M^{11}\rangle\phi(t)dt}{R^5}\Big|^2 +$$

$$\Big|\frac{\int_{-\infty}^{\infty}\langle J^1M^1|B|J^{11}M^{11}\rangle\phi(t)dt}{R^5}\Big|^2 + \Big|\frac{\int_{-\infty}^{\infty}\langle J^1M^1|C|J^{11}M^{11}\rangle\phi(t)dt}{R^5}\Big|^2$$

$$+ \Big|\frac{\int_{-\infty}^{\infty}\langle J^1M^1|D|J^{11}M^{11}\rangle\phi(t)dt}{R^5}\Big|^2 + \Big|\frac{\int_{-\infty}^{\infty}\langle J^1M^1|E|J^{11}M^{11}\rangle\phi(t)dt}{R^5}\Big|^2\Big\}$$

where $\phi(t) = \exp\{-i\Delta E(v^{11}J^{11}v^1J^1)t\}$

The form of $F(J^1,J^{11})$ depends on A, B, C, D, and E and therefore on the co-ordinate system used (see equations III(2.9) and III(2.10)).

a. Rotating Co-ordinate System (see § III.6)

$$F(J^1,J^{11}) = \Sigma_{M^{11}M^1}\Sigma_m\left|\frac{\int_{-\infty}^{\infty}\langle J^1M^1|f_m|J^{11}M^{11}\rangle e^{-i\Delta Et}dt}{R^5}\right|^2$$

where $f_m = a_m Y_2^m(\text{mol})$, a_m is a numerical constant. III(4.3)

Hence $F(J^1,J^{11}) = Q\Sigma_{M^{11}M^1}a_M^2\langle J^1M^1|2M|J^{11}M^{11}\rangle^2$, $M = M^1-M^{11}$

$$= \frac{5(2J^{11}+1)}{4\pi(2J^1+1)}\langle J^{11}2oo|J^{11}2J^1o\rangle^2 Q\Sigma_{M^{11}M^1}a_M^2$$

$$\langle J^{11}2M^{11}M|J^{11}2J^1M^1\rangle^2$$

from III(2.7) $$= \frac{5(2J^{11}+1)}{4\pi(2J^1+1)}\langle J^{11}2oo|J^{11}2J^1o\rangle^2 Q\Sigma_M a_M^2\Sigma_{M^{11}}$$

$$\langle J^{11}2M^{11}M|J^{11}2J^1(M^{11}+M)\rangle^2$$

$$Q = \left|\frac{\int_{-\infty}^{\infty}e^{-i\Delta Et}dt}{R^5}\right|^2$$

and $\Sigma_{M^{11}}\langle J^{11}2M^{11}M|J^{11}2J^1(M^{11}+M)\rangle^2 = \frac{(2J^1+1)}{5}\Sigma_{M^{11}}\langle J^{11}J^1M^{11}-(M^{11}+M)|$

$$J^{11}J^12-M\rangle^2 = (2J^1+1)/5$$

Finally, evaluating the Clebsch-Gordan Coefficients,

$$F(J^{11},J^1) = \alpha(J)Q(\Delta E) \qquad \text{III(4.4)}$$

where $\alpha(J) = \frac{35J(J-1)}{12\pi(2J-1)}$, $J^1 = J^{11}+2$ and J is the larger of J^1 and J^{11}.

$$= \frac{35J(J+1)(2J+1)}{18\pi(2J-1)2J+3)} \quad , \; J^1 = J^{11} \neq 0$$

b. Space-fixed Co-ordinate System

$$F(J^1,J^{11}) = \Sigma_{M^{11}M^1}\Sigma_f \left| \int_{-\infty}^{\infty} \langle J^1 M^1 | f | J^{11} M^{11} \rangle e^{-i\Delta E t} dt \right|^2 \qquad \text{III(4.5)}$$

R^5

where $f = \Sigma_m \alpha^f_m Y^m_2$(molecule) = A, B, ... E.

Proceeding as before it can be shown that

$$F(J^{11},J^1) = \alpha(J)\, Q(\Delta E) \qquad \text{III(4.6)}$$

where $\alpha(J) = \frac{7J(J-1)}{192\pi(2J-1)}$, $J^1 = J^{11}-2$ and J is the larger of J^1 and J^{11}.

or $\alpha(J) = \frac{7J(J+1)(2J+1)}{288\pi(2J-1)(2J+3)}$, $J^1 = J^{11} \neq 0$

*

in which f_1, f_2, ..., f_5 are defined in equations III(2.10). In both co-ordinate systems $F(J^{11}-2,J^{11}) = F(J^{11},J^{11}-2)$.

The cross-sections were calculated according to equations III(1.11):

* and $$Q(\Delta E) = \frac{5}{4}\left|\int_{-\infty}^{\infty} f_1 \frac{e^{-i\Delta E t}}{R^5} dt\right|^2 + 2\left|\int_{-\infty}^{\infty} f_2 \frac{e^{-i\Delta E t}}{R^5} dt\right|^2 + \left|\int_{-\infty}^{\infty} f_3 \frac{e^{-i\Delta E t}}{R^5} dt\right|^2$$

$$+350\left|\int_{-\infty}^{\infty} f_4 \frac{e^{-i\Delta E t}}{R^5} dt\right|^2 + \frac{175}{4}\left|\int_{-\infty}^{\infty} f_5 \frac{e^{-i\Delta E t}}{R^5} dt\right|^2$$

$$\sigma^{V^1J^1j^1}_{V^{11}J^{11}j^{11}}(v_i) = 2\pi\int_o^\infty bP(b)db = \left[\beta(j^1,j^{11})H(j^1V^1J^1:j^{11}V^{11}J^{11})\right]^2$$

$$\mathcal{A}(J^{11})\sigma(v_i,\Delta E) \qquad \text{III(4.7)}$$

where $\sigma(v_i,\Delta E) = 2\pi\int_o^\infty bQ(\Delta E)db$, $\Delta E = \Delta E(j^1V^1J^1:j^{11}V^{11}J^{11})$, and the integral was evaluated by Gaussian Quadrature (the evaluation of $Q(\Delta E,b)$ will be discussed below). Finally, the rate constant $k^{j^1}_{j^{11}}(T)$ was calculated according to equation III(1.6):

$$k^{j^1}_{j^{11}}(T) = \frac{1}{(2j^{11}+1)}\sum_{V^{11}J^{11}}\sum_{V^1J^1}\frac{f_T(V^{11}J^{11})}{(2J^{11}+1)}\ k^{V^1J^1j^1}_{V^{11}J^{11}j^{11}}(T) \quad ; \quad k^{V^1J^1j^1}_{V^{11}J^{11}j^{11}}(T) =$$

$$\int_{v_o}^\infty v_i f_T(v_i)\sigma^{V^1J^1j^1}_{V^{11}J^{11}j^{11}}(v_i)dv_i$$

Hence,

$$k^{j^1}_{j^{11}}(T) = \frac{1}{(2j^{11}+1)}\sum_{V^{11}J^{11}}\sum_{V^1J^1}\frac{f_T(V^{11},J^{11})}{(2J^{11}+1)}\left[\beta(j^1,j^{11})H(j^1V^1J^1:j^{11}V^{11}J^{11})\right]^2$$

$$\alpha(J)k(\Delta E,T) \qquad \text{III(4.8)}$$

where $k(\Delta E,T) = \int_{v_o}^\infty v_i f_T(v_i)\sigma(v_i,\Delta E)dv_i$

For ease of computation, $k(\Delta E,T)$ was written as

$$k(\Delta E,T) = \bar{v}e^{-(E_o/kT)}\int_o^\infty (y+x_o)e^{-y}\sigma(v_i)dy \qquad \text{III (4.9)}$$

where $y = (v_i/v_m)^2 - x_o$, $x_o = (v_o/v_m)^2$

$\bar{v} = (8kT/\pi\mu)^{\frac{1}{2}}$ and $v_m = (2kT/\mu)^{\frac{1}{2}}$

The integral was evaluated by 4-point Gaussian-Lagrange Quadrature, $\sigma(v_i)$ being evaluated only at the four quadrature points.

Evaluation of $Q(\Delta E)$

$Q(\Delta E)$ (equations III(4.4) and III(4.6)) involves integrals of the form

$$I = \int_{-\infty}^{\infty}(e^{-i\Delta E t}/R^5)dt$$

and $$I_\theta = \int_{-\infty}^{\infty}\frac{f(\theta)e^{-i\Delta E t}}{R^5}dt \qquad \text{III(4.10)}$$

which require for their evaluation, a knowledge of R and θ as functions of time. The classical trajectory analysis is useful here in that the equations of relative motion (see part 1) are then known, at least for elastic encounters:

$$\dot{R} = v(1-b^2/R^2-u(R)/E)^{\frac{1}{2}}$$

$$\dot{\theta} = vb/R^2 \qquad \text{III(4.11)}$$

$$\dot{\Phi} = o$$

if, as assumed, the A-BC potential, u, is a function of R alone.

For Iodine $(5^2P_{3/2})$ and D_2 the parameterised form

$$u(R) = a\varepsilon\{(\sigma/R)^{30} - (\sigma/R)^6\} \qquad \text{III(4.12)}$$

where $a = (5^{-\frac{1}{4}}-5^{-5/4})^{-1}$, $\varepsilon = 5.3\times10^{-4}$ A.U., $\sigma = 7.153815$ a.u.,

figure 8

$u(R)\times10^{3}$/A.u. (III(4.12)) vs R/a.u., $v = v_m(300K)$

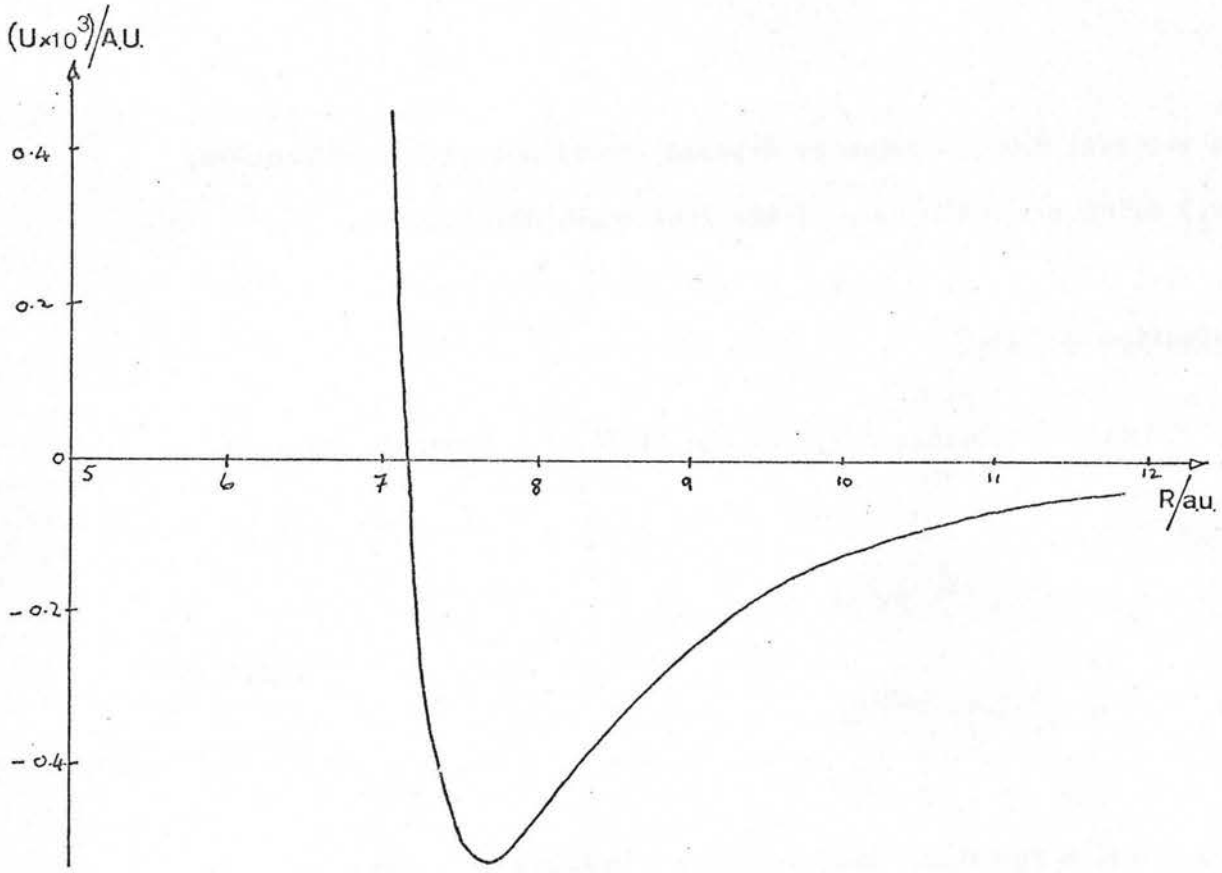

figure 9

Deflection function χ/radians vs impact parameter b/a.u.

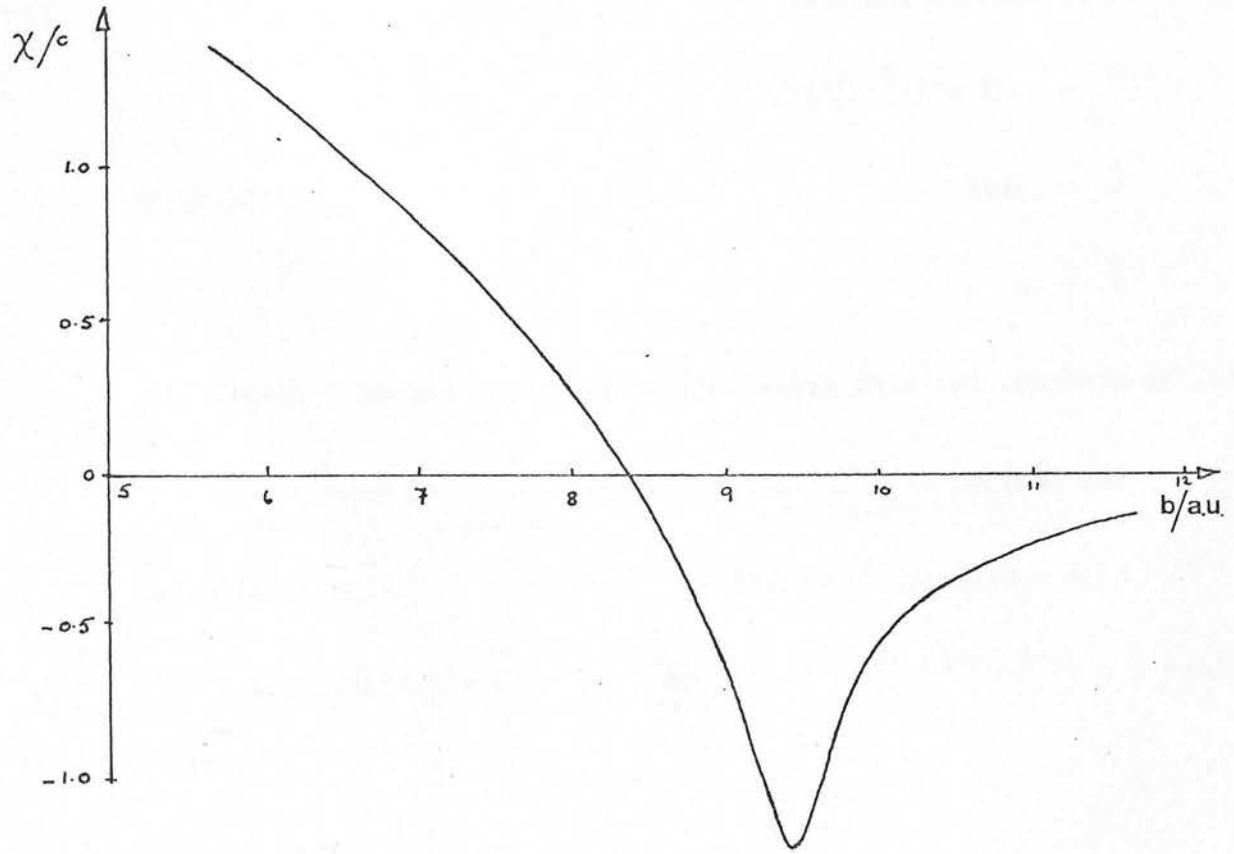

has been established from elastic scattering data (WON74). The $I-H_2$ and I-HD potentials were assumed to be identical to III(4.12) and this was the parameterisation adopted. This potential and the corresponding deflection function are displayed in Figures 8 and 9. The choice of ε and σ for other colliding pairs will be discussed in section 5. Since, classically, in a quenching collision the colliding partners are $I(5^2P_{\frac{1}{2}})$ and D_2 for part of the trajectory and $I(5^2P_{3/2})$ and D_2 for part of the trajectory, the selection of ε and σ values is somewhat arbitrary.

U(R) may be written

$$U(R) = C^{30}/R^{30} - C^6/R^6$$

in which $C^{30} = a\varepsilon\sigma^{30}$ and $C^6 = a\varepsilon\sigma^6$

C^6 is related to the polarisabilities of the collision partners, and the polarisability of $I(5^2P_{\frac{1}{2}})$ is not identical to that of $I(5^2P_{3/2})$. Nonetheless it was assumed that the two potential surfaces for $I(5^2P_{\frac{1}{2}}) + D_2$ and for $I(5^2P_{3/2}) + D_2$ are essentially parallel for a large range of internuclear separation. A more serious criticism is that, at thermal energies, the quenching collisions are markedly inelastic. In this case, for a real collision, neither v nor b are well defined. A symmetrised trajectory was used in an attempt to overcome this difficulty. That is v in equation III(4.11) was defined not as the initial relative velocity at infinite separation, but as

$$v = (v_i v_f)^{\frac{1}{2}}$$

figure 10

Co-ordinate system for evaluation of trajectory integrals

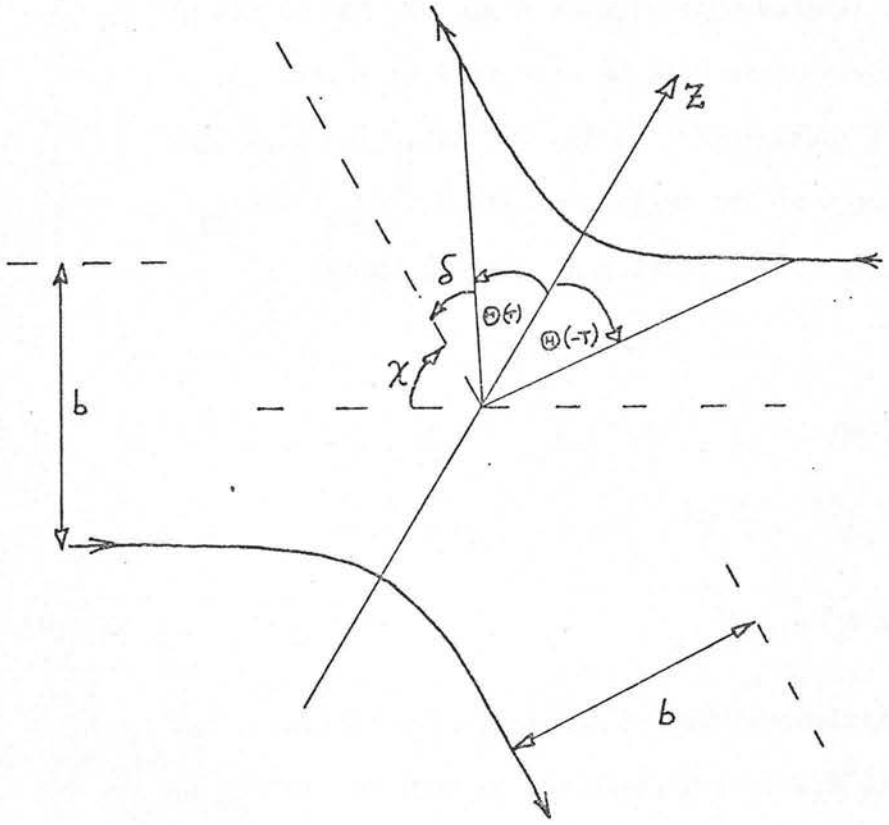

where $v_f = v_i(1-\Delta E/E_i)^{\frac{1}{2}}$ III(4.13)

and v_i is the initial velocity.

The co-ordinate system adopted was one in which the apse line of the trajectory was chosen as the Z axis, as shown in Figure 10, and the zero of time was taken to be that time when the interparticle vector coincides with the apse line. In this co-ordinate system

$$R(-t) = R(t) \quad \text{and} \quad \theta(-t) = \theta(t),$$

and as a result I and I_θ in equation III(4.10) are given by

$$I = 2\int_o^\infty (\cos\Delta Et/R^5)dt \text{ and } I_\theta = 2\int_o^\infty (f_\theta \cos\Delta Et/R^5)dt$$

These integrals were evaluated by numerically integrating the system of equations.

$$\dot{I} = 2\cos\Delta Et/R^5$$

or $\dot{I}_\theta = 2f(\theta)\cos\Delta Et/R^5$ III(4.14)

together with III(4.8), from t = o to t = T where T is such that

i. $|U(R_T)/E| < 10^{-3}|1-b^2/R^2|$ (straight line trajectory for $R>R_T$)

ii. $\delta = \sin^{-1}(b/R) < 0.1^c$ (θ constant for $R>R_T$)

iii. $b/R_T < 0.1$ where $R_T = R(T)$ III(4.15)

Under these conditions the remaining contributions to I and I_θ , ΔI and ΔI_θ, can be evaluated analytically to a good approximation

$$\Delta I = 2\Delta$$

$$\Delta I_\theta = 2f(\Theta_T).\Delta, \quad \Theta_T = \Theta(T)$$

$$\Delta = (\alpha^4/v)\{\left[\cos(|\Delta E|T)\cos x_o + \sin(|\Delta E|T)\sin x_o\right]C$$

$$+ \left[\cos(|\Delta E|T)\sin x_o - \sin(|\Delta E|T)\cos x_o\right]S\} \qquad \Delta E>o \text{ or } <o$$

where $\alpha = |\Delta E|/v$, $x_o = \alpha R_T$

and $C = \int_{x_o}^{\infty} \frac{\cos x dx}{x^5}$, $S = \int_{x_o}^{\infty} \frac{\sin x dx}{x^5}$ are standard integrals.

III(4.16)

In addition the time step-length Δt, was so chosen that

a. $\Delta\Theta = \Theta\Delta t = \frac{vb\Delta t}{R_o^2} < \frac{\pi}{40}$, R_o = distance of closest approach

(steps smaller than 1/10 period of oscillations in $f(\Theta)$)

b. $\Delta t < 2\pi/10\Delta$ III(4.17)

(steps smaller than 1/10 period of $\cos\Delta Et$ oscillations).

The boundary conditions are $R(o) = R_o$

$$\Theta(o) = o$$

where R_o was found from an iterative solution of the equation

$$1 - b^2R^2 - U(R)/E = o$$

figure 12 $\sigma(v_i)/\mathring{A}^2$ as a function of v_i/v_m

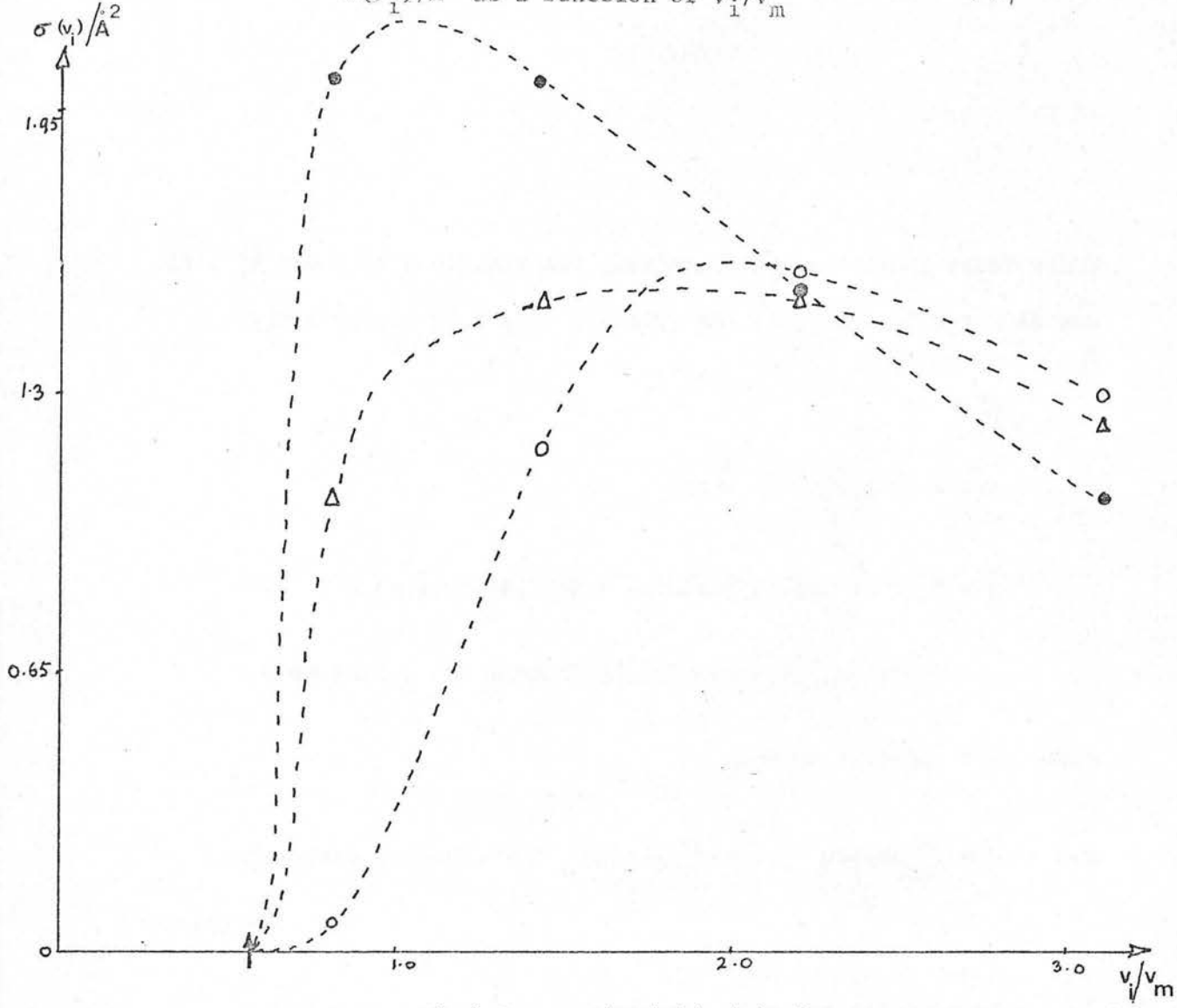

a. $\sigma(v_i)$ for III(5.5)(a) † indicates threshold velocity

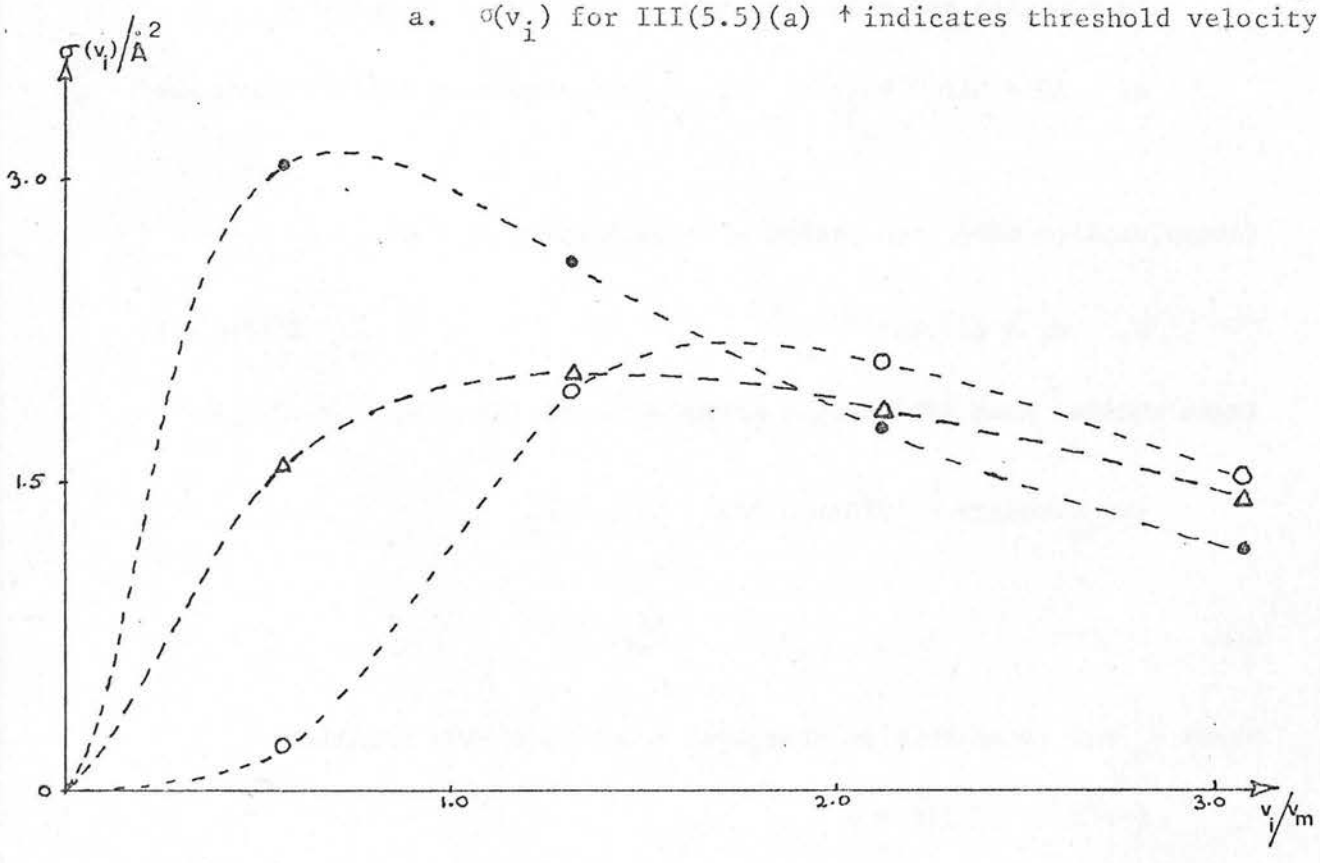

b. $\sigma(v_i)$ for III(5.5)(b). are for the space fixed co-ordinate system, Δ for the rotating co-ordinate system, and 0 for the straight line trajectory.

figure 11

$Q(\Delta E,b)$ as a function of b/a.u. for

$\Delta E = 6.8\ cm^{-1}$. (Te/H_2) $v = 3.07\ v_m$

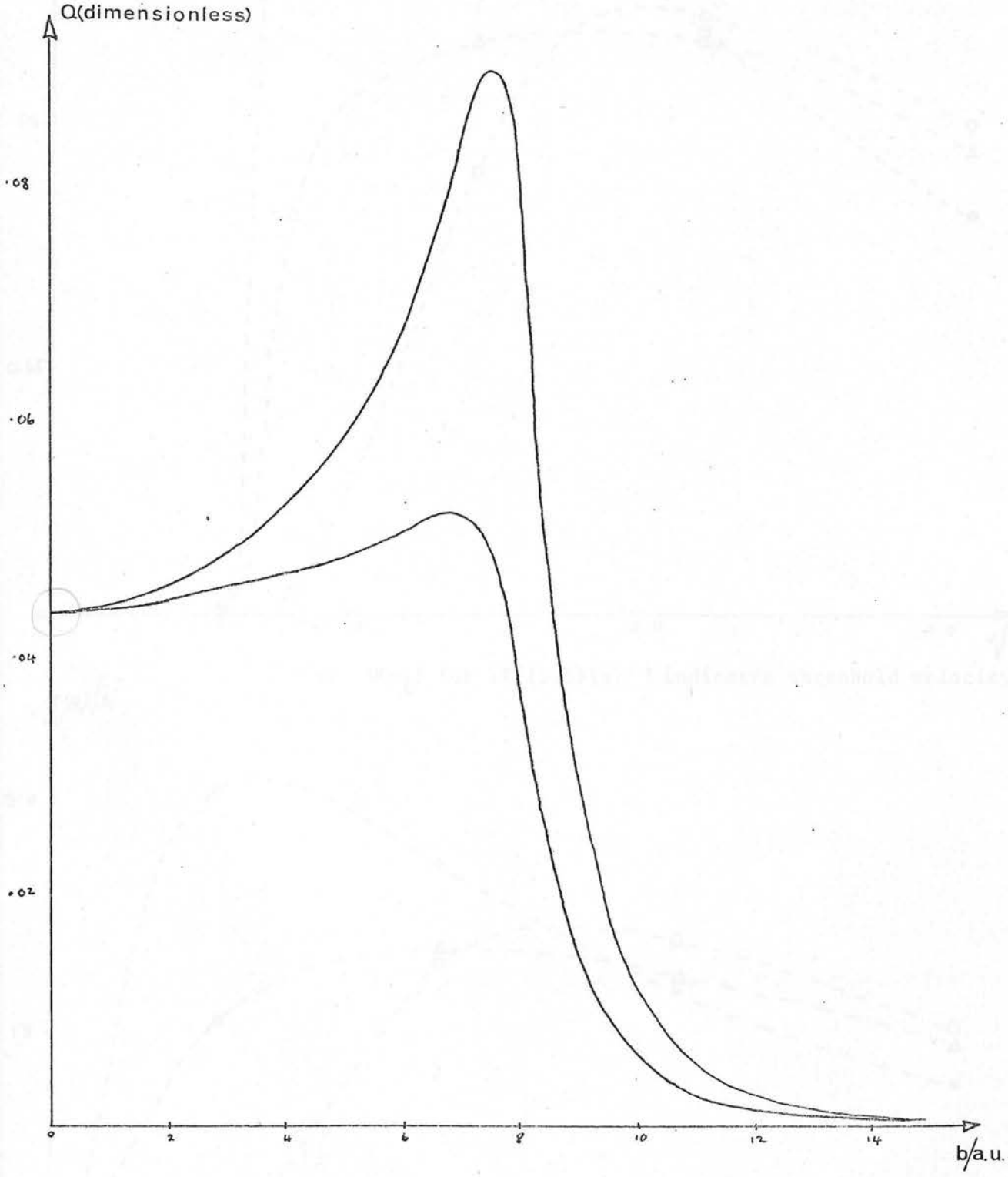

lower curve is for space-fixed co-ordinates

Hannings Modified predictor - corrector method (RAL60) was used to solve equations III(4.11). It is a fourth order method using four preceeding points for computation of a new vector of the dependent variables. A fourth order Runge-Kutta method was used for adjustment of the initial increment and for computation of starting values, and the program automatically adjusted the increment during the whole computation by halving or doubling. Typical $Q(\Delta E,b)$ curves, for both space fixed and rotating co-ordinate frames, are depicted as functions of b in Figure 11, and some cross-sections $\sigma(v_i)$ are displayed as functions of velocity in Figure 12 (see section III.5).

$Q(\Delta E,b)$ and $\sigma(v_i)$ have been weighted by factors 7/192 and 35/12 for space-fixed and rotating co-ordinate systems respectively.

III.5 Results and Discussion

Before considering the results of the calculations described in sections III.2 - III.4, the selection of potential parameters ε and σ for systems other than I/H_2 will be discussed.

The potential III(4.12) may be written

$$U(R) = C^{(30)}R^{-30} - C^{(6)}R^{-6} \qquad \text{III(5.1)}$$

where $C^{(6)} = 132.7867 \text{ AU } a_o^6$ is the dispersion force coefficient for $I - H_2$. The following assumptions were made

i. $\varepsilon(A/H_2) = \varepsilon(A/HD) = \varepsilon(A/D_2)$

$\sigma(A/H_2) = \sigma(A/HD) = \sigma(A/D_2)$

ii. $\sigma = \sigma(H_2) + \sigma(I)$

iii. $\sigma(I5^2P_{3/2}) = \langle I5p^2P_{3/2}|r^2|I5p^2P_{3/2}\rangle^{\frac{1}{2}}$

iv. $\sigma(I5^2P_{\frac{1}{2}}) = \sigma(I5^2P_{3/2}) = \sigma(I)$

(V) $C^{(6)}(I/H_2) \simeq C^{(6)}(Tl/H_2) \simeq C^{(6)}(Hg/H_2) \simeq C^{(6)}(Te/H_2)$

Assumptions iii. and iv. were made for all atoms. The σ values for Tl, Hg and Te were calculated as follows:

$$\sigma(Tl) = \sigma(I) \times \frac{r_{max}(Tl)}{r_{max}(I)}$$

where $r_{max}(A)$ is the outermost maximum in the relativistic Hartree-Fock wave function (WAB65) for A.

TABLE 6

Trajectory Potential Parameters for

Te/H_2, I/H_2, Hg/H_2 Tl/H_2

Atom	σ/a.u.	$(a\varepsilon/A.U.)\times10^4$
Te	7.363115	8.33269
I	7.153815	9.906686
Hg	8.848706	2.76615
Tl	8.777415	2.90372

a.u. = 0.5292 Å, A.U. = 27.2106 eV

$$\sigma(Hg) = \frac{\sigma(Tl) \times \sigma^{Coul}(Hg\ ^3P_o)}{\sigma^{Coul}(Tl\ ^2P_{\frac{1}{2}})}$$

where σ^{Coul} was calculated from iii. using Coulomb wave functions.

$\sigma(Te)$ was calculated from iii. using Hartree-Fock-Slater wave functions.

The values of σ and ε selected for the various systems are displayed in Table 6.

The optimum number of velocity integral (III(4.9)) quadrature points Nv and the optimum number of time steps N_t (in solving III(4.14)) were established by evaluating $k(\Delta E,T)$ (III(4.8)) for the process

$$I(^2P_{\frac{1}{2}}) + H_2(V=0,J=2) \rightarrow I(^2P_{3/2}) + H_2(V=2,J=0) \quad \Delta E = 129.4\ cm^{-1}$$

The calculation was performed using three sets of Ny and Nt:

a. Nt = 250, Nv = 4 $k = 5.03 \times 10^{-11}\ cm^3 sec^{-1}$

b. Nt = 500, Nv = 4 $k = 4.89 \times 10^{-11}$ " "

c. Nt = 250, Nv = 8 $k = 5.07 \times 10^{-11}$ " "

Hence, for $\Delta E = 129.4\ cm^{-1}$, the trajectory integrals were reliably evaluated using 250 steps and the velocity integrals were calculated without significant loss of accuracy by means of a 4-point Quadrature. It was assumed that this scheme was suitable for all J^1, J^{11} and ΔE.

TABLE 7 (continued)

2.HD	Initial V	J	→	Final V	J	$\Delta E/cm^{-1}$
d.	0	4	→	2	2	50.2
	0	5	→	2	3	-141.5
e.	0	3	→	2	5	-33.9
	0	4	→	2	6	85.5

3.D_2

a. and b. For J^{11} up to 8, there are no quadrupole - allowed spin conserving transitions with $\Delta E < 500\ cm^{-1}$ for V=0→1 and V=0→3. For 0 8 → 2 6, $\Delta E \simeq 200\ cm^{-1}$. ($f(J=8) \simeq 1 \times 10^{-4}$).

c.	0	7	→	3	5	177.0
	0	8	→	3	6	33.6
d.	0	2	→	2	4	-156.6
	0	3	→	2	5	-62.0
	0	4	→	2	6	26.2
	0	5	→	2	7	107.7
e.	0	6	→	3	4	128.3
	0	7	→	3	5	-12.5

TABLE 7

Near-resonant, quadrupole allowed spin conserving transitions

$$A(j^{11}) + BC(V^{11},J^{11}) \rightarrow A(j^{1}) + BC(V^{1}J^{1})$$

Atomic transitions

		$\Delta E/cm^{-1}$	Ref.
a.	$Te(5^3P_o) \rightarrow Te(5^3P_2)$	-4706.7	BAC32
b.	$Te(5^3P_1) \rightarrow Te(5^3P_2)$	-4751.0	BAC32
c.	$I(5^2P_{\frac{1}{2}}) \rightarrow I(5^2P_{3/2})$	-7603.2	HUS71
d.	$Hg(6^3P_2) \rightarrow Hg(6^3P_o)$	-6397.9	BAC32
e.	$Tl(6^2P_{3/2}) \rightarrow Tl(6^2P_{\frac{1}{2}})$	-7792.7	BAC32

1.H_2	Initial V	J	→	Final V	J	$\Delta E/cm^{-1}$
a.	0	1	→	1	3	6.2
b.	0	1	→	1	3	-38.1
	0	2	→	1	4	166.0
c.	0	2	→	2	0	129.4
	0	3	→	2	1	-114.9
d.	0	7	→	2	5	68.8
e.	0	2	→	2	0	-60.1

2.HD						
a.	0	5	→	1	7	-73.1
	0	6	→	1	8	49.1
	0	7	→	1	9	161.2
b.	0	5	→	1	7	-117.4
	0	6	→	1	8	4.8
	0	7	→	1	9	116.9
c.	0	1	→	2	3	-118.7
	0	2	→	2	4	24.1
	0	3	→	2	5	155.6

The dependence of the calculated rate constant on σ and ε was then investigated and it was found that

a. Allowing $C^{(6)}$ to double by doubling ε increases k by ~10% and

b. Doubling $C^{(6)}$ by increasing σ by a factor of $2^{1/6}$ decreases k by a factor of ~2.5 for $\Delta E \simeq \pm 120$ cm^{-1}.

It was felt, therefore, that uncertainty in the calculated rate constants due to uncertainty in ε and σ probably did not amount to more than a factor of 2 or 3.

One of the features of the mechanism proposed for electronic to vibrational plus rotational energy transfer from atoms to small molecules is that the energy transferred to translation, often referred to as the energy mismatch, ΔE, should be minimised. This assumption will be further discussed below, but in the meantime only those transitions for which $\Delta E \lesssim 200$ cm^{-1} (≈kT at 300K) will be considered. In evaluating ΔE, energy differences for the V-J states of H_2, HD and D_2 must be known. These were calculated from the best available spectroscopic data (FIN65, ST057, BRE73), and tables are presented in Appendix IV. Transitions and energy mismatches are listed in Table 7. In constructing the table it was assumed that for long range energy transfer processes, nuclear spin states are unaffected. On the assumption that the transitions listed in Table 7 provide the dominant contribution to the rate constants $k^{j^1}_{j^{11}}$

TABLE 8

Experimental and Calculated rate constants at 300K

$A(j^{11} \rightarrow j^{1})/EC$	$k_{calc.}/cm^3 sec^{-1}$	$k_{exp.}/cm^3 sec^{-1}$
$Te(5^3P_o) \rightarrow Te(5^3P_2)$ /H_2	1.8×10^{-11}	(1.0×10^{-11} ($^3P_1$ and ^3P_o)
$Te(5^3P_1) \rightarrow Te(5^3P_2)$ /H_2	8.6×10^{-12}	(
$I(5^2P_{\frac{1}{2}}) \rightarrow I(5^2P_{3/2})$ /H_2	4.2×10^{-15}	1.3×10^{-13}
$Hg(6^3P_2) \rightarrow Hg(6^3P_o)$ /H_2	4.4×10^{-21}	
$Tl(6^2P_{3/2}) \rightarrow Tl(6^2P_{\frac{1}{2}})$ /H_2	1.3×10^{-15}	4.9×10^{-13}
$Te(5^3P_o) \rightarrow Te(5^3P_2)$ /HD	3.7×10^{-14}	
$Te(5^3P_1) \rightarrow Te(5^3P_2)$ /HD	1.4×10^{-14}	
$I(5^2P_{\frac{1}{2}}) \rightarrow I(5^2P_{3/2})$ /HD	1.5×10^{-13}	3.2×10^{-13}
$Hg(6^3P_2) \rightarrow Hg(6^3P_o)$ /HD	1.6×10^{-16}	
$Tl(6^2P_{3/2}) \rightarrow Tl(6^2P_{\frac{1}{2}})$ /HD	8.8×10^{-15}	
$Te(5^3P_o) \rightarrow Te(5^3P_2)$ D_2	$<1 \times 10^{-19}$	(
$Te(5^3P_1) \rightarrow Te(5^3P_2)$ /D_2	$<1 \times 10^{-19}$	(8.8×10^{-15}
$I(5^2P_{\frac{1}{2}}) \rightarrow I(5^2P_{3/2})$ /D_2	2.2×10^{-20}	1.0×10^{-15}
$Hg(6^3P_2) \rightarrow Hg(6^3P_o)$ /D_2	2.9×10^{-15}	
$Tl(6^2P_{3/2}) \rightarrow Tl(6^2P_{\frac{1}{2}})$ /D_2	1.6×10^{-20}	4.9×10^{-14}

defined in equation III(1.6), the rate constants listed in Table 8 were calculated using the space-fixed co-ordinate system.

In a complete calculation of the cross-sections $\sigma_{v^{11}J^{11}j^{11}}^{v^1J^1j^1}$ the coupled equations III(1.7) would be solved (numerically) without further approximation and the cross-sections and rate constants calculated would be independent of the choice of co-ordinate system. However, this is not true of a first order perturbation calculation. For this reason, some rate constants and cross-sections were calculated using a basis defined relative to the rotating co-ordinate system. Equations III(1.7) reduce to III(1.8) only if

$$\partial\phi_q/\partial t = o$$

This condition is only valid when the basis is defined relative to fixed axes but not when it is defined relative to rotating axes when equation III(1.9) becomes

$$^{(1)}C_f(t) = (i\hbar)^{-1}\int_{-\infty}^{t} G_{fi}\exp(i\omega_{fi}t^1)dt^1, \quad \hat{G} = V - i\hbar\partial/\partial t$$

(provided $i\hbar\,\partial/\partial t$ can be treated as part of the perturbation).

III(5.3)

However, $\partial/\partial t$ may be written

$$\partial/\partial t = \dot{R}\partial/\partial R + \dot{\Theta}\partial/\partial\Theta \qquad (\dot{\Phi} = o,\ \text{III(4.11)})$$

$$\langle \phi_f | \partial/\partial t | \phi_i \rangle = \langle \Omega_f : j_f m_f J_f M_f | \Omega_i : j_i m_i : J_i M_i \rangle \langle V_f J_f | \partial/\partial t | V_i J_i \rangle$$

$$+ \langle \Omega_f : j_f m_f : J_f M_f | \partial/\partial t | j_i m_i : J_i M_i \rangle \langle V_f J_f | V_i J_i \rangle$$

$$= o(j_i m_i \neq j_f m_f \text{ and } V_f J_f \neq V_i J_i).$$

Thus III(5.3) becomes

$$^{(1)}C_f(t) = (i\hbar)^{-1} \int_{-\infty}^{t} V_{fi} \exp(i\omega_{fi} t^1) dt^1 \qquad \text{III(5.4)}$$

as before except that V is now written in terms of the rotating co-ordinate system.

k(ΔE,T) and $\sigma(v_i)$ (III(4.7) and III(4.8)) were calculated in both co-ordinate systems for the processes

$$\left.\begin{array}{ll} \text{a.} & Hg(^3P_2) + H_2(V=0,J=7) \rightarrow Hg(^3P_o) + H_2(V=2,J=5) + 68.8\,cm^{-1} \\ \text{b.} & Tl(^2P_{3/2}) + H_2(V=0,J=2) \rightarrow Tl(^2P_{\frac{1}{2}}) + H_2(V=2,J=0) - 60.1\,cm^{-1} \\ \text{c.} & Te(^3P_o) + H_2(V=0,J=1) \rightarrow Te(^3P_2) + H_2(V=1,J=3) \qquad 6.2\,cm^{-1} \end{array}\right\} \text{III(5.5)}$$

and the results are presented in Table 9 (the entries under "k (rotating/straight line)" will be discussed below).

Itis clear that the results of the two calculations do not differ by more than a factor of two.

TABLE 9

$k(\Delta E, T)$ in Space-Fixed and Rotating Co-ordinate Systems, T=300K

	k(space-fixed)/ $cm^3 sec^{-1}$	k(rotating)/ $cm^3 sec^{-1}$	k(rotating/straight line)/ $cm^3 sec^{-1}$
a.	3.4×10^{-11}	2.3×10^{-11}	1.5×10^{-11}
b.	4.5×10^{-11}	3.4×10^{-11}	2.9×10^{-11}
c.	3.7×10^{-10}	6.1×10^{-10}	1.0×10^{-9}

a., b. and c. refer respectively to the processes

III(5.5) a., b. and c.

k(space-fixed) has been multiplied by 7/192 and k(rotating) has been multiplied by 35/12.

In calculations of the sort described here, a straight line trajectory is frequently employed to evaluate integrals of the form III(4.10), and this approach is particularly useful when the form of the A-BC potential is not known. To estimate the error introduced by this approximation, $k(\Delta E,T)$ and $\sigma(v_i)$ were calculated in the rotating co-ordinate system, the trajectory integral being evaluated on the assumption of a rectilinear trajectory:

$$\left|\frac{\int_{-\infty}^{\infty} e^{i\Delta E t}\,dt}{R^5}\right|^2 = \frac{16}{9b^8v^2} \quad ; \Delta E = 0$$

$$= \frac{4\Delta E^4}{9b^4v^6}\left[K_2\left(\frac{\Delta E b}{v}\right)\right]^2 \qquad \text{III(5.6)}$$

where $K_2(x)$ is a second order Modified Bessel function of the first kind. Clearly this form is not applicable for very small impact parameters (when the result for $\Delta E=0$ also applies for $\Delta E\neq 0$) and it was therefore assumed that

$$\left|\frac{\int_{-\infty}^{\infty} e^{i\Delta E t}\,dt}{R^5}\right|^2 = p(\sigma) \qquad b \leq \sigma \qquad \text{III(5.7)}$$

where σ is one of the σ values listed in Table 6 and $p(\sigma)$ is the value of the absolute square of the integral for $b = \sigma$.

The values of $k(\Delta E,T)$ calculated in this manner for III(5.5) a. b. and c. are listed in the third column of Table 9. All of these values lie within a factor of 2 of the values obtained from 'bent trajectory calculations'. $\sigma(v_i)$ for all three calculations for the processes III(5.5) a. and b. are displayed as functions of v_i in

TABLE 10

$k^*(300)$ as a function of energy mismatch, ΔE

$\Delta E/cm^{-1}$	$k^*(300)$
-400	3.5×10^{-8}
-350	2.1×10^{-7}
-300	1.3×10^{-6}
-250	9.5×10^{-6}
-200	7.3×10^{-5}
-150	6.2×10^{-4}
-100	6.3×10^{-3}
- 50	7.8×10^{-2}
0	1
50	7.0×10^{-2}
100	4.6×10^{-3}
150	3.6×10^{-4}
200	3.4×10^{-5}
250	3.5×10^{-6}
300	5.3×10^{-7}
350	4.9×10^{-8}
400	6.5×10^{-9}

$k^*(300)$ is defined in equation III(5.8)

Figures 12(a) and 12(b) respectively.

In view of the agreement between straight line and full trajectory calculations and the similar agreement between rotating and stationary co-ordinate system calculations, it seems likely that the straight line trajectory calculation will provide at least a qualitative estimate of the dependence of $k(\Delta E,T)$ on ΔE. For this purpose, average values of reduced mass, σ, and $\bar{v}$ were used and

$$k^*(300) = k(\Delta E,300)/k(0,300) \qquad \text{III(5.8)}$$

was calculated for $\Delta E = -400 \rightarrow +400$ cm^{-1}. The results are presented in Table 10 from which it can be seen that, neglecting rotational and J-state population factors, a process which differs in ΔE from the nearest resonant process by more than 200 cm^{-1} (at 300K) may be neglected. In determining which processes provide the dominant contribution to the various rate constants, each set of transitions

$$A(j^{11}) \rightarrow A(j^{1}) \ /BC$$

must be considered individually. Consider, for example,

$$I(5^2P_{\frac{1}{2}}) \rightarrow I(5^2P_{3/2}) \ /H_2$$

The transitions in H_2 which have been included in Table 7 are

$$\text{a.} \quad H_2(V=o,J=2) \rightarrow H_2(V=2,J=o), \quad \Delta E = 129.4 \ cm^{-1} \qquad \text{III(5.9)}$$

$$\text{b.} \quad H_2(V=o,J=3) \rightarrow H_2(V=2,J=1), \quad \Delta E = -114.9 \ cm^{-1}$$

figure 13

$k(\Delta E, T)/cm^3 sec^{-1}$ as a function of T/K.

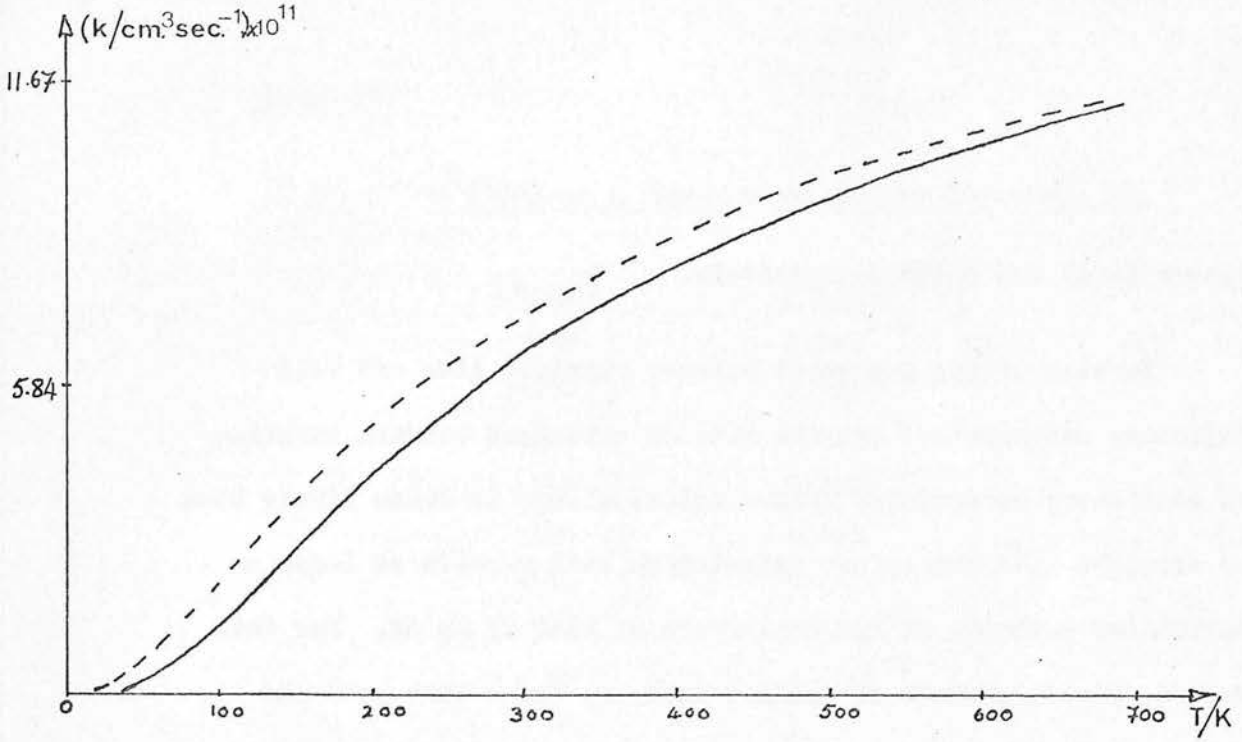

(a) $\Delta E = 50\,cm.^{-1}$ (——) and $\Delta E = -50\,cm.^{-1}$ (- -)

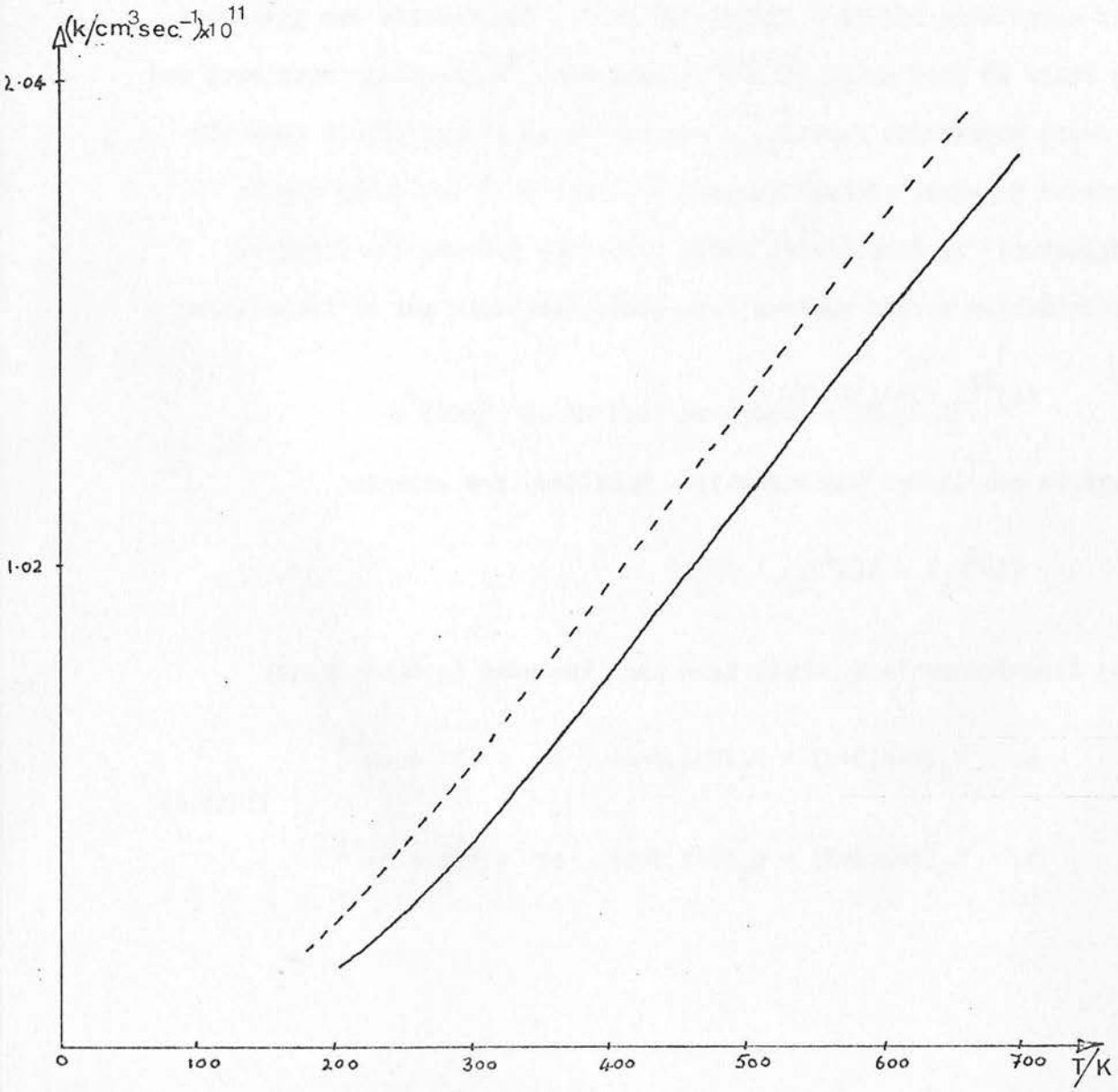

(b) $\Delta E = 100\,cm.^{-1}$ (——) and $\Delta E = -100\,cm.^{-1}$ (— —)

Some other transitions which might have been included are:

a.	o 1 → 2 3	+1001.0 cm^{-1}		
b.	o 2 → 2 4	1182.3 cm^{-1}		
c.	o 3 → 2 5	1345.3 cm^{-1}		III(5.10)
d.	o 4 → 2 2	- 365.6 cm^{-1}		
e.	o 4 → 2 6	1488.6 cm^{-1}		

III(5.10) d. and e. may immediately be discounted because not only is $f(J=4) \sim (1/20)f(J=3)$, but also ΔE is enormous compared to III(5.9) a. or b. III(5.10) b. obviously makes a negligible contribution to the rate constant compared to III(5.9) a., and the same is true of III(5.10) c. and III(5.9) b. Although the J = 1 state has ~ 6x the population of the J=2 state, this factor cannot compensate for the enormous reduction in the rate constant for III(5.10) a., compared to III(5.9) a. or b., due to the large energy mismatch. It is clear from the tables in Appendix IV that no other $V^{11} \rightarrow V^{1}$ transitions are near-resonant. Similar arguments can be applied to all the other transitions in Table 7. Hence it was concluded that the rate constants calculated from the transitions listed in Table 7 were probably ~ 80-90% of the rate constants for all quadrupole-allowed transitions.

Possible temperature dependences of the rate constants $k(\Delta E,T)$ were also considered. $k(\Delta E,T)$ was calculated for the rotating co-ordinate system with straight line trajectory using average values of reduced mass, $\bar{v}$ and σ. $k(\Delta E,T)$ for $\Delta E = \pm 50\ cm^{-1}$ and $\Delta E = \pm 100\ cm^{-1}$ is displayed as a function of T in Figures 13(a) and 13(b) respectively. It is evident that the rate constants $k_{j^{11}}^{j^{1}}$

(III(4.7), III(4.8))

i. increase with increasing T if those channels for which $f_T(v^{11},J^{11}).k(\Delta E,T)$ increases dominate those for which it decreases.

ii. decrease with increasing T if those channels for which $f_T(v^{11},J^{11}).k(\Delta E,T)$ decreases dominate those for which it increases.

$f_T(v^{11},J^{11}).k(\Delta E,T)$ can only decrease with increasing T for any channel if the decrease in $f_T(v^{11}J^{11})$ dominates the increase in $k(\Delta E,T)$.

Type i. behaviour has been observed for I/H_2, and type ii. has been observed for I/D_2 (DEA72).

An approximation that is frequently made, for example when estimating cross-sections from rate constants and vice versa, is that $\sigma(v_i)$ varies much more slowly with v_i than does $v_i f_T(v_i)$ in which case

$$k(\Delta E,T) = \int_{v_o}^{\infty} v_i f_T(v_i)\sigma(v_i)dv_i$$

may be approximated by

$$k(\Delta E,T) \simeq \bar{v}\sigma(v_m) \qquad (v_o=o) \qquad \text{III(5.11)}$$

$$\simeq (1+E_o/kT)e^{-E_o/kT}\bar{v}\sigma(v_m), \quad v_o = (2E_o/\mu)^{\frac{1}{2}}$$

TABLE 11

Comparison of calculated and approximate rate constants

		Space-fixed	Rotating	Rotating and straight line
Calculated	(a.	3.4×10^{-11}	2.3×10^{-11}	1.5×10^{-11}
	(b.	4.5×10^{-11}	3.4×10^{-11}	2.9×10^{-11}
Approximate	(a.	3.7×10^{-11}	2.3×10^{-11}	0.59×10^{-11}
	(b.	5.3×10^{-11}	3.5×10^{-11}	2.1×10^{-11}

a. and b. refer respectively to the processes

$$Hg(^3P_2)+H_2(V=0,J=7) \rightarrow Hg(^3P_0)+H_2(V=2,J=5)+68.8\ cm^{-1}$$

$$Tl(^2P_{3/2})+H_2(V=0,J=2) \rightarrow Tl(^2P_{\frac{1}{2}})+H_2(V=2,J=0)-60.1\ cm^{-1}$$

and approximate values refer to the approximation

$$k(\Delta E,T) \approx \bar{v}\sigma(v_m) \quad (v_o=0)$$

$$\approx (1+E_o/kT)e^{-E_o/kT}\bar{v}\sigma(v_m),\ v_o=(2E_o/\mu)^{\frac{1}{2}}$$

where v_m is the most probable velocity in the distribution. This approximation was applied to the processes III(5.5) a. and b. for cross-sections and rate constants calculated from

i. a space-fixed co-ordinate system

ii. a rotating co-ordinate system

iii. a rotating co-ordinate system and straight line trajectory.

The results are displayed in Table 11 from which it can be seen that, provided the $\sigma(v_i)$ curve is not too rapidly varying around $v = v_m$, the approximation III(5.11) is accurate to within a factor of two.

Conclusions

i. The quadrupole-quadrupole mechanism alone cannot account for all the observed rate constants though it does account almost entirely for near-resonant processes. (Te/H_2, I/HD). In particular, isotopic ratios, which are largely independent of the details of the electronic eigen functions, are not correctly predicted. Nevertheless, the long-range mechanism is clearly an important one and cannot be dismissed.

ii. Neglecting rotational and populational factors, processes which differ in ΔE from the nearest resonant process by more than 200 cm^{-1} at 300K may be neglected.

iii. The calculated rate constants are not sensitive to the choice of co-ordinate system.

iv. For the rotating co-ordinate system calculations, the symmetrised, straight line trajectory is a useful approximation.

v. The observed rate constants may increase or decrease with increasing temperature.

vi. Provided $\sigma(v)$ does not vary too rapidly around $v=v_m$, the approximation $k = \bar{v}\sigma(v_m)$ is a useful one.

APPENDIX I

The matrices $\underset{\sim}{S}$, $\underset{\sim}{S}^{-1}\{\partial/\partial\Theta\}$, $\underset{\sim}{S}^{-1}\{\partial/\partial R\}$, $\underset{\sim}{S}^{-1}\{H\}$ and $\underset{\sim}{D}(\Theta)$ for the system $M(^2S_{\frac{1}{2}}) + X(^1S_o) \rightleftarrows M^+ + X^-(^2P_{3/2})$

$$\underset{\sim}{S} = \begin{vmatrix} 1 & o & o & o & o & o \\ o & 1 & o & o & x & o \\ o & o & 1 & o & o & x \\ o & o & o & 1 & o & o \\ o & x & o & o & 1 & o \\ o & o & x & o & o & 1 \end{vmatrix} \qquad x = (\sqrt{2}/\sqrt{3})\langle P_o^X | S^M \rangle$$

In this model $= \langle \phi^X_{3/2} \pm \tfrac{1}{2} | \psi^M_{\frac{1}{2}} \pm \tfrac{1}{2} \rangle = (\sqrt{2}/\sqrt{3})\langle P_o^X | S^M \rangle$ so that x = . Proceeding in a fashion identical to that of § I.4, the matrices $\underset{\sim}{S}^{-1}\{\partial/\partial\Theta\}$, $\underset{\sim}{S}^{-1}\{\partial/\partial R\}$ and $\underset{\sim}{S}^{-1}\{H\}$ were evaluated:

$$\underset{\sim}{S}^{-1}\{\partial/\partial\Theta\} = \begin{vmatrix} o & -\sqrt{3}/2 & o & o & o & o \\ \sqrt{3}/2 & o & -1 & o & o & o \\ o & 1 & o & -\sqrt{3}/2 & o & o \\ o & o & \sqrt{3}/2 & o & o & o \\ o & o & o & o & o & -\tfrac{1}{2} \\ o & o & o & o & \tfrac{1}{2} & o \end{vmatrix}$$

$$\underset{\sim}{S}^{-1}\{\partial/\partial R\} = x^1(1-x^2)^{-1} \begin{vmatrix} o & o & o & o & o & o \\ o & -\alpha x & o & o & \beta & o \\ o & o & -\alpha x & o & o & \beta \\ o & o & o & o & o & o \\ o & \alpha & o & o & -\beta x & o \\ o & o & \alpha & o & o & -\beta x \end{vmatrix}$$

where $x^1 = dx/dR$, $\alpha = m_M/(m_M + m_X)$ and $\beta = m_X/(m_M + m_X)$

$$\underline{S}^{-1}\{H\} = \begin{vmatrix} H_{11}(1-x^2) & o & o & o & o & o \\ o & (H_{22}-Hx) & o & o & (H-H_{55}x) & o \\ o & o & (H_{22}-Hx) & o & o & (H-H_{55}x) \\ o & o & o & (H_{11}(1-x^2) & o & o \\ o & (H-H_{22}x) & o & o & (H_{55}-Hx) & o \\ o & o & (H-H_{22}x) & o & o & (H_{55}-Hx) \end{vmatrix} (1-x^2)^{-1}$$

$H_{11} = H_{44}$; $H_{22} = H_{33}$; $H_{55} = H_{66}$; $H_{25} = H_{52} = H_{36} = H_{63} = H$, and

$H = (\sqrt{2}/\sqrt{3})\langle X^I_{o \pm \frac{1}{2}} | H | X^K_{o \pm \frac{1}{2}} \rangle$

$$\underline{D}(\theta) = \begin{vmatrix} c^3 & -\sqrt{3}c^2s & \sqrt{3}cs^2 & -s^3 & o & o \\ \sqrt{3}c^2s & c(3c^2-2) & s(3s^2-2) & \sqrt{3}cs^2 & o & o \\ \sqrt{3}cs^2 & -s(3s^2-2) & c(3c^2-2) & -\sqrt{3}c^2s & o & o \\ s^3 & \sqrt{3}cs^2 & \sqrt{3}c^2s & c^3 & o & o \\ o & o & o & o & c & -s \\ o & o & o & o & s & c \end{vmatrix}$$

in which $c = \cos\theta/2$, $s = \sin\theta/2$

$$\langle|m_1,m_2|\partial/\partial R||m_3,m_4|\rangle^X = \alpha\{\langle\psi^X_{j_2m_2}|\psi^X_{j_4m_4}\rangle\partial/\partial R\langle\psi^M_{j_1m_1}|\psi^X_{j_3m_3}\rangle$$

$$-\langle\psi^X_{j_2m_2}|\psi^X_{j_3m_3}\rangle\partial/\partial R\langle\psi^M_{j_1m_1}|\psi^X_{j_4m_4}\rangle\}$$

where $\alpha = m_M/(m_M + m_X)$ and $\beta = 1 - \alpha$

From the above it can readily be shown that

$$\underline{S}^{-1}\{\partial/\partial\theta\} = \begin{vmatrix} 0 & -1/\sqrt{2} & 0 & 0 & 0 \\ 1/\sqrt{2} & 0 & -1/\sqrt{2} & 0 & 0 \\ 0 & 1/\sqrt{2} & 0 & 0 & 0 \\ 0 & 0 & 0 & 0 & 0 \\ 0 & 0 & 0 & 0 & 0 \end{vmatrix}$$

(Only components of the $^3\Sigma$ state are 'mixed' by Coriolis Coupling)

and

$$\underline{S}^{-1}\{\partial/\partial R\} = x^1(1-x^2)^{-1} \begin{vmatrix} -x & 0 & 0 & 0 & 0 \\ 0 & -x & 0 & 0 & 0 \\ 0 & 0 & -x & 0 & 0 \\ 0 & 0 & 0 & x(\alpha-\beta) & \sqrt{2}\alpha \\ 0 & 0 & 0 & \sqrt{3}(\beta-\alpha x^2) & -2\alpha x \end{vmatrix}$$

where $x^1 = dx/dR$

The matrix of the Hamiltonian was evaluated as in § I.4 and § I.5, and $\underline{S}^{-1}\{H\}$ was found to be given by

$$\underline{S}^{-1}\{H\} = (1-x^2)^{-1} \begin{vmatrix} H_{11} & o & o & o & o \\ o & H_{11} & o & o & o \\ o & o & H_{11} & o & o \\ o & o & o & (H_{44}-\sqrt{2}xH) & (H-\sqrt{2}xH_{55}) \\ o & o & o & (H(1-x^2)-\sqrt{2}xH_{44}) & (H_{55}(1+x^2)-\sqrt{2}xH) \end{vmatrix}$$

$$H_{11} = H_{22} = H_{33}$$

$$H_{45} = H_{54} = H$$

$$\underline{D}^{a}(\theta) = \begin{vmatrix} c^2 & -\sqrt{2}cs & s^2 & \sqrt{2}cs & o \\ cs/\sqrt{2} & c^2 & -cs/\sqrt{2} & -s^2 & o \\ s^2 & \sqrt{2}cs & c^2 & \sqrt{2}cs & o \\ cs/\sqrt{2} & -s^2 & -cs/\sqrt{2} & c^2 & o \\ o & o & o & o & 1 \end{vmatrix}$$

$$\underline{D}^{b}(\theta) = \begin{vmatrix} c^2 & -\sqrt{2}\,cs & s^2 & \sqrt{2}cs & o \\ cs/\sqrt{2} & c^2 & -cs/\sqrt{2} & s^2 & o \\ s^2 & \sqrt{2}cs & c^2 & \sqrt{2}cs & o \\ -cs/\sqrt{2} & s^2 & cs/\sqrt{2} & c^2 & o \\ o & o & o & o & 1 \end{vmatrix}$$

APPENDIX III

The matrices $\underset{\sim}{S}$, $\underset{\sim}{S}^{-1}\{\partial/\partial\Theta\}$, $\underset{\sim}{S}^{-1}\{\partial/\partial R\}$, $\underset{\sim}{S}^{-1}\{H\}$, $\underset{\sim}{R}(\Theta_o)$, $\underset{\sim}{Q}^o$, $\underset{\sim}{D}^a(\Theta)$, $\underset{\sim}{D}^b(\Theta)$ for the system $M(^2S_{\frac{1}{2}}) + X(^2P_{3/2}) \rightleftarrows M^+(^1S_o) + X^-(^1S_o)$

The overlap matrix in the molecular basis (I(7.1) is given by

$$\underset{\sim}{S} = \begin{vmatrix} (1+x^2) & o & o & o & -\sqrt{2}x/\sqrt{3} & o & o & o & o \\ o & 1 & o & o & o & o & o & o & o \\ o & o & 1 & o & o & o & o & o & o \\ o & o & o & (1-x^2) & o & o & o & o & o \\ -\sqrt{2}x/\sqrt{3} & o & o & o & 1 & o & o & o & o \\ o & o & o & o & o & (1-x^2) & o & o & o \\ o & o & o & o & o & o & (1-x^2) & o & o \\ o & o & o & o & o & o & o & 1 & o \\ o & o & o & o & o & o & o & o & 1 \end{vmatrix}$$

where $x = (\sqrt{2}/\sqrt{3}) \langle p_o^x | s^M \rangle$

In this model

$$\zeta = \langle | \psi^x_{3/2-\frac{1}{2}}, \psi^M_{\frac{1}{2}\frac{1}{2}} | \Big| \phi_5 \rangle = (\sqrt{2}/3) \langle s^M | p_o^x \rangle$$

so that $x = \sqrt{3}\,\zeta$

Proceeding as in § (I.6) the matrices $\underset{\sim}{S}^{-1}\{\partial/\partial\Theta\}$, $\underset{\sim}{S}^{-1}\{\partial/\partial R\}$ and $\underset{\sim}{S}^{-1}\{H\}$ were evaluated:

$$\underline{S}^{-1}\{\partial/\partial\Theta\} = \begin{vmatrix} 0 & 0 & \sqrt{3}/2 & -\frac{1}{2} & 0 & 0 & 0 & 0 & 0 \\ 0 & 0 & -\frac{1}{2} & -\sqrt{3}/2 & 0 & 0 & 0 & 0 & 0 \\ -\sqrt{3}/2 & \frac{1}{2} & 0 & 0 & 0 & 0 & 0 & 0 & 0 \\ \frac{1}{2} & \sqrt{3}/2 & 0 & 0 & 0 & 0 & 0 & 0 & 0 \\ 0 & 0 & 0 & 0 & 0 & 0 & 0 & 0 & 0 \\ 0 & 0 & 0 & 0 & 0 & 0 & -3/2 & \sqrt{3}/2 & 0 \\ 0 & 0 & 0 & 0 & 0 & 3/2 & 0 & 0 & \sqrt{3}/2 \\ 0 & 0 & 0 & 0 & 0 & -\sqrt{3}/2 & 0 & 0 & -\frac{1}{2} \\ 0 & 0 & 0 & 0 & 0 & 0 & -\sqrt{3}/2 & \frac{1}{2} & 0 \end{vmatrix}$$

$$\underline{S}^{-1}\{\partial/\partial R\} = \begin{vmatrix} (3-2\beta)x & 0 & 0 & 0 & -\sqrt{6}\alpha & 0 & 0 & 0 & 0 \\ \frac{1}{D}\frac{dx}{dR} & 0 & 0 & 0 & 0 & 0 & 0 & 0 & 0 \\ 0 & 0 & 0 & 0 & 0 & 0 & 0 & 0 & 0 \\ 0 & 0 & 0 & -Dx/(1-x^2) & 0 & 0 & 0 & 0 & 0 \\ \sqrt{6}(\alpha x^2 - \beta) & 0 & 0 & 0 & -\sqrt{6}\alpha x & 0 & 0 & 0 & 0 \\ 0 & 0 & 0 & 0 & 0 & -Dx/(1-x^2) & 0 & 0 & 0 \\ 0 & 0 & 0 & 0 & 0 & 0 & -Dx/(1-x^2) & 0 & 0 \\ 0 & 0 & 0 & 0 & 0 & 0 & 0 & 0 & 0 \\ 0 & 0 & 0 & 0 & 0 & 0 & 0 & 0 & 0 \end{vmatrix}$$

$$D = (3+x^2),\ \alpha = m_M/(m_M + m_X),\ \beta = (1-\alpha)$$

$$\underset{\sim}{S}^{-1}(H) = \begin{vmatrix} (3H_{11}+\sqrt{6}Hx)/D & 0 & 0 & 0 & (3H+\sqrt{6}xH_{55})/D & 0 & 0 & 0 & 0 \\ 0 & H_{22} & 0 & 0 & 0 & 0 & 0 & 0 & 0 \\ 0 & 0 & H_{22} & 0 & 0 & 0 & 0 & 0 & 0 \\ 0 & 0 & 0 & H_{44}/(1-x^2) & 0 & 0 & 0 & 0 & 0 \\ \sqrt{6}xH_{11}+3H(1+x^2)/D & 0 & 0 & 0 & \sqrt{6}xH+3H_{55}(1+x^2)/D & 0 & 0 & 0 & 0 \\ 0 & 0 & 0 & 0 & 0 & H_{44}/(1-x^2) & 0 & 0 & 0 \\ 0 & 0 & 0 & 0 & 0 & 0 & H_{44} & 0 & 0 \\ 0 & 0 & 0 & 0 & 0 & 0 & 0 & H_{22} & 0 \\ 0 & 0 & 0 & 0 & 0 & 0 & 0 & 0 & H_{22} \end{vmatrix}$$

$$H_{22} = H_{33} = H_{88} = H_{99},\ H_{44} = H_{66} = H_{77},\ H_{15} = H_{51} = H$$

$$\underset{\sim}{R}(\Theta_o) = \begin{vmatrix} D_{81} & (1+D_{82}) & D_{83} & D_{84} & D_{85} & D_{86} & D_{87} & D_{88} & D_{89} \\ D_{31} & D_{32} & D_{33} & D_{34} & D_{35} & D_{36} & D_{37} & D_{38} & (1+D_{39}) \\ D_{41} & D_{42} & D_{43} & D_{44} & D_{45} & (1+D_{46}) & D_{47} & D_{48} & D_{49} \\ -D_{61} & -D_{62} & -D_{63} & (1-D_{64}) & -D_{65} & -D_{66} & -D_{67} & -D_{68} & -D_{69} \\ -D_{91} & -D_{92} & (1-D_{93}) & -D_{94} & -D_{95} & -D_{96} & -D_{97} & -D_{98} & -D_{99} \\ -D_{21} & -D_{22} & -D_{23} & -D_{24} & -D_{25} & -D_{26} & -D_{27} & (1-D_{28}) & -D_{29} \\ (1+D_{71}) & D_{72} & D_{73} & D_{74} & D_{75} & D_{76} & D_{77} & D_{78} & D_{79} \\ -D_{11} & -D_{12} & -D_{13} & -D_{14} & -D_{15} & -D_{16} & (1-D_{17}) & -D_{18} & -D_{19} \\ D_{51} & D_{52} & D_{53} & D_{54} & (1+D_{55}) & D_{56} & D_{57} & D_{58} & D_{59} \end{vmatrix}$$

$$Q^{0} = \begin{vmatrix} (2p_1^{o})^{\frac{1}{2}} \\ (2p_2^{o})^{\frac{1}{2}} \\ (2p_3^{o})^{\frac{1}{2}} \\ (2p_4^{o})^{\frac{1}{2}} \\ (2p_5^{o})^{\frac{1}{2}} \\ (2p_6^{o})^{\frac{1}{2}} \\ (2p_7^{o})^{\frac{1}{2}} \\ (2p_8^{o})^{\frac{1}{2}} \\ 2(p_9^{o})^{\frac{1}{2}} \end{vmatrix}$$

and the matrix $D(\theta_o)$ is defined by

$$D(\theta) = D^b(\theta)\, D^{a^{-1}}(\theta)$$

where $D^a(\theta) =$

$c^2(3c^2-2)$	$\sqrt{3}c^2s^2$	$\sqrt{3}cs^3$	$sc(3s^2-2)$	0	$sc(3c^2-2)$	$s^2(3s^2-2)$	$\sqrt{3}c^2s^2$	$\sqrt{3}c^3s$
$\sqrt{3}c^2s^2$	c^4	$-cs^3$	$-\sqrt{3}cs^3$	0	$-\sqrt{3}c^3s$	$\sqrt{3}c^2s^2$	s^4	$-sc^3$
$-\sqrt{3}cs^3$	cs^3	c^4	$-\sqrt{3}c^2s^2$	0	$\sqrt{3}c^2s^2$	$\sqrt{3}c^3s$	$-sc^3$	$-s^4$
$-cs(3s^2-2)$	$\sqrt{3}cs^3$	$-\sqrt{3}c^2s^2$	$c^2(3c^2-2)$	0	$-s^2(3s^2-2)$	$cs(3c^2-2)$	$-\sqrt{3}c^3s$	$\sqrt{3}c^2s^2$
0	0	0	0	1	0	0	0	0
$-sc(3c^2-2)$	$\sqrt{3}c^3s$	$\sqrt{3}c^2s^2$	$-s^2(3s^2-2)$	0	$c^2(3c^2-2)$	$cs(3s^2-2)$	$-\sqrt{3}cs^3$	$-\sqrt{3}c^2s^2$
$s^2(3s^2-2)$	$\sqrt{3}c^2s^2$	$-\sqrt{3}c^3s$	$-sc(3c^2-2)$	0	$-sc(3s^2-2)$	$c^2(3c^2-2)$	$\sqrt{3}c^2s^2$	$-\sqrt{3}cs^3$
$\sqrt{3}c^2s^2$	s^4	sc^3	$\sqrt{3}c^3s$	0	$\sqrt{3}cs^3$	$\sqrt{3}c^2s^2$	c^4	cs^3
$-\sqrt{3}c^3s$	c^3s	$-s^4$	$\sqrt{3}c^2s^2$	0	$-\sqrt{3}c^2s^2$	$\sqrt{3}cs^3$	$-cs^3$	c^4

and $D^b(\theta) =$

$c^2(3c^2-2)$	$\sqrt{3}c^2s^2$	$\sqrt{3}cs^3$	$sc(3s^2-2)$	0	$-sc(3c^2-2)$	$-s^2(3s^2-2)$	$-\sqrt{3}c^2s^2$	$-\sqrt{3}c^3s$
$\sqrt{3}c^2s^2$	c^4	$-cs^3$	$-\sqrt{3}cs^3$	0	$\sqrt{3}c^3s$	$-\sqrt{3}c^2s^2$	$-s^4$	sc^3
$-\sqrt{3}cs^3$	cs^3	c^4	$-\sqrt{3}c^2s^2$	0	$-\sqrt{3}c^2s^2$	$-\sqrt{3}c^3s$	c^3s	s^4
$-sc(3s^2-2)$	$\sqrt{3}cs^3$	$-\sqrt{3}c^2s^2$	$c^3(3c^2-2)$	0	$s^2(3s^2-2)$	$sc(3c^2-2)$	$\sqrt{3}c^3s$	$-\sqrt{3}c^2s^2$
0	0	0	0	1	0	0	0	0
$sc(3c^2-2)$	$-\sqrt{3}c^3s$	$-\sqrt{3}c^2s^2$	$s^2(3s^2-2)$	0	$c^2(3c^2-2)$	$sc(3s^2-2)$	$-\sqrt{3}cs^3$	$-\sqrt{3}c^2s^2$
$-s^2(3s^2-2)$	$-\sqrt{3}c^2s^2$	$\sqrt{3}c^3s$	$sc(3c^2-2)$	0	$-sc(3s^2-2)$	$c^2(3c^2-2)$	$\sqrt{3}c^2s^2$	$-\sqrt{3}cs^3$
$-\sqrt{3}c^2s^2$	$-s^4$	$-c^3s$	$-\sqrt{3}c^3s$	0	$\sqrt{3}cs^3$	$\sqrt{3}c^2s^2$	c^4	cs^3
$\sqrt{3}c^3s$	$-c^3s$	s^4	$-\sqrt{3}c^2s^2$	0	$-\sqrt{3}c^2s^2$	$\sqrt{3}cs^3$	$-cs^3$	c^4

APPENDIX IV

Tables are presented of the energy differences in cm^{-1} for

$H_2(V^{11}J^{11}) \rightarrow H_2(V^1,J^1)$

$V^{11}=0,\ V^1=1,2$

$J^{11}=0 \rightarrow 10,\ J^1=0,10$, (FIN65)

$HD(V^{11},J^{11}) \rightarrow HD(V^1,J^1)$

$V^{11}=0,\ V^1=1,2$

$J^{11}=0 \rightarrow 10,\ J^1=0 \rightarrow 10$, (STO57)

$D_2(V^{11},J^{11}) \rightarrow D_2(V^1J^1)$

$V^{11}=0,\ V^1=1;\ J^{11}=0 \rightarrow 6,\ J^1=0 \rightarrow 6$

$V^{11}=0,\ V^1=2,3;\ J^{11}=0 \rightarrow 8,\ J^1=0 \rightarrow 8$ (BRE73)

as well as the populations $f_T(J^{11})$ $(V^{11}=0)$, $J^{11}=0 \rightarrow 10$ for H_2, HD and D_2 at 300, 400 and 500K.

Energy Differences for H_2 (V=0 → V=1)

J^{11} \ J^{1}	0	1	2	3	4	5	6	7	8	9	10
0	4161.2	4273.7	4497.8	4831.4	5271.4	5814.0	6454.5	7187.7	8008.0	8909.4	9886.3
1	4042.7	4155.3	4379.4	4712.9	5152.9	5695.5	6336.0	7069.2	7889.5	8790.9	9767.8
2	3806.8	3919.4	4143.5	4477.0	4917.0	5459.6	6100.1	6833.3	7653.6	8555.1	9531.9
3	3455.7	3568.2	3792.3	4125.9	4565.9	5108.5	5749.0	6482.2	7302.4	8203.9	9180.8
4	2992.4	3105.0	3329.1	3662.6	4102.6	4645.2	5285.7	6018.9	6839.2	7740.7	8717.5
5	2421.1	2533.7	2757.7	3091.3	3531.3	4073.9	4714.4	5447.6	6267.9	7169.3	8146.2
6	1746.5	1859.0	2083.1	2416.7	2856.7	3399.2	4039.7	4773.0	5593.2	6494.7	7471.6
7	973.9	1086.5	1310.6	1644.1	2084.1	2626.7	3267.2	4000.4	4820.7	5722.2	6699.0
8	109.2	221.8	445.9	779.4	1219.4	1762.0	2402.5	3135.7	3956.0	4857.5	5834.3
9	-841.8	-729.2	-505.1	-171.5	268.5	811.0	1451.5	2184.7	3005.0	3906.5	4883.4
10	-1873.2	-1760.6	-1536.5	-1202.9	-762.9	-220.4	420.1	1153.3	1973.6	2875.1	3852.0

Energy Differences for H_2(V=0 → V=2)

J^{11} \ J^{1}	0	1	2	3	4	5	6	7	8	9	10
0	8087.0	8193.8	8406.4	8722.7	9139.8	9654.0	10260.6	10954.4	11729.8	12580.8	13501.4
1	7968.5	8075.3	8287.9	8604.2	9021.4	9535.5	10142.1	10835.9	11611.3	12462.3	13382.9
2	7732.6	7839.4	8052.0	8368.3	8785.5	9299.6	9906.2	10600.0	11375.4	12226.4	13147.0
3	7381.5	7488.3	7700.9	8017.2	8434.3	8948.5	9555.1	10248.9	11024.2	11875.3	12795.9
4	69182	7025.0	7237.6	7553.9	7971.1	8485.2	9091.8	9785.6	10561.0	11412.0	12332.6
5	6346.9	6453.7	6666.3	6982.6	7399.8	7913.9	8520.5	9214.3	9989.7	10840.7	11761.3
6	5672.3	5779.1	5991.6	6308.0	6725.1	7239.3	7845.8	8539.7	9315.0	10166.1	11086.7
7	4899.7	5006.5	5219.1	5535.4	5952.6	6466.7	7073.3	7767.1	8542.5	9393.5	10314.1
8	4035.0	4141.8	4354.4	4670.7	5087.9	5602.0	6208.6	6902.4	7677.8	8528.8	9449.4
9	3084.1	3190.9	3403.4	3719.8	4136.9	4651.1	5257.6	5951.4	6726.8	7577.7	8498.5
10	2052.7	2159.5	2372.0	2688.4	3105.5	3619.7	4226.2	4920.0	5695.4	6546.4	7467.1

Energy Differences for HD(V=0 → V=1)

J^{11} \ J^{1}	0	1	2	3	4	5	6	7	8	9	10
0	3632.1	3717.4	3887.6	4141.4	4477.1	4892.4	5384.6	5950.9	6587.7	7291.8	8059.7
1	3542.8	3678.2	3798.4	4052.2	4387.8	4803.1	5295.4	5861.6	6498.5	7202.6	7970.4
2	3365.0	3450.4	3620.6	3874.3	4210.0	4625.3	5117.6	5683.8	6320.7	7024.7	7792.6
3	3099.8	3185.1	3355.3	3609.1	3944.8	4360.1	4852.3	5418.6	6055.4	6759.5	7527.4
4	2748.9	2834.3	3004.5	3258.3	3593.9	4009.2	4501.5	5067.7	5704.6	6408.7	7176.5
5	2314.8	2400.2	2570.4	2824.1	3159.8	3575.1	4067.4	4633.6	5270.5	5974.6	6742.4
6	1800.1	1885.5	2055.7	2309.5	2645.1	3060.5	3552.7	4118.9	4755.8	5459.9	6227.8
7	1208.1	1293.5	1463.7	1717.4	2053.1	2468.4	2960.7	3526.9	4163.8	4867.9	5635.7
8	542.1	627.5	797.7	1051.4	1387.1	1802.4	2294.7	2860.9	3497.8	4201.9	4969.7
9	-194.3	-1o8.9	61.3	315.1	650.7	1066.0	1558.3	2124.5	2761.4	3465.5	4233.3
10	-997.4	-912.0	-741.8	-488.1	-152.4	262.9	755.2	1321.4	1958.3	2662.4	3430.2

Energy Differences for HD(V=0 → V=2)

J^{11} \ J^{1}	0	1	2	3	4	5	6	7	8	9	10
0	7087.0	7168.6	7331.2	7573.7	7894.4	8291.1	8761.3	9302.0	9910.1	10582.2	11315.0
1	6997.8	7079.4	7242.0	7484.5	7805.2	8201.9	8672.1	9212.8	9820.8	10492.9	11225.8
2	6819.9	6901.5	7064.1	7306.6	7627.3	8024.1	8494.2	9034.9	9643.0	10315.1	11048.0
3	6554.7	6636.3	6798.9	7041.4	7362.1	7758.8	8229.0	8769.7	9377.8	10049.9	10782.7
4	6203.8	6285.4	6448.1	6690.6	7011.3	7408.0	7878.2	8418.9	9026.9	9699.0	10431.9
5	5769.7	5851.3	6013.9	6256.4	6577.1	6973.9	7444.0	7984.7	8592.8	9264.9	9997.8
6	5255.1	5336.7	5499.3	5741.8	6062.5	6459.2	6929.4	7470.1	8078.1	8750.2	9483.1
7	4663.0	4744.6	4907.3	5149.8	5470.4	5867.2	6337.3	6878.0	7486.1	8158.2	8891.1
8	3997.0	4078.6	4241.3	4483.8	4804.4	5201.2	5671.3	6212.0	6820.1	7492.2	8225.1
9	3260.6	3342.2	3504.9	3747.4	4068.1	4464.8	4935.0	5475.7	6083.7	6755.8	7488.7
10	2457.5	2539.1	2701.7	2944.2	3264.9	3661.7	4131.8	4672.5	5280.6	5952.7	6685.6

Energy Differences for D_2 (V=0 → V=1)

J^{11} \ J^{1}	0	1	2	3	4	5	6
0	2993.6	3051.3	3166.3	3338.2	3566.2	3849.2	4186.0
1	2933.8	2991.5	3106.5	3278.4	3506.4	3789.4	4126.2
2	2814.6	2872.3	2987.3	3159.2	3387.2	3670.2	4007.0
3	2636.4	2694.0	2809.0	2981.0	3209.0	3492.0	3828.8
4	2400.0	2457.6	2572.6	2744.6	2972.6	3255.6	3592.4
5	2106.5	2164.2	2279.2	2451.1	2679.1	2962.1	3298.9
6	1757.2	18149	1929.9	2101.8	2329.8	2612.8	2949.6

Energy Differences for D_2 (V=0 → V=2)

J^{11} \ J^{1}	0	1	2	3	4	5	6	7	8
0	5868.5	5924.0	6034.9	6200.4	6420.3	6693.1	7017.7	7392.6	7815.9
1	5808.7	5864.2	5975.1	6140.6	6360.5	6633.3	6958.0	7332.9	7756.1
2	5689.5	5745.0	5855.9	6021.4	6241.3	6514.1	6838.7	7213.6	7636.9
3	5511.2	5566.8	5677.6	5843.1	6063.0	6335.9	6660.5	7035.4	7478.7
4	5274.8	5330.4	5441.2	5603.7	5826.6	6099.5	6424.1	6799.0	7212.3
5	4981.4	5036.9	5147.8	5313.3	5533.2	5806.0	6130.7	6505.6	6928.8
6	4632.1	4687.6	4798.5	4964.0	5183.9	5456.7	5781.4	6156.3	6579.5
7	4228.4	4283.9	4394.8	4560.3	4780.2	5053.0	5377.7	5752.6	6175.8
8	3772.1	3827.7	3938.5	4104.0	4323.9	4596.7	4921.4	5296.3	5719.5

Energy Differences for D_2 (V=0 → V=3)

J^{11} \ J^{1}	0	1	2	3	4	5	6	7	8
0	8625.7	8679.2	8786.1	8945.7	9157.4	9420.3	9733.1	10094.2	10504.2
1	8565.9	8619.5	8726.3	8885.9	9097.6	9360.5	9673.3	10034.4	1044.4
2	8446.7	8500.2	8607.1	8766.7	8978.4	9241.3	9554.1	9915.2	10325.2
3	8288.5	8322.0	8428.9	8588.5	8800.2	9063.0	9375.9	9737.0	10147.0
4	8032.1	8085.6	8192.5	8352.1	8563.8	8826.7	9139.5	9500.6	9910.6
5	7738.6	7792.2	7899.0	8058.7	8270.3	8533.2	8846.1	9207.1	9617.1
6	7389.3	7442.9	7549.7	7709.4	7921.0	8183.9	8496.8	8857.8	9267.8
7	6985.6	7039.2	7146.0	7305.6	7517.3	7780.2	8093.0	8454.1	8864.1
8	6529.4	6582.9	6689.8	6849.4	7061.1	7323.9	7636.8	7997.9	8407.9

Populations of V=0 rotational states for H_2, HD and D_2 at T=300, 400 and 500K

H_2	J	$f_{300}(J)$	$f_{400}(J)$	$f_{500}(J)$
	0	1.29×10^{-1}	9.87×10^{-2}	7.99×10^{-2}
	1	6.57×10^{-1}	5.80×10^{-1}	5.12×10^{-1}
	2	1.18×10^{-1}	1.38×10^{-1}	1.44×10^{-1}
	3	9.17×10^{-2}	1.64×10^{-1}	2.20×10^{-1}
	4	4.26×10^{-3}	1.33×10^{-2}	2.49×10^{-2}
	5	1.01×10^{-3}	6.23×10^{-3}	1.76×10^{-2}
	6	1.56×10^{-5}	2.17×10^{-4}	9.97×10^{-4}
	7	1.33×10^{-6}	4.66×10^{-5}	3.74×10^{-4}
	8	7.94×10^{-9}	7.84×10^{-7}	1.17×10^{-5}
	9	2.78×10^{-10}	8.60×10^{-8}	2.55×10^{-6}
	10	7.29×10^{-12}	7.75×10^{-10}	4.82×10^{-8}
HD	0	1.98×10^{-1}	1.51×10^{-1}	1.22×10^{-1}
	1	3.88×10^{-1}	3.29×10^{-1}	2.83×10^{-1}
	2	2.75×10^{-1}	2.89×10^{-1}	2.83×10^{-1}
	3	1.08×10^{-1}	1.56×10^{-1}	1.85×10^{-1}
	4	2.58×10^{-2}	5.68×10^{-2}	8.65×10^{-2}
	5	3.93×10^{-3}	1.46×10^{-2}	3.03×10^{-2}
	6	3.94×10^{-4}	2.70×10^{-3}	8.15×10^{-3}
	7	2.66×10^{-5}	3.71×10^{-4}	1.71×10^{-3}
	8	1.23×10^{-6}	3.83×10^{-5}	2.85×10^{-4}
	9	4.04×10^{-8}	3.03×10^{-6}	3.83×10^{-5}
	10	9.48×10^{-10}	1.86×10^{-7}	4.20×10^{-6}
D_2	0	1.81×10^{-1}	1.37×10^{-1}	1.11×10^{-1}
	1	2.04×10^{-1}	1.66×10^{-1}	1.40×10^{-1}
	2	3.84×10^{-1}	3.61×10^{-1}	3.30×10^{-1}
	3	1.14×10^{-1}	1.33×10^{-1}	1.38×10^{-1}
	4	9.47×10^{-2}	1.46×10^{-1}	1.80×10^{-1}
	5	1.42×10^{-2}	3.11×10^{-2}	4.73×10^{-2}
	6	6.26×10^{-3}	2.09×10^{-2}	4.09×10^{-2}
	7	5.22×10^{-4}	2.82×10^{-3}	7.39×10^{-3}
	8	1.33×10^{-4}	1.24×10^{-3}	4.51×10^{-3}
	9	6.53×10^{-6}	1.12×10^{-4}	5.87×10^{-4}
	10	1.01×10^{-6}	3.37×10^{-5}	2.63×10^{-4}

Appendix V

Phase shifts, partial wave summations and Semi-classical Analysis of elastic and inelastic Scattering.

Phase Shifts for elastic and inelastic Scattering.

(a) Elastic Scattering

$$\delta_1 = -\int_{-\infty}^{t_\rho} H_{11}\, dt = -\int_{\infty}^{\rho} \frac{H_{11}}{\dot{R}}\, dR$$

and $\dot{R} = -(p_0/\mu)\left(1 - b^2/R^2 - H_{11}/\epsilon\right)^{1/2}$, $p_0 = (2\epsilon\mu)^{1/2}$

b is the impact parameter.

It is assumed that at the energies considered (200 eV), the use of a straight line trajectory

$$\dot{R} = -(p_0/\mu)\left(1 - b^2/R^2\right)^{1/2}$$

is a useful approximation.

Subject to this approximation, and making use of the relation

$$p_o b = (\ell + \tfrac{1}{2})$$

it can be shown that

$$\zeta_1 = \left[\alpha/(\ell+\tfrac{1}{2})^9\right]\cdot\left[I_{10}(0) - I_{10}(\pi/2)\right] \qquad (1)$$

$$\alpha = A_1 \mu p_o^8$$

where $I_{10}(\theta) = \int^{\theta} \sin^8\theta d\theta = \frac{1}{16}(35\theta/8+\sin 8\theta/64+7\sin 4\theta/8-4\sin 2\theta+2\sin^3 2\theta/3)$

Similarly

$$\zeta_2 = -\left\{\int_{\infty}^{R_c} \frac{H_{11}}{\dot{R}} dR + \int_{R_c}^{b} \frac{H_{22}}{\dot{R}} dR \right\}$$

is approximated by

$$\zeta_2 = \frac{\alpha}{(\ell+\frac{1}{2})^9}\left[I_{10}(o)-I_{10}(\theta_c)\right] + \frac{\beta}{(\ell+\frac{1}{2})^7}\left[I_8(\theta_c)-I_8(\pi/2)\right] -$$

$$\gamma\left[(R_c p_o)^2 - (\ell+\tfrac{1}{2})^2\right]^{1/2}; \beta = A_2 \mu p_o^6 , \gamma = E_2 \mu/p_o^2 , \qquad (2)$$

$$\theta_c = \sin^{-1}(b/R_c)$$

and $I_8 = \int \sin^6\theta d\theta = \frac{1}{8}\left(5\theta/2-2\sin 2\theta+\frac{3}{8}\sin 4\theta+\sin^3 2\theta/6\right)$.

Since E_2 (~1.6 eV) << E(~200 eV), any momentum change following transitions between the two states has been neglected (and angular momentum is conserved).

In the same manner it can be shown that

$$\bar{\zeta}_1 = \left[\alpha/(\ell+\tfrac{1}{2})^9\right]\cdot\left[I_{10}(o) - I_{10}(\pi/2)\right] \qquad (3)$$

b. Inelastic Scattering

$$\zeta_3 = -\tfrac{1}{2}\left\{\int_{\infty}^{R_c} \frac{H_{11}}{\dot{R}}dR + 2\int_{R_c}^{\rho} \frac{H_{11}}{\dot{R}}dR - \int_{R_c}^{\infty} \frac{H_{22}}{\dot{R}}dR\right\}$$

$$\zeta_4 = -\tfrac{1}{2}\left\{\int_{\infty}^{R_c} \frac{H_{11}}{\dot{R}}dR + 2\int_{R_c}^{\rho} \frac{H_{22}}{\dot{R}}dR - \int_{R_c}^{\infty} \frac{H_{22}}{\dot{R}}dR\right\}$$

The tricky integral to evaluate is $\int_{R_c}^{\infty} H_{22}dR/\dot{R}$, because $H_{22}(\infty)\neq o$. The method used was to replace the upper limit by r, where r is defined by

$$\left|\int_{R_c}^{r} (H_{22}-E_2)/\dot{R}\, dR - \int_{R_c}^{r+R_c} (H_{22}-E_2)/\dot{R}\, dR\right| < 10^{-3}$$

Hence, proceeding in the same manner as in the evaluation of the elastic phase shifts, the results were obtained:

$$\zeta_3 = (\tfrac{1}{2})\left\{\frac{\alpha}{(\ell+\frac{1}{2})^9}\left[I_{10}(\theta_c)-\frac{70\pi}{16}\right] + \frac{\beta}{(\ell+\frac{1}{2})^7}\left[I_8(\theta_r) - I_8(\theta_c)\right] + \right.$$

$$\left.\gamma\left[(R_c p_o)^2-(\ell+\tfrac{1}{2})^2\right]^{\frac{1}{2}} - \gamma\left[(rp_o)^2 - (\ell+\tfrac{1}{2})^2\right]^{\frac{1}{2}}\right\} \qquad (4)$$

$$\zeta_4 = (\tfrac{1}{2})\left\{\frac{\beta}{(\ell+\frac{1}{2})^7}\left[I_8(\theta_c)+I_8(\theta_r)-\frac{10\pi}{4}\right]-\frac{\alpha I_{10}(\theta_c)}{(\ell+\frac{1}{2})^9} -\gamma\left[(R_c p_o)^2-\right.\right.$$

$$\left.\left.(\ell+\tfrac{1}{2})^2\right]^{\frac{1}{2}}-\gamma\left[(rp_o)^2-(\ell+\tfrac{1}{2})^2\right]^{\frac{1}{2}}\right\} \qquad (5)$$

where $\theta_r = \sin^{-1}(b/r)$.

For reasons that will be discussed below, the above formulae for ζ_1 etc, were used only for $\ell > \ell_n$ where ℓ_n is such that

$$2\left(\frac{\partial \zeta_n}{\partial \ell}\right)_{\ell_n} = \pi \qquad (6)$$

For $\ell < \ell_n$, a linear fit was used

$$\zeta_n = \zeta_n(\ell_n) - (\pi/2)\,(\ell_n - \ell) \qquad (7)$$

Evaluation of Partial Wave Summation

As already noted (II(2.1)), the elastic and inelastic scattering amplitudes are given by

$$f_{el}(\theta) = (1/2i/k_{e\ell}) \sum_{\ell=o}^{\infty} (2\ell+1)(S_{\ell\ell}^{e\ell} - 1) P_\ell(\cos\theta)$$

$$f_{inel}(\theta) = (1/2ik\ \ ) \sum_{\ell=o}^{\infty} (2\ell+1) S_{\ell\ell}^{inel}\ P_\ell(\cos\theta)$$

In the region $o \lesssim \ell \lesssim \ell_c$, $S_{\ell\ell}^{e\ell}$ and $S_{\ell\ell}^{inel}$ are given by II(2.4), and in the region $\ell_c + 1 \lesssim \ell \lesssim L$, where L is such that $\overline{\zeta}_1$ ( ) is $< 10^{-2}\pi$, $S_{\ell\ell}^{e\ell}$ and $S_{\ell\ell}^{inel}$ are given by II(2.5). In the region $L \lesssim \ell < \infty$

$$S_{\ell\ell}^{e\ell} \simeq 1, \quad S_{\ell\ell}^{inel} = o \quad (\overline{\zeta}_1 \simeq o)$$

Hence the final result is

$$f_{el}(\theta) = (1/2ik_{el})\sum_{\ell=o}^{L}(2\ell+1)(S_{\ell\ell}^{e\ell}-1)P_{\ell}(\cos\theta)$$

$$\text{and} \qquad f_{inel}(\theta) = (1/2ik_{\ell})\sum_{\ell=o}^{\ell_c}(2\ell+1)S_{\ell\ell}^{inel}P_{\ell}(\cos\theta) \qquad (8)$$

$I_{el}(\theta) = |f_{el}(\theta)|^2$ and $I_{inel}(\theta) = |f_{inel}(\theta)|^2$ are displayed as functions of θ (θ=1-2°) in Figure 5 for $H_{12}(R_c)$=0.25 eV , and in Figure 6 for $H_{12}(R_c)$=0.35 eV , and $I_{el}(\theta)$ and $I_{inel}(\theta)$ are presented as functions of θ (=0.3° → 4.7°) in Figure 7.

Semi-classical Analysis of Elastic and Inelastic Differential Cross Sections

The following analysis is essentially that of Ford and Wheeler (FOR59).

Making use of the asymptotic form

$$P_{\ell}(\cos\theta) \sim \left[2/(\ell+\tfrac{1}{2})\pi\sin\theta\right]^{\frac{1}{2}}\sin\left[(\ell+\tfrac{1}{2})\theta+\pi/4\right] \quad , \quad \sin\theta>1/\ell$$

and replacing the summation over partial waves by an integral, the elastic scattered amplitude is found to be

$$f_{el}(\theta) = \left[\sqrt{2}/ik_{el}(\pi\sin\theta)^{\frac{1}{2}}\right]\int_o^{\infty}(\ell+\tfrac{1}{2})^{\frac{1}{2}}S_{\ell\ell}^{e\ell}\sin\left[(\ell+\tfrac{1}{2})\theta+\pi/4\right]d\ell \qquad (9)$$

a. Elastic Scattering

Noting that

$$S^{e\ell}_{\ell\ell} = pe^{2i\zeta_1} + (1-p)e^{2i\zeta_2} \qquad 0 \lesssim \ell \lesssim \ell_c$$

$$= e^{2i\bar{\zeta}_1} \qquad \ell > \ell_c$$

and that $\sin(\ell+\frac{1}{2})\theta+\pi/4 = (1/2i)\left[\exp(i\phi)-\exp(-i\phi)\right]$, $\phi=(\ell+\frac{1}{2})\theta+\pi/4$,

(9) may be written as

$$f_{el}(\theta) = -\left[1/k_{el}(2\pi\sin\theta)^{\frac{1}{2}}\right]\{\int_o^{\ell_c}(\ell+\tfrac{1}{2})^{\frac{1}{2}}p(e^{i\phi^+_1}-e^{i\phi^-_1})d\ell +$$

$$\int_o^{\ell_c}(\ell+\tfrac{1}{2})^{\frac{1}{2}}(1-p)(e^{i\phi^+_2}-e^{i\phi^-_2})d\ell + \int_{\ell_c}^{\infty}(\ell+\tfrac{1}{2})^{\frac{1}{2}}(e^{i\phi^+_1}-e^{i\phi^-_1})d\ell\} \qquad (10)$$

in which $\phi^{\pm}_n = 2\zeta_n \pm \left[(\ell+\frac{1}{2})\theta+\pi/4\right]$

The principal contribution to an integral of the form

$\int_o^L f(\ell)\exp(i\phi(\ell))d\ell$, where $f(\ell)$ is a slowly-varying function of ℓ, comes from regions of ℓ in which

$$\frac{\partial\phi}{\partial\ell} \simeq o$$

- so-called regions of stationary phase. The regions of stationary phase in the integrals of (10) are defined by

$$\frac{\partial\phi^{\pm}_n}{\partial\ell} = o \quad \text{ie} \quad \frac{2\partial\zeta_n}{\partial\ell} = \begin{matrix} - \\ + \end{matrix} \theta$$

the value of ℓ at which this identity is satisfied is denoted ℓ_θ

It is convenient, then, to define "deflection functions", χ_n:

$$\chi_n = 2\partial\zeta_n/\partial\ell \qquad (11)$$

in terms of which the form of $f_{el}(\theta)$ may be analysed. Of course the phase shifts are only related to the true deflection functions χ,

$$\chi = \pi - \int_{\text{trajectory}} (\dot{\theta}/\dot{R})\,dR$$

in the manner of (11) if the phase shifts, ζ, are defined as

$$\zeta = \int_{\text{trajectory}} dR/\lambda - \int_{\substack{\text{zero potential}\\ \text{trajectory}}} dR/\lambda \ , \quad \lambda = \hbar/\mu\dot{R}$$

However, the usefulness of the definition (11) will soon become apparent.

There are two elastic deflection functions χ_1 and χ_2:

$$\chi_1 = 315\pi\alpha/128(\ell+\tfrac{1}{2})^{10} \qquad (12)$$

$$\chi_2 = 2\left\{\frac{-9\alpha}{(\ell+\frac{1}{2})^{10}}\left[I_{10}(0)-I_{10}(\theta_c)\right] - \frac{\alpha}{(\ell+\frac{1}{2})^{9}} I^1_{10}(\theta_c)\right.$$

$$- \frac{7\beta}{(\ell+\frac{1}{2})^{8}}\left[I_8(\theta_c)-I_8(\pi/2)\right] + \frac{\beta}{(\ell+\frac{1}{2})^{7}} I^1_8(\theta_c) +$$

$$\left.\gamma(\ell+\tfrac{1}{2})\left[(R_c p_o)^2 - (\ell+\tfrac{1}{2})^2\right]^{-\frac{1}{2}}\right\} \qquad (13)$$

where $I^1_8(\theta) = (\tfrac{1}{8})\left[5/2-4\cos2\theta+(3/2)\cos4\theta+\sin^2 2\theta\cos2\theta\right]\theta^1$,

$$I^1_{10}(\theta) = (1/16)\left[35/8 + \cos8\theta/8 +(7/2)\cos4\theta-8\cos2\theta+4\sin^2 2\theta\right.$$

$$\left.\cos2\theta\right]\theta^1 \ ,$$

$$\theta^1 = \left[(p_o R)^2 - (\ell+\tfrac{1}{2})^2\right]^{-\frac{1}{2}}$$

and α, β, γ and θ_c are defined in equation (5). $\bar{\chi}_1$ has the same functional form as χ_1.

As can be seen in Figure 8, where χ_1 and χ_2 are displayed as functions of ℓ, χ_1 has a single branch and χ_2 has two branches.

Since χ_1 and χ_2 are defined in the range $0 \to \pi$, the first and third of the integrals in equation (10) cannot simultaneously include a point of stationary phase since χ_1 is a monotonic function of ℓ. However, if χ_1 and $\chi_2 \to \infty$ as $\ell \to 0$ (as they would if they were computed unmodified on the assumption of a rectilinear trajectory) additional, spurious points of stationary phase would be introduced, since θ and $\pi+\theta$ are physically indistinguishable. It is for this reason that the phase shifts were modified according to equation (7).

Hence the expression for $f_{el}(\theta)$ reads:

$$f_{el}(\theta) = \left[1/k_{el}(2\sin\theta)^{\frac{1}{2}}\right]\{a_1\exp(i\beta_1)+a_1^1\exp(i\beta_1^1)+a_2\exp(i\beta_2)+ a_2^1\exp(i\beta_2^1)\} \qquad (14)$$

where $\beta_n = \left[2\zeta_n - 2(\ell+\tfrac{1}{2})\zeta_n^1 - (2-\zeta_n^{11}/|\zeta_n^{11}| - \zeta_n^1/|\zeta_n^1|)\pi/4\right]\ell_\theta$

$$a_1 = \left[(\ell+\tfrac{1}{2})^{\frac{1}{2}} p(\ell)/|\zeta_1^{11}|^{\frac{1}{2}}\right]\ell_{1\theta}, \quad a_2 = \left[(\ell+\tfrac{1}{2})^{\frac{1}{2}}(1-p(\ell)/|\zeta_2^{11}|^{\frac{1}{2}}\right]\ell_{2\theta}$$

$a_1^1 = \left[(\ell+\frac{1}{2})^{\frac{1}{2}} p(\ell)/|\zeta_1^{11}|^{\frac{1}{2}}\right]_{\ell_{1\theta}^1}$ is the contribution arising from the point of stationary phase for ℓ greater than the value (ℓ_c) for which $\chi_1 = \chi_2$ and $a_2^1 = \left[(\ell+\frac{1}{2})^{\frac{1}{2}}(1-p(\ell)/|\zeta_2^{11}|^{\frac{1}{2}}\right]_{\ell_{2\theta}^1}$ is the contribution arising from the point of stationary phase on the large ℓ side of the minimum in χ_2. $\chi_1 = \chi_2 = \chi_c = 0.0375$ (2.15^o) at $\ell_c = 2884$ and $\chi_2^{min} = 0.0245^c$ (1.4^o) at $\ell_2^{min} = 2710$ (see Figure 8). For $\theta>\chi_c$ only a_1 and a_2 can be non-zero. For $\chi_2^{min}<\theta<\chi_c$, a_1^1, a_2 and a_2^1 can all be non-zero and for $\theta<\chi_2^{min}$ only a_1^1 can be non-zero. Hence $f_{el}(\theta)$ is given by

$$\left[k_{el}(2\sin\theta)^{\frac{1}{2}}\right]f_{el}(\theta) = a_1\exp(i\beta_1)+a_2\exp(i\beta_2) \quad , \quad \theta>\chi_c$$

$$= a_1^1\exp(i\beta_1^1)+a_2\exp(i\beta_2)+a_2^1\exp(i\beta_2^1), \chi_2^{min}<\theta<\chi_c$$

$$= a_1^1\exp(i\beta_1^1) \quad , \quad \theta<\chi_2^{min}$$

and the elastic differential cross section, $I_{el}(\theta)$ is given by

$$(2k_{el}^2\sin\theta)I_{el}(\theta) = a_1^2 + a_2^2 + 2a_1a_2\cos(\beta_1-\beta_2) \quad , \quad \theta>\chi_c$$

$$= a_1^{1^2} + a_2^2 + a_2^{1^2} + 2a_1^1a_2\cos(\beta_1^1-\beta_2)+2a_1^1a_2^1\cos(\beta_1^1-\beta_2^1)$$

$$+2a_2a_2^1\cos(\beta_2-\beta_2^1) \quad , \quad \chi_2^{min}<\theta<\chi_c$$

$$= a_1^{1^2} \quad , \quad \theta<\chi_2^{min} \qquad (15)$$

TABLE 1

Amplitudes from Regions of Stationary Phase in Elastic Scattering

	$H_{12}(R_c)=0.25$ eV	$H_{12}(R_c)=0.35$ eV
$a_1^1(2990)$	8.2×10^3	8.2×10^3
$a_2(2580)$	4.5×10^3	7.5×10^3
$a_2^1(2850)$	6.3×10^3	9.4×10^3

The elastic d.c.s. is structureless for $\theta < \chi_2^{min}$ (1.4^o). For $1.4^o < \theta < 2.15^o$ there are three sets of oscillations since a_1^1, a_2 and a_2^1 are all of comparable magnitude (see Table 1). For $\theta > 2.15^o$ there is only one source of oscillations in $I_{el}(\theta)$.

Consider $\theta = 1.5^o$ (0.0262^c). $\chi_1 = \theta$ at $\ell_\theta \simeq$ 2990, $\chi_2 = \theta$ at $\ell_\theta \simeq$ 2805 and at $\ell_\theta \simeq$ 2580. The appropriate values of a_1^1 etc calculated from (14), are presented in Table 1 for $H_{12}(R_c) = 0.25$ eV and 0.35 eV. Clearly a_1^1, a_2 and a_2^1 are all non-zero (see Figure 8). The 'wavelengths' of the three oscillations (see (15)) that is the angular increment in θ required to go from I_{max} to I_{min} and back to I_{max}, around $\theta = 1.5^o$ will be

$$\delta_{1\theta} = 2\pi/(2990 - 2850) = 2.6^o$$

$$\delta_{2\theta} = 2\pi/(2990 - 2580) = 0.9^o$$

$$\delta_{3\theta} = 2\pi/(2850 - 2580) = 1.3^o \quad \text{(see Ford and Wheeler)}$$

b. Inelastic Scattering

$$S_{\ell\ell}^{inel} = \left[p(1-p)\right]^{\frac{1}{2}}\{e^{2i\zeta_3} - e^{2i\zeta_4}\} \qquad 0 \lesssim \ell \lesssim \ell_c$$

$$S_{\ell\ell}^{inel} = 0 \qquad \ell > \ell_c$$

Hence

$$f_{inel}(\theta) = -\left[1/k_{\ell\ell} \quad (2\pi\sin\theta)^{\frac{1}{2}}\right]\{\int_0^{\ell_c}(\ell+\tfrac{1}{2})\left[p(1-p)\right]^{\frac{1}{2}}\left[\exp(i\phi_3^+) - \exp(i\phi_3^-)\right] d\ell$$

$$-\int_0^{\ell_c}(\ell+\tfrac{1}{2})\left[p(1-p)\right]^{\frac{1}{2}}\left[\exp(i\phi_4^+) - \exp(i\phi_4^-)\right] d\ell\} \qquad (16)$$

The 'deflection functions' χ_3 and χ_4 appropriate to inelastic scattering are defined by the equations

$$\chi_3 = \frac{-9\alpha}{(\ell+\frac{1}{2})^{10}}\left[I_{10}(\theta_c)-\frac{70\pi}{16}\right]+\frac{\alpha}{(\ell+\frac{1}{2})^{9}}\,I'_{10}(\theta_c)-\frac{7\beta}{(\ell+\frac{1}{2})^{8}}\left[I_8(\theta_r)-I_8(\theta_c)\right]$$

$$+\frac{\beta}{(\ell+\frac{1}{2})^{7}}\left[I'_8(\theta_r)-I'_8(\theta_c)\right]-\gamma(\ell+\tfrac{1}{2})\left\{\left[(R_cp_o)^2-(\ell+\tfrac{1}{2})^2\right]^{-\frac{1}{2}}\right.$$

$$\left.-\left[(rp_o)^2-(\ell+\tfrac{1}{2})^{\frac{1}{2}}\right]^{-\frac{1}{2}}\right\}$$

$$\chi_4 = \frac{-7\beta}{(\ell+\frac{1}{2})^{8}}\left[I_8(\theta_c)+I_8(\theta_r)-\frac{10\pi}{4}\right]+\frac{\beta}{(\ell+\frac{1}{2})^{7}}\left[I'_8(\theta_c)+I'_8(\theta_r)\right]$$

$$-\frac{\alpha}{(\ell+\frac{1}{2})^{10}}\,I'_{10}(\theta_c)+\frac{9\alpha I_{10}(\theta_c)}{(\ell+\frac{1}{2})^{9}}+\gamma(\ell+\tfrac{1}{2})\left\{\left[(R_cp_o)^2-(\ell+\tfrac{1}{2})^2\right]^{-\frac{1}{2}}\right.$$

$$\left.+\left[(rp_o)^2-(\ell+\tfrac{1}{2})^2\right]^{-\frac{1}{2}}\right\} \qquad (17)$$

χ_3 and χ_4 are displayed as functions of ℓ in Figure 9. Proceeding as before in the evaluation of $f_{inel}(\theta)$, the result is obtained

$$\left[k_{\ell\ell}\ (2\sin\theta)^{\frac{1}{2}}\right]f_{inel}(\theta) = 0\ ;\quad \theta<\chi_4^{min}$$

$$= -a_4\exp(i\beta_4)-a'_4\exp(i\beta'_4)\ ;\ \chi_4^{min}<\theta<\chi_c$$

$$= a_3\exp(i\beta_3)-a_4\exp(i\beta_4)\ ;\ \theta>\chi_c \qquad (18)$$

TABLE 2

Amplitudes from Regions of Stationary Phase

in Inelastic Scattering

	$H_{12}(R_c) = 0.25$ eV	$H_{12}(R_c) = 0.35$ eV
$a_3(2877)$	1.3×10^2	0.9×10^3
$a_4(2485)$	4.3×10^3	4.7×10^3

where $a_3 = \left[(\ell+\frac{1}{2})p(1-p)/|\zeta_3''|\right]^{\frac{1}{2}}_{\ell_{3\theta}}$, $a_4 = \left[(\ell+\frac{1}{2})p(1-p)/|\zeta_4''|\right]^{\frac{1}{2}}_{\ell_{4\theta}}$

and $a_4' = \left[(\ell+\frac{1}{2})p(1-p)/|\zeta_4''|\right]^{\frac{1}{2}}_{\ell_{4\theta}}$,

is the contribution arising from the point of stationary phase on the large ℓ side of the minimum in χ_4. a_4 and a_4' are obviously of comparable magnitude. $\chi_4^{min} = 0.0175^c$ (1.0^o) at $\ell_4^{min} = 2780$ and $\chi_3 = \chi_4 = \chi_c = 0.021^c$ (1.2^o) at $\ell_c = 2884$. The inelastic differential cross section, $I_{inel}(\theta)$ is given by

$$(2k^2_{\ell} \sin\theta) I_{inel}(\theta) = o \quad , \quad \theta < \chi_4^{min}$$

$$= a_4^2 + a_4'^2 + 2a_4 a_4' \cos(\beta_4 - \beta_4'), \quad \chi_4^{min} < \theta < \chi_c$$

$$= a_3^2 + a_4^2 - 2a_3 a_4 \cos(\beta_3 - \beta_4), \quad \theta > \chi_c \qquad (19)$$

The inelastic d.c.s. is zero for $\theta < \chi_4^{min}$ (1.0^o). For $1.0^o < \theta < 1.2^o$ and also for $\theta > 1.2^o$ there is only one source (different in the two angular ranges) of oscillations in $I_{inel}(\theta)$.

Consider $\theta = 1.5^o$ $\chi_3 = \theta$ at $\ell_\theta \simeq 2877$, $\chi_4 = \theta$ at $\ell_\theta \simeq 2485$. The appropriate values of a_3 and a_4 are presented in Table 2 for $H_{12}(R_c) = 0.25$ and 0.35 eV. It can be seen that for $H_{12} = 0.25$ eV $I_{inel}(\theta)$ should show quite strong oscillations of period $\sim 0.9^o$. around $\theta = 1.5^o$ and for $H_{12} = 0.35$ eV these oscillations should be less strong.

REFERENCES

BA032 BACHER, R.F. and GOUDSMIT, S., "Atomic Energy States", McGraw-Hill, N.Y. and London (1932).

BA139 BATES, D.R. and BOTTARD, A., Phil. Trans. Roy. Soc., A 242, 101 (1949).

BE073 BELOVED, B. and BERENDS, G., Can. J. Phys., 51(9), 967 (1973).

BU059 BUCKINGHAM, A.D., Quarterly Rev., 13, 183 (1959).

BU274 BUTCHER, R.J., DUNCAN, R.J. and STRAIN, R.N., Far Trans II, 70(11), 1837 (1974).

CA059 CARLSON, B.C. and SUSSKIND, S.S., Proc. Camb. Phil. Soc., 56, 628 (1960).

CH169 CHILD, M.S., Mol. Phys., 16 313 (1969).

CO052 CONDON, E.U. and SHORTLEY, G.H., "Theory of Atomic Spectra", C.U.P. (1953).

DA070(a) DASHEVSKAYA, E.I., KITAYEV, L.E. and KRASNOV, A.I., J.C.P., 53, 1129 (1970).

DA070(b) DASHEVSKAYA, E.I., KITAYEV, L.E. and KRASNOV, A.I., Opt. Spectrosc., 29, 340 (1970).

DU172 DUNCAN, J.L. and HUSAIN, D., J.C.S. Far.II, 68, 1803 (1972).

DU071 DUNCAN, R.J. and HUSAIN, D., Ann. Rep. (A) 68, 124 (1971).

BAC32 BACHER, R.F. and GOUDSMIT, S., "Atomic Energy States", McGraw-Hill, N.Y. and London (1932).

BAT39 BATES, D.R. and DAMGAARD, A., Phil. Trans. Roy. Soc., A 242, 101 (1949).

BRE73 BREDOHL, H. and HERZBERG, G., Can. J. Phys., 51(9), 867 (1973).

BUC59 BUCKINGHAM, A.D., Quarterly Rev., 13, 183 (1959).

BUT74 BUTCHER, R.J., DONOVAN, R.J. and STRAIN, R.H., Far Trans II, 70(11), 1837 (1974).

CAR50 CARLSON, B.C. and RUSHBROOKE, G.S., Proc. Camb. Phil. Soc., 46, 626 (1950).

CHI69 CHILD, M.S., Mol. Phys., 16 313 (1969).

CON53 CONDON, E.U. and SHORTLEY, G.H., "Theory of Atomic Spectra", C.U.P. (1953).

DAS70(a) DASHEVSKAYA, E.I., NIKITIN, E.E. and REZNIKOV, A.I., J.C.P., 53, 1175 (1970).

DAS70(b) DASHEVSKAYA, E.I., NIKITIN, E.E. and REZNIKOV, A.I., Opt. Spectrosc., 29, 540 (1970).

DEA72 DEAKIN, J.J. and HUSAIN, D., J.C.S. Far.II, 68, 1603 (1972).

DON71 DONOVAN, R.J. and HUSAIN, D., Ann. Rep. (A) 68, 124 (1971).

ADDENDUM

HAR 27 HARTREE, D.R., Proc. Camb. Phil. Soc., 24, 89 (1927)

HAR 38 HARTREE, D.R. and HARTREE, W., Proc. Roy. Soc., A164 (1938)

KER 74 KERR, J.H., Ph. D. Thesis, University of Edinburgh (1974)

DON72 DONOVAN, R.J., HUSAIN, D. and KIRSCH, L.J., Ann. Rep. (A) 69, 19 (1972).

DON73 DONOVAN, R.J. and LITTLE, D.J., J.C.S. Far. II, 69, 952 (1973).

DON74 DONOVAN, R.J. and GILLESPIE, H.M., S.P.R., Reaction Kinetics, 1, 14, Chem. Soc., London (1975).

EDM57 EDMONDS, A.R., "Angular Momentum in Quantum Mechanics", Princetown (1957).

EWI74 EWING, JJ., C.P. Lett., 29 50 (1974).

FIN65 FINK, U., WIGGINS, T.A. and RANK, D.H., J. Mol. Spec., 18, 384 (1965).

FOR59 FORD, K.W. and WHEELER, J.A., Ann. of Physics, 7, 259 (1959).

GAL64 GALLAGHER, A. and LURIO, A., Phys. Rev., A136, 87 (1964).

GAR57 GARSTANG, R.H., Proc. Camb. Phil. Soc., 53, 214 (1957).

GAR64 GARSTANG, R.H., J. Res. Nat. Bur. Stand., A68, 61 (1964).

GOL50 GOLDSTEIN, H., "Classical Mechanics", Addison-Wesley (1950).

GRI74 GRICE, R., and HERSCHBACH, D.R., Mol. Phys., 27, 159 (1974).

HER50 HERZBERG, G., "Spectra of Diatomic Molecules", 2nd Edn., Van Nostrand, Princetown (1950).

HER63 HERMAN, F. and SKILLMAN, S., "Atomic Structure Calculations", Prentice-Hall (1963).

HUS67 HUSAIN, D. and WIESENFELD, J.R., Trans. Far. Soc., 63, 1394 (1967).

JAM33 JAMES, H.M., and COOLIDGE, H.S., J.C.P., 1, 825 (1933).

JAM67 JAMES, T.C. and KLEMPERER, J., J.C.P., 40. 914 (1964).

KOL65 KOLOS, W. and WOLNIEWICZ, L., J.C.P., 43. 2429 (1965).

KOT69 KOTOVA, L.P., Sov. Phys., JETP, 28, 719 (1969).

KRY62 KRYLOV, V.I., "Approximate Calculation of Integrals", McMillan, N.Y. and London (1962).

LIJ72 Lijnse, P.L., "Review of Literature on Quenching, excitation and mixing collision cross sections for the first resonance doublet of the alkalis". (1972).

MOO73 MOORE, C.B., Adv. Chem. Phys., 23, 41 (1973).

MUL30 MULLIKEN, R.S., Rev. Mod. Phys., 2, 60 (1930).

NIK65(a) NIKITIN, E.E., Opt. Spectrosc., 19, 91 (1965).

NIK65(b) NIKITIN, E.E., J.C.P., 43, 744 (1965).

OLS71 OLSON, R.E., SMITH, F.T. and BAUER, E., Appl. Optics, 10, 1848 (1971).

PAU35 PAULING, L. and WILSON, E.B., "Introduction to Quantum Mechanics", McGraw-Hill (1935).

POR73 PORTER, G. and WEST, M.A., "Investigation of rates and mechanisms of reactions", 2nd Edn., part II, Ed. HAMMES, G.G., Wiley Interscience (1973).

RAA73 RAABE, G.P., Z. Naturforschung, 28A, 1642 (1973).

RAL60 RALSTON, A. and WILF, H.S., "Mathematical Methods for Digital Computers", Wiley, N.Y. and London (1960).

RAN62 RANK, D.H. *et al*, J. Opt. Soc. Amer., 52, 1004, (1962).

RAN63 RANK, D.J. and FOLZ, J.V., Astrophys. J., 138, 1319 (1963).

RIT51 RITTNER, E.S., J.C.P., 19, 1030 (1951).

ROS57 ROSE, M.E., "Elementary Theory of Angular Momentum", Wiley, (1957).

SCH49 SCHIFF, L.I., "Quantum Mechanics", McGraw-Hill (1949).

SHA73 SHARMA, R.D., CHEN, H.L. and SZOKE, A, J.C.P., 58, 3519 (1973).

SMI71 SMITH, I.W.M. and HANCOCK, G., Appl. Opt., 10, 1827 (1971).

STO57 STOICHEFF, B.P., Can. J. Phys., 35, 730 (1957).

STR73 STRAIN, R.H., McLEAN, J. and DONOVAN, R.J., C.P. Lett., 20, 504 (1973).

STU32 STUECKELBERG, E.C.G., Helv. Phys. Acta., 5, 370 (1932).

WAB65 WABER, J.T., and CROMER, D.T., J.C.P., 42, 416 (1965).

WIE73 WIESENFELD, J.R., C.P. Lett., 21, 517 (1973).

WOL66 WOLNIEWICZ, L., J.C.P., 45, 515 (1966).

WON74 WONG, Y.C. and LEE, Y.T., J.C.P., 60, 4619 (1974).

ZEN32 ZENER, C., Proc. Roy. Soc., A137, 696 (1932).